Alma Mater Studiorum - Università di Bologna

DOTTORATO DI RICERCA IN

CHIMICA

Ciclo 34

Settore Concorsuale: 03/C1 - CHIMICA ORGANICA

Settore Scientifico Disciplinare: CHIM/06 - CHIMICA ORGANICA

NEW CATALYTIC STRATEGIES FOR THE SYNTHESIS OF COMPLEX (HETERO)-CYCLIC COMPOUNDS

Presentata da: Alessandro Cerveri

Coordinatore Dottorato

Domenica Tonelli

Supervisore

Marco Bandini

Co-supervisore

Marco Lucarini

Esame finale anno 2022

Abstract

The aim of this Doctoral Thesis is the development of new catalytic transformation for efficient and sustainable processes, with the main purpose of easily access the incredible diversity and complexity of bio-relevant compounds. The tuning of general synthetic strategies is a flourishing field in organic chemistry, and can rapidly give access to libraries of products with small to big modifications from a hypothetical lead compound. Whit this in mind, in the modern era of organic synthesis, many aspects are pivotal in the design of a new catalytic procedure, such as reproducibility, generality over the main functional groups, mild conditions and easily accessible starting materials and catalysts. Particularly, another fundamental aspect is the generation of complexity in one single step, to conveniently assemble the scaffold of the class of compounds studied. During the course of my PhD, two main strategies were analyzed to tackle these challenges, namely de-aromatization and ring construction through cyclization.

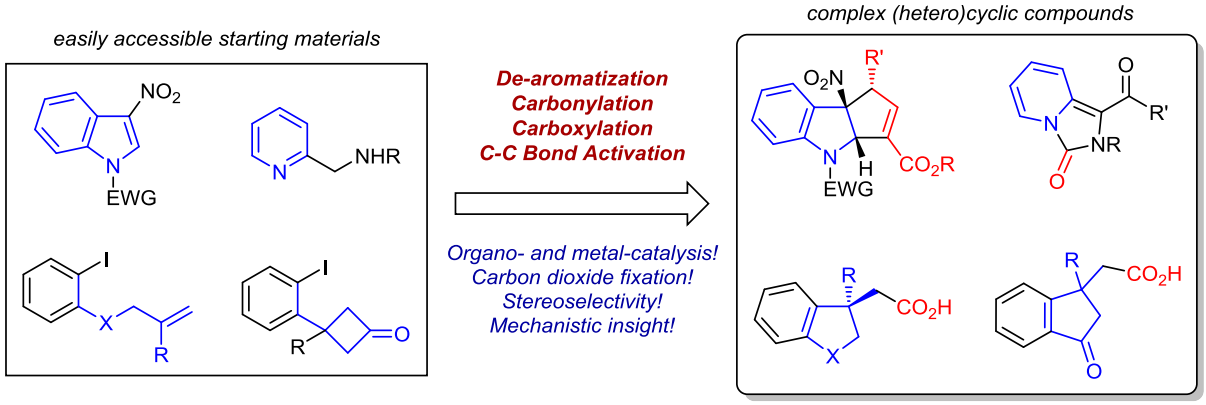

These methodologies have been deeply investigated both in organo- and metal-catalyzed fashions, and conceptually new protocols have been developed. Particular attention has been devoted at the study and optimization of the reaction conditions and catalyst structure, in order to maximize yield and selectivity of the processes as well as minimizing the catalyst loading and using the mildest conditions. The substrate scope has been thoroughly investigated to demonstrate the broad applicability of the proposed transformations, as well as the performance of synthetic elaborations illustrating the usefulness of the developed methods. Despite the conceptual diversity, the proposed protocols are connected by their potential further development into useful tools for the bio-molecule synthetic scenario.

The diastereoselective phosphine-catalyzed dearomative cyclization of 3-NO_2-indoles and allenyl-esters is described. This methodology provides high yields (up to 96%) with good

functional group tolerance (18 examples) in the synthesis of densely functionalized indolines, under mild reaction conditions (rt, air, reagent-grade solvent). Computational simulations and labeling experiments revealed the stepwise-[3+2] nature of the mechanism, and a full stereochemical profile of the reaction accounting for the selectivity observed is proposed.

A novel TBD assisted three-component carbonylation of pyridine-2-methanamines is documented by means of CO_2 as a benign CO surrogate. The redox-neutral methodology enables the realization of densely functionalized imidazo-pyridinones in high yields (up to 93%), and excellent chemoselectivity and functional group tolerance (25 examples). Computational and experimental efforts on the investigation of the mechanism revealed an unprecedented electrophilic activation system of carbon dioxide based on the combined action of acid chlorides and TBD.

A novel asymmetric nickel-based carbo-carboxylation procedure has been developed, featuring atmospheric CO_2 as carboxylating reagent. A new rationally designed chiral ligand has been prepared and shown to achieve enantiomeric excesses (up to 99%) and better performances. The overall process efficiently furnishes chiral 2,3-dihydrobenzofuran-3-ylacetic acids, an important class of bioactive products, from readily available starting materials. A combined experimental and computational efforts revealed the key steps of the catalytic cycle and suggested the unexpected participation of Ni(I) species in the stereodetermining cyclization event.

The nickel catalyzed cascade C-C bond activation/carboxylation of cyclobutanones derivatives is described. Through mild conditions and the use of carbon dioxide as environmentally benign carboxylating agent, a range of dihydroindanones bearing a quaternary carbon centre and a carboxylic moiety were synthesized (12 examples) in moderate to good yields (up to 76% yield). A new tetrahedral sterically demanding nickel complex has been prepared for this transformation and has been characterized by means of X-ray spectroscopy. Moreover, based on previous reports and experimental observation a rationally designed mechanism is proposed.

Table of Contents

1. Introduction

1.1. The Meeting Point Between Nature and Synthesis

Historically, natural products (secondary metabolites) have been used since ancient times and in folklore for the treatment of many diseases and illnesses. Classical chemistry methodologies enabled a vast array of bioactive compounds from terrestrial and marine sources to be discovered. Many of these natural products have gone on to become current drug candidates. The earliest record of natural product extraction and utilization date back to Mesopotamian civilizations in (2600 B.C.) which documented oils from *Cupressus sempervirens* (Cypress) and *Commiphora* species (myrrh) which are still used today to treat coughs, colds and inflammation.[1] Since then, the knowledge of natural compounds evolved over the century, gradually becoming an ever more precise and calculated science. To date, the global knowledge of natural products chemistry is incredibly advanced, and big steps have been taken in the extraction, purification and formulation in active principle of those bio-active entities.[2]

Traditional medicinal practices have formed the basis of most of the early medicines followed by subsequent clinical, pharmacological and chemical studies.[3] Probably the most famous and well known example to date would be the synthesis of the *anti*-inflammatory agent, acetylsalicylic acid (aspirin, Scheme 1) derived from the natural product, salicin isolated from the bark of the willow tree *Salix alba* L.[4] Investigation of *Papaver somniferum* L. (opium poppy) resulted in the isolation of several alkaloids including morphine, a commercially important drug, first reported in 1803. *Digitalis purpurea* L. (foxglove) had been traced back to Europe in the 10th century but it was not until the 1700s that the active constituent digitoxin, a cardiotonic glycoside, was found to enhance cardiac conduction, thereby improving the strength of cardiac contractibility. Digitoxin and its analogues have long been used in the management of congestive heart failure and have possible long term detrimental effects and are being replaced by other medicines in the treatment of "heart deficiency". The anti-malarial drug quinine was isolated from the bark of *Cinchona succirubra* Pav. ex Klotsch, and had been used for centuries for the treatment of malaria, fever, indigestion,

[1] G.M. Cragg, D.J. Newman, *Pure Appl. Chem.* **2005**, *77*, 7–24.
[2] a) B.B. Mishra,; V.K. Tiwari, *Eur. J. Med. Chem*. **2011**, *46*, 4769–4807; b) J. Rey-Ladino, A.G. Ross, A.W. Cripps, D.P. McManus, R. Quinn, *Vaccine* **2011**, *29*, 6464–6471; c) B. Haefner, *Drug Discov. Today* **2003**, *8*, 536–544.
[3] M.S. Butler, *J. Nat. Prod.* **2004**, *67*, 2141–2153.
[4] A. Der Marderosian, J.A. Beutler, *The Review of Natural Products*, 2nd ed.; Facts and Comparisons; Seattle, WA, USA, **2002**; pp. 13–43.

mouth and throat diseases and cancer. Formal use of the bark to treat malaria was established in the mid 1800s when the British began the worldwide cultivation of the plant. Pilocarpine found in *Pilocarpus jaborandi* (Rutaceae) is an L-histidine-derived alkaloid, which has been used as a clinical drug in the treatment of chronic open-angle glaucoma and acute angle-closure glaucoma for over 100 years. In 1998, an oral preparation of pilocarpine was approved for the management of Sjogren's syndrome, an autoimmune disease that damages the salivary and lacrimal glands.

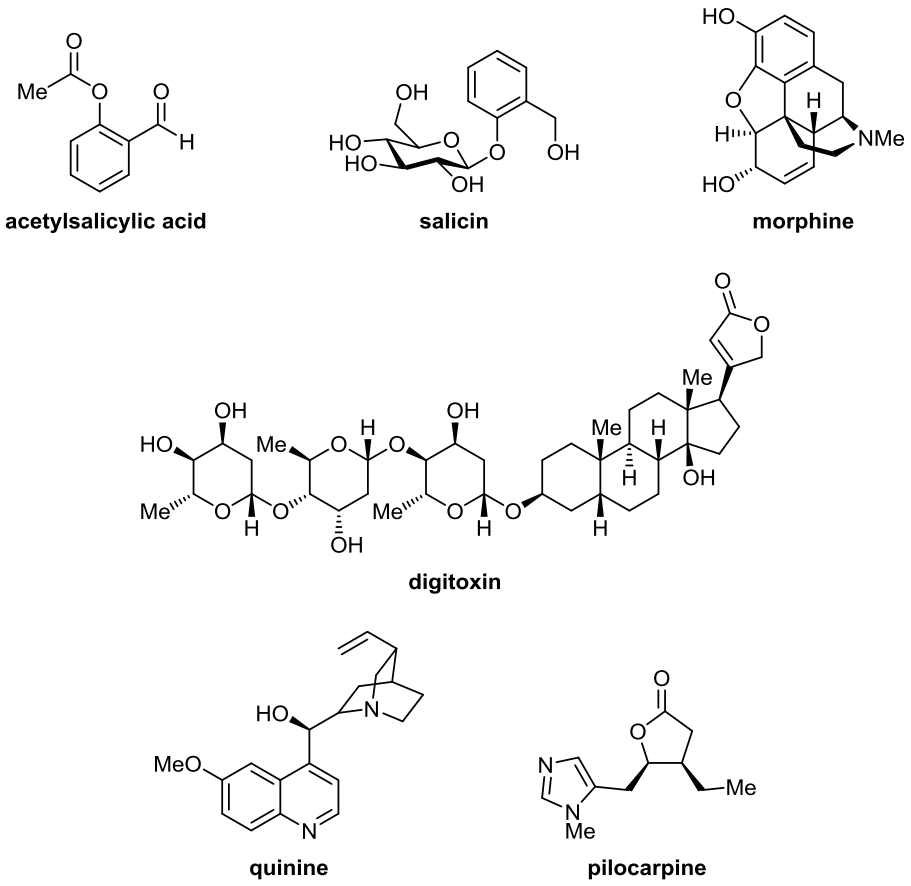

Scheme 1: Historically well known natural compounds.

Among these pivotal examples it's already possible to note some of the fundamental characteristics of the bio-active small molecules, that are shared in most cases. Particularly common is the structural complexity, the presence of various defined stereogenic centers, the abundance of different functional groups and hetero-atoms, and finally small hetero-cyclic scaffolds, both aromatic and not. Apart from acetylsalicylic acid, all the drugs shown in scheme 1 are characterized by all these distinctive features.

As a matter of fact, natural products continue to provide unique inspiration of structural diversity. Since less than 10% of the world's biodiversity has been evaluated for potential

biological activity, many more useful lead compounds await discovery, and combinatorial chemistry is a perfect tool to speed the process to access this chemical diversity. This challenge has been repeatedly faced by synthetic organic chemistry, which led overtime to the development of different strategies, as well as extraction and purification, also total synthesis and semi-synthesis of the various complex scaffolds. Unfortunately, the amount of possibly useful secondary metabolites is overwhelming, and even few changes of their molecular structure can bring to drastic changes in their activity, and even on the overall effect in a living organism.[5] As a consequence, in order to find the most effective version of a hypothetic lead compound, is necessary to prepare as many modified molecules as possible. Particularly, in view of the synthesis of libraries of analogues of known compounds, the synthetic methodology scenario offers different strategies for the general construction of specific structures with small modifications from the model substrate.

1.2. Hetero-Cyclic Natural Compounds

As previously exposed, hetero-cyclic compounds are ubiquitous in nature, and they are also often the effective core of the bio-active molecules. Generally, five- and six-membered rings are predominant, but also smaller or bigger cycles can be found. Particularly frequent are hetero-aromatic rings (*i.e.* pyridine, pyrrole or furan), and their non-aromatic counterparts. These compounds are common in the metabolism of most living beings thanks to their stability and versatility, and the organism use them in a number of transformations. Accordingly, in the area of synthetic methodologies the straightforward preparation of hetero-cyclic derivatives is an aspect of critical importance, and a tremendous number of new strategies are continuously produced by the scientific community. Nevertheless, any synthetic method is specifically optimized for the production of a precise scaffold, and is necessary to further increase the knowledge about the chemical reactivity of these compounds to obtain more efficient procedures for the fast assembly of molecular complexity. Since (hetero)aromatic compounds are so frequent, their reactivity is well studied, and their chemical manipulation is a flourishing research field. Particularly attractive is the strategy based on breaking the aromaticity generating non aromatic (hetero)cycles, namely "de-aromatization". All the different aromatics are possibly subjected to de-aromatization reactions in various modes, like oxidation, reduction and isomerization, according to their specific electronic as well as structural properties (Scheme 2).

[5] N. Vargesson *Birth Defects Res C Embryo Today*, **2015**, *105*(2), 140-156.

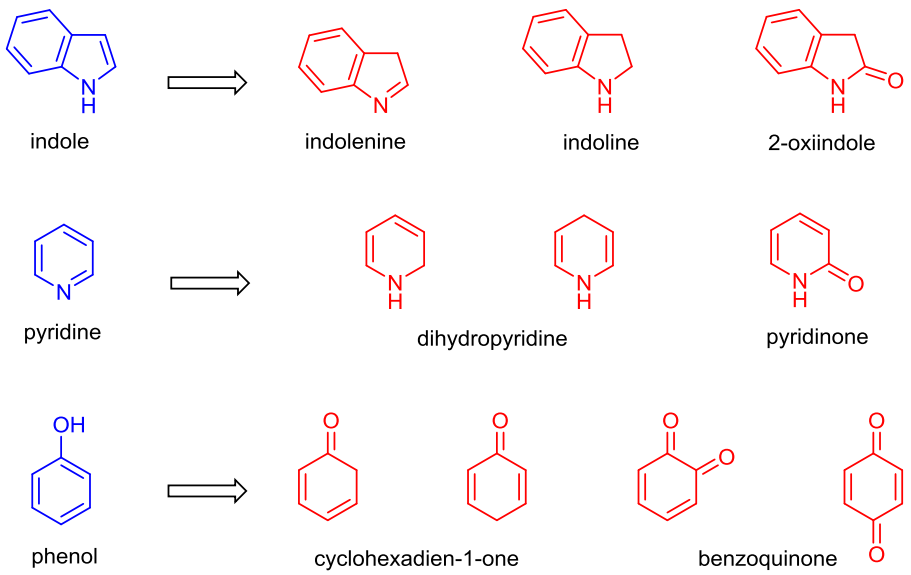

Scheme 2: Commonly widespread in nature aromatic compounds (blue) and their possible de-aromatized versions (red).

For example the electron-rich cyclo-fused indole is nucleophilic, particularly at the C(3), and can be de-aromatized by making it react with various electrophiles. In nature it's widespread in all the possible modes, such as the isomerized (indolenine), reduced (indoline) or oxidized (2-oxindole). Similarly to indole, pyridine and phenol are among the most common aromatics in the bio-chemical world, and the oxidative or reductive processes they can undergo in a living organism produces a variety of derivatives such as dihydroyridines and cyclohexadienones (dearomatized by electrophilic or nucleophilic substitution) or pyridinones and benzoquinones (oxidized forms). Equally relevant are five-membered aromatic rings, benzo-fused and not, such as furan, pyrrole, thiophene and the de-aromatized counterparts. In scheme 3 are summarized some pivotal examples of relevant bio-active compounds, both aromatic and de-aromatized, which easily underlines the chemical complexity and variety of nature.

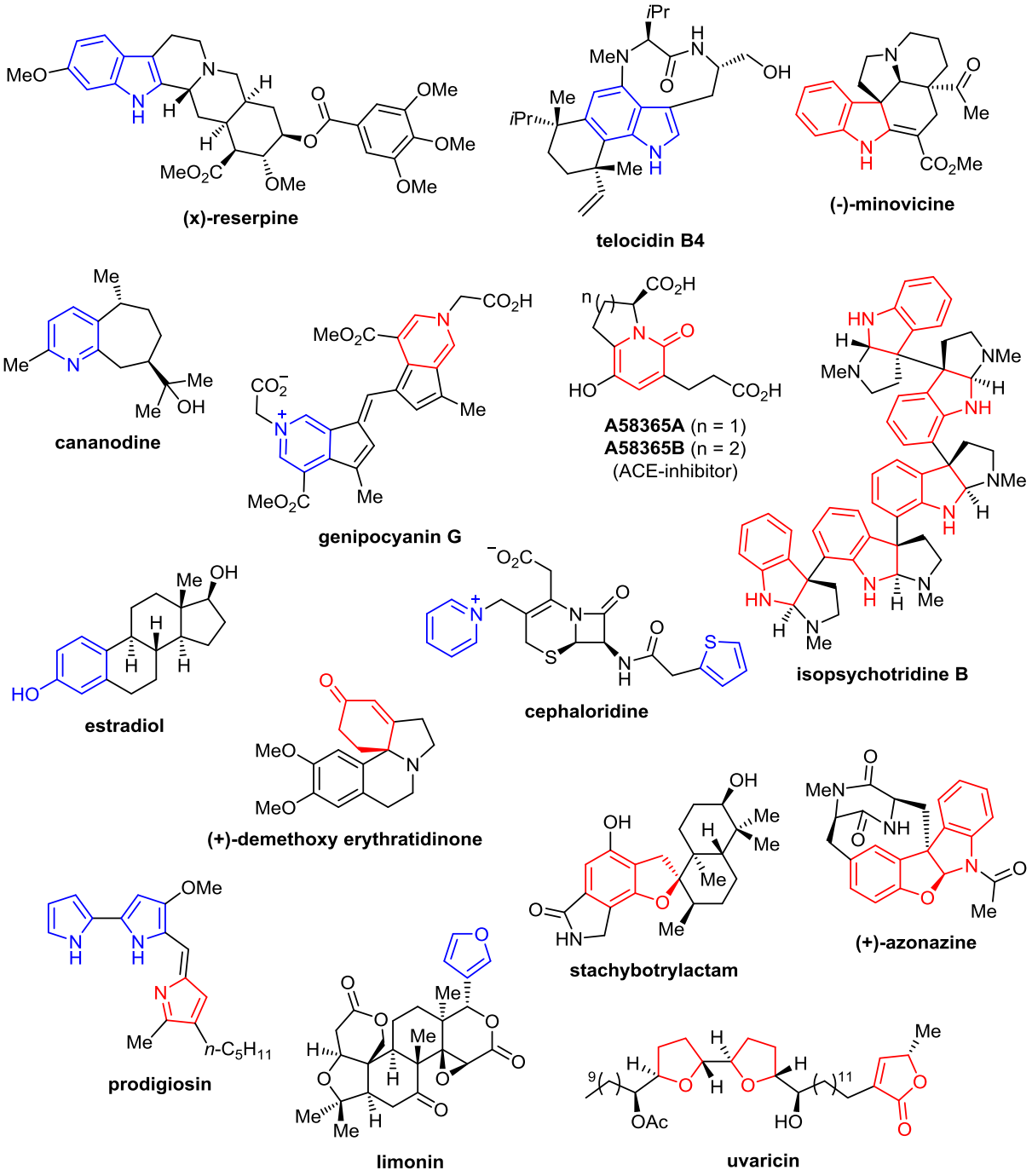

Scheme 3: Examples of (hetero)cycle-based natural products, deriving from indole, pyridine, phenol, pyrrole, (benzo)furan and thiophene.

1.3. New Strategies for the Synthesis of Complex Hetero-Cyclic Compounds

The need of reliable methodologies for the preparation of complex bio-molecules brought the organic synthesis field to exponentially expand over the last century. Incredible steps forward

have been taken since Wöhler achieved the synthesis of urea in 1828,[6] and more and more complex natural products, from acetic acid to glucose to vitamin B_{12} to palytoxin and so on, have been synthesized.[7] Danishefsky achieved the total synthesis of a homogeneous, wild-type erythropoietin (EPO) with a relative molecular mass of 17868 in 2013, reaching a new milestone of natural product synthesis.[8] Today, organic chemists have demonstrated they are capable of synthesizing nearly any molecule with enough effort and time. The present state-of-the-art processes for the synthesis of most complex natural products are not efficient enough to generate sufficient quantities for biological studies. Thus, the development of efficient synthetic routes for the scalable production of complex natural compounds is still a challenging task facing chemists.[9] Nevertheless impressive efforts have been directed in the development of highly efficient protocols, and catalysis can be often a pivotal strategy to achieve efficient and sustainable processes.

(-)-Flustramine B (**4a**) and (-)-debromoflustramine B (**4b**) belong to a family of marine alkaloids isolated from the Bryozoa *Flustra foliacea*, which possess skeletal and smooth muscle relaxant activity and significant butyrylcholinesterase inhibitory activity, respectively.[10] Their embedded HPI core structure makes them popular targets in recent asymmetric total synthesis studies.[11] In 2004, MacMillan and co-workers reported their enantioselective synthesis of both those indole-based alkaloids (Scheme 4).[12] In the presence of an imidazolidinone catalyst **2**,[13] 6-bromo-substituted tryptamine derivative **1** reacted smoothly with acrolein in a cascade dearomative addition/cyclization sequence. The enantioenriched compound **3** with a pendant primary alcohol group was achieved in 78%

[6] F. Wö hler, Ueber Kü nstliche Bildung Des Harnstoffs. *Ann. Phys.* **1828**, 88, 253−256

[7] a) K.C. Nicolaou, D. Vourloumis, N. Winssinger, P.S. Baran, *Angew. Chem., Int. Ed.* **2000**, *39*, 44−122; b) K.C. Nicolaou*, J. Org. Chem*. **2009**, *74*, 951−972; c) K.C. Nicolaou, J.S. Chen, WileyVCH: Weinheim, Germany, **2011**; d) R.W. Hoffmann, *Angew. Chem., Int. Ed.* **2013**, *52*, 123−130; e) J.D. Keasling, A. Mendoza, P.S. Baran, *Nature* **2012**, *492*, 188−189.

[8] P. Wang, S. W. Dong, J. H. Shieh, E. Peguero, R. Hendrickson, M. A. S. Moore, S. J. Danishefsky, *Science* **2013**, *342*, 1357−1360.

[9] a) J. B. J. Hendrickson, *Am. Chem. Soc.* **1975**, *97*, 5784−5800; b) T. Gaich, P. S. Baran, *J. Org. Chem.* **2010**, *75*, 4657−4673; c) C. A. Kuttruff, M. D. Eastgate, P. S. Baran, *Nat. Prod. Rep.* **2014**, *31*, 419−432; d) J. Mulzer, *Nat. Prod. Rep.* **2014**, *31*, 595−603; e) P. Wender, *A. Nat. Prod. Rep.* **2014**, *31*, 433−440.

[10] J. S. Carle and C. Christophersen, *J. Am. Chem. Soc.* **1979**, *101*, 4012–4013.

[11] a) D. Crich and A. Banerjee, *Acc. Chem. Res.* **2007**, *40*, 151–161; b) A. Steven and L. E. Overman, *Angew. Chem., Int. Ed.* **2007**, *46*, 5488–5508; c) P. Ruiz-Sanchis, S. A. Savina, F. Albericio and M. Alvarez, ´ *Chem.–Eur. J*. **2011**, *17*, 1388–1408

[12] J. F. Austin, S.-G. Kim, C. J. Sinz, W.-J. Xiao, D. W. C. MacMillan, *Proc. Natl. Acad. Sci. U. S. A.* **2004**, *101*, 5482–5487.

[13] G. Lelais, D. W. C. MacMillan, *Aldrichimica Acta*, **2006**, *39*, 79–87.

yield with 90% *ee* after in situ reduction by $NaBH_4$. This pivotal scaffold was then engaged in the divergent synthesis of **4a** and **4b**.

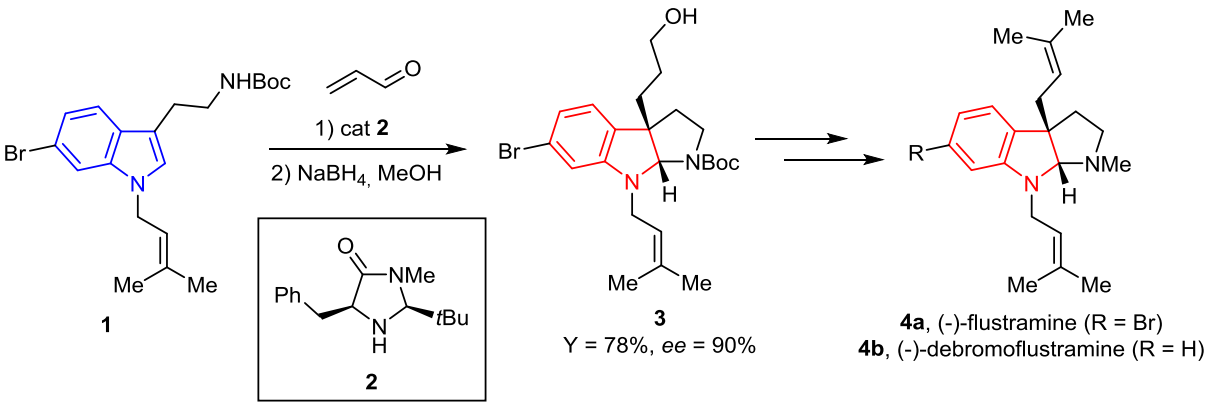

Scheme 4: Enantioselective organocatalyzed construction of the indolinic core of flustramine alkaloids.

Porco and co-workers described in 2005 the synthesis of (-)-mitorubrin (**8**) and related azaphilone natural products employing enantioselective oxidative dearomatization of resorcinols (Scheme 5).[14] Dearomatization of the resorcinol aldehyde **5** using the *in-situ* formed [{(-)-sparteine}$_2$$Cu_2O_2$] complex was achieved in a regioselective manner with high enantioslectivity to afford vinylogous acid **6**. This enyne was subjected to CuI-catalyzed cycloisomerization to afford the mitorubrin core structure **7** (58% for two steps, 97% ee). Further esterification and final deprotection afforded the desired azaphilone (-)-mitorubrin (**8**). This convergent synthesis featured an interesting highly enantioselective oxidative dearomatization of resorcinol aldehydes using a readily accessible chiral copper complex.

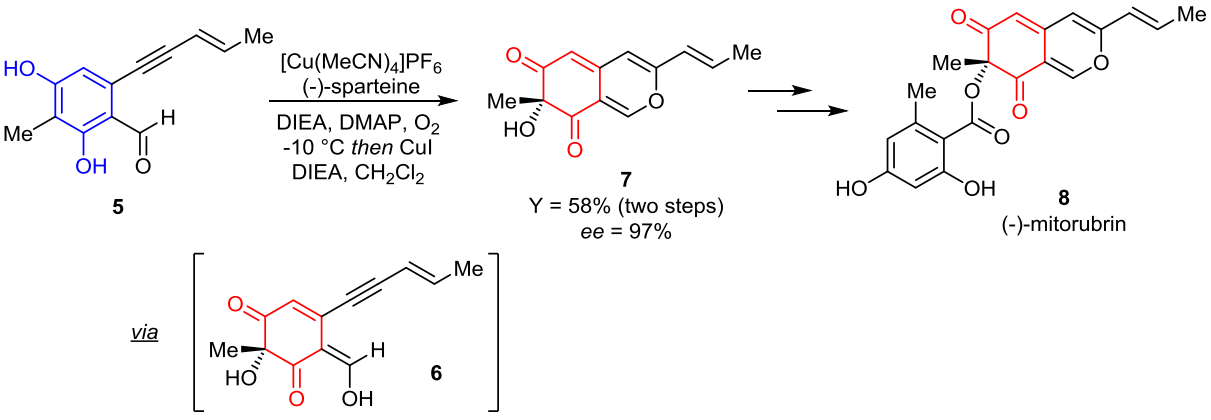

Scheme 5: Copper-catalyzed enantioselective dearomative oxidation of resorcinol aldehyde by means of molecular oxygen as stoichiometric oxidant.

[14] a) J. Zhu, N. P. Grigoriadis, J. P. Lee, J. A. Porco, Jr., *J. Am. Chem. Soc.* **2005**, *127*, 9342 – 9343; b) J. Zhu, J. A. Porco, Jr., *Org. Lett.* **2006**, *8*, 5169 – 5171.

Another interesting example of catalytic de-aromatization reaction applied to the synthesis of natural compounds was disclosed by Frontier and co-workers in 2008, which reported the stereoselective total synthesis of the pentacyclic sesquiterpene dilactone (±)-merrilactone A (**12**) featuring the catalytic Nazarov cyclization of 2-silyloxyfurans (Scheme 6).[15] Recently, catalytic Nazarov cyclizations have been reported employing a wide range of transition-metal complexes and have demonstrated that dienones with high electron density at one terminus of the pentadienyl cation intermediate exhibit high cyclization reactivity. In this context, Frontier and co-workers employed iridium complex **10** to catalyze the Nazarov cyclization of trialkyl-2-silyloxyfuranyl enone **9**. The authors suggested that the iridium(III) complex or a Lewis acidic silicon species could be involved in the dearomatization of silyloxyfuran via coordination and activation of the enone moiety leading to the bicyclic framework which may be followed by silyl transfer to give the product. This approach for catalytic enone activation triggered the dearomatization of the 2-silyoxyfuran and afforded the desired trisubstituted Nazarov product **11** bearing two adjacent, highly crowded stereogenic centers in 82% yield. Few other steps concluded an elegant synthesis of (±)-merrilactone A (**12**).

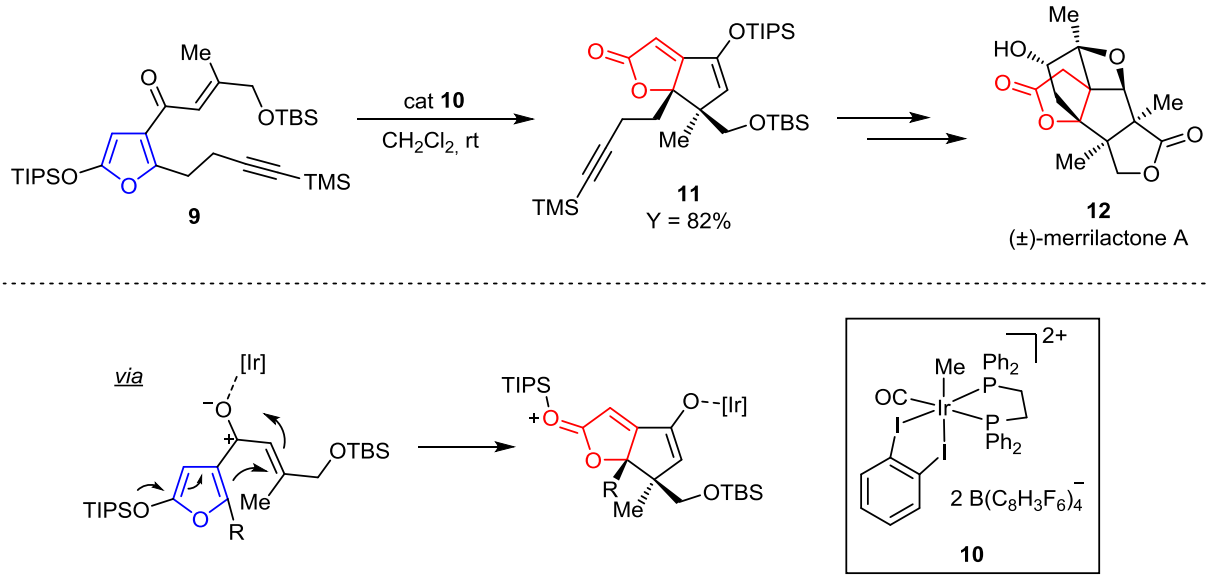

Scheme 6: Stereoselective catalytic Nazarov dearomative cyclization applied in the total synthesis of the terpenoid merrilactone A.

In 2016, Kitamura, Fukuyama and coworkers disclosed the enantioselective total synthesis of (+)-hinckdentine A (**16**),[16] which was isolated from the marine Bryozoan *Hincksinoflustra*

[15] W. He, J. Huang, X. Sun, A. J. Frontier, *J. Am. Chem. Soc*. **2008**, *130*, 300 – 308.
[16] A. J. Blackman, T. W. Hambley, K. Picker, W. C. Taylor, N. Thirasasana, *Tetrahedron Lett*. **1987**, *28*, 5561–5562.

denticulate, based on a catalytic asymmetric dearomatization reaction (Scheme 7).[17] The key enantioenriched intermediate was obtained in a Pd-catalyzed dearomative Heck-type cyclization of N-acyl 5-oxotetrahydrocarbazole **13**. With the Feringa ligand **14** as the optimal ligand, the desired dearomative Heck reaction could be performed on a 10 gram scale, affording the screwshape intermediate **15** in 98% yield with 86% ee.

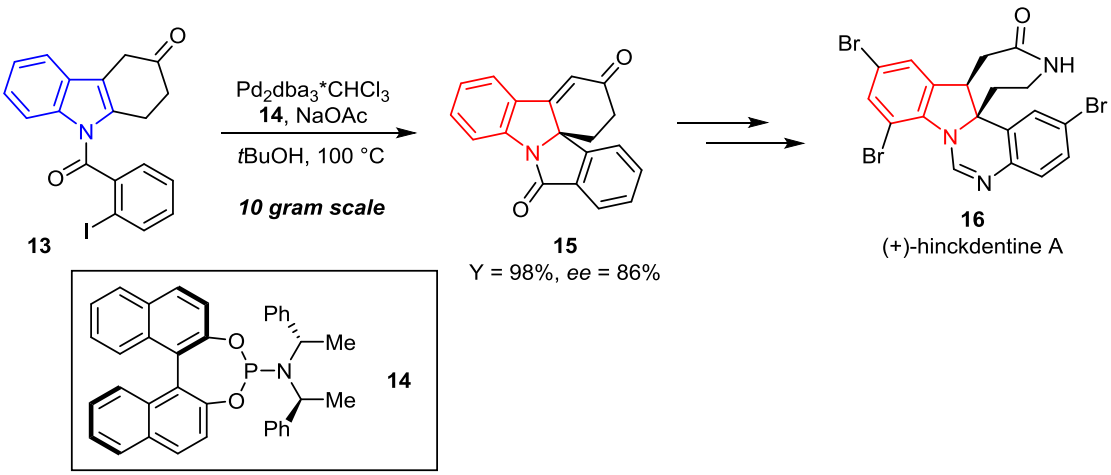

Scheme 7: Intramolecular dearomative Heck-coupling for the construction of the congested tetra-substituted stereogenic center of hinckdentine A.

A silver-catalyzed dearomative isomerization of pyridine was reported in 2016 by Unsworth and co-workers (Scheme 8).[18] With this protocol quinazolinones **18** were obtained in high yield by means of mild conditions, subjecting pyridine-ynones **17** to a cyclization/ dearomatization sequence catalyzed by small amount of the cheap silver nitrate. The cyclo-fused product was then easily modified by selective reduction to obtain the natural quinolizidine alkaloid lasubine II (**19**) in straightforward manner with high overall yield.

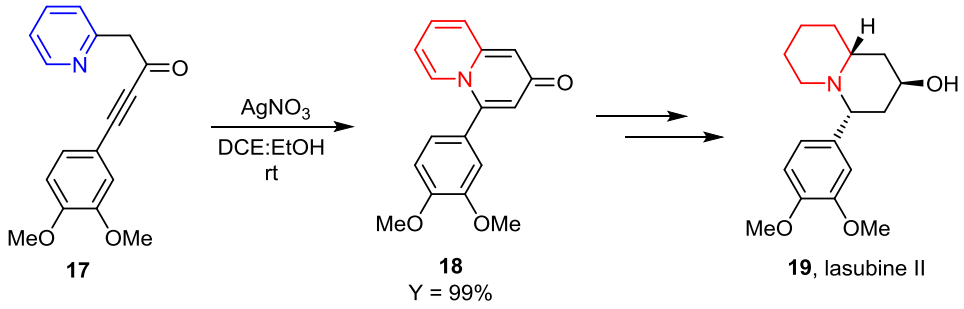

Scheme 8: Lewis acid-catalyzed cycloisomerization/dearomatization of pyridine derivatives in the synthesis of quinolizidine-based natural compounds.

[17] K. Douki, H. Ono, T. Taniguchi, J. Shimokawa, M. Kitamura, T. Fukuyama, *J. Am. Chem. Soc.* **2016**, *138*, 14578–14581.
[18] M. J. James, N. D. Grant, P. O'Brien, R. J. K. Taylor, W. P. Unsworth, *Org. Lett.* **2016**, *18*, 6256−6259.

Although one of the earliest known dearomative methods, the hydrogenation of arenes and hetero-arenes remains a vibrant and active field of research to this day. Advances in enantioselective catalysis as well as functional-group and heterocyclic tolerance have established dearomative hydrogenation as one of the premier methods for generating complex, saturated cyclic structures.[19] A demonstrative example of the powerfully simplifying disconnections made possible through enantioselective hydrogenation of arenes is found in the 2019 synthesis of (-)-jorumycin (**23**) from Stoltz and co-workers (Scheme 9).[20] Many successful syntheses of the bis-tetrahydroisoquinoline (bis-THIQ) alkaloid natural products have been disclosed before, but almost all rely upon stepwise construction of individual THIQ rings through Pictet-Spengler and other electrophilic aromatic substitution-based cyclization methods. The elegant approach reported from the Stoltz group leverages the power of modern cross-coupling to quickly assemble **20** from two simple, flat isoquinoline motifs. This is followed by a newly developed, enantioselective dearomative isoquinoline hydrogenation that sets four stereocenters and triggers cyclization to the bisTHIQ core **22** through lactamization. From this complex intermediate, Stoltz and co-workers were able to complete the syntheses of (-)-jorunnamycin (not shown) and (-)-jorumycin (**23**), as well as a series of unnatural analogs, in a rapid and efficient manner.

[19] M.P. Wiesenfeldt, Z. Nairoukh, T. Dalton, F. Glorius, *Angew. Chem. Int. Ed.* **2019**, *58*, 10460–10476.
[20] E.R. Welin, A. Ngamnithiporn, M. Klatte, G. Lapointe, G.M. Pototschnig, M.S.J. Mcdermott, D. Conklin, C.D. Gilmore, P.M. Tadross, C.K. Haley, et al. *Science,* **2019**, *363*, 270–275.

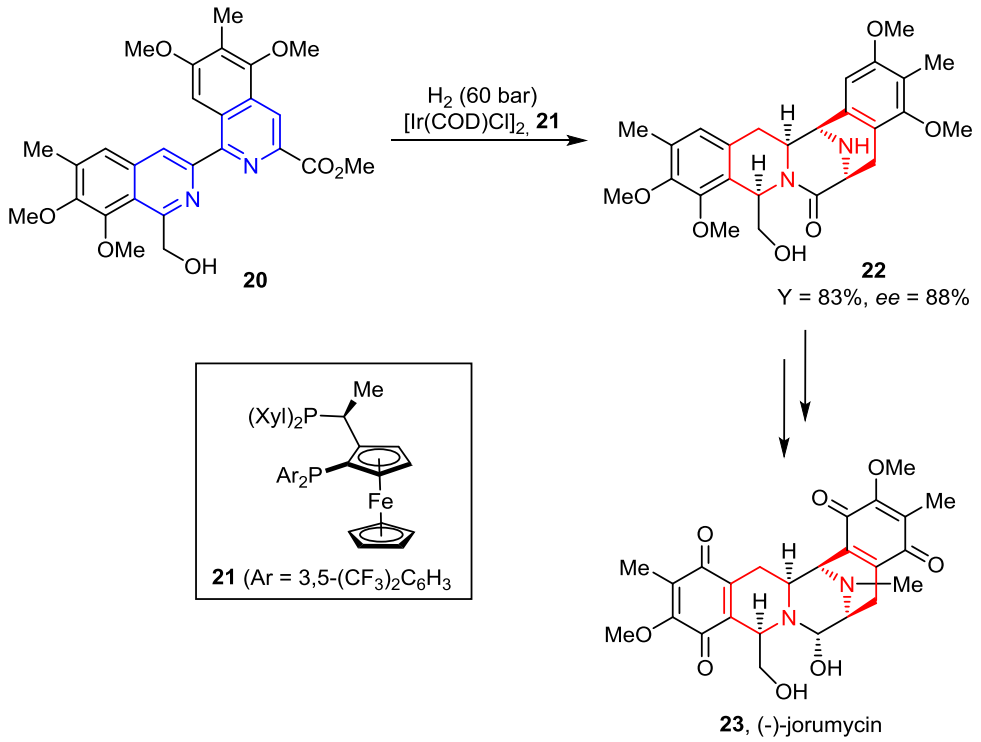

Scheme 9: Iridium-catalyzed enantioselective hydrogenation in the synthesis of complex bis-tetrahydroisoquinolines alkaloids.

In the previous examples the construction of densely functionalized hetero-cyclic scaffolds was obtained through de-aromatization of pre-built hetero-arenes intermediates, but another important strategy is certainly the direct construction of the cyclic framework, possibly in a tandem functionalization/cyclization sequence. With this purpose Ma and co-workers in 2012 elegantly disclosed the nickel-catalyzed hydro-carboxylation of alkynes using the environmentally benign CO_2 as C(1) synthon,[21] applied in the total synthesis of heteroplexisolide E (**25**), a natural compound isolated from *Heteroplexis micocephala* in 2009 (Scheme 10).[22] By subjecting the homo-propargylic alcohol **24** to nickel-hydride regime and atmospheric pressure of CO_2 the geometrically defined α,β-unsaturated carboxylic acid is obtained in the carboxylation step after the *syn* addition of nickel on the triple bond. The un-isolated intermediate was then easily cyclized in the α-alkylidene-γ-butyrolactone (**25**) in acidic conditions, directly delivering the target product in 77% yield over two steps.

[21] Li, S. and Ma, S. *Chem. Asian J.*, **2012**, *7*: 2411-2418.
[22] X. Fan, J. Zi, C. Zhu, W. Xu, W. Cheng, S. Yang, Y. Guo, J. Shi, *J. Nat. Prod.* **2009**, *72*, 1184.

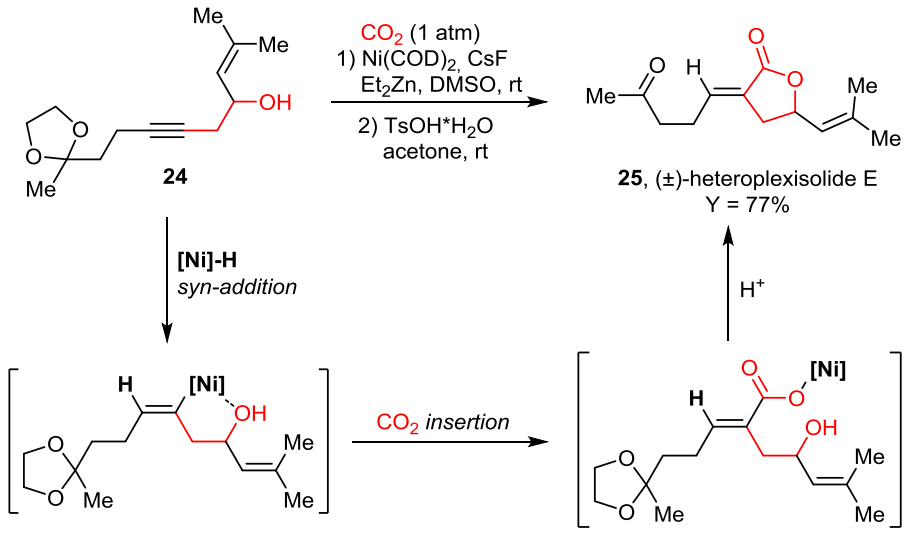

Scheme 10: Nickel-catalyzed hydro-carboxylation of alkynes and following cyclization for the construction of butyrolactone scaffold in heteroplexidolide E.

In the following chapters those two main strategies (namely de-aromatization and ring construction), will be deeply analyzed, for what regards their background and what are some promising research field. New catalytic methodologies for the synthesis of densely functionalized relevant scaffolds will be presented, focusing on mechanistic novelty, efficiency as well as sustainability of the processes. In particular, with regard to this latter point, carbon dioxide will be further discussed, being a promising sustainable source of C(1) building block to be implemented in the synthesis of *fine chemicals*.

2. Aim of the Thesis

The aim of this Doctoral Thesis is the development of new catalytic transformation for efficient and sustainable processes, with the main purpose of easily access the incredible diversity and complexity of bio-relevant compounds. The tuning of general synthetic strategies is a flourishing field in organic chemistry, and can rapidly give access to libraries of products with small to big modifications from a hypothetical lead compound. Whit this in mind, in the modern era of organic synthesis, many aspects are pivotal in the design of a new catalytic procedure, such as reproducibility, generality over the main functional groups, mild conditions and easily accessible starting materials and catalysts. Particularly, another fundamental aspect is the generation of complexity in one single step, to conveniently assemble the scaffold of the class of compounds studied. During the course of my PhD, two main strategies were analyzed to tackle these challenges, namely de-aromatization and ring construction through cyclization.

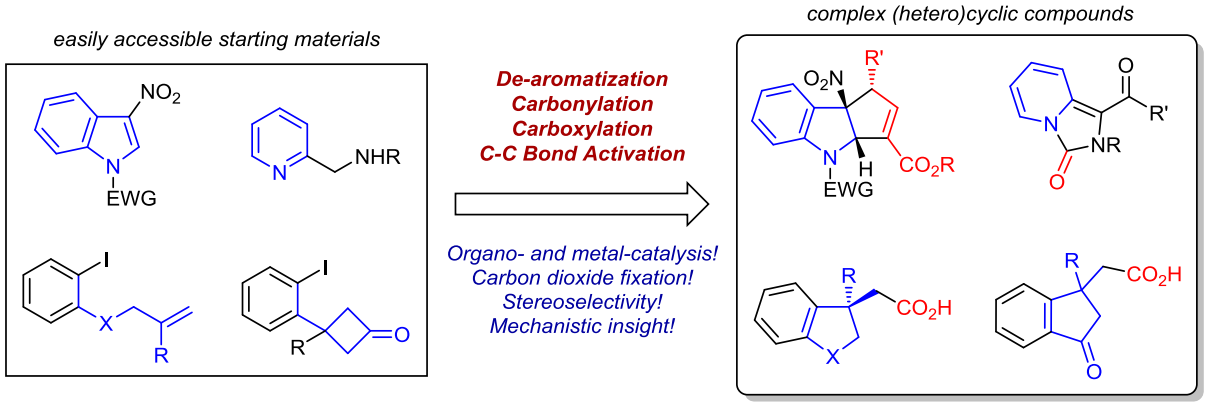

These methodologies have been deeply investigated both in organo- and metal-catalyzed fashions, and conceptually new protocols have been developed. Particular attention has been devoted at the study and optimization of the reaction conditions and catalyst structure, in order to maximize yield and selectivity of the processes as well as minimizing the catalyst loading and using the mildest conditions. The substrate scope has been thoroughly investigated to demonstrate the broad applicability of the proposed transformations, as well as the performance of synthetic elaborations illustrating the usefulness of the developed methods. Despite the conceptual diversity, the proposed protocols are connected by their potential further development into useful tools for the bio-molecule synthetic scenario.

3. Phosphine-Catalyzed Stereoselective Dearomatization of 3-NO_2-Indoles with Allenoates

All the procedures and results here described can be found in:

- A. Cerveri, O. Nieto Faza, C. Silva López, S. Grilli, M. Monari, M. Bandini, "Phosphine-catalyzed stereoselective dearomatization of 3-NO_2-indoles with allenoates" *J.Org.Chem.* **2019**, *84*, 6347-6355.

ABSTRACT

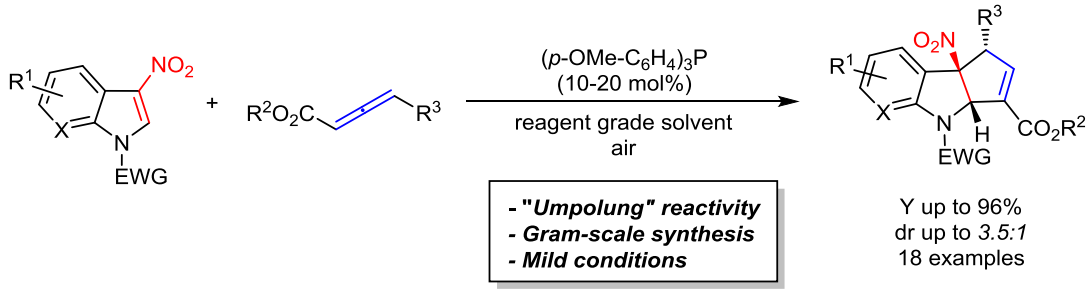

The diastereoselective phosphine-catalyzed dearomative cyclization of 3-NO_2-indoles and allenyl-esters is described. This methodology provides high yields (up to 96%) with good functional group tolerance (18 examples) in the synthesis of densely functionalized indolines, under mild reaction conditions (rt, air, reagent-grade solvent). Computational simulations and labeling experiments revealed the stepwise-[3+2] nature of the mechanism, and a full stereochemical profile of the reaction accounting for the selectivity observed is proposed.

3.1. Background

Catalytic dearomatization reactions represent a powerful tool in the synthetic organic chemistry scenario for convenient conversion of largely available 2D compounds into the more structurally elaborated 3D chemical space.[23] This approach commonly involves electron-rich arenes, such as indole, pyrrole, 2-naphthol and phenol, that react following their intrinsic nucleophilic profile and site-selectivity. Over the past few decades, the indole ring has become a common chemical benchmark to text the efficiency of catalytic systems for

[23] a) A. R. Pape, K. P. Kaliappan, E. P. Kündig, *Chem. Rev.* **2000**, *100*, 2917−2940; b) S. P. Roche, J. A. Porco, *Angew. Chem., Int. Ed.* **2011**, *50*, 4068−4093; c) C.-X. Zhuo, W. Zhang, S.-L. You, *Angew. Chem., Int. Ed*. **2012**, *51*, 12662−12686; d) C. Zheng, S.-L. You, *Chem*. **2016**, *1*, 830−857; e) E. Manoni, A. De Nisi, M. Bandini, *Pure Appl. Chem.* **2016**, *88*, 207−214; f) S. Park, S. Chang, *Angew. Chem., Int. Ed*. **2017**, *56*, 7720−7738; g) J. An, M. Bandini, *Chimia* **2018**, *72*, 610−613.

arene manipulations due to its innate nucleophilicity.[24] This prerogative paralleled the well consolidate role of indolyl cores as platforms to prepare densely functionalized polycyclic fused hetero-scaffolds. Accordingly, a growing interest towards the realization of always more performing and sustainable protocols for the preparation[25] and site-selective manipulation[26] of the indole ring is on-going.

A more recent trend in the field evaluates the possibility to expand significantly the chemical diversity accessible via dearomative protocols by means of the so far less explored "dark side" reactivity of electron-rich arenes, namely electrophilicity.[27] This peculiar "umpolung"-like reactivity is particularly attractive for the indolyl core where, apart from several seminal works based on stoichiometric reagents,[28] the area has remained unexpectedly silent up to recently.[29] In this context, catalysis is opportunely considered the ultimate synthetic tool to boost the impact of the nucleophilic manipulation of indoles in organic synthesis. The "hidden" electrophilic profile of indole faced a unique historical behavior. Upon the pioneering work by Szmuszkovicz in the early 60s, that involved the regioselective condensation of 3-acylindoles **26** with PhMgBr (Scheme 11a),[28a] the approach remained silent for almost 50 years until Liu and coworkers re-discovered the introduction of carboxylic-EWGs (*i.e.* 3-acetylindoles) in the hetero-arene perimeter to "reverse" the indole reactivity. Here, the stereochemical profile of a three-component variant was controlled (Scheme 11b).[30]

[24] a) R. J. Sundberg, in *The Chemistry of Indoles*, Academic Press, New York, **1970**; b) R. J. Sundberg, in *Indoles: Best Synthetic Methods*, Academic Press, New York, **1996**.
[25] A. Palmieri, M. Petrini, *Syntheisis* **2019**, *51*, 829-841.
[26] a) J. Bariwal, L. G. Voskerssensky, E. V. Van der Eycken, *Chem. Soc. Rev.* **2018**, *47*, 3831-3848; b) A. Palmieri, M. Petrini, *Synthesis* **2019**, *51*, 829-841; c) G.-G. Huang, B.-L. Yin, *Adv. Synth. Catal.* **2019**, *361*, 405-425.
[27] a) M. Bandini, *Org. Biomol. Chem.* **2013**, *11*, 5206−5212; b) C. C. J. Loh, D. Enders, *Angew. Chem., Int. Ed.* **2012**, *51*, 46−48.
[28] a) J. J. Szmuszkovicz, *Org. Chem.* **1962**, *27*, 511−514; b) R. J. Sundberg, *J. Org. Chem*. **1965**, *30*, 3604−3610.
[29] Caramenti, P.; Nicolai, S.; Waser, J. *Chem. Eur. J.* **2017**, *23*, 14702−14706.
[30] L. Wang, Y. Shao, Y. Liu, *Org. Lett.*, **2012**, *14*, 3978-3981.

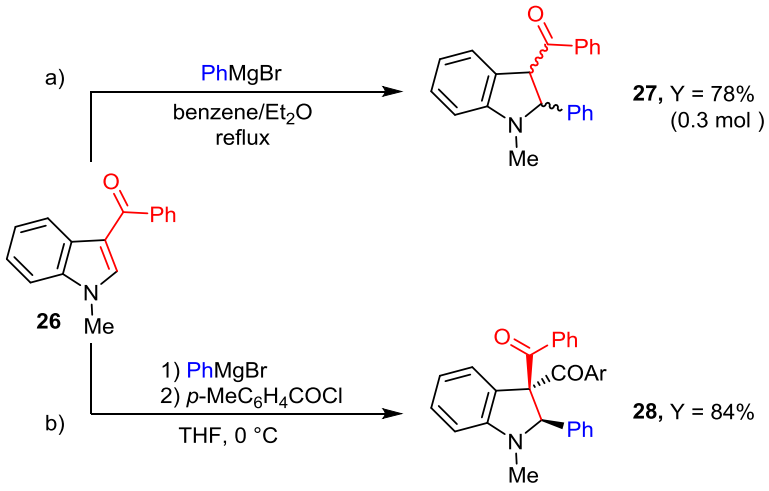

Scheme 11: a) Szmuszkovicz pioneering research on the *umpolung* de-aromatization of indoles; b) and modern reinterpretation of the process in a diastereoselective fashion.

However, across the years, the combination of EWGs (ketones, esters, NO_2) at C(2)- and C(3)-positions and leaving groups (*i.e.* OH, OMs, OTs, SO_2R) at the N(1)-site of the indole core was extensively investigated resulting in the development of several regioselective Michael type- as well as S_N2-type nucleophilic addition processes.[31] Those strategies enabled the realization of important synthetic shortcut towards the formation of C-C and C-X bonds via inter- as well as intramolecular processes. Additionally, final rearomatization or dearomatization of the pyrrolyl core can occur opening unprecedented scenario to access 3D chemical space from the 2D ones.

The exploitation of the strong electron-withdrawing nitro-group to reverse the natural indole reactivity[32] is probably the most effectively used approach in catalytic and stereoselective methodologies. In particular, C(3)-NO_2-indoles **29** are commonly employed resulting into the construction of cyclic compounds through annulation processes. In many cases, an additional EWG group located at the N(1)-position is needed to guarantee satisfying reactivity of the indolyl core. The process offers several possibilities for the stereoselectivity fine-tuning such as LA or BA-type activation of the NO_2-indole group and electrophilic as well as nucleophilic activation of the reaction partner.

The field was pioneered by Arai and Awata in the 2014 that reported the first example of CADA (Catalytic Asymmetric De-Aromatization reaction) with *umpolung* reactivity on the

[31] a) T. Nagayoshi, S. Saeki, M. Hamana, *Heterocycles* **1977**, *6*, 1666-1674; b) W. R. Ashcroft, M. G. Bead and J. A. Joule, *J. Chem. Soc., Chem. Commun*. **1981**, 994-995; c) M. M. Cooper I. M. Lovell, J. A. Joule, *Tetrahedron Lett*. **1996**, *37*, 4283-4286; d) E. T. Pelkey, T. C. Barden, G. W. Gribble, *Tetrahedron Lett*. **1999**, *40*, 7615-7619.
[32] a) M. Makosza, *Chem. Soc. Rev.* **2010**, *39*, 2855-2868; b) M. Makosza, *Synthesis*, **2011**, 2341-2356.

indole unit by means of the nitro-group at the C(3). The [3+2] cycloaddition was performed under Lewis Acid (LA) catalysis, using copper triflate to activate a glycine imino ester **30a** (Scheme 12).[33] The protocol was subsequently extended to alanine analogous **30b** by Stanley and Gerten under similar approach.[34]

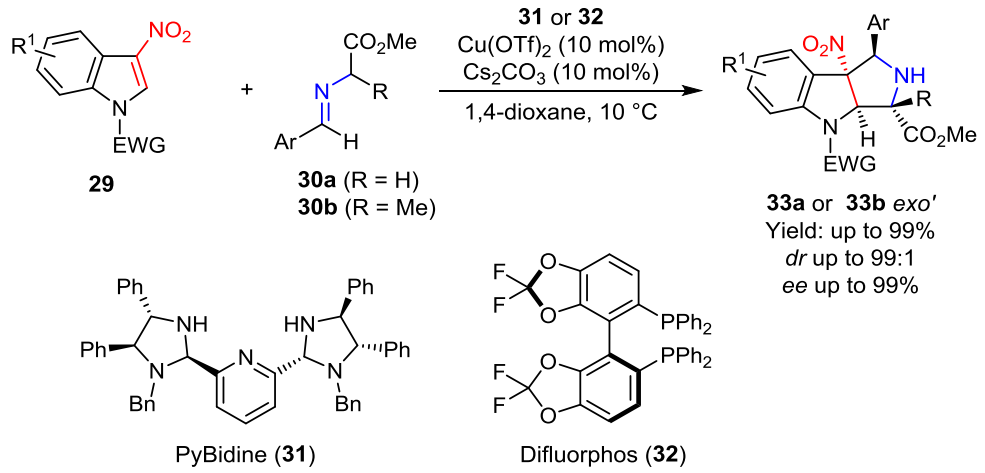

Scheme 12: Copper-catalyzed formal [3+2] dearomative cycloaddition between 3-NO_2-indoles and glycine or alanine imino-derivatives.

Almost concomitantly, another elegant dearomatization reaction of *N*-phenylsulfonyl-3-NO_2 indoles **29a** was reported by Trost and coworkers.[35] The [3+2]-type cycloaddition performed under phosphoramidite-[Pd(0)] activation of the allyl acetate **34** to give the trimethylenemethane dipolar intermediate **A**. The chiral ligand **14** provided the bicyclic nitro-indoline **35** with a moderate enantiomeric excess (66%, Scheme 13). Interestingly, although only a couple of examples of indole dearomatizations were reported, the strategy could be effectively applied to other electron-poor arenes, like 5-nitroquinolines.

[33] A. Awata, T. Arai, *Angew. Chem. Int. Ed.* **2014**, *53*, 10462-10465.
[34] A. L. Gerten, L. M. Stanley, *Org. Chem. Front.* **2016**, *3*, 339-343.
[35] B. M. Trost, V. Ehmke, B. M. O'Keefe, D. A. Bringley, *J. Am. Chem. Soc.* **2014**, *136*, 8213-8216.

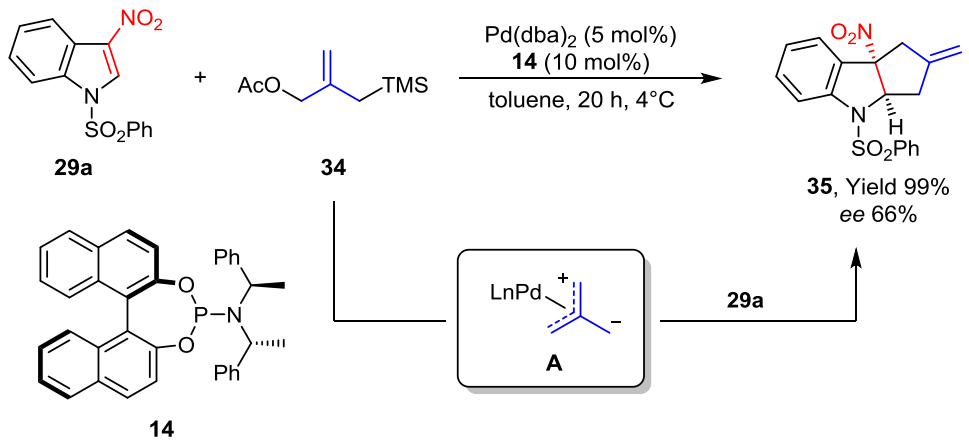

Scheme 13: Pd-catalyzed [3+2] cycloaddition through generation *in situ* of a dipolar allyl-Pd species.

The use of Pd-based ambipolar intermediates was subsequently adopted by using strained functionalized three-member ring precursors with achiral as well as chiral-Pd catalysts. In particular, highly diastereo- as well as enantioselective [3+2]-cycloadditions were documented with vinylepoxides (**36a**)[36a] vinylaziridines (**36b**)[36b] and vinylcyclopropanes (**36c**, Scheme 14).[36d]

[36] a) Q. Cheng, F. Zhang, Y. Cai, Y.-L. Guo, S.-L. You, *Angew. Chem. Int. Ed.* **2018**, *57*, 2134-2138; b) J.-J. Suo, W. Liu, J. Du, C.-H. Ding, X.-L. Hou, *Chem. Asian J.* **2018**, *13*, 959-936; c) J.-Q. Zhang, F. Tong, B.-B. Sun, W.-T. Fan, J.-B. Chen, D. Hu, *J. Org. Chem.* **2018**, *83*, 2882-2891; d) M. Sun, Z.- Q. Zhu, L. Gu, X. Wan, G.-J. Mei, F. Shi, *J. Org. Chem.* **2018**, *83*, 2341-2348.

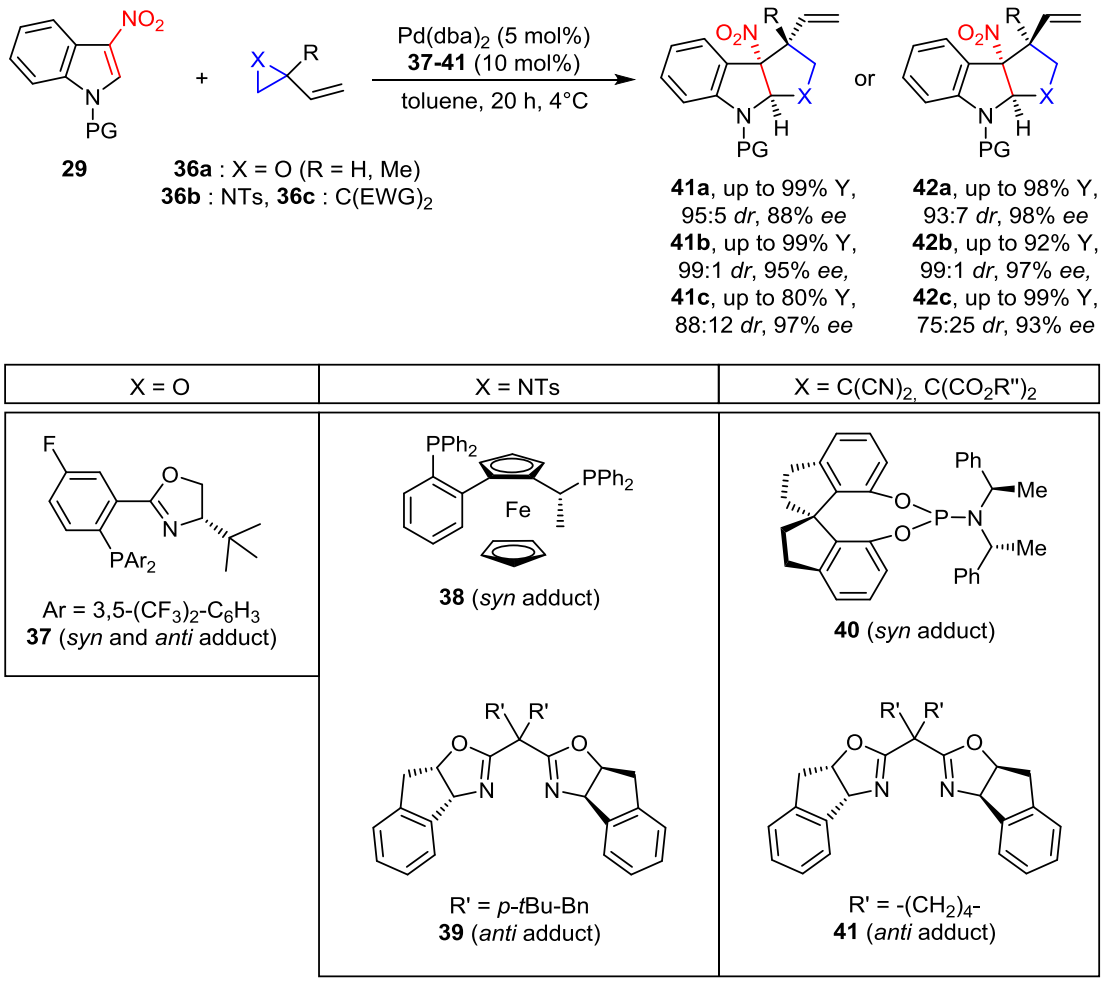

Scheme 14: Stereodivergent and complementary strategies for the enantioselective cyclization of indole with strained vinyl-cycles.

Interestingly the different methodologies gave access to both the possible diastereoisomers, in accordance with the ligand and the conditions employed. Among them, the case-study proposed by You and Guo faced an interesting solvent-based diastereodivergency. In particular, when toluene was used as the solvent the *syn* adduct was mainly formed, while in acetonitrile, the *anti* isomer was predominant under invariant conditions.

A different approach for the metal-catalyzed enantioselective dearomatization of electron-poor indoles was proposed in the 2015 by Yuan and coworkers.[37] In this highly selective [3+2]-cyclization reaction a bis(oxazoline)-Zn(OTf)$_2$ complex promoted the activation of 3-isothiocyanato oxindoles **43**, enabling the selective condensation with **29b** and delivering the densely functionalized polycyclic spirooxindoles **44**. From mechanistic experiments and nonlinear effect studies a double role of the catalyst was revealed. While the Zn(II) core acts

[37] J.-Q. Zhao, Z.-J. Wu, M.-Q. Zhou, X.-Y. Xu, X.-M. Zhang, W.-C. Yuan, *Org. Lett.* **2015**, *17*, 5020-5023.

as Lewis Acid for the activation of the nitro moiety, the linking NH group was proven fundamental to trigger the C(3)-attack to the oxindole (Scheme 15).

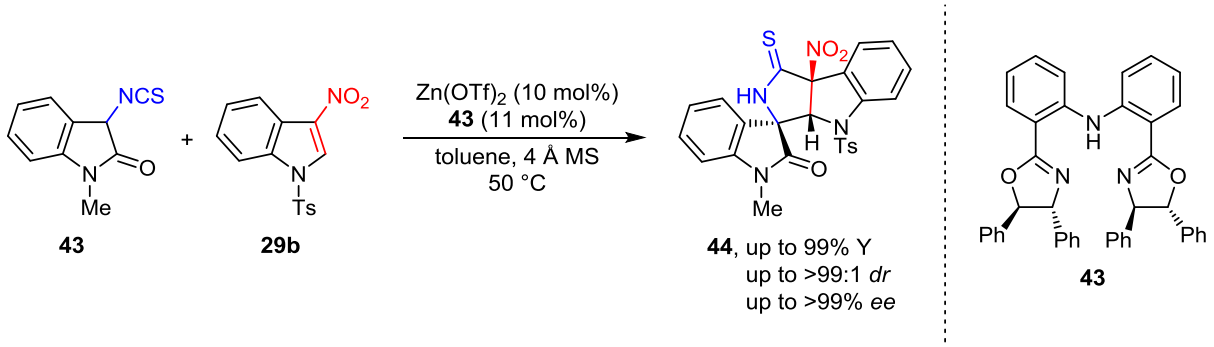

Scheme 15: Highly stereoselective Zn-catalyzed construction of spirocyclic fused scaffolds via 3-NO_2-indole dearomatization.

Moving to a metal-free chemical space, the enantioselective [4+2]-cycloaddition between 3-nitroindoles **29** and *in situ* formed chiral trienamine **48** was elegantly reported by Jørgensen and coworkers in the presence of prolineurea organocatalyst **47**.[38] From a mechanistic view-point, the initial formation of the dearomatized polycyclic indoline led to a fast elimination of nitrous acid to deliver the final densely functionalized dihydrocarbazoles **49** (Scheme 16). The overall stereochemical profile of the protocol was attributed to the synergic action of the proline moiety (formation of chiral trienamine **48**) and to the thiourea group (hydrogen-bond activation of NO_2 group). The possibility to extend the substrate scope to 3-nitrobenzothiophenes **45** was also documented.

[38] Y. Li, F. Tur, R. P. Nielsen, H. Jiang, F. Jensen, K. A. Jørgensen, *Angew. Chem. Int. Ed.* **2016**, *55*, 1020-1024.

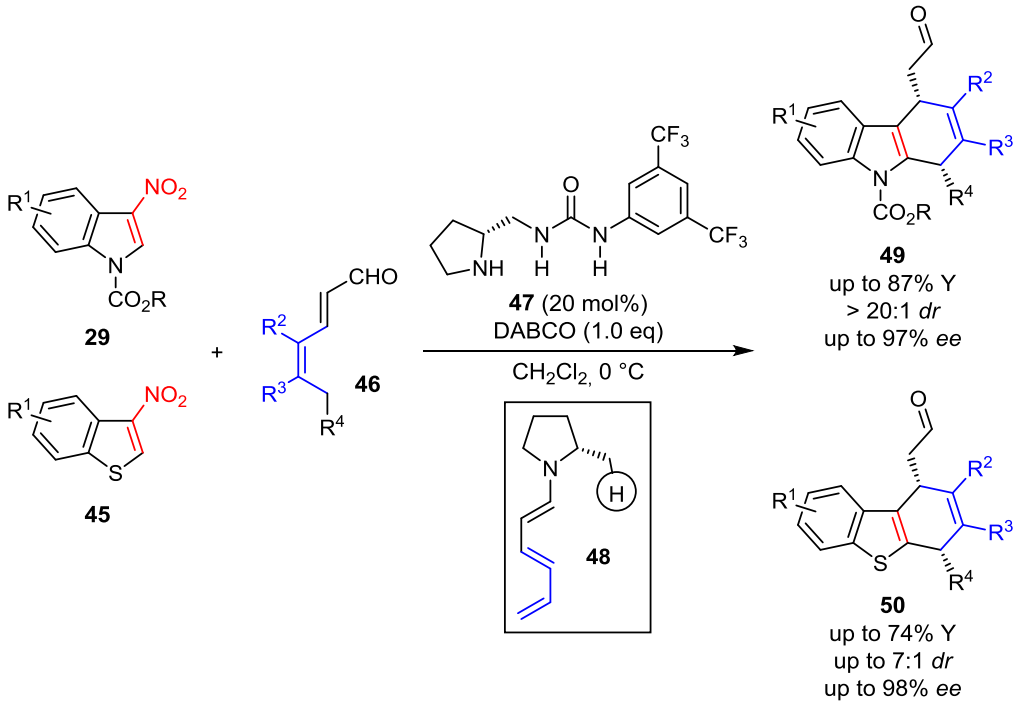

Scheme 16: Enantioselective organo-catalyzed [4+2] cycloaddition of chiral trienamine.

Subsequently a different enantioselective organocatalyzed [4+2]-dearomative cyclization was proposed by Yuan and coworkers, by combining the Nazarov reagent **51** and 3-nitroindole **29** to form fully dearomatized hydrocarbazole skeletons **53**, using a chinchona-thiourea bi-functional organocatalyst **52** (Scheme 17).[39]

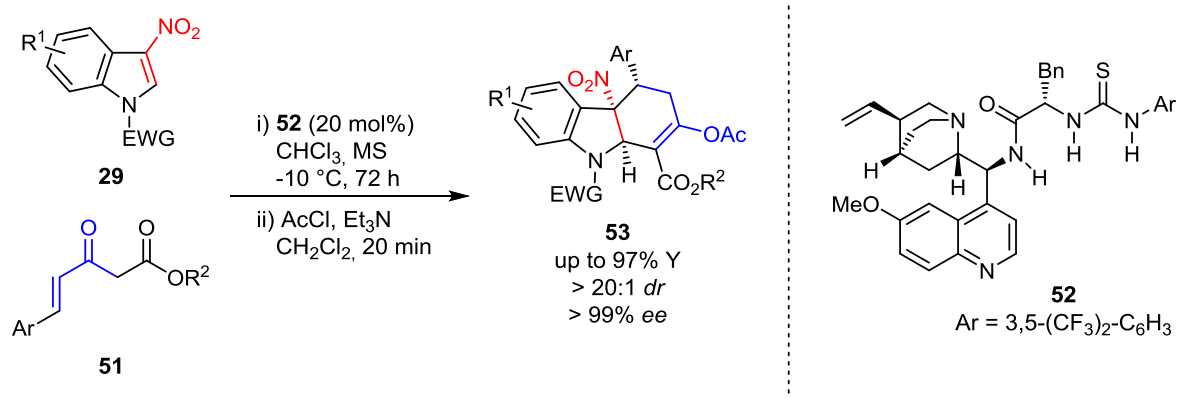

Scheme 17: Bi-functional chinchona-thiourea catalyst for the dearomative [4+2] cycloaddition of 3-NO_2-indoles and Nazarov reagent.

Given those selected examples, becomes clear the actual effectiveness of this "umpolung" strategy for the synthesis of densely functionalized polycyclic 3D structures, and further investigations in the field are required to increase the potential applications of this chemistry.

[39] D.-F. Yue, J.-Q. Zhao, X.-Z. Chen, Y. Zhou, X.-M. Zhang, X.-Y. Xu, W.-Cheng Y. *Org. Lett.* **2017**, *19,* 4508-4511.

3.2. Aim of the Project

In line with the research group interests addressing the catalytic manipulation of arenes,[40] was previously introduced the electrophilic activation of electron-rich allenes (i.e., allenamides) as a valuable tool for the dearomatization of indoles via conventional reactivity profiles. Interestingly, the use of allenes in umpolung-type dearomatizations of indoles was still unknown. The idea was that by switching from electron-rich to electron-deficient allenes (i.e., allenoates)[41] it could be possible to match the intrinsic electrophilic character of nitroindoles with the well-known nucleophilic activation of allenoates.[42] Eventually, an interesting [3 + 2]-type dearomative cycloaddition could occur, leading to densely functionalized C(2)/C(3)-fused polycyclic indoline derivatives **57** (Scheme 18).

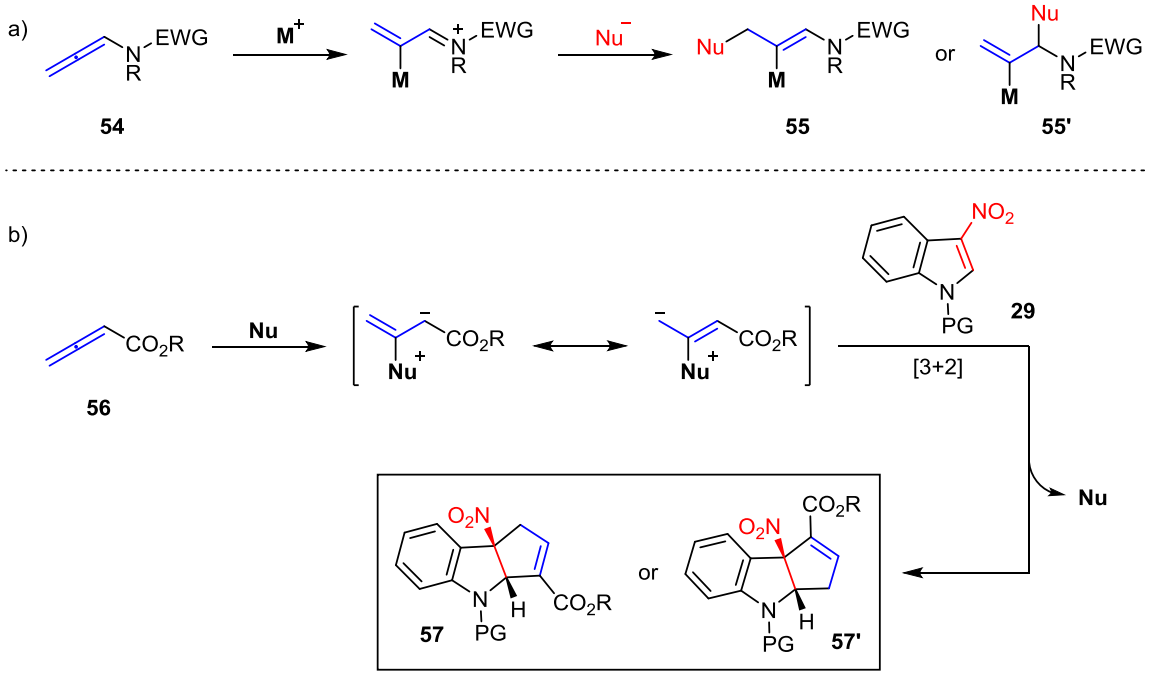

Scheme 18: a) Electrophilic activation mode of allenamides; b) Nucleophilic activation of allenoate for the generation of a reactive dipolar intermediate.

However, numerous regiochemical (α-addition vs γ-addition, **57** vs **57'**) as well as stereochemical issues can theoretically challenge the process, making the design and optimization of both the catalytic systems and the reaction parameters a pivotal aspect of the whole methodology.

[40] a) Q.-Q. Yang, M. Marchini, W.-J. Xiao, P. Ceroni, M. Bandini, *Chem. Eur. J.* **2015**, *21*, 18052−18056; b) J. An, A. Parodi, M. Monari, M. C. Reis, C. S. Lopez, M. Bandini, *Chem. Eur. J.* **2017**, *23*, 17473−17477.
[41] a) Q.-Y. Zhao, Z. Lian, Y. Wei, M. Shi, *Chem. Commun*. **2012**, *48*, 1724−1732; b) Z. Wang, X. Xu, O. Kwon, *Chem. Soc. Rev*. **2014**, *43*, 2927−2940.
[42] a) C. Zhang, X. Lu, *J. Org. Chem.* **1995**, *60*, 2906−2908; b) Z. Xu, X. Lu, *Tetrahedron Lett.* **1997**, *38*, 3461−3464; c) Z. Xu, X. Lu, *J. Org. Chem.* **1998**, *63*, 5031−5041.

3.3. Discussion and Results

From an extensive survey of reaction conditions, optimal reaction parameters for the condensation of allenoate **56a** with *N*-Boc-3-NO_2-indole **29c** (model substrates) were initially found in the use of Ph_3P (20 mol % as the catalyst), reagent-grade toluene, and rt/air (Table 1, entry 13). Notably, the exclusive formation of the diastereomerically enriched compound **57ac** (65% yield) was recorded.

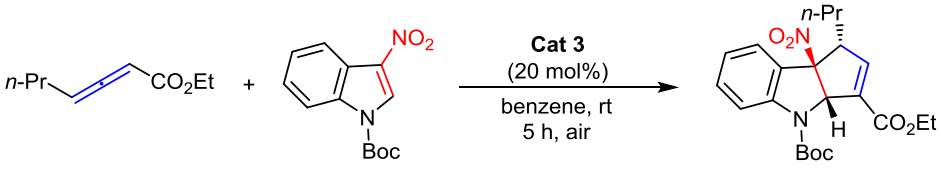

56a **29c** (+/-)-**57ac**

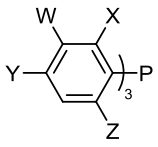

Cat 1: W/XYZ = H
Cat 2: W = H, X/Y/Z = OMe
Cat 3: W/X/Z = H, Y = OMe
Cat 4: X = OMe, W/Y/Z = H
Cat 5: X = F, W/Y/Z = H
Cat 6: W = Me, X/Y/Z = H

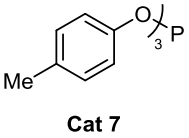

Cat 7

$(nBu)_3P$
Cat 8

Cat 9

Entry	Deviation from optimal	Yield **57** (%)[b]	Dr[c]
1		85	3.5:1
2	**Cat 1**	74	3:1
3	**Cat 2**	NR	
4	**Cat 4**	35	2.5:1
5	**Cat 5**	11	3.5:1
6	**Cat 6**	20	3.5:1
7	**Cat 7**	NR	
8	**Cat 8**	48	3.5:1
9	**Cat 9**	NR	
10	IPr*HCl/K_2CO_3	NR	
11	0 °C	55	4:1
12	65 °C	63	2.5:1
13	**Cat 1**, toluene, 20 h	65	2:1
14	**Cat 1**, CH_2Cl_2, 12 h	33	ND
15	**Cat 1**, MeCN, 12 h	37	ND
16	**Cat 1**, *n*-Hex, 12 h	39	2.5:1
17	**Cat 1**, $PhCF_3$, 12 h	41	1.5:1

18	**Cat 3** (10 mol%)	55	3.5:1

Table 1: [a] Optimal reaction conditions: **56a** (0.15 mmol), **29c** (0.1 mmol), in benzene (0.5 mL). [b] Determined after flash chromatography. [c] Determined by ^{1}H NMR on the reaction crude. NR = no reaction. ND: not determined.

Deviations from these parameters caused a remarkable drop in performance of the whole protocol. A screening of several P and N-based nucleophilic catalysts (**Cat 1-9**) revealed the electron-rich (*p*-$MeOC_6H_4)_3P$ phosphine (**Cat 3**) as the optimal catalyst (20 mol %, entry 1), delivering **57ac** in 85% yield and 3.5:1 diastereoselectivity. Differently, less nucleophilic (*o*-$FC_6H_4)_3P$ phosphine (**Cat 5**, entry 5) and phosphite **Cat 7** led to disappointing outcomes. Besides electronic aspects, steric constraints also showed some peculiarities on the reaction profile as well. In fact, ortho-substituted and meta-substituted phosphines **Cat 2/4/6** proved less competent with respect to **Cat 3**. Variations on the reaction temperature did not affect significantly the overall process (entries 11 and 12), and benzene proved to be superior over a range of solvents (i.e., CH_2Cl_2, *n*-Hex, toluene, $PhCF_3$) in the presence of PPh_3 as the catalyst (entries 13-17). Therefore, optimal reaction conditions were applied to the condensation of a range of allenoates (**56b-f**) and differently substituted C(3)-NO_2-indoles (**29d-m**, Scheme 19). In terms of allenoate tolerance, it is worth mentioning that substitutions at the ester (EWG = CO_2Bn, CO_2tBu, and $CO_2(3,5\text{-}(Me)_2C_6H_3)$) moiety proved competent in the model protocols, delivering the corresponding [3 + 2]-cycloadducts from moderate to excellent yield and diastereoselection up to 3.5:1. The γ-substitution pattern was then analyzed, and although the γ,γ'-$(Me)_2$ allenoate **56e** did not take part in the process, the mono-substituted congener **56d** (R = H) delivered the desired product in a satisfactory 72% isolated yield. Additionally, a large tolerance toward indole functionalization resulted from a screening of 4-, 5-, and 6-substituted-3-NO_2-indoles (**29d-j**). Indoles containing both EDG and EWG groups reacted satisfyingly, delivering the corresponding cycloadducts (**57ad-aj**) in moderate to excellent yield (51−92%) and moderate diastereoselectivity (up to 3.5:1). Analogously, the 7-azaindole **29m** worked nicely in the [3 + 2]-cycloaddition processes, producing the dearomatized compounds **57am**, **57cm**, and **57fm** in 96%, 71%, and 91% yield, respectively. Last, different carbamates were also examined as potential protecting groups at the N(1) position (**29k** and **29l**), and no significant variations in terms of isolated yield as well as stereoinduction were observed.

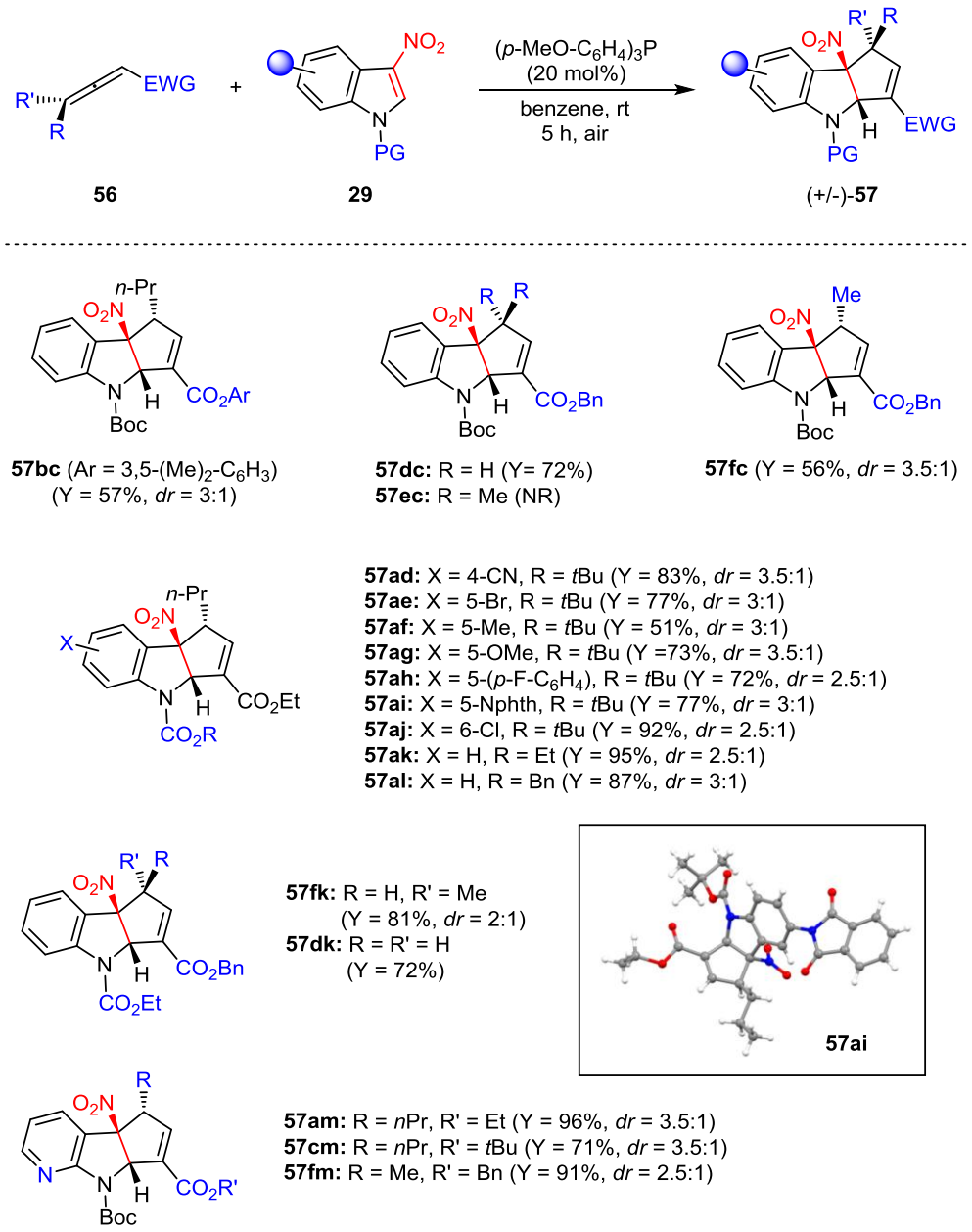

Scheme 19: Substrate scope for the phosphine catalyzed dearomative [3+2] cycloaddition.

Stereochemical assignment on the cycloadduct was initially performed by NOE-^{1}H NMR investigations on **57ac**, providing a *trans* correlation of the bi-cyclic junction and the stereogenic center installed into the formed γ-carbon of the allenyl unit. This evidence was also supported by single-crystal X-ray analysis performed on compound **57ai** (crystallization from *n*-pentane/DCM solution, in collaboration with Prof. Magda Monari, University of Bologna). These results suggest that the reaction mechanism may not be a simple concerted [3 + 2] dipolar cycloaddition, leaving open the question on how is determined the diastereoselectivity. The reaction mechanism also must be compatible with the rather mild conditions employed, untypical for thermal pericyclic processes. With this purpose was

carried out a thorough mechanistic exploration of the possible pathways for this dearomatization reaction (Scheme 20) at the M06-2X/6-31+G(d,p) level (in collaboration with Prof. Carlos Silva Lopez, University of Vigo).

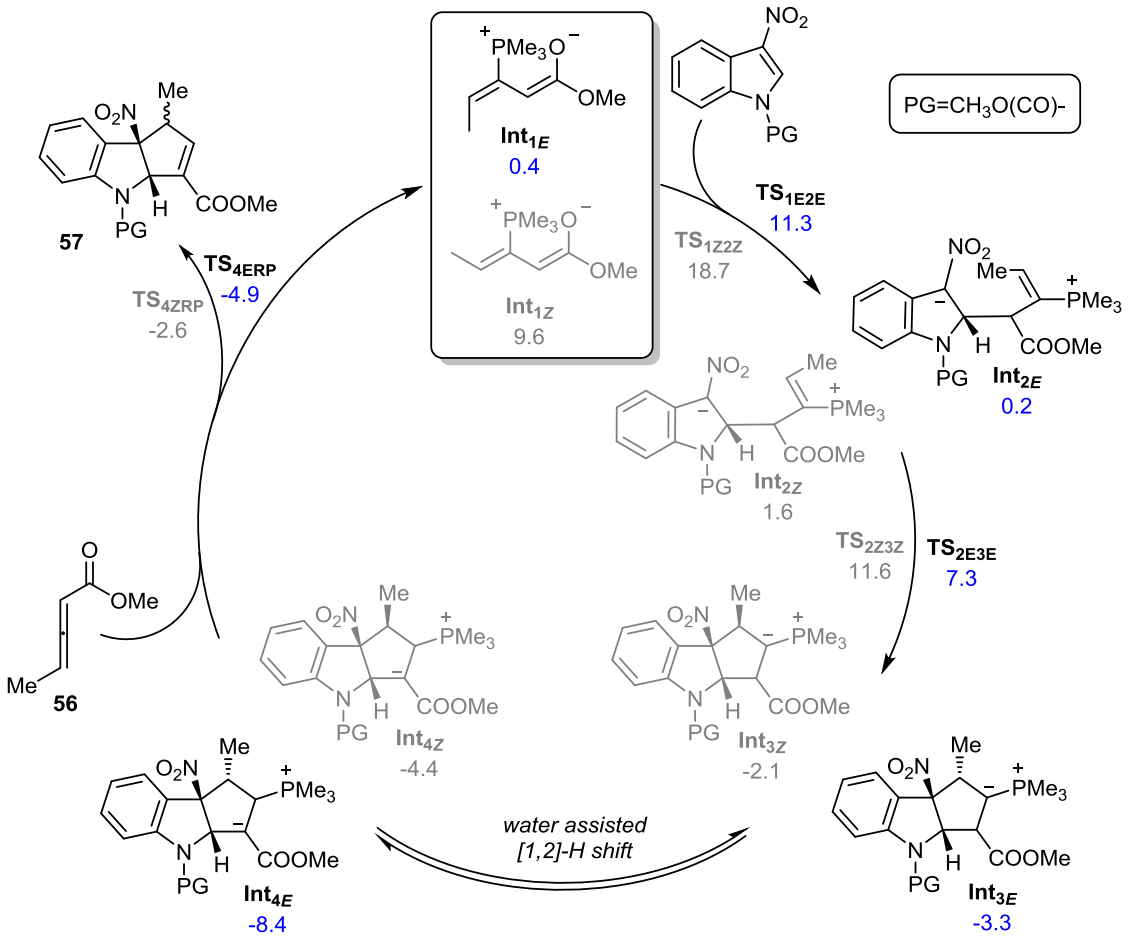

Scheme 20: Proposed mechanistic hypothesis for the catalytic system optimized.

The general mechanism operates mostly as expected: the allene is nucleophilically activated by the phosphine, yielding intermediate **Int$_1$**, which undergoes a subsequent dearomative cyclization. The details of the cyclization and the source of diastereoselection, however, are less obvious. First, was considered that the formation of geometric isomers upon nucleophilic activation of the allenoate followed by a concerted [3 + 2] dipolar cycloaddition could account for the observed chemistry. All attempts to locate the transition state for the concerted cycloaddition however were unsuccessful and ended in structures compatible with a stepwise pathway. Furthermore, the drastic stability difference (more than 9 kcal/mol) between the two geometric isomers of the activated allenoate, **Int$_1$**, suggested that **Int$_{1Z}$** may not participate in the reaction at all. The energy barriers associated with the less stable activated allenoate confirmed this (structures in gray in Scheme 20). Once **Int$_{1Z}$** was excluded from this

chemistry, was explored the possibility of interconversion between **Int_{2E}** and **Int_{2Z}** (through a simple E → Z isomerization step) to account for the formation of the minor stereoisomer, but the computed barrier was very high (53.8 kcal/mol). Interestingly **Int_{2E}** is conformationally active, so it was studied if the conformational equilibrium at this intermediate could justify the formation of diastereomers. The study of this equilibrium provides a justification not only to the formation of a diastereomer as minor product but also to the intriguing effect of seemingly distant groups in this selectivity. The conformational rotations depicted in Scheme 21 are strongly coupled.

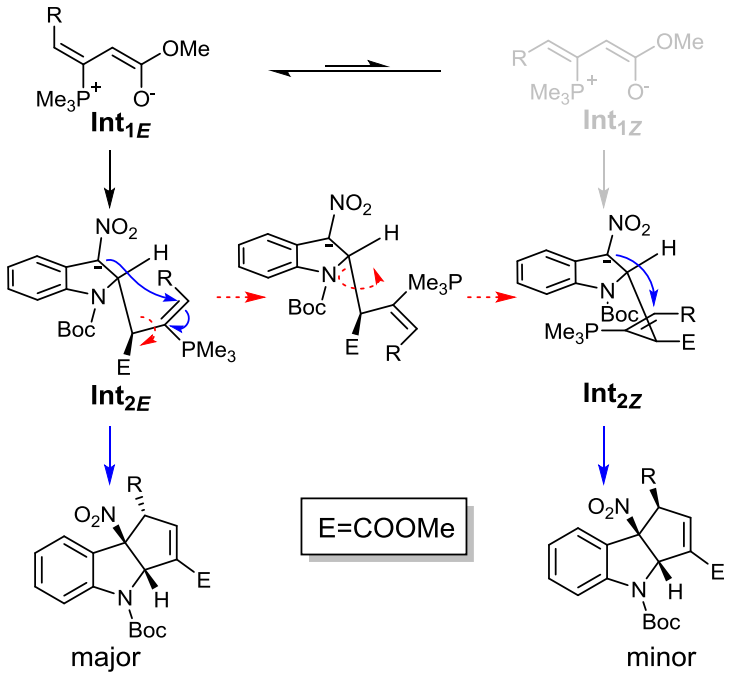

Scheme 21: Insight of the possible reason behind the diastereoselectivities observed.

Both dihedral angles rotate in concert to avoid strong contacts between the acyclic branch (featuring bulky groups like the phosphine) and the indole protecting group or the nitro group. This motion was estimated to have a kinetic cost of about 10 kcal/mol. This is not only compatible with the reaction conditions but also competitive with the ring closure to yield **Int_{3E}**. It thus seems that **Int_{2E}** is a key intermediate where a mechanistic bifurcation occurs. Most molecules arriving to **Int_{2E}** complete the cyclization to yield the major diastereoisomer, but a fraction of molecules undergoes conformational scrambling before the second C-C bond can be formed, and this leads to formation of the minor diastereomer. Since the bond rotation is hindered by the volume of the phosphine and its steric contacts with groups at N1 and C3, increasing the size of these groups should therefore result in increased diastereoselection. This effect is observed in **57fc-fk** and **57ac-ak** pairs as illustrated in Scheme 19. After the stepwise

[3 + 2] cycloaddition a key [1,2]-H shift occurs to form **Int_{4e}**. This step was initially assumed to occur in an intramolecular fashion, but the associated activation barriers computed for this process were extremely high in energy (more than 45 kcal/mol). With this information was then considered that perhaps a water-mediated [1,2]-H shift could be the operating mechanism.[43] Calculations with an explicit water molecule provided energy barriers compatible with the reaction conditions (less than 9.0 kcal/mol). This mechanism was also confirmed via deuterium-labeling experiments as illustrated in Scheme 22. This water-mediated [1,2]-H shift leaves the reacting molecule ready for the departure of the catalyst through a very facile transition state (**TS_{4ERP}**, with an activation barrier of less than 2 kcal/mol).

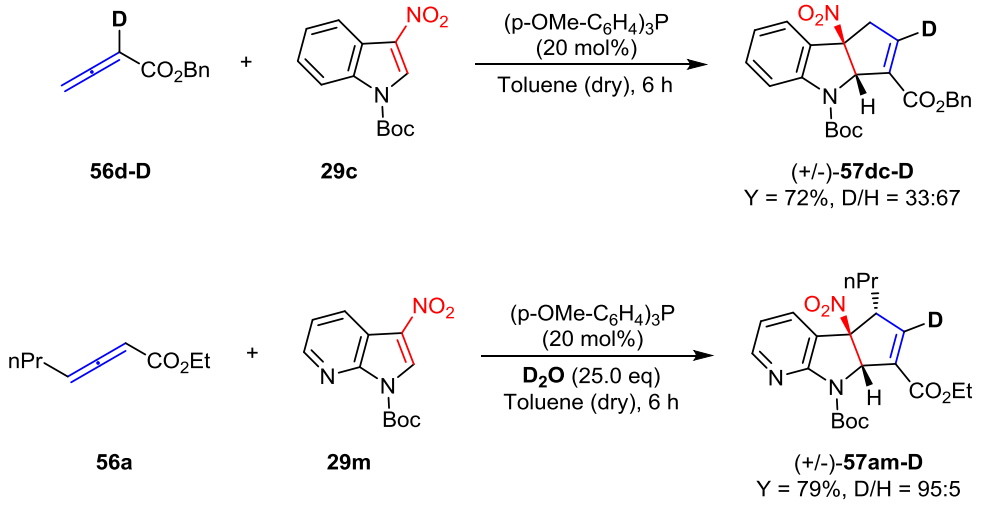

Scheme 22: Labeling experiments with deuterium modified allenoate (up) and D_2O as a free source of deuterium (down).

At this point the synthetic flexibility of the cyclo-fused indoline was tested with different useful transformations. In particular, regioselective reduction of the C=C bond was effectively realized by means of $NaBH_4$ as well as NO_2 group with Zn/TMSCl systems, respectively (Scheme 23a). The corresponding saturated cyclopentyl derivative **58am** was isolated in 93% yield as a 9:3:3:1 mixture of diastereoisomers. The reduction of the nitro-group worked smoothly, providing the amino compound in 97% yield that was subsequently acetylated to compound **59am** in 75% yield (two-steps) and 6.7:1 dr. Finally, the N-Boc protecting group was efficiently removed under acid treatment (i.e., HCl 4N) of compound **57am**, resulting in the N(1)-H indoline **60am** in 85% yield. The aza-containing heterocycle **29m** was also

[43] Y. Xia, Y. Liang, Y. Chen, M. Wang, L. Jiao, F. Huang, S. Liu, Y. Li, Z.-X. Yu, *J. Am. Chem. Soc*. **2007**, *129*, 3470−3471.

employed to verify the extendibility of the protocol to a gram-scale synthesis. Interestingly, when 4 mmol of **29m** and 6 mmol of **56a** were treated with **Cat 3** (10 mol %), the corresponding indoline **57am** was isolated in 93% yield (ca. 1.5 gr) with no erosion on the stereochemical profile (Scheme 23b).

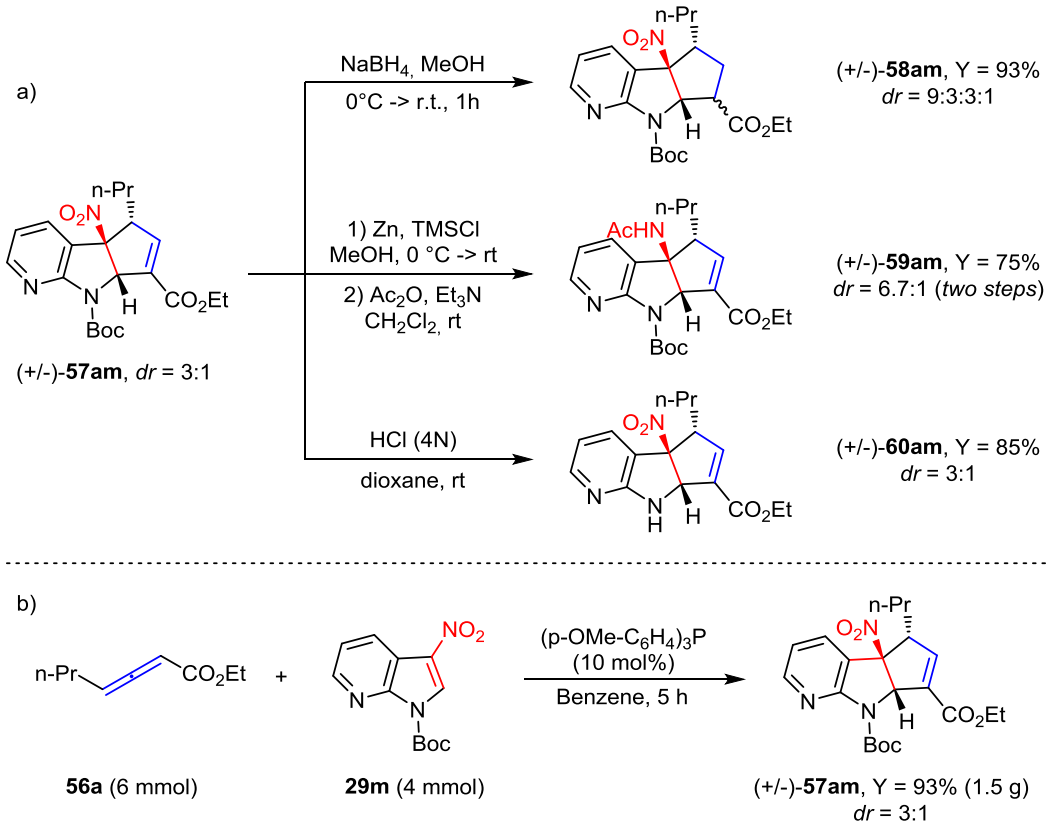

Scheme 23: a) Synthetic transformation of the compound **57am**; b) Gram-scale reaction.

3.4. Conclusion

A new protocol for the stereoselective phosphine-catalyzed dearomatization of 3-NO_2-indoles with allenoates is presented. The methodology enabled the realization of a number of polycyclic-fused indoline derivatives in high yields and moderate to good stereoselectivity. The hetero-cyclic compounds can be produced on gram-scale without varying the reaction conditions, and they are versatile platforms for late-stage selective modification. Moreover, suitability of the metal-free approach for the gram-scale synthesis and full mechanistic/stereochemical rational via DFT calculations were also provided.

3.5. General Procedures and Product Characterization

3.5.1. Materials and Methods

^{1}H NMR spectra were recorded on a Varian 400 (400 MHz) spectrometer. Chemical shifts are reported in ppm from TMS with the solvent resonance as the internal standard (deuterochloroform 7.24 ppm). Data are reported as follows: chemical shift, multiplicity (s = singlet, d = doublet, t = triplet, q = quartet, sext = sextet, sept = septet, p = pseudo, b = broad, m = multiplet), coupling constants (Hertz). ^{13}C NMR spectra were recorded on a Varian 400 (100 MHz) spectrometer with complete proton decoupling. Chemical shifts are reported in ppm from TMS with the solvent as the internal standard (deuterochloroform 77.0 ppm). Monodimensional NOE experiment (400 MHz, $CDCl_3$, 25 °C) was performed by using a DPFGSE-NOE sequence with a 50 Hz pulse and a mixing time of 1.5 s. Irradiation at the frequency of proton H^{11} (6.44 ppm) showed a strong positive NOE response of the H^4 frequency, confirming the sin-relationship. Weaker NOE effects were also observed for the vinylic H^5 proton. GC-MS spectra were taken by EI ionization at 70 eV on a Hewlett-Packard 5971 with GC injection. They are reported as m/z (relative. intensity). LC-electrospray ionization mass spectra were obtained with an Agilent Technologies MSD1100 single-quadrupole mass spectrometer. Chromatographic purification was done with 240−400 mesh silica gel. Other anhydrous solvents were supplied by Sigma-Aldrich in Sureseal bottles and used without any further purification. Commercially available chemicals were purchased from Sigma-Aldrich, Stream, and TCI and used without any further purification. Melting points were determined with a Bibby Stuart Scientific Melting Point Apparatus SMP 3 and are not corrected. An Agilent Technologies LC/MSD Trap 1100 series (nebulizer 15.0 PSI, dry gas 5.0 L/min, dry temperature 325 °C, capillary voltage positive scan 4000 mA, capillary voltage negative scan 3500 mA) was used. Preparation of α-allenyl esters, **56**[44] N-Boc-3-nitroindoles **29**[45] and nitroindoles **29k** and **29l**[46] was accomplished following the reported procedures.

[44] Y. Liu, M. Daka, M. Bandini, *Synthesis* **2018**, *50*, 3187−3196.
[45] Q. Cheng, F. Zhang, Y. Cai, Y.-L. Guo, S.-L. You, *Angew. Chem., Int. Ed*. **2018**, *57*, 2134−2138.
[46] G. W. Gribble, E. T. Pelkey, W. M. Simon, H. A. Trujillo, *Tetrahedron* **2000**, *56*, 10133−10140.

tert-Butyl 4-Cyano-3-nitro-1H-indole-1-carboxylate (**29d**)

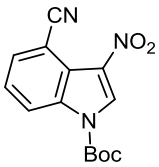

Yellow solid, **M.p.** = 178.2−179.4 °C. **^{1}H NMR** (400 MHz, $CDCl_3$) δ = 8.60 (s, 1H), 8.55 (d, J = 8.6 Hz, 1H), 7.77 (dd, J = 7.5, 0.8 Hz, 1H), 7.51 (t, J = 8.1 Hz, 1H), 1.70 (s, 9H). **^{13}C NMR** (100 MHz, $CDCl_3$) δ = 147.2, 134.9, 132.8, 131.7, 130.0, 126.3, 120.4, 120.0, 117.1, 104.4, 88.2, 27.9. (3C). **LC-MS** (m/z): $[M+H]^+$ = 288.2. **Anal. Calc.** for $C_{14}H_{13}N_3O_4$ (287.28): C, 58.53; H, 4.56. Found: C, 58.42; H, 4.45.

tert-Butyl 5-(4-Fluorophenyl)-3-nitro-1H-indole-1-carboxylate (**29h**)

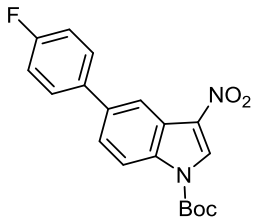

Orange solid, **M.p.** = 166.2−169.0 °C. **^{1}H NMR** (400 MHz, $CDCl_3$) δ = 8.50 (s, 1H), 8.37 (d, J = 1.2 Hz, 1H), 8.22 (d, J = 8.8 Hz, 1H), 7.59 (dt, J = 8.6, 3.6 Hz, 3H), 7.12 (t, J = 8.7 Hz, 2H),1.68 (s, 9H). **^{13}C NMR** (100 MHz, $CDCl_3$) δ = 162.5 (d, J =246.3 Hz), 147.9, 146.7 (2C), 137.8, 136.6 (d, J = 3.0 Hz), 129.0 (d, J = 8.3 Hz), 128.9, 128.2, 125.8, 121.9, 118.6, 115.8, 115.6 (d, J = 21.2 Hz), 86.8, 85.0, 27.9 (3C). **^{19}F NMR** (376 MHz, $CDCl_3$) δ = −115.39. **LC-MS** (m/z): $[M+H]^+$ = 357.2. **Anal. Calc.** for $C_{19}H_{17}FN_2O_4$ (356.35): C, 64.04; H, 4.81. Found: C, 63.87; H, 4.72.

tert-Butyl 5-(1,3-Dioxoisoindolin-2-yl)-3-nitro-1H-indole-1-carboxylate (**29i**)

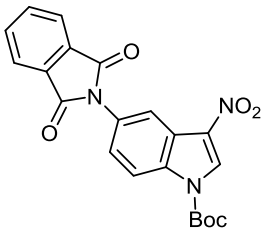

White solid, **M.p.** = 256.2−258.4 °C. **^{1}H NMR** (400 MHz, CDCl3) δ = 8.60 (s, 1H), 8.36 (d, J = 7.6 Hz, 1H), 8.35 (s, 1H), 7.98 (dd, J = 5.4, 3.1 Hz, 2H), 7.82 (dd, J = 5.4, 3.1 Hz, 2H), 7.52 (dd, J = 8.9, 2.1 Hz, 1H), 1.72 (s, 9H). **^{13}C NMR** (100 MHz, $CDCl_3$) δ = 167.2 (2C), 158.0, 148.2, 134.1 (2C), 132.2, 131.8 (2C), 130.0 (2C), 128.9, 128.0, 122.5, 116.5, 116.3, 102.3, 86.6, 28.2 (3C). **LC-MS** (m/z): $[M+H]^+$ = 408.2. **Anal. Calc.** for $C_{21}H_{17}N_3O_6$ (407.11): C, 61.92; H, 4.21. Found: C, 61.72; H, 4.04.

3.5.2. General Procedure for Phosphine-Catalyzed Dearomatization of 3-Nitroindoles with Allenoates

A scintillation vial was charged with reagent-grade benzene (0.5 mL), allenoate **56** (0.15 mmol), nitro-indole **29** (0.1 mmol), and last (p-OMe-$C_6H_4)_3$P (7 mg, 20 mol %). The reaction was then kept stirring at room temperature until **29** was completely consumed (TLC). Last, the solution was directly transferred into a silica gel column (*c*-Hex:EtOAc = 40:1 → 15:1) to afford compounds **57**.

(±)-4-(*tert*-Butyl) 3-Ethyl-8b-nitro-1-propyl-3a,8b-dihydrocyclopenta[b]indole-3,4(1H) dicarboxylate (**57ac**)

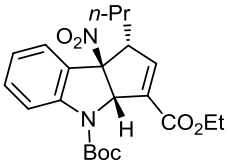

Colorless oil, yield = 85%, dr = 3.5:1 (35.4 mg). **^{1}H NMR** (400 MHz, $CDCl_3$) δ = 7.75 (d, J = 8.2 Hz, 1H), 7.58 (d, J = 7.7 Hz, 1H), 7.40 (dd, J = 11.5, 4.1 Hz, 1H), 7.07 (t, J = 7.6 Hz, 1H), 6.68 (s, 1H), 6.44 (s, 1H), 4.30−4.14 (m, 2H), 3.69 (d, J = 6.2 Hz, 1H), 2.31−2.18 (m, 1H), 1.66−1.56 (s, 9H), 1.55−1.38 (m, 3H), 1.29 (t, J = 7.1 Hz, 3H), 1.02 (t, J = 7.0 Hz, 3H). **^{13}C NMR** (100 MHz, $CDCl_3$) δ = 163.0, 152.0, 143.9, 143.6, 132.5, 131.8, 127.8, 124.5, 122.9, 117.8, 101.4, 82.5, 72.1, 61.0, 52.3, 33.7, 28.4 (3C), 21.4, 14.4, 14.2; minor isomer, diagnostic signals δ = 132.0, 123.7. **LC-MS** (m/z): $[M\text{-}Boc+H]^+$ = 317.0, $[2M+Na]^+$ = 855.2. **Anal. Calc.** for $C_{22}H_{28}N_2O_6$ (416.19): C, 63.45; H, 6.78. Found: C, 63.31; H, 6.55.

(±)-4-(*tert*-Butyl) 3-Ethyl-8-cyano-8b-nitro-1-propyl-3a,8b-dihydrocyclopenta[b]indole-3,4(1H)-dicarboxylate (**57ad**)

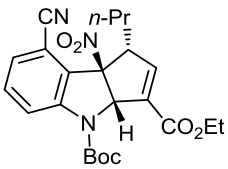

Pale yellow solid, yield = 83%, dr = 3.5:1 (36.6 mg). **M.p.** = 133.3−133.7 °C. **^{1}H NMR** (400 MHz, $CDCl_3$) δ = 8.02 (d, J = 8.1 Hz, 1H), 7.51−7.44 (m, 1H), 7.44−7.36 (m, 1H), 6.74 (d, J = 1.5 Hz, 1H), 6.00 (s, 1H), 4.30−4.14 (m, 2H), 3.97 (d, 1H), 2.02−1.89 (m, 1H), 1.58 (s, 9H), 1.48 (m, 2H), 1.37 (m, 1H), 1.29 (m, 3H), 0.89 (t, J = 7.3 Hz, 3H). **^{13}C NMR** (100 MHz, $CDCl_3$) δ = 163.4, 162.2, 151.2, 145.1, 144.4, 133.2 132.3, 131.7, 127.8, 121.1, 116.6, 111.0, 102.1, 83.9, 75.8, 61.1, 53.3, 33.7, 28.1 (3C), 20.5, 14.2; minor isomer, diagnostic signals δ = 145.5, 131.8, 116.5, 111.3, 60.9, 33.3. **LC-MS** (m/z): $[M\text{-}Boc+H]^+$ = 342.0, $[2M+Na]^+$ = 905.2. **Anal. Calc.** for $C_{23}H_{27}N_3O_6$ (441.19): C, 62.57; H, 6.16. Found: C, 62.36; H, 6.01.

(±)-4-(tert-Butyl) 3-Ethyl-7-bromo-8b-nitro-1-propyl-3a,8b-dihydrocyclopenta[b]indole-3,4(1H)-dicarboxylate (**57ae**)

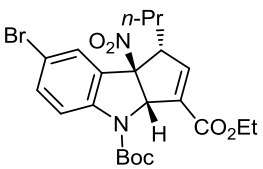

Yellow oil, yield = 77%, dr = 3:1 (38.1 mg). **^{1}H NMR** (400 MHz, $CDCl_3$) δ = 7.66 (s, 1H), 7.64 (d, J = 13.6 Hz, 2H), 7.49 (d, J = 8.8 Hz, 1H), 6.66 (s, 1H), 6.41 (s, 1H), 4.25−4.14 (m, 2H), 3.66 (d, J = 6.6 Hz, 1H), 2.21−2.11 (m, 1H), 1.63−1.38 (m, 12H), 1.27 (t, J = 7.1 Hz, 3H), 1.02 (t, J = 7.1 Hz, 3H). **^{13}C NMR** (100 MHz, $CDCl_3$) δ = 162.5, 151.5, 143.3, 134.6, 132.1, 130.4, 118.9, 115.1, 100.4, 82.7, 72.1, 60.9, 52.1, 32.2, 28.1 (3C), 26.9, 22.6, 21.1, 14.1, 13.8; minor isomer, diagnostic signals δ = 126.0, 142.8. **LC-MS** (m/z): $[M\text{-}Boc+H]^+$ = 395.0,

$[2M+Na]^+$ = 1012.0. **Anal. Calc.** for $C_{22}H_{27}BrN_2O_6$ (494.11): C, 53.34; H, 5.49. Found: C, 53.25; H, 5.29.

(±)-4-(*tert*-Butyl) 3-Ethyl-7-methyl-8b-nitro-1-propyl-3a,8b-dihydrocyclopenta[b]indole-3,4(1H)-dicarboxylate (**57af**)

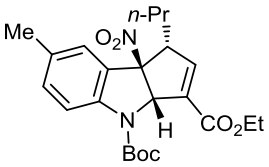

Colorless oil, yield = 51%, dr = 3:1 (21.9 mg). **^{1}H NMR** (400 MHz, $CDCl_3$) δ = 7.60 (d, J = 7.9 Hz, 1H), 7.33 (s, 1H), 7.19 (d, J = 8.2 Hz, 1H), 6.65 (s, 1H), 6.40 (s, 1H), 4.27−4.14 (m, 2H), 3.66 (d, J = 6.3 Hz, 1H), 2.33 (s, 3H), 2.26−2.15 (m, 1H), 1.75−1.38 (m, 12H), 1.26 (t, J = 7.1 Hz, 3H), 1.01 (t, J = 7.0 Hz, 3H). **^{13}C NMR** (100 MHz, $CDCl_3$) δ = 162.8, 151.9, 143.3, 141.5, 132.4, 127.7, 124.4, 117.3, 100.9, 82.0, 72.0, 60.7, 51.9, 51.2, 33.5, 32.3, 28.2, 28.2 (3C), 21.1, 14.0, 13.9; minor isomer, diagnostic signals δ = 132.55, 20.15. **LC-MS** (m/z): $[M-Boc+H]^+$ = 331.2, $[2M+Na]^+$ 883.2. **Anal. Calc.** for $C_{23}H_{30}N_2O_6$ (430.21): C, 64.17; H, 7.02. Found: C, 64.31; H, 7.18.

(±)-4-(*tert*-Butyl) 3-Ethyl-7-methoxy-8b-nitro-1-propyl-3a,8b-dihydrocyclopenta[b]indole-3,4(1H)-dicarboxylate (**57ag**)

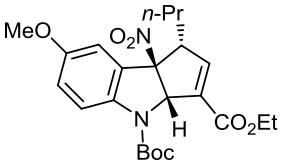

Colorless oil, yield = 73%, dr = 3.5:1 (32.6 mg). **^{1}H NMR** (400 MHz, $CDCl_3$) δ = 7.63 (d, J = 8.1 Hz, 1H), 7.08 (d, J = 2.4 Hz, 1H), 6.95 (dd, J = 9.1, 2.4 Hz, 1H), 6.66 (s, 1H), 6.40 (s, 1H), 4.24−4.15 (m, 2H), 3.78 (s, 3H), 3.66 (d, J = 6.3 Hz, 1H), 2.26−2.13 (m, 1H), 1.64−1.35 (m, 12H), 1.27 (t, J = 7.1 Hz, 3H), 1.00 (t, J = 7.0 Hz, 3H). **^{13}C NMR** (100 MHz, $CDCl_3$) δ = 162.8, 155.4, 152.0, 143.2, 132.4, 125.4, 118.3, 117.1, 113.2, 100.9, 82.0, 72.2, 60.7, 55.9, 52.0, 32.4, 28.2, 28.2 (3C), 21.2, 14.2, 13.9; minor isomer, diagnostic signals δ = 137.5, 117.8, 110.8, 33.6. **LC-MS** (m/z): $[M-Boc+H]^+$ = 347.2, $[2M+Na]^+$ = 915.2. **Anal. Calc.** for $C_{23}H_{30}N_2O_7$ (446.21): C, 61.87; H, 6.77. Found: C, 61.72; H, 6.51.

(±)-4-(*tert*-Butyl) 3-Ethyl-7-(4-fluorophenyl)-8b-nitro-1-propyl-3a,8b-dihydrocyclopenta[b]indole-3,4(1H)-dicarboxylate (**57ah**)

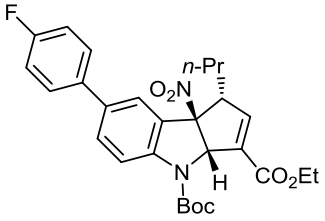

Yellow oil, yield = 72%, dr = 2.5:1 (36.7 mg). **^{1}H NMR** (400 MHz, $CDCl_3$) δ = 7.80 (d, J = 11.5 Hz, 1H), 7.69 (d, J = 1.5 Hz, 1H), 7.56 (dd, J = 8.5, 1.8 Hz, 1H), 7.45 (dd, J = 8.7, 5.3 Hz, 2H), 7.12 (dd, J = 12.2, 5.1 Hz, 2H), 6.69 (s, 1H), 6.47 (s, 1H),

4.28−4.15 (m, 2H), 3.75−3.69 (m, 1H), 2.29 (dd, J = 19.7, 13.8 Hz, 1H), 1.66−1.41 (m, 12H), 1.28 (t, J = 7.2, 2.3 Hz, 3H), 1.02 (t, J = 7.1 Hz, 3H). **^{13}C NMR** (100 MHz, $CDCl_3$) δ = 162.7, 162.4 (d, J = 250.9 Hz), 151.7, 143.3, 136.4 (d, J = 3.0 Hz), 135.3, 132.3, 130.6, 128.5 (J = 16.6 Hz), 126.0, 117.7, 115.7 (d, J = 21.2 Hz), 100.8, 82.4, 72.2, 60.8, 52.0, 32.5, 31.6, 28.2 (3C), 22.6, 21.1, 14.2, 13.9; minor isomer, diagnostic signals δ = 130.7, 128.8 (d, J = 7.6 Hz), 117.8, 115.8 (d, J = 21.2 Hz), 115.6, 51.3, 33.6. **^{19}F NMR** (376 MHz, $CDCl_3$) δ = −115.6. **LC-MS** (m/z): $[M\text{-Boc+H}]^+ = [2M+Na]^+$ = 1043.6. **Anal. Calc.** for $C_{28}H_{31}FN_2O_6$ (510.22): C, 65.87; H, 6.12. Found: C, 65.61; H, 6.00.

(±)-4-(*tert*-Butyl) 3-Ethyl-7-(1,3-dioxoisoindolin-2-yl)-8b-nitro-1-propyl-3a,8b-dihydrocyclopenta[b]indole-3,4(1H)-dicarboxylate (**57ai**)

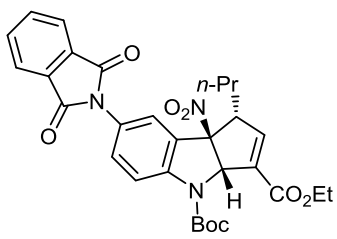

White solid, yield = 77%, dr = 3:1 (43.2 mg). **M.p.** = 195.8−197.2 °C. **^{1}H NMR** (400 MHz, $CDCl_3$) δ = 7.94 (dd, J = 5.5, 3.0 Hz, 2H), 7.85 (d, J = 8.5 Hz, 1H), 7.78 (dd, J = 5.4, 3.0 Hz, 2H), 7.67 (d, J = 2.0 Hz, 1H), 7.49 (dd, J = 8.8, 2.1 Hz, 1H), 6.69 (s, 1H), 6.49 (s, 1H), 4.21 (m, 2H), 3.69 (dd, J = 10.9, 4.5 Hz, 1H), 2.28−2.16 (m, 1H), 1.69−1.42 (m, 12H), 1.28 (t, J = 7.1 Hz, 3H), 1.03 (t, J = 7.3 Hz, 3H). **^{13}C NMR** (100 MHz, $CDCl_3$) δ = 167.0 (2C), 162.6, 151.5, 143.5, 134.5 (2C), 134.4 (2C), 132.1, 131.7, 129.8, 126.2, 126.2, 123.8 (2C), 117.7, 100.4, 82.6, 72.2, 60.8, 52.4, 32.3, 28.2, 28.1 (3C), 21.1, 14.2, 13.8; minor isomer, diagnostic signals δ = 143.0, 51.6, 13.9. **LC-MS** (m/z): $[M\text{-Boc+H}]^+$ = 462.0, $[2M+Na]^+$ 1145.2. **Anal. Calc.** for $C_{30}H_{31}N_3O_8$ (561.21): C, 64.16; H, 5.56. Found: C, 63.98; H, 5.52.

(±)-4-(*tert*-Butyl) 3-Ethyl-6-chloro-8b-nitro-1-propyl-3a,8b-dihydrocyclopenta[b]indole-3,4(1H)-dicarboxylate (**57aj**)

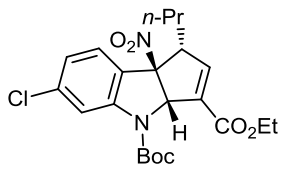

Colorless oil, yield = 92%, dr = 2.5:1 (41.4 mg). **^{1}H NMR** (400 MHz, $CDCl_3$) δ = 7.81 (s, 1H), 7.49 (d, J = 8.4 Hz, 1H), 7.05 (dd, J = 8.4, 2.0 Hz, 1H), 6.67 (s, 1H), 6.43 (s, 1H), 4.29−4.16 (m, 2H), 3.67 (d, J = 6.1 Hz, 1H), 2.23−2.14 (m, 1H), 1.60 (s, 9H), 1.56−1.44 (m, 3H), 1.29 (t, J = 7.1 Hz, 3H), 1.02 (t, J = 7.0 Hz, 3H). **^{13}C NMR** (100 MHz, $CDCl_3$) δ = 162.7, 151.4, 144.7, 143.3, 137.9, 132.1, 128.5, 122.9, 117.8, 100.3, 82.8, 72.3, 60.9, 52.2, 32.4, 28.1 (3C), 26.9, 21.1, 14.2, 13.9; minor isomer, diagnostic signals δ = 122.6. **LC-MS** (m/z): $[M\text{-Boc+H}]^+$ = 351.0, $[2M+Na]^+$ = 923.2. **Anal. Calc.** for $C_{22}H_{27}ClN_2O_6$ (450.16): C, 58.60; H, 6.04. Found: C, 58.39; H, 6.22.

(±)-Diethyl-8b-nitro-1-propyl-3a,8b-dihydrocyclopenta[b]-indole-3,4(1H)-dicarboxylate (**57ak**)

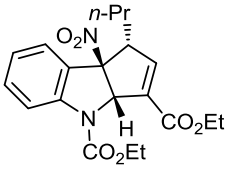

Light yellow oil, yield = 95%, dr = 2.5:1 (36.9 mg). **^{1}H NMR** (400 MHz, $CDCl_3$) δ = 7.81 (d, J = 8.0 Hz, 1H), 7.57 (d, J = 7.7 Hz, 1H), 7.41 (dd, J = 11.4, 4.1 Hz, 1H), 7.08 (t, J = 7.7 Hz, 1H), 6.70 (s, 1H), 6.46 (s, 1H), 4.47−4.11 (m, 4H), 3.68 (d, J = 6.2 Hz, 1H), 2.26−2.16 (m, 1H), 1.62−1.34 (m, 5H), 1.27 (t, J = 7.1 Hz, 3H), 1.00 (t, J = 7.0 Hz, 3H). **^{13}C NMR** (100 MHz, $CDCl_3$) δ = 162.8, 152.9, 145.4, 143.9, 131.8, 127.6, 123.0, 117.2, 101.1, 71.7, 69.2, 62.4, 60.9, 52.2, 51.2, 32.5, 21.1, 14.4, 14.1, 14.0; minor isomer, diagnostic signals δ = 143.3, 132.1, 132.0, 126.0, 33.5, 20.1, 14.5, 14.1. **LC-MS** (m/z): $[M+H]^+$ = 389.2. **Anal. Calc.** for $C_{20}H_{24}N_2O_6$ (388.16): C, 61.85; H, 6.23. Found: C, 61.71; H, 6.01.

(±)-4-Benzyl 3-Ethyl-8b-nitro-1-propyl-3a,8b-dihydrocyclopenta[b]indole-3,4(1H)-dicarboxylate (**57al**)

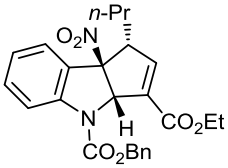

Light yellow oil, yield = 87%, dr = 3:1 (39.1 mg). **^{1}H NMR** (400 MHz, $CDCl_3$) δ = 7.82 (d, J = 6.9 Hz, 1H), 7.58 (dd, J = 7.8, 0.6 Hz, 1H), 7.49−7.28 (m, 5H), 7.08 (td, J = 7.8, 1.0 Hz, 1H), 6.72 (t, J = 1.7 Hz, 1H), 6.50 (s, 1H), 5.39 (d, J = 12.3 Hz, 1H), 5.24 (d, J = 12.3 Hz, 1H), 4.21−4.04 (m, 2H), 3.68 (dd, J = 8.4, 2.0 Hz, 1H), 2.29−2.14 (m, 1H), 1.62−1.36 (m, 3H), 1.22 (t, J = 7.1 Hz, 3H), 1.01 (t, J = 7.0 Hz, 3H). **^{13}C NMR** (100 MHz, $CDCl_3$) δ = 162.7, 152.8, 145.6, 144.1, 135.8, 131.9, 131.9, 128.5 (2C), 128.2, 128.1 (2C), 127.6, 123.9, 123.1, 117.3, 101.0, 71.7, 68.1, 60.9, 52.1, 32.4, 21.1, 14.1, 13.9; minor isomer, diagnostic signals δ = 132.1, 33.5, 20.1. **LC-MS** (m/z): $[M+H]^+$ = 451.2. **Anal. Calc.** for $C_{25}H_{26}N_2O_6$ (450.18): C, 66.66; H, 5.82. Found: C, 66.41; H, 5.68.

(±)-8-(*tert*-Butyl) 7-Ethyl-4b-nitro-5-propyl-5,7a-dihydrocyclopenta[4,5]pyrrolo[2,3-b]pyridine-7,8(4bH)-dicarboxylate (**57am**)

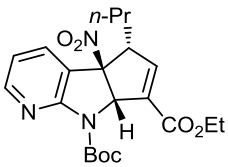

Yellow oil, yield = 96%, dr = 3.5:1 (40.0 mg). **^{1}H NMR** (400 MHz, $CDCl_3$) δ = 8.48 (dd, J = 4.9, 1.4 Hz, 1H), 7.89 (dd, J = 7.7, 1.4 Hz, 1H), 7.02 (dd, J = 7.7, 5.0 Hz, 1H), 6.66 (s, 1H), 6.45 (s, 1H), 4.19 (q, J = 7.1 Hz, 2H), 3.64 (d, J = 6.1 Hz, 1H), 2.18−2.06 (m, 1H), 1.57 (s, 9H), 1.56−1.51 (m, 1H), 1.44 (m, 2H), 1.27 (t, J = 7.1 Hz, 3H), 1.00 (t, J = 7.0 Hz, 3H). **^{13}C NMR** (100 MHz, $CDCl_3$) δ = 162.4, 156.2, 151.8, 150.3, 143.1, 137.0, 132.6, 118.2, 118.1, 98.9,

82.8, 70.6, 60.9, 52.3, 32.6, 28.0 (3C), 21.0, 14.2, 13.9; minor isomer, diagnostic signals δ = 135.1, 33.3. **LC-MS** (m/z): $[M\text{-Boc}+H]^+$ = 318.2, $[M+H]^+$ = 418.2. **Anal. Calc.** for $C_{21}H_{27}N_3O_6$ (417.19): C, 60.42; H, 6.52. Found: C, 60.39; H, 6.39.

(±)-4-(*tert*-Butyl) 3-(3,5-Dimethylphenyl)-8b-nitro-1-propyl-3a,8b-dihydrocyclopenta[b]indole-3,4(1H)-dicarboxylate (**57bc**)

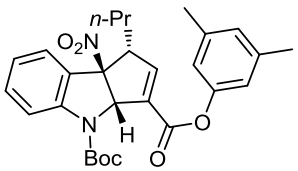

Colorless oil, yield = 57%, dr = 3:1 (28.0 mg). **^{1}H NMR** (400 MHz, $CDCl_3$) δ = 7.77 (d, J = 7.8 Hz, 1H), 7.59 (d, J = 7.8 Hz, 1H), 7.42 (t, J = 7.8 Hz, 1H), 7.09 (t, J = 7.6 Hz, 1H), 6.90 (s, 1H), 6.85 (s, 1H), 6.72 (s, 2H), 6.54 (s, 1H), 3.76 (d, J = 8.4 Hz, 1H), 2.29 (s, 6H), 2.29−2.20 (m, 1H), 1.67−1.44 (m, 12H), 1.02 (t, J = 7.0 Hz, 3H). **^{13}C NMR** (100 MHz, $CDCl_3$) δ = 161.3, 151.9, 150.1, 145.6, 139.2 (2C), 131.7, 127.7, 127.6, 124.3, 122.8, 119.1 (2C), 117.7, 100.9, 82.4, 71.9, 52.3, 32.5, 28.1 (3C), 26.9 (2C), 21.2, 21.2, 14.0; minor isomer, diagnostic signals δ = 143.8, 123.7, 33.5. **LC-MS** (m/z): $[M\text{-Boc}+H]^+$ = 393.0, $[2M+Na]^+$ = 1007.2. **Anal. Calc.** for $C_{28}H_{32}N_2O_6$ (492.23): C, 68.28; H, 6.55. Found: C, 68.31; H, 6.41.

(±)-Di-*tert*-butyl 4b-Nitro-5-propyl-5,7a-dihydrocyclopenta[4,5]-pyrrolo[2,3-b]pyridine-7,8(4bH)-dicarboxylate (**57cm**)

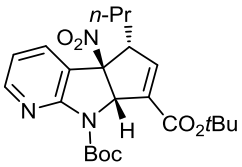

Light yellow oil, yield = 71%, dr = 3.5:1 (31.6 mg). **^{1}H NMR** (400 MHz, $CDCl_3$) δ = 8.43 (d, J = 3.7 Hz, 1H), 7.85 (d, J = 7.5 Hz, 1H), 6.98 (dd, J = 7.4, 5.1 Hz, 1H), 6.47 (s, 1H), 6.38 (s, 1H), 3.59 (d, J = 5.6 Hz, 1H), 2.08 (m, 1H), 1.54 (m, 1H), 1.53 (s, 9H), 1.41 (m, 2H), 1.41 (s, 9H), 0.95 (t, J = 6.8 Hz, 3H). **^{13}C NMR** (100 MHz, $CDCl_3$) δ = 161.4, 156.2, 151.7, 150.4, 141.7, 136.9, 133.8, 118.1, 118.0, 98.7, 82.7, 81.5, 70.7, 52.1, 32.5, 28.0 (3C), 27.9(3C), 20.9, 13.9; minor isomer, diagnostic signals δ = 143.0, 118.9, 66.7, 33.4. **LC-MS** (m/z): $[M+H]^+$ = 446.2. **Anal. Calc.** for $C_{23}H_{31}N_3O_6$ (445.52): C, 64.01; H, 7.01. Found: C, 63.88; H, 6.85.

(±)-3-Benzyl 4-(*tert*-Butyl) 8b-Nitro-3a,8b-dihydrocyclopenta[b]-indole-3,4(1H)-dicarboxylate (**57dc**)

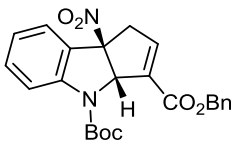

Colorless oil, yield = 72% (31.4 mg). **^{1}H NMR** (400 MHz, $CDCl_3$) δ= 7.71 (s, 1H), 7.48 (d, J = 7.4 Hz, 1H), 7.43−7.37 (m, 1H), 7.35−7.28 (m, 5H), 7.10 (dd, J = 11.0, 4.2 Hz, 1H), 6.72 (s, 1H), 6.44 (s, 1H), 5.18 (dd, J = 27.0, 12.4 Hz, 2H), 3.56 (d, J = 18.6 Hz, 1H), 3.36 (d, J = 18.6 Hz, 1H), 1.55 (s, 9H). **^{13}C**

NMR (100 MHz, $CDCl_3$) δ = 162.1, 151.9, 142.9, 141.1, 135.6, 133.8, 132.0, 128.5 (2C), 128.3, 128.2 (2C), 124.5, 123.6, 117.8, 96.8, 82.3, 71.8, 66.5, 42.0, 28.1 (3C), 26.9. **LC-MS** (m/z): $[M\text{-}Boc+H]^+$ = 337.0. **Anal. Calc.** for $C_{24}H_{24}N_2O_6$ (436.16): C, 66.05; H, 5.54. Found: C, 65.89; H, 5.35.

(±)-3-Benzyl 4-Ethyl 8b-nitro-3a,8b-dihydrocyclopenta[b]indole-3,4(1H)-dicarboxylate (**57dk**)

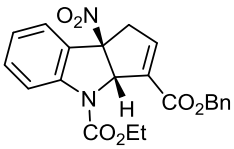

Colorless oil, yield = 72% (29.4 mg). **^{1}H NMR** (400 MHz, $CDCl_3$) δ = 7.76 (s, 1H), 7.50 (d, J = 7.7 Hz, 1H), 7.42 (t, J = 7.8 Hz, 1H), 7.37−7.28 (m, 5H), 7.12 (t, J = 7.6 Hz, 1H), 6.76 (s, 1H), 6.47 (s, 1H), 5.21 (d, J = 12.3 Hz, 1H), 5.12 (d, J = 12.3 Hz, 1H), 4.34−4.20 (m, 1H), 4.13 (m, 1H), 3.58 (d, J = 18.8 Hz, 1H), 3.38 (d, J = 17.7 Hz, 1H), 1.30 (t, J = 7.1 Hz, 3H). **^{13}C NMR** (100 MHz, $CDCl_3$) δ = 162.2, 153.1, 141.5, 135.4, 133.7, 132.2, 128.5, 128.4, 128.3, 124.5, 123.9, 117.6, 97.0, 71.7, 66.7, 62.4, 42.0, 27.9, 26.9, 14.3. **LC-MS** (m/z): $[M+H]^+$ = 409.2. **Anal. Calc.** for $C_{22}H_{20}N_2O_6$ (408.13): C, 64.70; H, 4.94. Found: C, 64.50; H, 4.79.

(±)-3-Benzyl 4-(*tert*-Butyl) 1-methyl-8b-nitro-3a,8b-dihydrocyclopenta[b]indole-3,4(1H)-dicarboxylate (**57fc**)

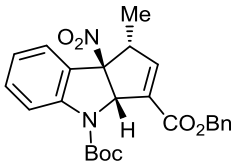

Colorless oil, yield = 56%, dr = 3.5:1 (25.2 mg). **^{1}H NMR** (400 MHz, $CDCl_3$) δ = 7.77 (d, J = 7.8 Hz, 1H), 7.54 (d, J = 7.4 Hz, 1H), 7.43−7.37 (m, 1H), 7.36−7.28 (m, 5H), 7.06 (t, J = 7.6 Hz, 1H), 6.52−6.46 (m, 2H), 5.18 (dd, J = 34.0, 12.4 Hz, 2H), 3.82 (dd, J = 14.6, 7.3 Hz, 1H), 1.55 (s, 9H), 1.49 (d, J = 7.3 Hz, 3H). **^{13}C NMR** (100 MHz, $CDCl_3$) δ = 162.4, 151.8, 146.0, 143.8, 135.6, 131.7, 131.6, 128.5 (2C), 128.3, 128.2(2C), 127.5, 122.6, 117.5, 100.8, 82.3, 71.9, 66.5, 47.1, 28.1(3C), 26.9, 16.2.; minor isomer, diagnostic signals δ = 132.0, 117.4, 46.7. **LC-MS** (m/z): $[M\text{-}Boc+H]^+$ = 351.2, $[2M+Na]^+$ = 923.4. **Anal. Calc.** for $C_{25}H_{26}N_2O_6$ (450.18): C, 66.66; H, 5.82. Found: C, 66.38; H, 5.65.

(±)-3-Benzyl 4-Ethyl-1-methyl-8b-nitro-3a,8b-dihydrocyclopenta[b]indole-3,4(1H)-dicarboxylate (**57fk**)

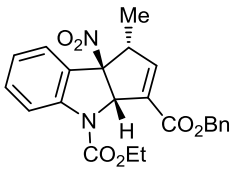

Pale yellow oil, yield = 81%, dr = 2:1 (34.2 mg). **^{1}H NMR** (400 MHz, $CDCl_3$) δ = 7.82 (d, J = 7.8 Hz, 1H), 7.56 (d, J = 7.8 Hz, 1H), 7.45−7.28 (m, 6H), 7.08 (td, J = 7.8, 1.0 Hz, 1H), 6.55 (d, J = 1.8 Hz, 1H), 6.52 (s,

1H), 5.21 (d, J = 12.3 Hz, 1H), 5.12 (d, J = 12.3 Hz, 1H), 4.25 (dq, J = 10.6, 7.1 Hz, 1H), 4.18−4.07 (m, 1H), 3.83 (q, J = 7.3 Hz, 1H), 1.50 (d, J = 7.3 Hz, 3H), 1.30 (td, J = 7.1, 3.8 Hz, 3H). **^{13}C NMR** (100 MHz, $CDCl_3$) δ = 162.5, 152.9, 146.6, 135.4, 131.9, 131.4, 128.6 (2C), 128.4 (2C), 127.5, 123.8, 122.9, 117.3, 101.0, 71.7, 69.0, 66.7, 62.4, 47.2, 26.9, 16.2, 14.3; minor isomer, diagnostic signals δ = 147.0, 143.4, 132.1, 128.4, 125. 9, 66.7, 46.7, 16.3, 14.4. **LC-MS** (m/z): $[M+H]^+$ = 423.2. **Anal. Calc.** for $C_{23}H_{22}N_2O_6$ (422.15): C, 65.40; H, 5.25. Found: C, 65.20; H, 5.17.

(±)-7-Benzyl 8-(*tert*-Butyl)-5-methyl-4b-nitro-5,7adihydrocyclopenta[4,5]pyrrolo[2,3-b]pyridine-7,8(4bH)-dicarboxylate (**57fm**)

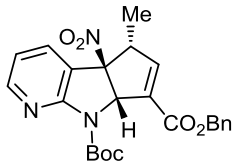

Yellow oil, yield = 91%, dr = 2.5:1 (41.0 mg). **^{1}H NMR** (400 MHz, $CDCl_3$) δ = 8.49 (dd, J = 4.9, 1.5 Hz, 1H), 7.88 (dd, J = 7.7, 1.5 Hz, 1H), 7.47−7.21 (m, 5H), 7.01 (dd, J = 7.8, 5.1 Hz, 1H), 6.51 (s, 1H), 6.49 (d, J = 1.6 Hz, 1H), 5.20−5.09 (m, 2H), 3.78 (dd, J = 14.5, 7.2 Hz, 1H), 1.56 (s, 9H), 1.44 (s, 3H). **^{13}C NMR** (100 MHz, $CDCl_3$) δ = 159.4, 153.7, 149.4, 147.7, 143.0, 134.3, 132.9, 129.4, 126.0 (2C), 125.8 (2C), 116.5, 115.6, 96.3, 80.3, 68.1, 65.9, 64.1, 44.8, 25.4 (3C), 13.5; minor isomer, diagnostic signals δ = 149.7, 143.5, 132.6, 125.8, 125.8, 115.8, 64.1, 44.3. **LC-MS** = $[M-Boc+H]^+$ = 352.2. **Anal. Calc.** for $C_{24}H_{25}N_3O_6$ (451.17): C, 63.85; H, 5.58. Found: C, 63.65; H, 5.65.

3.5.3. Gram-Scale Reaction

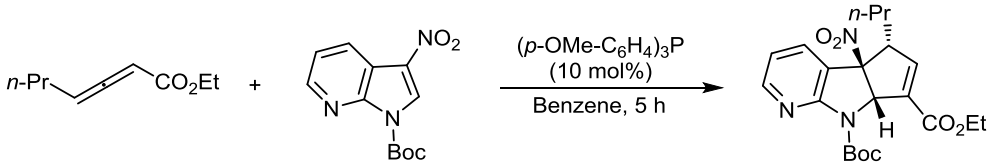

A one-necked 100 mL flask was charged with reagent-grade benzene (15 mL), substrate **29m** (1.05 g, 4.0 mmol, 1.0 equiv), substrate **56a** (308 mg, 2 mmol, 0.5 equiv), and tris(4-methoxyphenyl)phosphine (141 mg, 10 mol %). Then the reaction was kept stirring at room temperature for 1 h. Therefore, other two aliquots of **56a** (2 × 308 mg, 2 mmol) were added every 30 min. The reaction was kept stirring at room temperature for 3 h, until **29m** was completely consumed (TLC). Last, the benzene was evaporated under reduced pressure, and the crude was transferred into silica gel column chromatography (*c*-Hex:EtOAc = 10:1) to afford compound **57am** as a orange oily solid (yield = 93%, dr = 3:1, 15.5 g).

3.5.4. Synthetic Application of Products

(±)-8-(*tert*-Butyl) 7-Ethyl-4bnitro-5-propyl-5,6,7,7a-tetrahydrocyclopenta[4,5]pyrrolo[2,3-b]-pyridine-7,8(4bH)-dicarboxylate (**58am**, major isomer).

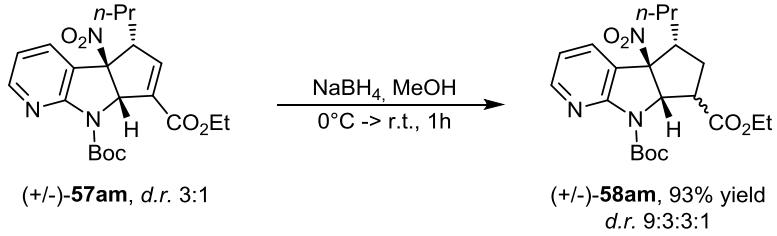

(+/-)-**57am**, *d.r.* 3:1

(+/-)-**58am**, 93% yield
d.r. 9:3:3:1

A one-necked flask was charged with reagent-grade methanol (2 mL), racemic **57am** (41.7 mg, 0.1 mmol, 1.0 equiv), and $NaBH_4$(0.3 mmol, 3.0 equiv) in sequence. The reaction was stirred for 1 h at rt. The solvent was removed under vacuum, then water was added, and the product was extracted three times with AcOEt. After dryness with Na_2SO_4 the volatiles were removed under vacuum. The ^{1}H NMR spectrum was collected on the crude mixture (dr = 3:1). Finally, the product was purified by flash chromatography (*c*-Hex:EtOAc = 10:1) to afford compound **58am** as a colorless oil (yield = 93%, dr = 9:3:3:1, 39.0 mg). **^{1}H NMR** (400 MHz, $CDCl_3$) δ = 8.54−8.37 (m, 1H), 7.85−7.76 (m, 1H), 6.98 (dd, J = 7.6, 5.1 Hz, 1H), 5.73 (s, 1H), 4.30−4.15 (m, 2H), 3.09 (d, J = 8.1 Hz, 1H), 3.06−2.92 (m, 1H), 2.30 (dd, J = 13.5, 5.7 Hz, 2H), 1.99−1.87 (m, 1H), 1.65 (m, 1H), 1.52 (s, 9H), 1.47−1.12 (m, 5H), 0.91 (t, J = 7.2 Hz, 3H). **^{13}C NMR** (100 MHz, $CDCl_3$) δ = 172.5, 156.7, 151.5, 136.8, 135.4, 117.7, 99.3, 83.0, 70.3, 61.4, 49.9, 49.0, 33.8, 32.0, 28.2 (3C), 26.9, 21.2, 14.2, 14.0; minor isomer, diagnostic signals δ = 151.4, 149.2, 83.4, 69.8, 61.1, 51.9, 28.1, **LC-MS** (m/z): $[M+H]^+$ = 419.2, $[2M+Na]^+$ = 861.2. **Anal. Calc.** for $C_{21}H_{29}N_3O_6$ (418.21): C, 60.13; H, 6.97. Found: C, 60.00; H, 6.65.

(±)-8-(*tert*-Butyl) 7-Ethyl-4b-amino-5-propyl-5,7adihydrocyclopenta[4,5]pyrrolo[2,3-b]pyridine-7,8(4bH)-dicarboxylate (**59am'**)

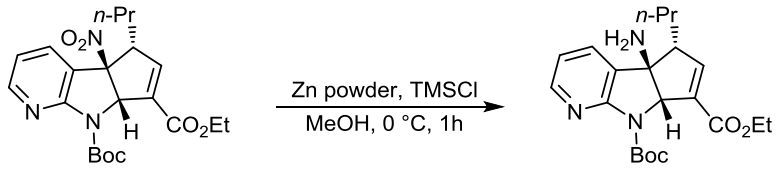

(+/-)-**57am**, *d.r.* 3:1

(+/-)-**59am'**, 97% yield
d.r. 3:1

Zinc powder (140.6 mg, 2.15 mmol, 21.5 equiv) was slowly added to a solution of **57am** (41.7 mg, 0.1 mmol, 1.0 equiv) and trimethylsilyl chloride (0.26 mL, 2.03 mmol, 20.3 equiv)

in methanol at 0 °C. After stirring the reaction suspension at 0 °C for 1 h, the suspension was filtered and washed with dichloromethane. Then the filtrate was washed with saturated $NaHCO_3$ and extracted with dichloromethane. The combined organic fractions were dried over Na_2SO_4, filtered, and concentrated by rotary evaporation. The ^1H NMR spectrum was collected on the crude mixture (dr = 3:1). Then the residue was purified by silica gel column chromatography (DCM:MeOH = 40:1) to afford the desired product **59am'** as a colorless oil (yield = 97%, dr = 3:1, 38.1 mg). **^{1}H NMR** (400 MHz, $CDCl_3$) δ = 8.32 (d, J = 3.7 Hz, 1H), 7.61 (d, J = 7.1 Hz, 1H), 6.89 (s, 1H), 6.67 (s, 1H), 5.27 (s, 1H), 4.19−4.09 (m, 2H), 2.89 (d, J = 10.6 Hz, 1H), 1.85 (d, J = 11.2 Hz, 1H), 1.75−1.30 (m, 12H), 1.24 (t, J = 6.7 Hz, 3H), 0.97 (t, J = 7.0 Hz, 3H). **^{13}C NMR** (100 MHz, $CDCl_3$) δ 163.7, 155.4, 149.2, 145.8, 134.86, 133.5, 127.3, 117.9, 81.8, 75.2, 70.4, 60.4, 54.5, 32.5, 28.2 (3C), 21.7, 20.8, 14.2, 14.1; minor isomer, diagnostic signals δ = 151.3, 149.4, 118.8, 67.7, 33.1. **LC-MS** (m/z): $[M\text{-Boc+H}]^+$ = 288.2, $[M+H]^+$ = 388.2. **Anal. Calc.** for ($C_{21}H_{29}N_3O_4$: 387.22): C, 65.10; H, 7.54. Found: C, 65.21; H, 7.35.

(±)-8-(*tert*-Butyl) 7-ethyl-(4b-acetamido-5-propyl-5,7adihydrocyclopenta[4,5]pyrrolo[2,3-b]pyridine-7,8(4bH)-dicarboxylate (**59am**)

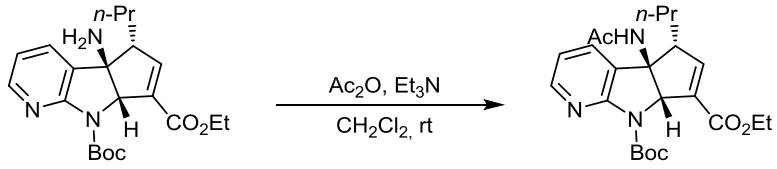

(+/-)-**59am'**, *d.r.* 3:1

(+/-)-**59am**, 97% yield
d.r. 6.7:1

To a solution of racemic **59am'** (38.7 mg, 0.1 mmol, 1.0 equiv) and Et_3N (15.2 mg, 0.15 mmol, 0.15 equiv) in DCM (1 mL) was slowly added Ac_2O (1.1 equiv), and the reaction was stirred for 3 h at rt. The solvent was removed under vacuum, then water was added, and the product was extracted three times with DCM. After dryness with Na_2SO_4, the volatiles were removed under vacuum. The ^1H NMR spectrum was collected on the crude mixture (dr = 6.7:1). Finally, the product was purified by flash chromatography (DCM:MeOH = 40:1) to afford compound **59am** as a colorless oil (yield = 77%, dr = 6.7:1, 33.1 mg). **^{1}H NMR** (400 MHz, $CDCl_3$) δ = 8.30 (d, J = 4.3 Hz, 1H), 7.68 (d, J = 7.4 Hz, 1H), 6.90 (dd, J = 7.4, 5.2 Hz, 1H), 6.72 (s, 1H), 6.06 (s, 1H), 5.87 (s, 1H), 4.13 (dd, J = 14.3, 7.2 Hz, 2H), 3.87 (d, J = 7.7 Hz, 1H), 1.93 (s, 3H), 1.86 (dd, J = 11.5, 5.5 Hz, 1H), 1.54 (m, 1H), 1.54 (s, 9H), 1.23 (t, J = 7.1 Hz, 3H), 0.96 (t, J = 7.1 Hz, 3H). **^{13}C NMR** (100 MHz, $CDCl_3$) δ 169.7, 163.2, 156.0, 151.2, 149.2, 146.4, 135.1, 132.7, 124.8, 117.7, 82.0, 70.3, 69.6, 60.3, 49.0, 32.4, 28.1 (3C),

23.9, 21.5, 14.3, 14.2; minor isomer, diagnostic signals δ = 148.9, 118.5, 60.5, 28.2, 20.4. **LC-MS** (m/z): $[M+H]^+$ = 430.2. **Anal. Calc.** for $C_{23}H_{31}N_3O_5$ (429.23): C, 64.32; H, 7.28. Found: C, 64.20; H, 7.15.

(±)-Ethyl-4b-nitro-5-propyl-4b,5,7a,8-tetrahydrocyclopenta-[4,5]pyrrolo[2,3-b]pyridine-7-carboxylate (**60am**)

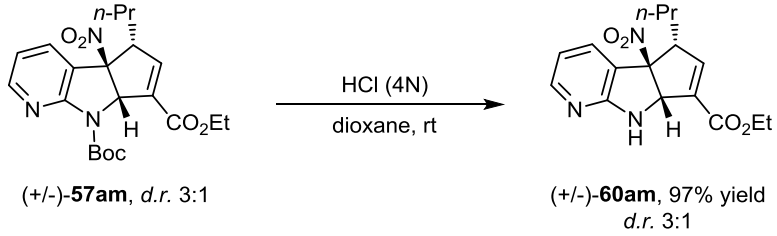

(+/-)-**57am**, *d.r.* 3:1

(+/-)-**60am**, 97% yield
d.r. 3:1

A one-necked flash was charged with racemic **57am** (41.7 mg, 0.1 mmol, 1.0 equiv) and HCl 4 N (in dioxane) (1.5 mL). The reaction was stirred for 1 h at rt. Then water was added, and the product extracted three times with AcOEt. After dryness with Na_2SO_4, the volatiles were removed under vacuum. The ^{1}H NMR spectrum was collected on the crude mixture (dr = 3:1). Finally, the product was purified by flash chromatography (DCM:MeOH = 40:1) to afford compound **60am** as an orange oil (yield = 85%, dr = 3:1, 26.9 mg). **^{1}H NMR** (400 MHz, $CDCl_3$) δ = 8.10 (d, J = 3.6 Hz, 1H), 7.72 (dd, J = 7.5, 1.2 Hz, 1H), 6.74 (s, 1H), 6.65 (dd, J = 7.5, 5.2 Hz, 1H), 5.86 (s, 1H), 5.74 (s, 1H), 4.29−4.20 (m, 2H), 3.68 (dd, J = 10.7, 3.1 Hz, 1H), 1.94 (ddd, J = 15.8, 10.9, 5.5 Hz, 1H), 1.58 (d, J = 6.8 Hz, 1H), 1.42 (dd, J = 14.7, 5.9 Hz, 2H), 1.30 (t, J = 7.1 Hz, 3H), 0.94 (t, J = 7.2 Hz, 3H). **^{13}C NMR** (100 MHz, $CDCl_3$) δ 163.1, 161.6, 151.2, 143.7, 136.5, 133.5, 114.4, 113.4, 102.2, 68.5, 61.2, 55.3, 33.5, 20.7, 14.2, 13.9; minor isomer, diagnostic signals δ = 151.3, 144.3, 135.3, 113.7, 66.7, 61.1, 54.6, 20.3. **LC-MS** (m/z): $[M+H]^+$ = 318.0. **Anal. Calc.** for $C_{16}H_{19}N_3O_4$ (317.35): C, 60.56; H, 6.04. Found: C, 60.35; H, 5.90.

3.5.5. Deuterated Experiments

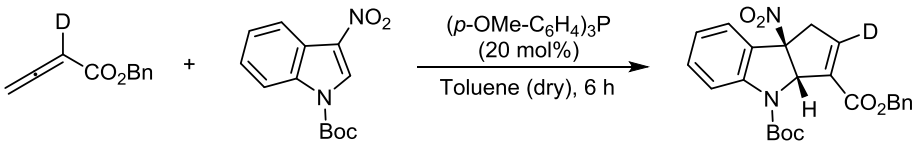

56d-D **29c**

(+/-)-**57dc-D**
Y = xx%, D/H = xx:xx

(a) An oven-dried Schlenk tube, filled with nitrogen atmosphere, was charged with dry toluene (0.5 mL), allenoate **D-56d** (26 mg, 0.15 mmol, 1.5 equiv, D/H > 95:5), nitroindole

29c (26 mg, 0.1 mmol, 1.0 equiv), and (p-OMe-C_6H_4)$_3$P (7 mg, 20 mol %). The reaction was then kept stirring at room temperature until **29c** was completely consumed (TLC). Last, the solution was directly transferred into a silica gel column (*c*-Hex:EtOAc = 40:1 → 15:1) to afford compound **D-57dc** (D/H = 33:67).

(b) The reaction was conducted with the same procedure with the addition of MS 4 Å, and it gave **57dc** in 42% yield (18 mg) and with no deuteration at the expected position.

(±)-D-57dc (from method a)

Colorless oil, yield = 72% (31.4 mg). **^{1}H NMR** (400 MHz, $CDCl_3$) δ= 7.71 (s, 1H), 7.48 (d, J = 7.4 Hz, 1H), 7.43−7.37 (m, 1H), 7.35−7.28 (m, 5H), 7.10 (dd, J = 11.0, 4.2 Hz, 1H), 6.72 (s, 1H), 6.44 (s, 1H), 5.18 (dd, J = 27.0, 12.4 Hz, 2H), 3.56 (d, J = 18.6 Hz, 1H), 3.36 (d, J = 18.6 Hz, 1H), 1.55 (s, 9H). **^{13}C NMR** (100 MHz, $CDCl_3$) δ = 156.8, 146.6, 137.6, 135.8, 130.3, 128.5, 126.7, 123.2 (2C), 123.0, 122.9 (2C), 119.2, 118.3, 112.6, 91.5, 77.0, 66.5, 61.2, 36.7 (3C), 22.9, 21.6. **LC-MS** (m/z): 338.0, 382.2.

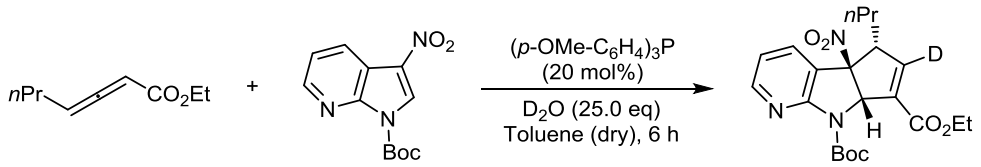

56a **29m** (+/-)-**57am-D**
Y = 79%, D/H = 95:5

An oven-dried Schlenk tube, filled with nitrogen atmosphere, was charged with dry toluene (0.5 mL), allenoate **56a** (23 mg, 0.15 mmol, 1.5 equiv), nitro-indole **29m** (26 mg, 0.1 mmol, 1.0 equiv), deuterated water (25.0 equiv), and (*p*-OMe-C_6H_4)$_3$P (7 mg, 20 mol %). The reaction was then kept stirring at room temperature until **29m** was completely consumed (TLC). Last, the solution was directly transferred into a silica gel column (*c*-Hex:EtOAc = 10:1) to afford compound **D-57am** (D/H > 95:5).

(±)-D-57am

Yellow oil, yield = 79% (33.0 mg, dr = 2.5:1). **^{1}H NMR** (400 MHz, $CDCl_3$) δ = 8.48 (dd, J = 4.9, 1.4 Hz, 1H), 7.89 (dd, J = 7.7, 1.4 Hz, 1H), 7.02 (dd, J = 7.7, 5.0 Hz, 1H), 6.45 (s, 1H), 4.19 (q, J = 7.1 Hz, 2H), 3.64 (d, J = 6.1 Hz, 1H), 2.18−2.06 (m, 1H), 1.57 (s, 9H), 1.56−1.51 (m, 1H), 1.44 (m, 2H), 1.27 (t, J = 7.1 Hz, 3H), 1.00 (t, J = 7.0 Hz, 3H). **^{13}C NMR** (100 MHz, $CDCl_3$) δ = 162.4, 156.2, 151.8, 150.3, 143.1, 137.0, 132.6, 118.2, 118.1, 98.9, 82.8, 70.6, 60.9, 52.3, 32.6, 28.0 (3C), 21.0, 14.2, 13.9; minor isomer, diagnostic signals δ = 135.1, 33.3.

LC-MS (m/z): $[M\text{-Boc}+H]^+$ = 319.0, $[M+H]^+$ = 419.2. **Anal. Calc.** for $C_{21}H_{26}DN_3O_6$ (418.20): C, 60.27; H, 6.74. Found: C, 60.12; H, 6.55.

4. Redox-neutral Metal-free Three-component Carbonylative Dearomatization of Pyridine Derivatives with CO_2

All the procedures and results here described can be found in:

- A. Cerveri, S. Pace, M. Monari, M. Lombardo, M. Bandini, " Redox-neutral Metal-free Three-component Carbonylative Dearomatization of Pyridine Derivatives with CO_2" *Chem.Eur.J.* **2019**, *25*, 15272-15276.

ABSTRACT

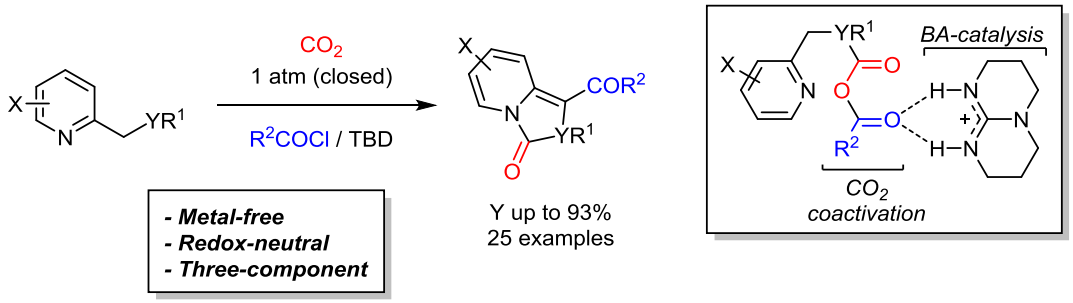

In this chapter, a novel TBD assisted three-component carbonylation of pyridine-2-methanamines is documented by means of CO_2 as a benign CO surrogate. The redox-neutral methodology enables the realization of densely functionalized imidazo-pyridinones in high yields (up to 93%), and excellent chemoselectivity and functional group tolerance (25 examples). Computational and experimental efforts on the investigation of the mechanism revealed an unprecedented electrophilic activation system of carbon dioxide based on the combined action of acid chlorides and TBD.

4.1. Background

Chemical industry is facing, along with its exponential growth, the increasing need of sustainable technologies, particularly in the area of the resource management.[47] Nowadays the majority of the carbon resources, used for a plethora of applications, are based on crude oil, natural gas and coal. Biomass is getting valorized more and more, and it's becoming an important tool in the sustainability route.[48] In addition to that, another strong candidate for a renewable carbon economy is CO_2, which is formed continuously by aerobic life on Earth and it's the major by-product of the chemical and energetic industries. Since the end of the 19th

[47] a) Dr. Kiran, D. Patil, *Journal of Current Trends in Chemical Engineering* **2014**, *2*, 2; b)J.F. Jenck, F. Agterberg, M.J. Droescher, *Green Chem.* **2004**, ***6***, 544-556.
[48] a) P. Ning, G. Yang, L.Hu, *et al. Biotechnol Biofuels* **2021**, *14,* 102. b) B. Song, R. Lin, C.H. Lam, H. Wu, T-H. Tsui, Y. Yu, *Renewable and Sustainable Energy Reviews* **2021**, *135*, 1364-0321.

century the Swedish scientist Arrhenius predicted that the growing amount of CO_2 in the atmosphere, caused by Industrialization, would have led to an increasing of the medium temperature, in relation to the already hypothesized green-house effect.[49] Although is clearly an urgent need the development of more efficient strategies for the capture and the recycle of CO_2, the chemical production alone is not enough to solve the problem, but in a sustainable perspective it can still benefit of this abundant nontoxic recyclable gas.

Carbon dioxide is the most oxidized state of carbon, which leads this linear apolar molecule to be thermodynamically stable and kinetically inert in many transformations. Due to this low-reactive nature, activation and utilization of CO_2 in the synthesis of valuable chemicals is still challenging and limited, although many efforts have been made and still are made for technologies that allow a more efficient handling.[50] There are several strategies that have been refined since the dawn of chemical industry, mainly based on the nucleophilic activation of CO_2 by adopting highly reactive substrates such as epoxides (Scheme 24a)[51] for the synthesis of cyclic carbonates or poly-carbonates, which is also an industrialized process, strong organo-metallic reagents (Scheme 24b)[52] or even phenolates and amines. For example, since the 1860s salicylic acid is majorly produced in the Kolbe-Schmitt process, in which a phenolate is directly carboxylated regio-selectively with CO_2, while in the 1922 started the production of urea by direct condensation of ammonia and CO_2 with the Bosch-Meiser process (Scheme 24c and 24d).[53]

[49] S. Arrhenius, *Philosophical Magazine* **1896**, *5(41)*, 237-276.
[50] a) M. Mikkelsen, M. Jorgensen, F. C. Krebs, *Energy Environ. Sci.* **2010,** *3*, 43–81; b) T. Sakakura, J.-C. Choi, H. Yasuda, *Chem. Rev.* **2007**, *107*, 2365–2387; c) C. Maeda, Y. Miyazaki, T. Ema, *Catal. Sci. Technol.* **2014,** *4*, 1482–1497.
[51] a) G. W. Coates, D. R. Moore, *Angew. Chem. Int. Ed*. **2004**, *43*, 6618–6639; b) T. Sakakura, K. Kohno*, The Chem. Commun.* **2009**, *11*, 1312–1330.
[52] a) G.R.M. Dowson, I. Dimitriou, R.E. Owen, D.G. Reed, R.W.K. Allen, P. Styring, *Faraday Discuss.* **2015**, *183*, 47-65; b) A. Correa, R. Martín, *Angewandte Chemie International Edition* **2009**, *48*, 6201-6204.
[53] a) D. Cameron, H. Jeskey, O. Baine, *J. Org. Chem.* **1950**, *15*, 233–236; b) W. Friedrich, *Annalen der Physik und Chemie* **1828**, *88*(2), 253-256.

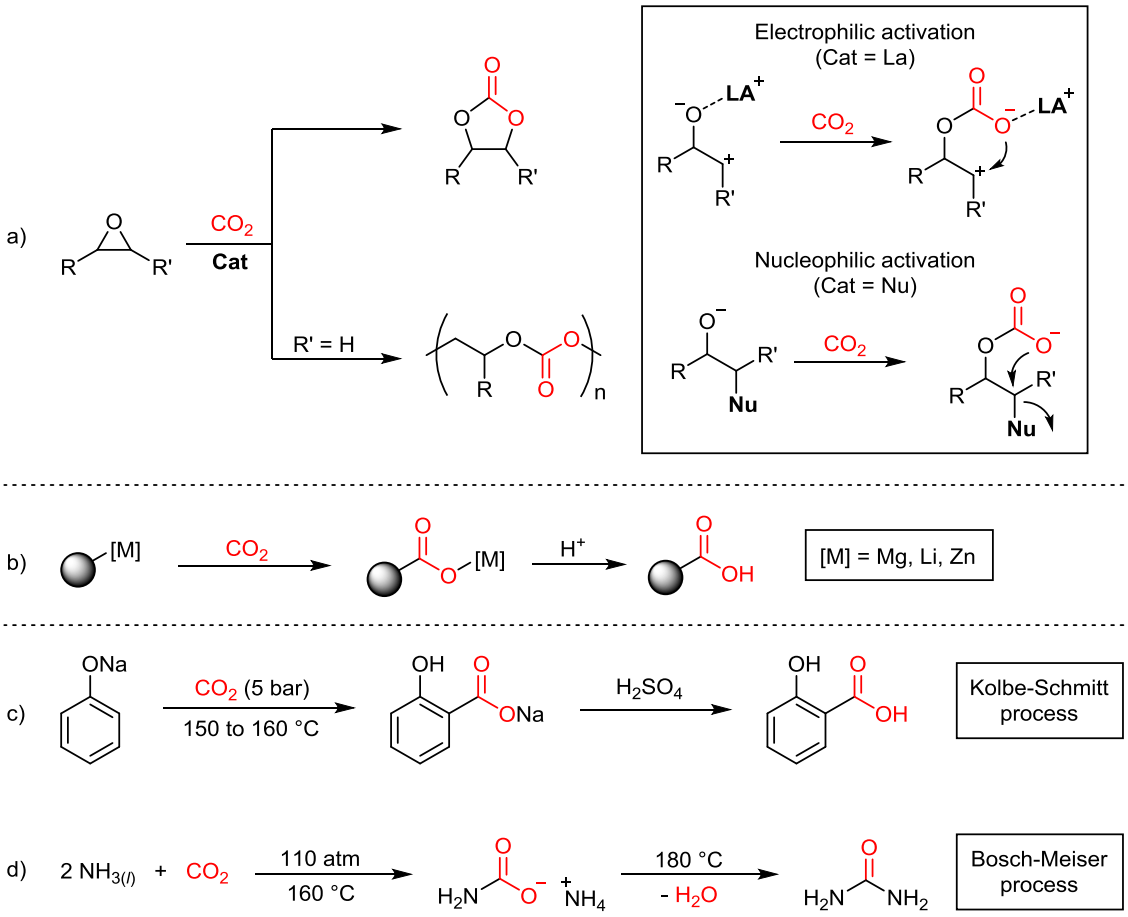

Scheme 24: a) Epoxides activation modes for the synthesis of cyclic- or poli-carbonates; b) CO_2 capture with highly reactive organo-metallic species; c) First industrialized processes employing CO_2 as C(1) synthon.

The carbonylation reaction of organic compounds is counted among the most useful synthetic methodology in organic as well as organometallic chemistry (Scheme 25a).[54] In this scenario, the ongoing seek for replacing highly toxic carbon monoxide with more environmentally benign and easy handling chemical entities is noteworthy. The use of CO_2 as a carbonylative surrogate is becoming a popular synthetic tool being a highly desirable, abundant, nontoxic one-carbon synthon.[55] Except for the synthesis of the urea, all the shown process, along with the vast majority of the CO_2 based reactions, are carboxylation reactions, meaning that the product is a carboxylic derivative (*i.e.* carboxylic acid, ester), and the product present both the oxygen atoms belonging to CO_2. Since CO_2 is electrophilic at the carbon, a strong nucleophile

[54] a) L. Kollar, in *Modern Carbonylation Methods*, Wiley-VCH, **2008**; b) M. Beller, X.-F. Wu, Transition Metal Catalyzed Carbonylation Reactions Carbonylative Activation of C-X Bonds, *Springer*, **2013**; c) S. Zhao, N.P. Mankad, *Catal. Sci. Technol.* **2019**, *9*, 3603-3613.

[55] a) Q. L, L. Wu, R. Jackstell, M. Beller, *Nat. Commun.* **2014**, *5*, 1-15; b) A. Tlili, E. Blondiaux, X. Frogneux, T. Cantat, *Green Chem.* **2015**, *17*, 157-168; c) J. Klankermayer; S. Wesselbaum, K. Beydoun, W. Leitner, *Angew. Chem. Int. Ed.* **2016**, *55*, 7296-7343; d) R. R. Shaikh, S. Pornpraprom, V. D' Elia, *ACS Catal.* **2018**, *8*, 419-450; e) C.S. Yeung, *Angew. Chem. Int. Ed.* **2019**, *58*, 2-13.

is needed to form a new C-C or C-X bond. In order to obtain a more functionalized carbonyl compound a second activation of the produced carboxylate must occur to give an activated intermediate that could further react with a second nucleophile. This activation is usually operated by an electrophile, which must be compatible with the system and not interfere with the first step of the transformation (Scheme 25).

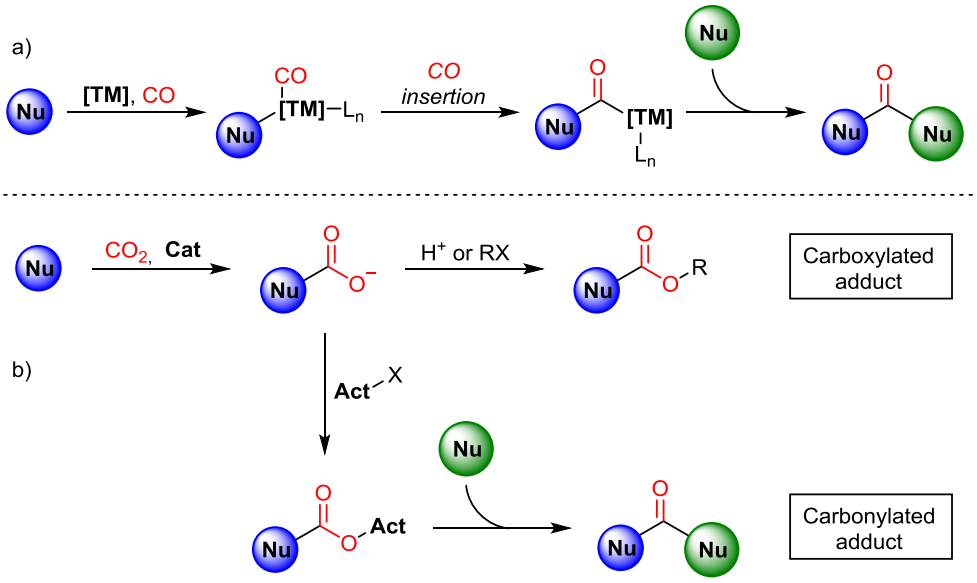

Scheme 25: a) Metal-catalyzed synthesis of carbonyl compounds using CO; b) Carbon dioxide as a surrogate of CO in carbonylation reactions.

To achieve this peculiar activation different strategies have been developed in the last decade, involving generally transition metals, strong bases, reducing agents and harsh reaction conditions. Pioneer of the field was Iwasawa and collaborators, which first developed a carbonylative C-H activation of *ortho*-alkenyl(aryl) phenols **61** to form benzo-fused six-membered conjugated cycle **62**, that was subsequently extended to aniline and ketone derivatives (Scheme 26).[56]

[56] a) K. Sasano, J. Takaya, N. Iwasawa, *J. Am. Chem. Soc.* **2013**, *135*, 10954-10957; b) Z. Zhang, L.-L. Liao, S.-S. Yan, L. Wang, Y.-Q. He, J.-H. Ye, J. Li, Y.-G. Zhi, D.-G. Yu, *Angew. Chem. Int. Ed.* **2016**, *55*, 7068-7072; c) W.-Z. Zhang, M.-W. Yang, X.-B. Lu, *Green Chem.* **2016**, *18*, 4181-4184.

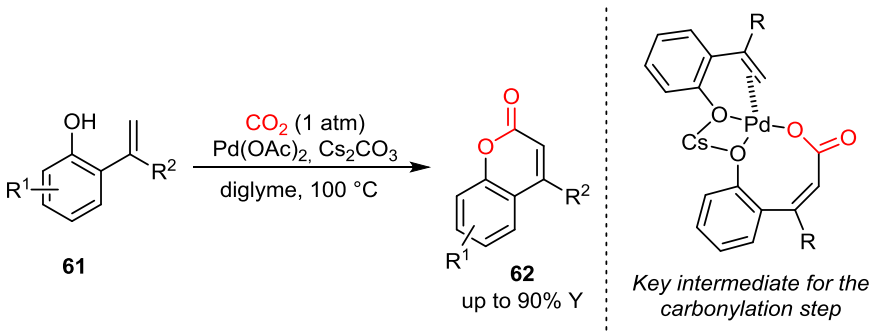

Scheme 26: Pd-catalyzed carbonylation of 2-alkenyl phenols with CO_2 by C-H activation.

This Pd-based approach is "redox-neutral", since the catalyst does not change its oxidation state, and consequently is not needed a stoichiometric reducing agent. The base, and particularly the metal counterion, plays a pivotal role in the outcome of the process. While using potassium or lithium bases is not possible to obtain the carbonylated adduct, cesium ion is capable to chelate the active palladium intermediate by the phenolic oxygen atoms, and facilitates the intramolecular condensation.

Another interesting transition metal-based carbonylation reaction has been subsequently reported by Wang and co-workers. This cyclo-carbonylation of isoquinolones **63** was performed under reductive conditions ($ZnMe_2$) and similarly to Iwasawa's procedure, is based on a directed intramolecular C-H activation of a sp^2 carbon for the synthesis of five-membered poly-cyclic scaffold **64** (Scheme 27).[57]

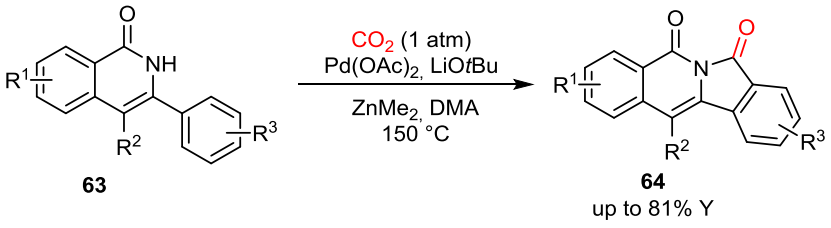

Scheme 27: Arylic C-H activation for the carbonylative cyclization of isoquinolones and CO_2.

The need of a 5d-TM and stoichiometric reductant make this process less attractive, notwithstanding the use of the poorly basic isoquinolonic nitrogen atom as directing group and the synthesis of strained cyclo-fused structures are main strengths of this process.

As evolution of this transition metal-based carbonylation chemistry, Li's group reported a ligand-promoted Rh(I)-catalyzed direct C-H carbonylation under "redox-neutral" conditions

[57] K. Yan, J. Jin, Y. Kong, B. Li, B. Wang, *Adv. Synth. Catal.* **2019**, *361*, 3080.

and atmospheric pressure of CO_2 which was assisted by the chelation of the amino group of *o*-aryl-anilines **65**, leading to the production of phenantridinones **66** (Scheme 28).[58]

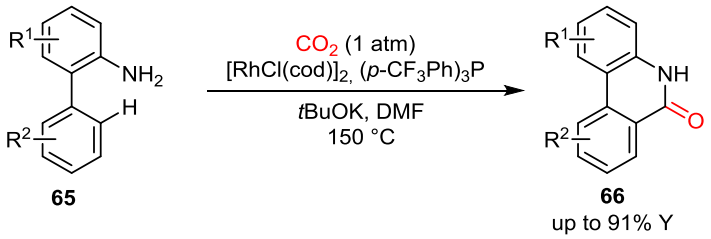

Scheme 28: Rhodium catalyzed C-H activation of 2-aryl anilines for the construction of phenantridinones scaffold.

This process, similarly, to the ones reported by Iwasawa and Wang, exploit the hetero-atom as a directing group for the metal-mediated C-H activation, which leads to the carboxylated adduct. The intermediate is then converted in the lactone/lactam derivative thanks to the combined action of the base and high temperature, favored also by the driving force of the intramolecular nature of the condensation.

Differently, when a metal-free approach is employed, the hetero-atom usually directly activates the CO_2 forming an unstable carbamic acid, which is *in-situ* activated to be trapped by the second nucleophile. Based on this concept is the recent work of Yu and co-workers,[59] which showed the metal-free carbonylation of *ortho*-alkenyl(aryl) anilines **67** by formal C-H activation (Scheme 29).

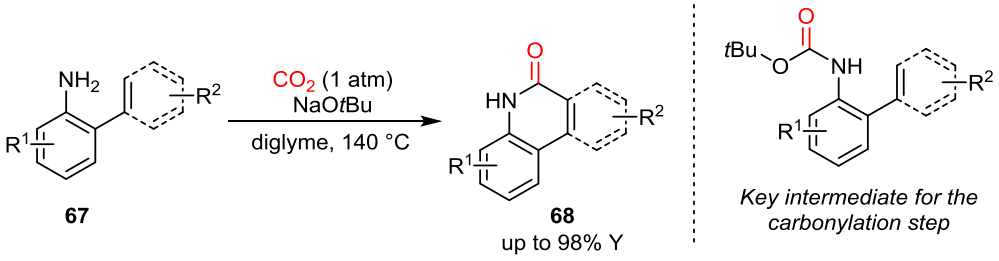

Scheme 29: Metal-free carbonylation of anylines with CO_2, by *in situ* formation of a reactive carbamate.

Various mechanistic experiments proved that the activation of the *in-situ* formed carboxylated aniline is operated by the *tert*-butoxide base, which at high temperatures can directly condensate to form the carbamate, reactive enough to engage a nucleophilic substitution with the double bond system. Also in this case the metal counter-ion of the base plays a crucial role

[58] Y. Gao, Z. Cai, S. Li, G. Li, *Org. Lett.* **2019**, *21*(10), 3663–3669.
[59] Z. Zhang, L-L. Liao, S-S. Yan, L. Wang, Y-Q. He, J-H. Ye, J. Li, Y.G. Zhi, D-G. Yu, *Angew. Chem. Int. Ed*. **2016**, *55*, 1-6.

for the chemical output; the sodium cation proved superior to other metals, acting as an oxophilic Lewis acid to promote the attack of the alkolate on the carbamic acid, leading to the elimination of sodium hydroxide and the formation of the reactive carbamate.

Another interesting example of metal-free CO_2 fixation on aromatic systems is the protocol reported by Xi and co-worker.[60] Analogously to the work of Li, 2-aryl anilines **65** were subjected to atmospheric pressure of CO_2 to obtain phenantridinones **66**, but in this case the activation for the formation of the lactam is operated by the combination of the strong electrophile MeOTf and the super-base TBD (Scheme 30). The guanidine-based hetero-cycle TBD (1,5,7-triazabicyclo[4.4.0]dec-5-ene), thanks to its charge delocalization and the engageable proton for hydrogen bonds, is capable to nucleophilic activate CO_2 and stabilize the zwitterionic intermediate that is formed. This species is formed quantitatively in solution under atmospheric pressure of CO_2 and is isolable as a stable white solid.

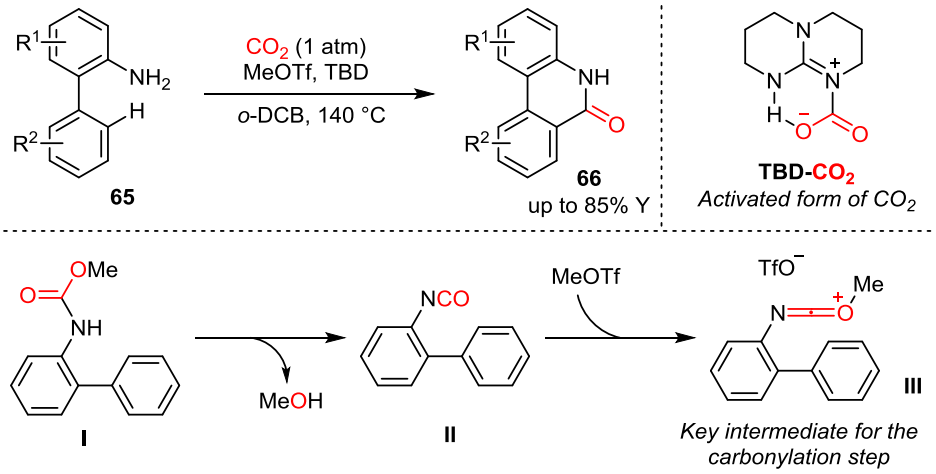

Scheme 30: MeOTf promoted carbonylation of 2-aryl anilines through formation of a highly reactive isocyanate.

The cooperation between the **TBD-CO_2** adduct and MeOTf led to the formation of the carbamate **I**, which evolves into the isocyanate **II** freeing methanol, and is further activated by a second equivalent of MeOTf forming the reactive intermediate **III** for the cyclization step.

Another particularly relevant class of molecules that can be employed in a carbonylative cyclization are pyridine derivatives. Differently from phenols and anilines, those aromatic substrates are electron-deficient and less reactive, but they also open-up an interesting strategic development: de-aromatization. Due to its nature, to lose aromaticity pyridine needs to be electrophilically activated. The so formed activated pyridinium can then evolve in two

[60] S. Wang, P. Shao, G. Du, C. Wi, *J. Org. Chem.* **2016**, *81*(15), 6672-6.

different dearomatized forms, depending on the substrate nature (Scheme 31).

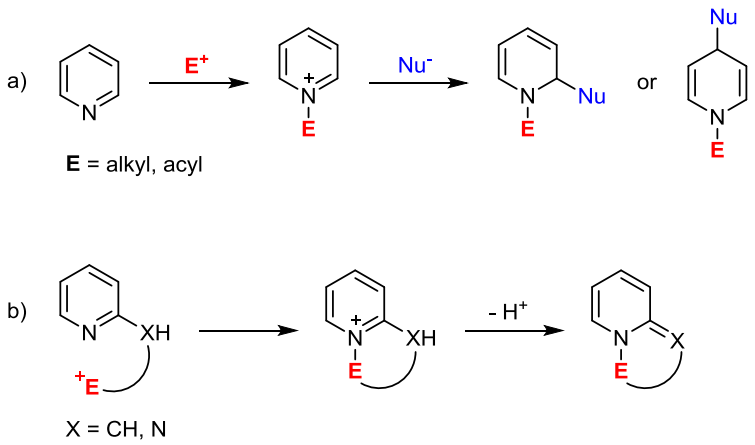

Scheme 31: a) Dearomatization of pyridine via electrophilic activation and nucleophilic attack; b) Substrate-dependant dearomatization mode of pyridine through deprotonation.

The first mode (Scheme 31a) is based on the formation of an iminium ion-like intermediate, which can be entrapped by a nucleophile in the 2- or 4- position of the aromatic ring, breaking the conjugation. This methodology has been vastly explored in the hetero-cyclic chemistry scenario achieving different regioselectivities with various nucleophiles, both organic and organo-metallic.[61] Way less explored is the intramolecular approach (Scheme 31b), where the appropriate molecular motif, after the formation of the pyridinium ion, permit the isomerization of the double bond operated by a base, leading to a differently dearomatized pyridinic scaffold. Interestingly in this case the conjugation is kept, and the resulting molecule is still planar, but Hückel's rules of aromaticity are no longer respected.

This peculiar strategy has been applied also in the formation of carbonylated dearomatized pyridines, and particularly two pivotal works of Zhu[62] showed the formation of six-membered lactams in Pd-catalyzed C(sp^2)-H activation, employing carbon monoxide as carbonyl source (Scheme 32).

[61] a) G. Bertuzzi, L. Bernardi, M. Fochi, Catalysts 2018, 8, 632; b) Q. Ding, X. Zhou, R. Fan, *Org. Biomol. Chem.*, **2014**, *12*, 4807-4815.
[62] a) D. Liang, Y. He, Q. Zhu, *Organic Letters* **2014**, *16*(10), 2748-2751; b) Z. Xie, S. Luo, Q. Zhu, *Chem. Commun.*, **2016**, *52*, 12873-12876.

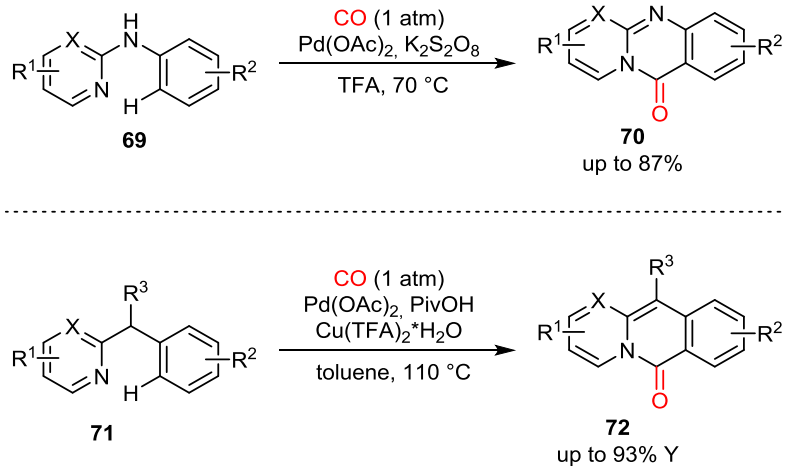

Scheme 32: Pd-catalyzed dearomative carbonylation of pyridine derivatives with CO_2.

As shown the isomerization/dearomatization step is obtainable with the appropriate conditions both with 2-amino- and 2-methylene pyridines **69** and **71**, and the so obtained cyclo-fused scaffolds **70** amd **72** are useful platforms for the synthesis of alkaloids and other relevant nitrogen based compounds. Main drawbacks of those methodologies are the need of stoichiometric oxidants needed for the turnover of the catalyst (*i.e.* $Cu(TFA)_2$, $K_2S_2O_8$) and the use of the highly toxic carbon monoxide. Accordingly, soon after a base-promoted dearomative annulation involving CO_2 as CO surrogate was disclosed by Cheng and co-workers,[63] leading to the synthesis of triazinones **74** starting from *N*-2-pyridyl amidines **73** (Scheme 33).

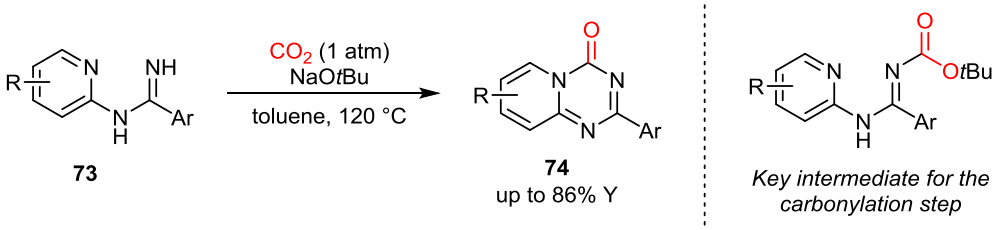

Scheme 33: Metal-free pyridyl amidines carbonylation with CO_2.

Similarly, to the carbonylation of alkenyl anilines reported by Yu, CO_2 is nuleophilically activated by the un-substituted nitrogen atom to form the carbamic acid intermediate, which is subsequently activated to undergo the acyclic nucleophilic substitution from the amino-pyridyl portion. Finally, a base-promoted isomerization breaks the aromaticity delivering the carbonylated hetero-cycle.

[63] M. Xia, W. Hu, S. Sun, J-T. Yu, J. Cheng, *Org. Biomol. Chem.*, **2017**, *15*, 4064.

Despite the undoubted efficiency of those various methodologies, various crucial issues need to be underlined. In the route to the sustainability, the requirements of TMs catalysis, strong inorganic bases (*i.e.* CsF, NaO*t*Bu, LiO*t*Bu) or super-stoichiometric electrophilic coactivators (*i.e.* MeOTf) are relatively big drawbacks, and possibly a limit in the further developments in the field.

4.2. Aim of the Project

To pursuit the topic of the dearomatization of electron-poor arenes, was decided to combine the aforementioned carbonylation strategies to tackle an ongoing "synthetic challenge" in the dearomatization reaction realm: the pyridine.[64] It should be emphasized that the use of "electrophilic" CO_2 as a reaction partner in dearomatization processes is almost unknown[65] and this can be conveniently rationalized by considering that both processes, namely CO_2 activation and aromaticity loss are highly energy demanding. Final target of the protocol would deal with the realization of a direct synthetic access to an important class of pharmacologically active bi-cyclic arenes: namely imidazo-pyridinones **A** (Scheme 34).[66] As such, a simple deconvolution of the acylated pyridinone scaffold instigated the need to verify the potential double role of acyl chlorides (*i.e.* acylating agents and electrophilic coactivators of CO_2) in a three component dearomative process involving pyridine-2-methanamines as the pyridyl reagent.

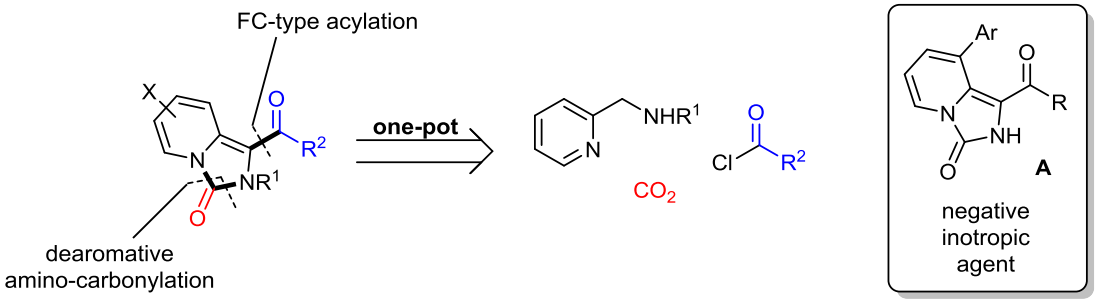

Figura 34: Working plan for the one-pot three component synthesis of imidazo-pyridinone scaffold.

[64] a) D.V. Gutsulyak, A. van der Est, G.I. Nikonov, *Angew. Chem., Int. Ed*. **2011**, *50*, 1384-1387; b) M. Zurro, S. Asmus, S. Beckendorf, C. Mu¨ck-Lichtenfeld, O.G. Manchen˜o, *J. Am. Chem. Soc*. **2014**, *136*, 13999-14002; d) Z.-P. Yang; C. Zheng, L. Huang, C. Qian, S.-L. You, *Angew. Chem. Int. Ed.* **2017**, *56*, 1530-1534.
[65] J.H. Ye, L. Zhu, S.-S. Yan, M. Miao, X.-C. Zhang, W.-J. Zhou, J. Li, Y. Lan, D.-G. Yu, *ACS Catal.* **2017**, *7*, 8324-9330.
[66] D. Davey, P.W. Erhardt, W.C. Lumma, Jr., J. Wiggins, M. Sullivan, D. Pang, E. Cantor, *J. Med. Chem.* **1987**, *30*, 1337-1342.

4.3. Discussion and Results

At the outset of the investigation, we addressed our attention to a metal-free methodology in order to positively impact the overall synthetic sustainability. In this direction, the superbase TBD was targeted as an organocatalyst[67] in the condensation of pyridine **75a** and benzoyl chloride (**76a**) under CO_2 atmosphere. Chemoselectivity (*i.e.* formation of the *N*-benzoyl-pyridine methanamide **77aa'**) as well as regioselectivity (*i.e.* site-selective final acylation) emerged as major obstacles to be faced in the titled transformation. However, upon an extensive screening of reaction conditions, it was found that the use of **75a**/**76a**/TBD/TEA (1/3/0.5/2.5) in MeCN at 140 °C (reaction time = 0.5 h) led to the pyridinyldene adduct **77aa** in 93% yield with specific acylation at the C(1)-position (Table 2, entry 1).

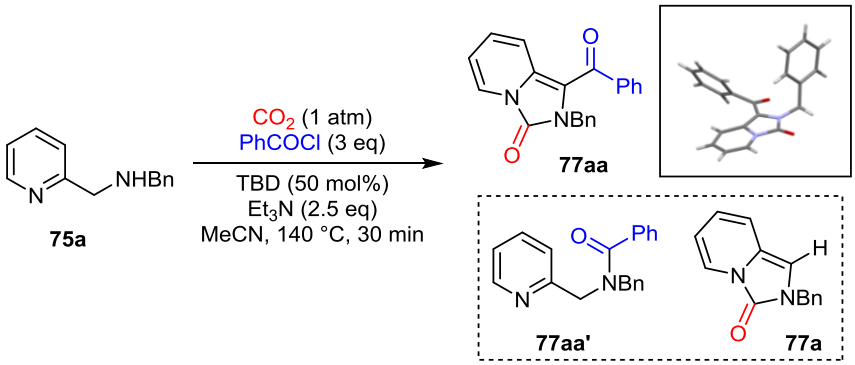

Entry[a]	Deviations from optimal	Yield (%) **77aa**[b]	Yield (%) **77aa'**[b]
1	_	93	Traces
2	No CO_2	_	95
3	TBD (3 eq) and no TEA	66	28
4[c]	Preformed TBD-CO_2 (3 eq)	55	40
5	DBU (3 eq) instead of TBD	31	58
6	DIPEA (2.5 eq) instead of TEA	71	15
7	DABCO (2.5 eq) instead of TEA	86	9
8	DABCO (50 mol%) instead of TBD	68	26
9[d]	No TBD and TEA (3 eq)	42	50
10	TBD (20 mol%) and TEA (2.8 eq)	53	41
11[d]	TESCl (3 eq) instead of PhCOCl	_	_
12[d]	Tf_2O (3 eq) instead of PhCOCl, rt	_	_
13[d]	$(PhCO)_2O$ (3 eq) instead of PhCOCl	_	91

[67] R. Nicholls, S. Kaufhold, B. N. Nguyen, *Catal. Sci. Technol.*, **2014**, *4*, 3458-3462.

14[d]	TsCl (3 eq) instead of PhCOCl	_	_

Table 2: [a] All the reactions were carried out with anhydrous solvents, unless otherwise specified. [b] Determined after flash chromatography. [c] Under N_2 atmosphere. [d] Reaction time = 3 h. X-ray structure of **77aa** is also represented.

Variations from optimal conditions resulted in a significant drop in reaction performance as highlighted in the Table 2. Interestingly, by comparing entries 3 and 4 emerged that the electrophilic activation exerted by TBD towards CO_2 was crucial for the carbonylation event. In fact, by adopting pre-formed TBD-CO_2 carbamate in the titled process (entry 4), **77aa** was isolated in comparable yield to entry 3 (55% *vs* 66%, respectively). Other tertiary amines (*i.e.* DABCO) proved less efficient with respect to TBD in the activation of the CO_2 (entry 8) while TEA was selected as acidity scavenger with respect to DIPEA and DABCO (entries 6 and 7) for the highest selectivity furnished. Attempts to lower further the TBD loading at 20 mol% (entry 10) caused a marked drop in **77aa** formation (yield = 53%) with the concomitant isolation of the amide **77aa'** in significant amount (41%). Finally, the crucial role of TBD in accelerating the CO_2 fixation was ascertained by running the model annulation with TEA (3 eq) as the only basic additive. The isolation of **77aa** in 42% yield in 3 h suggested that moderate CO_2 activation could also be exerted by the methanamine **75a** itself, probably in combination with the weak activation provided by the TEA.[68] Finally different scavengers from benzoyl chloride were tested (Table 2, entry 11-14), ranging from poorly reactive silyl chlorides to strongly electrophilic activators as triflic anhydride, but none was able to promote the desired reactivity. It is worthy to mention that in some sporadic cases the formation of **77a** in traces was observed. The protocol proved extremely high flexibility in terms of functional group tolerance performing effectively for a large variety of multi-component one-pot dearomative events. Variations on the pyridine amine congeners were operated both at the amine group and pyridyl core (**75b-q**). From the data collected in the Scheme 35 emerged that secondary benzylamines worked excellently in the process delivering the corresponding three-component adduct **77** in very good yields (up to 85%) regardless size, electronic features and substitution patterns at the benzylic site (**77ba-fa**). It is worth of mention that, also electron-rich heteroarenes (*i.e.* thiophenes) were adequately tolerated, showing high regioselectivity towards the final C(1)-imidazo-FC-acylation (**77ga**, yield = 78%). The replacement of the benzylic groups with other C(sp^3) units (*i.e.* *n*-C_5H_{11}, allyl, propargyl and $CH(C_2H_5)_2$) was also envisioned (**77ha-ka**) and good to excellent yields (up to 88%) were achieved in all

[68] J. C. Meredith, K. P. Johnston, J. M. Seminario, S. G. Kazarian and C. A. Eckert, J. *Phys. Chem.,* **1996**, *100*, 10837-10848.

cases. On the contrary, the primary pyridine-2-methanamine **75l** proved unsuitable for the titled transformation, delivering the amide **77la'** as the exclusive product. Modifications on the pyridine ring were also assessed by employing the quinoline analogous **75m** and the 6-Br derivative **75n**. In these reactions, moderate to good yields (35-54%) were obtained. Finally, the protocol was not exclusively restricted to nitrogen-based species, but also pyridyl alcohols 75**p-q** reacted smoothly under optimal conditions delivering the corresponding 3*H*-oxazolo[3,4-*a*]pyridin-3-ones **77pa** and **77qa** in 65% and 52% yield, respectively.

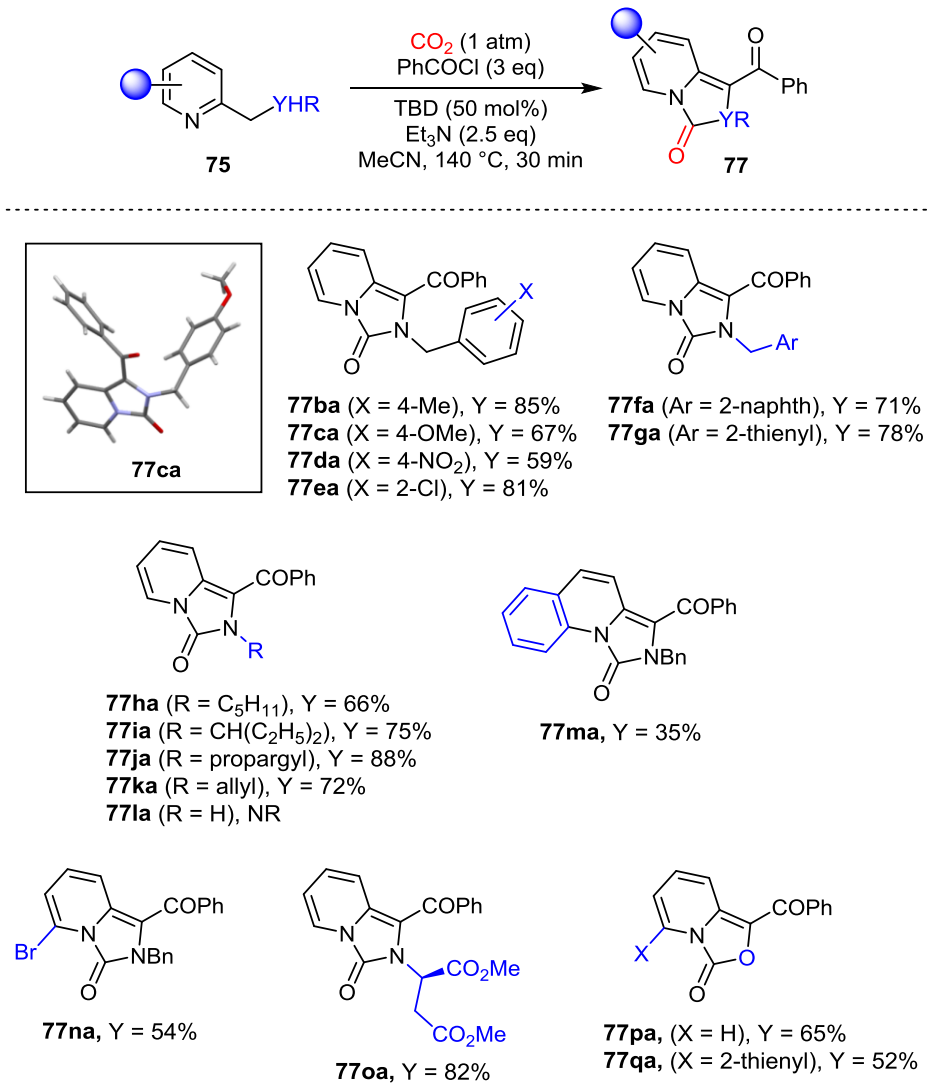

Scheme 35: Pyridine scope for the dearomative carbonylation with CO_2.

Therefore, a survey of acylating agents **76b-j** was undergone and the results collected in Scheme 36. Aromatic carboxylic acid chlorides proved effectiveness regardless the electronic nature of the substituents as well as pattern of functionalization. They can easily accommodate both electrondonating and electronwithdrawing groups delivering the

corresponding ketones **77** in up to 81% yield. Aliphatic acylating agents (**76h-i**) were also effectively tested in the titled reaction delivering the three-component adduct in useful yields: 84% and 79% respectively. Finally, was supposed that the installation of a trichloroacetyl unit at the C(1)-position would open interesting opportunities to generate carboxylic derivatives. In this regard, it was effectively verified that trichloroacetyl chloride **76j** worked smoothly in the three-component strategy resulting in **77aj** with 69% yield.

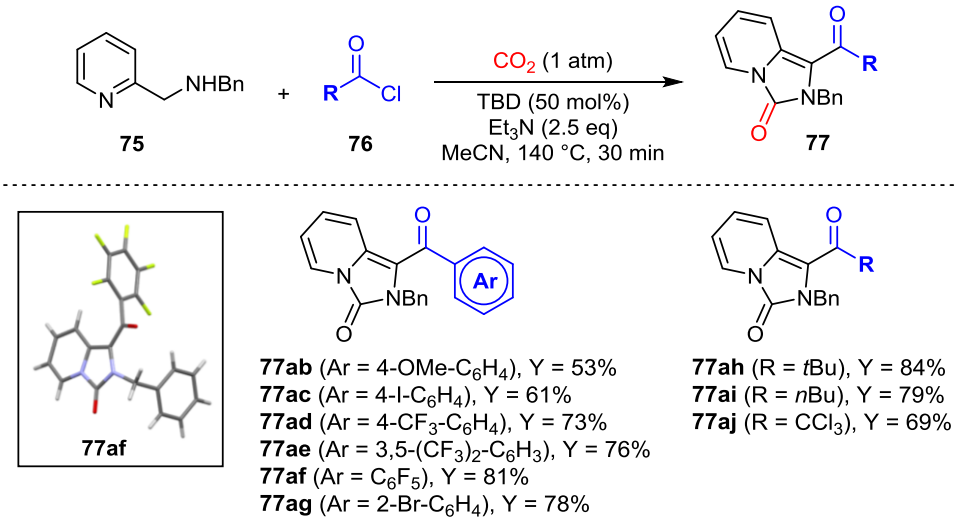

Scheme 36: Acid chloride scope for the dearomative carbonylation with CO_2.

The synthetic manipulation described in Scheme 37 clearly underlined the chemical modulability of the final compounds **77**. In particular, the trichloro derivative **77aj** was effectively subjected to methanolysis in the presence of NaH/MeOH to give the corresponding methyl ester **79aj** in 98% yield (Scheme 37b). Additionally, the partially dearomatized pyridine ring provides an expedient platform that can be conveniently (88% yield) and selectively reduced to a piperidinyl core (*i.e.* **78ia**) by means of mild reducing conditions ($Pd(OH)_2/H_2$/MeOH, Scheme 37a).

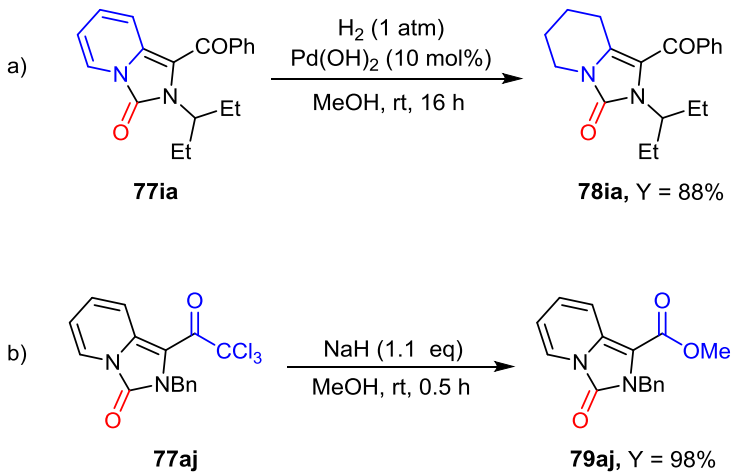

Scheme 37: Synthetic manipulation of the imidazo-pyridinone scaffold.

The attention was then moved to shed some light on the reaction profile by means of a series of dedicated experimental, spectroscopic and computational investigations. Firstly, was investigated if the species **77a** is an effective intermediate for the formation of **77aa** by subjecting it to FC-acylation in comparable conditions with the model protocol (Scheme 38a). The carbonylative events involving TBD and benzylamine **75a** was then studied. Interestingly, by monitoring the reaction of preformed TBD-CO_2[69] and **75a** in CD_3CN under nitrogen, (^{1}H-NMR and FT-IR), was discovered that a quantitative CO_2 transfer from TBD-carbamate to **75a**-CO_2 analogous occurred both at rt and 140 °C in 30 min (Scheme 38b; on the contrary, no carbonylation of **75a** occurs in absence of TBD). Therefore, **75a**-CO_2^- /$TBDH^+$ mixture (1 eq) was allowed to react with TEA (2 eq) and **76a** (3 eq) under two different environmental regimes at rt: CO_2 and N_2. Here, while the cyclization under CO_2 performed poorly, providing a **77aa**/**77a**/**77aa'** mixture only in 30% overall yield (4/3/1 ratio by ^{1}H-NMR crude), the presence of nitrogen conditions enabled the formation of a **77aa**/**77a** mixture in 82% overall yield at rt (2.2/1 ratio, Scheme 38c).

[69] C. Villiers, J.-P. Dognon, R. Pollet, P. Thuéry, M. Ephritikhine, *Angew. Chem. Int. Ed.* **2010**, *49*, 3465-3468.

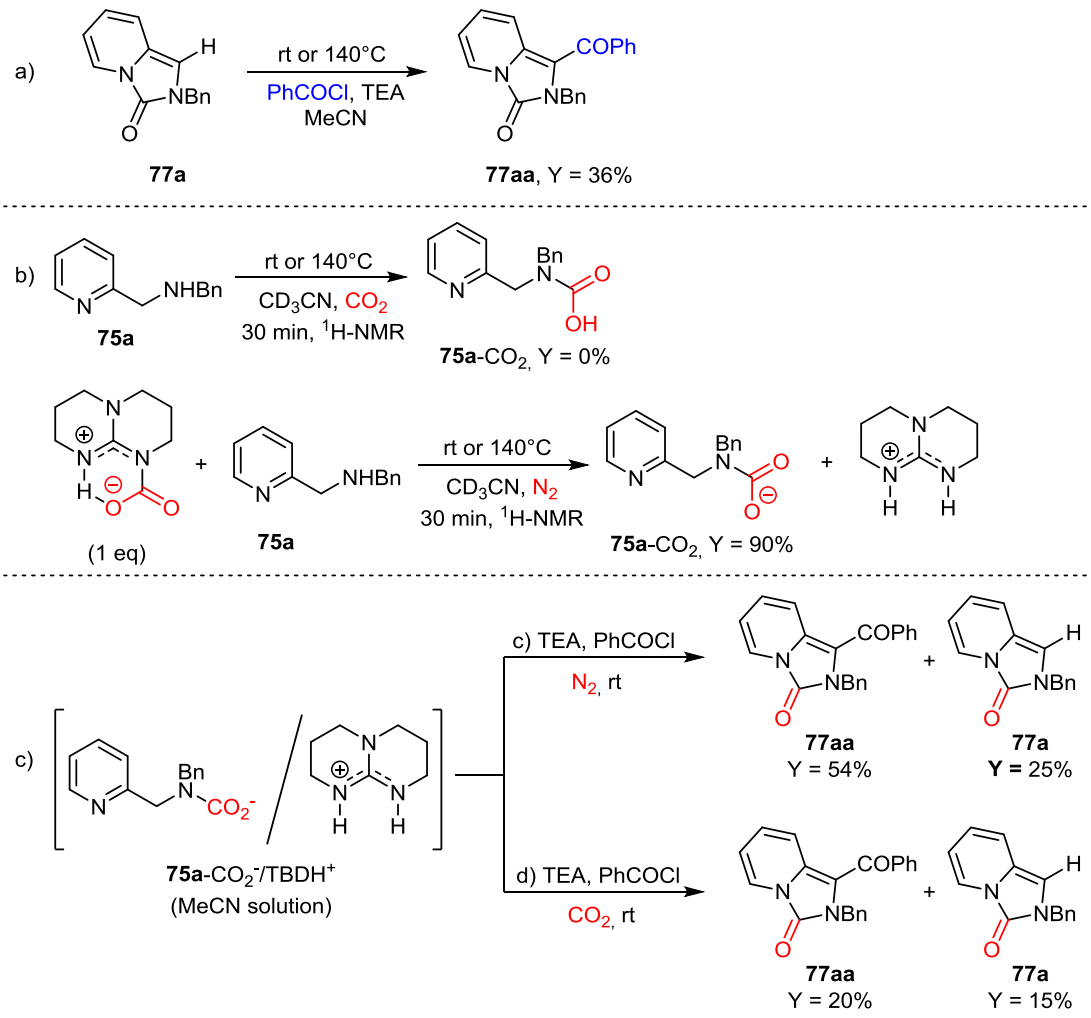

Scheme 38: Mechanistic experiments on the activation modes of the catalytic system.

These results clearly prove that 1) free TBD is essential during the whole reaction course and specifically in the initial carbonation of **75a** and during the dearomatization event of the pyridine and 2) **77a** is an intermediate of the reaction pathway that could undergo subsequent acylation reaction with the excess of chloride **76a** to leave compound **77aa**. The structural determinations of three compounds, namely **77aa**, **77ca** and **77af** by SC-XRD studies were carried out (in collaboration with Prof. Magda Monari, University of Bologna). Loss of the aromaticity involving the pyridine unit has been detected in all cases since an alternation of double and single C-C bonds was observed in the pyridine rings. Additionally, the reaction proved competence also at rt, however higher temperatures enable both better performance and the one-pot addition of all the reaction partners can be operable, concomitantly. These intriguing mechanistic insights prompted us to further explore the real role of TBD as a catalyst and the possible multiple-role played by the acid chloride. Therefore, a detailed DFT computational investigation of the reaction course relative to the formation of **77aa** was

carried out at the ω B97X-D/6-31G(d) level of theory in CH_3CN (in collaboration with Prof. Marco Lombardo, University of Bologna). From this analysis the catalytic cycle depicted in the Scheme 39 is proposed.

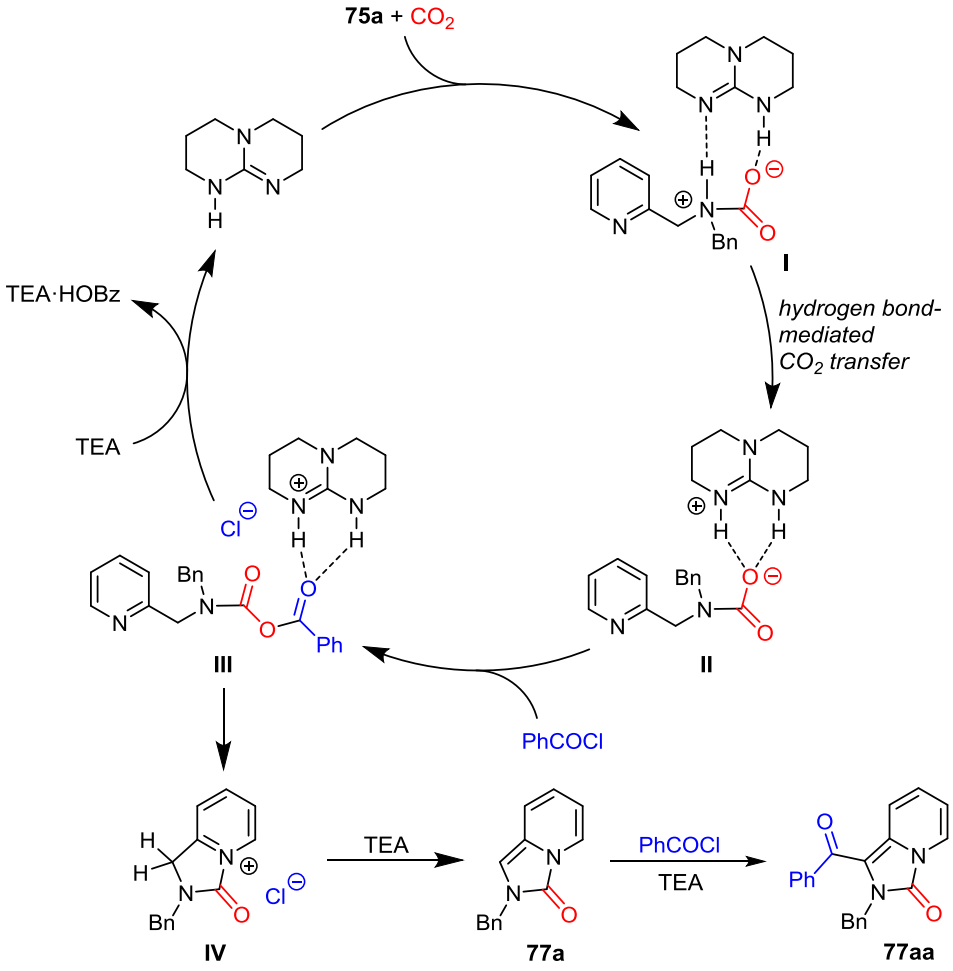

Scheme 39: Proposed catalytic cycle for the TBD-promoted dearomative carbonylation.

Interestingly, no direct transfer between TBD-CO_2 adduct and **75a** was located. Indeed, free TBD acts as a bi-functional activator first templating the approach of **75a** and CO_2 then quickly deprotonating the intermediate **I** and finally strongly stabilizing the final adduct **II** through a hydrogen-bonding network with the carbamate moiety.[70] TBD plays also a crucial role in the subsequent PhCOCl promoted cyclization of intermediate **II** to give the annulated zwitterionic intermediate **IV**. It should be emphasized also the pillar activating role played by the acyl chloride that was found in forming the highly electrophilic mixed anhydride of the carbamic acid **III**, responsible for the final dearomatization event. In this process, transition states ($\mathbf{TS_{II\text{-}III}}$ and $\mathbf{TS_{III\text{-}IV}}$) are characterized by a S_N2-like concerted mechanism, where no

[70] C. Zhang, Y. Lu, R. Zhao, W. Menberu, J. Guo, Z.-X. Wang, *Chem. Commun*. **2018**, *54*, 10870-10873.

tetrahedral intermediate is located.[71] Here the role of TBD as a Brønsted acid is again pivotal in making the benzoate unit a much better leaving group, allowing the nucleophilic attack by the pyridyl nitrogen and leading to the formation of the zwitterionic product **IV**. The final deprotonation step of **IV** to the neutral intermediate **77a** was modeled using both TEA and TDB as the base leading to very favourable exergonic reaction paths. Furthermore, the three-component adduct **77aa** could be easily obtained via Friedel-Crafts type acylation.

4.4. Conclusion

In conclusion, a redox-neutral metal-free dearomative carbonylation of pyridine derivatives with CO_2 is documented. The three-component one-pot methodology enables the realization of a large library of densely functionalized and synthetically flexible imidazo- and oxazolo-pyridinones in excellent yield and chemo/regioselective manner. The intriguing role of TBD as a promoter and RCOCl as an electrophilic CO_2 coactivator and acylating agent are proposed and disclosed by means of combined experimental, spectroscopic, and computational investigations.

[71] F. Ruff, Ö. Farkas, *J. Phys. Org. Chem.* **2011**, *24*, 480-491.

4.5. General Procedures and Product Characterization

4.5.1. Materials and Methods

^{1}H-NMR spectra were recorded on Varian 400 (400 MHz) spectrometer. Chemical shifts are reported in ppm from TMS with the solvent resonance as the internal standard (deuterochloroform: 7.26 ppm). Data are reported as follows: chemical shift, multiplicity (s = singlet, d = doublet, t = triplet, q = quartet, sext = sextet, sept = septet, p = pseudo, b = broad, m = multiplet, dm = double multiplet), coupling constants (Hz). ^{13}C-NMR spectra were recorded on a Varian 400 (100 MHz) spectrometer with complete proton decoupling. Chemical shifts are reported in ppm from TMS with the solvent as the internal standard (deuterochloroform: 77.0 ppm). GC-MS spectra were taken by EI ionization at 70 eV on a Hewlett-Packard 5971 with GC injection. They are reported as: m/z (rel. intensity). LC-electrospray ionization mass spectra were obtained with an Agilent Technologies MSD1100 (nebulizer: 15.0 PSI, dry Gas: 5.0 L/min, dry temperature: 325 °C, capillary voltage positive scan: 4000 mA, capillary voltage negative scan: 3500 mA) single quadrupole mass spectrometer. Chromatographic purification was done with 240-400 mesh silica gel. Anhydrous solvents were supplied by Sigma Aldrich in Sureseal® bottles and used without any further purification. Commercially available chemicals were purchased from Sigma Aldrich, Stream and TCI and used without any further purification. Melting points were determined with Bibby Stuart Scientific Melting Point Apparatus SMP 3 and are not corrected.

4.5.2. General procedure for the synthesis of 2-pyridylmethanamines from 2-picolylamine

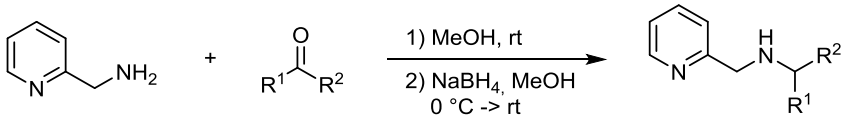

S-1 **75**

A mixture of 2-picolylamine **S-1** (5.0 mmol) and aldehyde (5.0 mmol) in 40 ml of MeOH was stirred at room temperature for 1 hours. The solution was cooled at 0 °C, $NaBH_4$ (10 mmol) was added in small portions. The mixture was slowly warmed at room temperature and stirred for 1 hour. Solvent was removed and the residue was re-dissolved in CH_2Cl_2, washed with a solution of NaOH 2M, then washed with saturated Na_2CO_3 solution twice, with a solution of brine and dried over with Na_2SO_4. Solvents were removed under vacuum to give the crude N-alkyl-1-(pyridin-2-yl)methanamine **75**. Further purification by flash column chromatography

yielded the product.

N-(4-methylbenzyl)-1-(pyridin-2-yl)methanamine (**75b**)

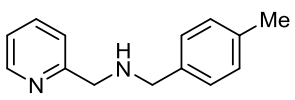

Pale yellow oil; yield = 78% (DCM:MeOH = 20:1). **^{1}H NMR** (400 MHz, $CDCl_3$) δ = 8.51 (d, J = 4.7 Hz, 1H), 7.55 (td, J = 7.6, 1.7 Hz, 1H), 7.25 (d, J = 7.5 Hz, 1H), 7.21 (d, J = 7.9 Hz, 2H), 7.08 (dd, J = 10.4, 6.7 Hz, 3H), 3.87 (s, 2H), 3.76 (s, 2H), 2.28 (s, 3H), 2.21 (s, 1H). **^{13}C NMR** (100 MHz, $CDCl_3$) δ = 159.8, 149.2, 137.1, 136.3, 129.0 (2C), 128.2 (2C), 122.2, 121.8, 54.4, 53.2, 21.1. **LC-MS** (m/z): $[M+H]^+$ = 213.0, $[M+Na]^+$ = 235.0. **Anal. Calc.** for ($C_{14}H_{16}N_2$: 212.30): C, 79.21; H, 7.60; found: C, 79.01; H, 7.38.

N-(4-methoxybenzyl)-1-(pyridin-2-yl)methanamine (**75c**)

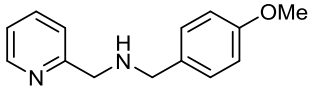

Yellow oil; yield = 75% (DCM:MeOH = 20:1). **^{1}H NMR** (400 MHz, $CDCl_3$) δ = 8.49 (d, J = 4.8 Hz, 1H), 7.55 (td, J = 7.7, 1.7 Hz, 1H), 7.26 – 7.19 (m, 3H), 7.07 (dd, J = 7.0, 5.3 Hz, 1H), 6.80 (dd, J = 9.0, 2.4 Hz, 2H), 3.85 (s, 2H), 3.74 – 3.68 (m, 5H), 2.42 (brs, 1H). **^{13}C NMR** (100 MHz, $CDCl_3$) δ = 159.7, 158.6, 149.2, 136.3, 132.2, 129.4 (2C), 122.3, 121.8, 113.7 (2C), 55.2, 54.3, 52.8. **LC-MS** (m/z): $[M+H]^+$ = 229.0, $[M+Na]^+$ =251.0, $[2M+Na]^+$ = 479.2. **Anal. Calc.** for ($C_{14}H_{16}N_2O$: 228.38): C, 73.66; H, 7.06; found: C, 73.41; H, 5.91.

N-(4-nitrobenzyl)-1-(pyridin-2-yl)methanamine (**75d**)

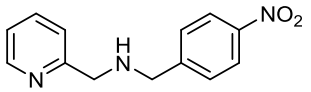

Orange oil; yield = 74% (DCM:MeOH = 20:1). **^{1}H NMR** (400 MHz, $CDCl_3$) δ = 8.55 (d, J = 4.2 Hz, 1H), 8.16 (d, J = 8.7 Hz, 2H), 7.63 (td, J = 7.7, 1.7 Hz, 1H), 7.53 (d, J = 8.8 Hz, 2H), 7.28 – 7.23 (m, 1H), 7.16 (dd, J = 7.2, 5.1 Hz, 1H), 3.93 (s, 2H), 3.91 (s, 2H), 2.21 (brs, 1H). **^{13}C NMR** (100 MHz, $CDCl_3$) δ = 158.8, 149.3, 147.7, 147.0, 136.6, 128.8 (2C), 123.6 (2C), 122.3, 54.2, 52.5. **LC-MS** (m/z): $[M+H]^+$ = 244.0, $[M+Na]^+$ = 266.2. **Anal. Calc.** for ($C_{13}H_{13}N_3O_2$: 243.27): C, 64.19; H, 5.39; found: C, 64.01; H, 5.20.

N-(2-chlorobenzyl)-1-(pyridin-2-yl)methanamine (**75e**)

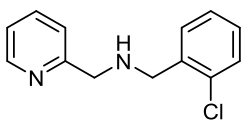

Colorless oil; yield = 73% (c-Hex:AcOEt = 1:1). **^{1}H NMR** (400 MHz, $CDCl_3$) δ = 8.49 – 8.46 (m, 1H), 7.53 (td, J = 7.7, 1.8 Hz, 1H), 7.37 (dd, J = 7.4, 1.8 Hz, 1H), 7.27 – 7.23 (m, 2H), 7.17 – 7.02 (m, 3H), 3.86 (s, 4H), 2.30 (brs, 1H). **^{13}C NMR** (100 MHz, $CDCl_3$) δ = 159.62, 149.19, 137.49, 136.31,

133.68, 130.01, 129.37, 128.18, 126.72, 122.14, 121.85, 54.43, 50.75. **LC-MS** (m/z): $[M+H]^+$ = 233.2, $[M+Na]^+$ = 256.2, $[2M+Na]^+$ = 489.4. **Anal. Calc.** for ($C_{13}H_{13}ClN_3$: 232.71): C, 67.10; H, 5.63; found: C, 67.00; H, 5.31.

1-(Naphthalen-2-yl)-*N*-(pyridin-2-ylmethyl)methanamine (**75f**)

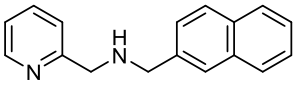

Yellow oil; yield = 68% (c-Hex:AcOEt = 4:1). **^{1}H NMR** (400 MHz, $CDCl_3$) δ = 8.55 (dd, J = 4.8, 0.7 Hz, 1H), 7.82 – 7.75 (m, 4H), 7.56 – 7.37 (m, 4H), 7.23 (d, J = 7.9 Hz, 1H), 7.09 – 7.03 (m, 1H), 3.96 (s, 2H), 3.93 (s, 2H), 2.29 (brs, 1H). **^{13}C NMR** (100 MHz, $CDCl_3$) δ = 159.8, 149.3, 137.8, 136.3, 133.5, 132.7, 128.0, 127.7, 126.6, 126.0, 125.5, 122.3, 121.9, 54.6, 53.6. **GC-MS** (m/z): 93 (100), 156 (61). **Anal. Calc.** for ($C_{17}H_{16}N_2$: 248.33): C, 82.22; H, 6.49; found: C, 82.02; H, 6.28.

N-(pyridin-2-ylmethyl)pentan-1-amine (**75h**)

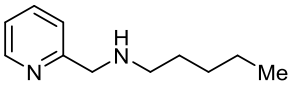

Yellow oil; yield = 43% (DCM:MeOH = 20:1). **^{1}H NMR** (400 MHz, $CDCl_3$) δ 8.51 – 8.41 (m, 1H), 7.59 – 7.51 (m, 1H), 7.27 – 7.19 (m, 1H), 7.06 (dd, J = 6.7, 5.1 Hz, 1H), 3.83 (s, 2H), 2.60 – 2.56 (m, 2H), 2.44 (brs, 1H), 1.47-1.44 (m, 2H), 1.28 – 1.12 (m, 4H), 0.87 – 0.69 (m, 3H). **^{13}C NMR** (100 MHz, $CDCl_3$) δ = 159.8, 149.2, 136.3, 122.2, 121.8, 55.2, 49.6, 29.7, 29.4, 22.5, 14.0. **GC-MS** (m/z): 121 (21); 93 (100). **Anal. Calc.** for ($C_{11}H_{18}N_2$: 178.28): C, 74.11; H, 10.18; found: C, 73.89; H, 10.06.

N-(pyridin-2-ylmethyl)pentan-3-amine (**75i**)

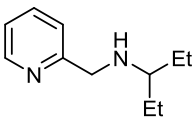

Yellow oil; yield = 34% (DCM:MeOH = 10:1). **^{1}H NMR** (400 MHz, $CDCl_3$) δ = 8.47 (d, J = 4.8 Hz, 1H), 7.55 (td, J = 7.7, 1.8 Hz, 1H), 7.29 – 7.22 (m, 1H), 7.08 – 7.02 (m, 1H), 3.82 (s, 2H), 2.39.2.37 (m, 1H), 2.07 (brs, 1H), 1.48 – 1.36 (m, 4H), 0.84 (t, J = 7.5 Hz, 6H). **^{13}C NMR** (100 MHz, $CDCl_3$) δ = 160.3, 149.1, 136.2, 122.2, 121.7, 59.7, 52.5, 25.7 (2C), 9.77 (2C). **LC-MS** (m/z): $[M+H]^+$ = 179.2; $[M+Na]^+$ = 201.0; $[2M+Na]^+$ = 379.2. **Anal. Calc.** for ($C_{11}H_{18}N_2$: 178.28): C, 74.11; H, 10.18; found: C, 73.99; H, 10.16.

4.5.3. General procedure for the synthesis of 2-pyridylmethanamines from 2-pyridinecarboxaldehydes

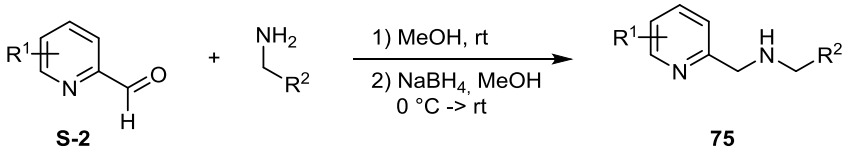

A mixture of 2-pyridinecarboxaldehyde **S-2** (2 mmol) and amine (2 mmol) in MeOH (16 mL) was stirred at room temperature for 1 h. The solution was cooled in an ice bath and $NaBH_4$ (4 mmol) was added in small portions. The mixture was slowly warmed at room temperature and stirred for 1 hour. Solvent was removed and the residue was re-dissolved in CH_2Cl_2, washed with a solution of NaOH 2M, then washed with saturated Na_2CO_3 solution twice and with a solution of brine and dried over Na_2SO_4. Solvents were removed by rotatory evaporation to give the crude mixture. Further purification by flash column chromatography yielded the product **75**.

N-(pyridin-2-ylmethyl)prop-2-en-1-amine (**75k**)

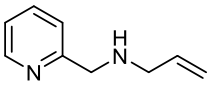

Orange oil; yield = 86% (DCM:MeOH = 10:1). **^{1}H NMR** (400 MHz, $CDCl_3$) δ = 8.39 (dd, J = 4.8, 0.7 Hz, 1H), 7.46 (td, J = 7.7, 1.8 Hz, 1H), 7.14 (d, J = 7.8 Hz, 1H), 7.02 – 6.92 (m, 1H), 5.78 (ddt, J = 17.1, 10.3, 6.0 Hz, 1H), 5.05 (ddd, J = 17.2, 1.6 Hz, 1H), 4.95 (ddd, J = 10.3, 3.0, 1.3 Hz, 1H), 3.75 (s, 2H), 3.14 (dt, J = 6.0, 1.4 Hz, 2H), 2.11 (s, 1H). **^{13}C NMR** (100 MHz, $CDCl_3$) δ = 159.6, 149.1, 136.5, 136.2, 122.1, 121.7, 115.9, 54.3, 51.8. **LC-MS** (m/z): $[M+H]^+$ = 149.0; $[M+Na]^+$ = 171.0. **Anal. Calc.** for ($C_9H_{12}N_2$: 148.21): C, 72.94; H, 8.16; found: C, 72.65; H, 8.01.

N-benzyl-1-(6-bromopyridin-2-yl)methanamine (**75n**)

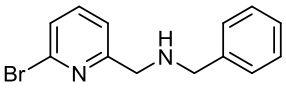

Pale yellow oil; yield = 79% (cHex:AcOEt = 4:1). **^{1}H NMR** (400 MHz, $CDCl_3$) δ = 7.45 (t, J = 7.7 Hz, 1H), 7.34 – 7.19 (m, 6H), 3.86 (s, 2H), 3.79 (s, 2H), 2.32 (brs, 1H). **^{13}C NMR** (100 MHz, $CDCl_3$) δ 161.6, 141.7, 139.8, 138.8, 128.4 (2C), 128.2 (2C), 127.1, 126.2, 121.0, 53.8, 53.4. **LC-MS** (m/z): $[M+H]^+$ = 278.0; $[M+Na]^+$ = 300.2; $[2M+Na]^+$ = 577.2. **Anal. Calc.** for ($C_{13}H_{13}BrN_2$: 277.17): C, 56.34; H, 4.73; found: C, 56.19; H, 4.69.

4.5.4. General procedure for TBD-catalyzed dearomatization of 2-picolylamines with acid chlorides

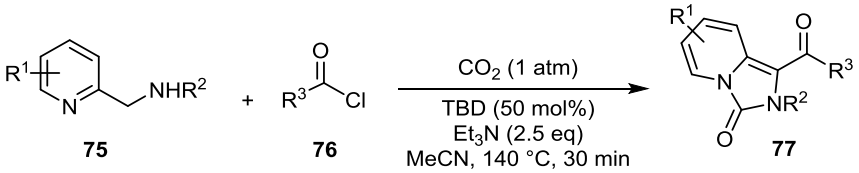

An oven-dried Schlenk tube, filled with nitrogen atmosphere, was charged with MeCN (1.0

mL), amine **75** (0.2 mmol, 1.0 eq), triethylamine (0.5 mmol, 2.5 eq) and 1,5,7-triazabicyclo[4.4.0]dec-5-ene (13.9 mg, 50 mol%). Then the nitrogen was evacuated, and the reactor was filled with CO_2 (1 atm). This procedure was repeated twice. Finally, the acyl chloride **76** was added (0.6 mmol, 3.0 eq) and the reactor was placed in a pre-heated oil bath at 140 °C. After 30 min the reaction was cooled at rt, and the solution was quenched with NaOH 2M (1 mL) and extracted with EtOAc (3 x 3 mL). The crude product was then purified by flash chromatography to afford pure compound **77**.

1-Benzoyl-2-benzylimidazo[1,5-a]pyridin-3(2H)-one (**77aa**)

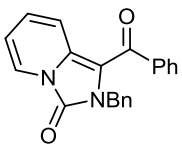

Yellow solid, yield = 93% (61 mg, cHex:AcOEt = 3:1). **M.p.** = 153.3-155.7 °C. **^{1}H NMR** (400 MHz, $CDCl_3$) δ = 7.95 (d, J = 7.1 Hz, 1H), 7.60 – 7.53 (m, 3H), 7.45 (dd, J = 9.0, 7.4 Hz, 4H), 7.32 – 7.22 (m, 3H), 6.76 (ddd, J = 9.5, 6.5, 1.0 Hz, 1H), 6.48 (dd, J = 10.0, 3.6 Hz, 1H), 6.34 (d, J = 9.5 Hz, 1H), 5.66 (s, 2H). **^{13}C NMR** (100 MHz, $CDCl_3$) δ = 183.20, 148.28, 140.57, 137.65, 133.67, 131.79, 130.26, 128.89 (2C), 128.63 (2C), 128.50 (2C), 128.47 (2C), 127.76, 124.25, 118.01, 111.94, 110.40, 46.49. **LC-MS** (m/z): $[M+H]^+$ = 329.0, $[M+Na]^+$ = 679.2.**Anal. Calc.** for ($C_{21}H_{16}N_2O_2$: 328.12): C, 76.81; H, 4.91; found: C, 76.59; H, 4.68.

2-Benzyl-1-(4-methoxybenzoyl)imidazo[1,5-a]pyridin-3(2H)-one (**77ab**)

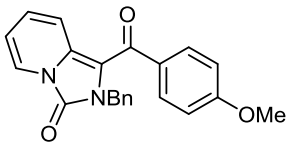

Green oil, yield = 53% (38 mg, cHex:AcOEt = 2:1). **^{1}H NMR** (400 MHz, $CDCl_3$) δ = 7.92 (d, J = 7.1 Hz, 1H), 7.60 (d, J = 8.7 Hz, 2H), 7.40 (d, J = 7.1 Hz, 2H), 7.25 (dt, J = 13.5, 5.9 Hz, 3H), 6.94 (d, J = 8.7 Hz, 2H), 6.75 (dd, J = 9.4, 6.5 Hz, 1H), 6.52 (d, J = 9.5 Hz, 1H), 6.44 (t, J = 6.7 Hz, 1H), 5.62 (s, 2H), 3.88 (s, 3H). **^{13}C NMR** (100 MHz, $CDCl_3$) δ = 182.30, 162.72, 148.11, 137.54, 132.69, 130.80, 130.74 (2C), 128.45 (2C), 128.27 (2C), 128.16, 127.54, 123.91, 117.94, 113.92 (2C), 111.44, 110.32, 55.43, 46.13. **LC-MS** (m/z): $[M+H]^+$ = 359.0, $[M+Na]^+$ = 381.2, $[2M+Na]^+$ = 739.2. **Anal. Calc.** for ($C_{22}H_{18}N_2O_3$: 358.13): C, 73.73; H, 5.06; found: C, 73.61; H, 4.81.

2-Benzyl-1-(4-iodobenzoyl)imidazo[1,5-a]pyridin-3(2H)-one (**77ac**)

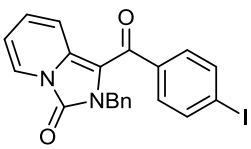

Yellow solid, yield = 61% (55 mg, cHex:AcOEt = 5:1). **M.p.** = 181.9-183.5 °C. **^{1}H NMR** (400 MHz, $CDCl_3$) δ = 7.96 (d, J = 7.1 Hz, 1H), 7.81 (d, J = 8.0 Hz, 2H), 7.41 (d, J = 7.1 Hz, 2H), 7.32 (d, J = 8.0 Hz, 2H), 7.30 – 7.22 (m, 3H), 6.84 (dd, J = 9.4, 6.5 Hz, 1H), 6.51 (t, J = 6.8 Hz, 1H), 6.44 (d, J =

9.5 Hz, 1H), 5.62 (s, 2H). **^{13}C NMR** (100 MHz, $CDCl_3$) δ = 181.70, 148.06, 139.69, 137.98 (2C), 137.38, 131.79, 129.96 (2C), 129.31, 128.49 (2C), 128.28 (2C), 127.66, 124.27, 117.67, 111.93, 109.91, 98.69, 46.33. **LC-MS** (m/z): $[M+H]^+$ = 455.2, $[M+Na]^+$ = 477.2, $[2M+Na]^+$ = 931.2. **Anal. Calc.** for ($C_{21}H_{15}IN_2O_2$: 454.02): C, 55.52; H, 3.33; found: C, 55.39; H, 3.18.

2-Benzyl-1-(4-(trifluoromethyl)benzoyl)imidazo[1,5-a]pyridin-3(2H)-one (**77ad**)

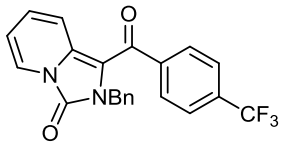

Green solid, yield = 73% (58 mg, cHex:AcOEt = 5:1). **M.p.** = 154.5-156.2 °C. **^{1}H NMR** (400 MHz, $CDCl_3$) δ = 7.95 (d, J = 7.1 Hz, 1H), 7.65 (dd, J = 19.5, 8.3 Hz, 4H), 7.38 (d, J = 7.0 Hz, 2H), 7.29 – 7.15 (m, 4H), 6.81 (dd, J = 9.3, 6.6 Hz, 1H), 6.50 (t, J = 6.8 Hz, 1H), 6.27 (d, J = 9.4 Hz, 1H), 5.60 (s, 2H). **^{13}C NMR** (100 MHz, $CDCl_3$) δ = 181.06, 148.05, 143.66, 137.34, 133.14 (q, J = 32.1 Hz, 1C), 132.25, 129.81, 128.62 (2C), 128.52 (2C), 128.30 (2C), 127.71, 125.82 (q, J = 3.7 Hz, 2C), 124.45,123.62 (q, J = 271.2 Hz, 1C), 117.42, 112.12, 109.85, 46.46. **^{19}F NMR** (376 MHz, $CDCl_3$) δ = -62.87. **LC-MS** (m/z): $[M+H]^+$ = 397.0, $[M+Na]^+$ = 419.2, $[2M+Na]^+$ = 815.2. **Anal. Calc.** for ($C_{22}H_{15}F_3N_2O_2$: 396.11): C, 66.67; H, 3.81; found: C, 66.50; H, 3.69.

2-Benzyl-1-(3,5-bis(trifluoromethyl)benzoyl)imidazo[1,5-a]pyridin-3(2H)-one (**77ae**)

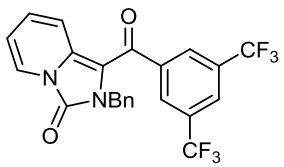

Brown oil, yield = 76% (71 mg, cHex:AcOEt = 6:1). **^{1}H NMR** (400 MHz, $CDCl_3$) δ = 8.02 (m, 3H), 7.41 (d, J = 6.8 Hz, 2H), 7.33 – 7.21 (m, 4H), 6.96 (ddd, J = 9.5, 6.6, 1.1 Hz, 1H), 6.68 – 6.61 (m, 1H), 6.36 (d, J = 9.5 Hz, 1H), 5.65 (s, 2H). **^{13}C NMR** (100 MHz, $CDCl_3$) δ = 178.51, 148.02, 142.10, 137.10, 132.63, 132.34 (q, J = 34.0 Hz, 2C), 130.74, 128.69 (d, J = 3.4 Hz, 2C), 128.58 (2C), 128.23 (2C), 127.84, 124.88, 124.79 (q, J = 3.8 Hz, 1C), 122.79 (q, J = 271.3 Hz, 2C), 116.78, 112.55, 109.45, 46.65. **^{19}F NMR** (376 MHz, $CDCl_3$) δ = -62.94. **LC-MS** (m/z): $[M+H]^+$ = 465.2, $[M+Na]^+$ = 487.2. **Anal. Calc.** for ($C_{23}H_{14}F_6N_2O_2$: 464.10): C, 59.49; H, 3.04; found: C, 59.32; H, 2.90.

2-Benzyl-1-(perfluorobenzoyl)imidazo[1,5-a]pyridin-3(2H)-one (**77af**)

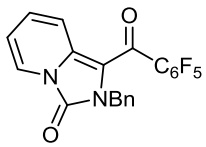

Yellow solid, yield = 81% (68 mg, cHex:AcOEt = 4:1). **M.p.** = 175.8-177.3 °C. **^{1}H NMR** (400 MHz, $CDCl_3$) δ = 8.12 (d, J = 7.0 Hz, 1H), 7.44 (d, J = 6.7 Hz, 2H), 7.34 – 7.25 (m, 3H), 7.14 (dd, J = 8.8, 7.2 Hz, 1H), 6.72 (t, J = 6.8 Hz, 1H), 6.41 (brs, 1H), 5.68 (s, 2H). **^{13}C NMR** (100 MHz, $CDCl_3$) δ = 166.00, 147.64, 143.49 (dm, J = 250.3 Hz, 2C), 142.24 (dm, J = 256.7 Hz, 1C), 137.76 (dm, J = 255.4Hz, 2C), 136.74, 133.83, 132.59, 128.48 (2C), 128.13, 127.76 (2C), 125.41, 115.95, 115.55 (t, J = 19.4

Hz, 1C), 113.17, 110.61, 46.92. **^{19}F NMR** (376 MHz, $CDCl_3$) δ = -141.56 (dd, J = 22.1, 7.3 Hz, 2F), -150.70 (t, J = 20.1 Hz, 1F), -158.98 (m, 2F). **LC-MS** (m/z): $[M+H]^+$ = 419.0, $[M+Na]^+$ = 441.2. **Anal. Calc.** for ($C_{21}H_{11}F_5N_2O_2$: 418.07): C, 60.30; H, 2.65; found: C, 60.19; H, 2.33.

2-Benzyl-1-(2-bromobenzoyl)imidazo[1,5-a]pyridin-3(2H)-one (**77ag**)

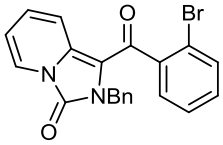

Yellow solid, yield = 78% (63 mg, cHex:AcOEt = 4:1). **M.p.** = 128.4-129.3 °C. **^{1}H NMR** (400 MHz, $CDCl_3$) δ = 8.00 (d, J = 7.0 Hz, 1H), 7.65 (d, J = 7.8 Hz, 1H), 7.53 (d, J = 7.5 Hz, 2H), 7.44 – 7.34 (m, 2H), 7.34 – 7.23 (m, 4H), 6.87 – 6.81 (m, 1H), 6.55 (t, J = 6.8 Hz, 1H), 5.87 (d, J = 9.4 Hz, 1H), 5.74 (d, J = 9.5 Hz, 2H). **^{13}C NMR** (100 MHz, $CDCl_3$) δ =179.86, 147.94, 141.91, 137.39, 133.48, 132.86, 131.11, 130.46, 128.61 (2C), 128.60, 128.38 (2C), 128.01, 127.61, 124.49, 119.72, 117.06, 112.32, 109.67, 46.65. **LC-MS** (m/z): $[M+H]^+$ = 407.2, $[M+Na]^+$ = 429.2, $[2M+Na]^+$ = 835.2. **Anal. Calc.** for ($C_{21}H_{15}BrN_2O_2$: 407.27): C, 61.93; H, 3.71; found: C, 61.65; H, 3.41.

2-Benzyl-1-pivaloylimidazo[1,5-a]pyridin-3(2H)-one (**77ah**)

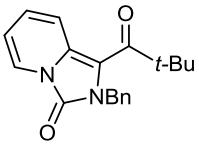

Brown solid, yield = 84% (52 mg, cHex:AcOEt = 4:1). **M.p.** = 130.8-131.6 °C. **^{1}H NMR** (400 MHz, $CDCl_3$) δ = 7.88 (d, J = 7.1 Hz, 1H), 7.34 (d, J = 9.6 Hz, 1H), 7.25 – 7.17 (m, 3H), 7.14 (d, J = 8.1 Hz, 2H), 6.92 (dd, J = 9.6, 6.4 Hz, 1H), 6.41 (t, J = 6.8 Hz, 1H), 5.43 (s, 2H), 1.13 (s, 9H). **^{13}C NMR** (100 MHz, $CDCl_3$) δ =197.07, 148.28, 137.69, 128.24, 127.91 (2C), 127.45 (2C), 127.37, 125.53, 124.18, 118.66, 110.41, 110.24, 46.44, 42.67, 27.22 (3C). **LC-MS** (m/z): $[M+H]^+$ = 309.0, $[M+Na]^+$ = 331.0, $[2M+Na]^+$ = 639.2. **Anal. Calc.** for ($C_{19}H_{20}N_2O_2$: 308.38): C, 74.00; H, 6.64; found: C, 73.88; H, 6.45.

2-Benzyl-1-pentanoylimidazo[1,5-a]pyridin-3(2H)-one (**77ai**)

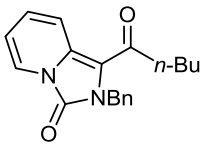

Yellow solid, yield = 79% (49 mg, cHex:AcOEt = 5:1). **M.p.** = 126.0-127.2 °C. **^{1}H NMR** (400 MHz, $CDCl_3$) δ = 7.99 (d, J = 7.1 Hz, 1H), 7.46 (d, J = 9.6 Hz, 1H), 7.39 (d, J = 7.2 Hz, 2H), 7.30 – 7.19 (m, 3H), 7.10 (ddd, J = 9.5, 6.5, 1.0 Hz, 1H), 6.54 (dd, J = 10.0, 3.6 Hz, 1H), 5.63 (s, 2H), 2.74 – 2.68 (m, 2H), 1.67 (dt, J = 15.1, 7.4 Hz, 2H), 1.35 (dq, J = 14.7, 7.4 Hz, 2H), 0.92 (t, J = 7.3 Hz, 3H). **^{13}C NMR** (100 MHz, $CDCl_3$) δ = 187.05, 147.97, 137.73, 129.47, 129.35, 128.29 (2C), 128.13 (2C), 127.36, 124.51, 117.89, 111.15, 110.49, 46.68, 41.02, 26.60, 22.41, 13.90. **LC-MS** (m/z): $[M+H]^+$ = 309.0, $[M+Na]^+$ = 331.2, $[2M+Na]^+$ = 639.2. **Anal. Calc.** for ($C_{19}H_{20}N_2O_2$:

308.38): C, 74.00; H, 6.64; found: C, 73.80; H, 6.49.

2-Benzyl-1-(2,2,2-trichloroacetyl)imidazo[1,5-a]pyridin-3(2H)-one (**77aj**)

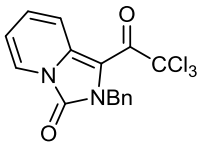

Yellow solid, yield = 69% (51 mg, cHex:AcOEt = 3:1). **M.p.** = 111.8-113.2 °C. **^{1}H NMR** (400 MHz, $CDCl_3$) δ = 8.16 (d, J = 7.0 Hz, 1H), 8.10 (d, J = 9.6 Hz, 1H), 7.35 (d, J = 6.8 Hz, 2H), 7.33 – 7.24 (m, 4H), 6.77 (t, J = 6.8 Hz, 1H), 5.61 (s, 2H). **^{13}C NMR** (100 MHz, $CDCl_3$) δ = 170.46, 148.30, 136.97, 131.35, 131.26, 128.45 (2C), 127.88 (2C), 127.59, 124.90, 121.30, 112.82, 104.15, 96.53, 47.48. **LC-MS** (m/z): $[M+H]^+$ = 369.2, $[2M+Na]^+$ = 759.4. **Anal. Calc.** for ($C_{16}H_{11}Cl_3N_2O_2$: 367.99): C, 51.99; H, 3.00; found: C, 51.70; H, 2.85.

1-Benzoyl-2-(4-methylbenzyl)imidazo[1,5-a]pyridin-3(2H)-one (**77ba**)

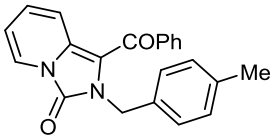

Pale brown solid, yield = 85% (58 mg, cHex:AcOEt = 3:1). **M.p.** = 121.3-125.1 °C. **^{1}H NMR** (400 MHz, $CDCl_3$) δ = 7.94 (d, J = 7.1 Hz, 1H), 7.63 – 7.53 (m, 3H), 7.45 (t, J = 7.5 Hz, 2H), 7.34 (d, J = 8.0 Hz, 2H), 7.09 (d, J = 8.0 Hz, 2H), 6.75 (ddd, J = 9.5, 6.5, 1.0 Hz, 1H), 6.46 (t, J = 6.4 Hz, 1H), 6.33 (d, J = 8.6 Hz, 1H), 5.62 (s, 2H), 2.29 (s, 3H). **^{13}C NMR** (100 MHz, $CDCl_3$) δ = 183.02, 148.07, 140.48, 137.25, 134.54, 133.37, 131.69, 131.59, 130.06, 129.14 (2C), 128.71 (2C), 128.36 (2C), 128.32 (2C), 124.07, 117.84, 111.70, 46.04, 21.07. **LC-MS** (m/z): $[M+H]^+$ = 343.0, $[M+Na]^+$ = 365.2, $[2M+Na]^+$ = 707.2. **Anal. Calc**. for ($C_{22}H_{18}N_2O_2$: 342.14): C, 77.17; H, 5.30; found: C, 76.95, H, 5.06.

1-Benzoyl-2-(4-methoxybenzyl)imidazo[1,5-a]pyridin-3(2H)-one (**77ca**)

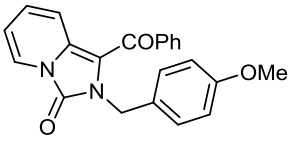

Green solid, yield = 67% (48 mg, cHex:AcOEt = 3:1). **M.p.** = 118.9-120.5 °C. **^{1}H NMR** (400 MHz, $CDCl_3$) δ = 7.94 (d, J = 7.1 Hz, 1H), 7.61 – 7.53 (m, 3H), 7.50 – 7.38 (m, 4H), 6.81 (d, J = 8.7 Hz, 2H), 6.78 – 6.68 (m, 1H), 6.47 (t, J = 6.8 Hz, 1H), 6.32 (d, J = 9.5 Hz, 1H), 5.59 (s, 2H), 3.76 (s, 3H). **^{13}C NMR** (100 MHz, $CDCl_3$) δ =183.04, 159.06, 148.04, 140.51, 131.72, 131.59, 129.93 (2C), 129.84, 128.73 (2C), 128.71, 128.30 (2C), 124.05, 117.85, 113.81 (2C), 111.70, 110.17, 55.16, 45.72. **LC-MS** (m/z): $[M+H]^+$ = 359.0, $[M+Na]^+$ = 381.2, $[2M+Na]^+$ = 739.2. **Anal. Calc**. for ($C_{22}H_{18}N_2O_3$: 358.13): C, 73.73; H, 5.06; found: C, 73.60, H, 4.88.

1-Benzoyl-2-(4-nitrobenzyl)imidazo[1,5-a]pyridin-3(2H)-one (**77da**)

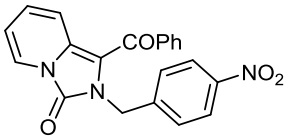

Yellow solid, yield = 59% (44 mg, cHex:AcOEt = 2:1). **M.p.** = 128.0-129.4 °C. **^{1}H NMR** (400 MHz, $CDCl_3$) δ = 8.16 (d, J = 8.6 Hz, 2H), 7.98 (d, J = 7.1 Hz, 1H), 7.63 (d, J = 8.6 Hz, 2H), 7.59 – 7.55 (m, 3H), 7.51 – 7.44 (m, 2H), 6.84 (dd, J = 9.5, 6.5 Hz, 1H), 6.55 (t, J = 6.8 Hz, 1H), 6.41 (d, J = 9.5 Hz, 1H), 5.71 (s, 2H). **^{13}C NMR** (100 MHz, $CDCl_3$) δ = 182.90, 148.08, 147.38, 144.70, 140.09, 131.91, 131.82, 129.42, 129.03 (2C), 128.85 (2C), 128.16 (2C), 124.07, 123.73 (2C), 117.87, 112.19, 109.93, 45.96. **LC-MS** (m/z): $[M+H]^+$ = 374.0, $[M+Na]^+$ = 396.2, $[2M+Na]^+$ = 769.2. **Anal. Calc**. for ($C_{21}H_{15}N_3O_4$: 373.11): C, 67.56; H, 4.05; found: C, 67.41, H, 3.78.

1-Benzoyl-2-(2-chlorobenzyl)imidazo[1,5-a]pyridin-3(2H)-one (**77ea**)

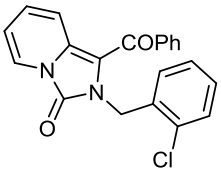

Yellow solid, yield = 81% (59 mg, cHex:AcOEt = 4:1). **M.p.** = 168.8-171.2 °C. **^{1}H NMR** (400 MHz, $CDCl_3$) δ = 7.97 (d, J = 7.0 Hz, 1H), 7.61 (d, J = 7.2 Hz, 2H), 7.56 (t, J = 7.4 Hz, 1H), 7.45 (t, J = 7.5 Hz, 2H), 7.39 – 7.33 (m, 1H), 7.19 – 7.14 (m, 2H), 7.02 – 6.97 (m, 1H), 6.82 (dd, J = 9.1, 6.6 Hz, 1H), 6.51 (t, J = 6.7 Hz, 1H), 6.45 (d, J = 9.5 Hz, 1H), 5.71 (s, 2H). **^{13}C NMR** (100 MHz, $CDCl_3$) δ = 182.75, 148.15, 140.09, 134.66, 132.78, 131.74, 131.35, 129.55, 128.89, 128.70 (2C), 128.42, 128.38 (2C), 127.80, 126.65, 124.05, 117.84, 111.78, 110.69, 44.80. **LC-MS** (m/z): $[M+H]^+$ = 363.0, $[M+Na]^+$ = 385.2, $[2M+Na]^+$ = 747.2. **Anal. Calc.** for ($C_{21}H_{15}ClN_2O_2$: 362.08): C, 69.52; H, 4.17; found: C, 69.31, H, 4.01.

1-Benzoyl-2-(naphthalen-2-ylmethyl)imidazo[1,5-a]pyridin-3(2H)-one (**77fa**)

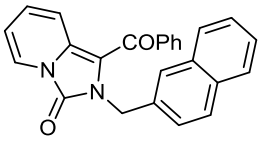

Yellow solid, yield = 71% (54 mg, cHex:AcOEt = 4:1). **M.p.** = 170.5-171.2 °C. **^{1}H NMR** (400 MHz, $CDCl_3$) δ = 7.97 (d, J = 7.1 Hz, 1H), 7.90 (s, 1H), 7.81 – 7.75 (m, 3H), 7.62 – 7.52 (m, 4H), 7.47 – 7.39 (m, 4H), 6.76 (ddd, J = 9.5, 6.5, 0.9 Hz, 1H), 6.48 (t, J = 6.6 Hz, 1H), 6.34 (d, J = 9.5 Hz, 1H), 5.82 (s, 2H). **^{13}C NMR** (100 MHz, $CDCl_3$) δ = 182.92, 148.03, 140.28, 134.86, 133.15, 132.69, 131.62, 131.46, 128.69, 128.59 (2C), 128.14 (2C), 128.09, 127.89, 127.39, 127.18, 126.18, 125.79, 125.69, 123.96, 117.73, 111.64, 110.10, 46.32. **LC-MS** (m/z): $[M+H]^+$ = 379.0, $[M+Na]^+$ = 401.2, $[2M+Na]^+$ = 779.2. **Anal. Calc**. for ($C_{25}H_{18}N_2O_2$: 378.14): C, 79.35; H, 4.79; found: C, 79.02, H, 4.52.

1-Benzoyl-2-(thiophen-2-ylmethyl)imidazo[1,5-a]pyridin-3(2H)-one (**77ga**)

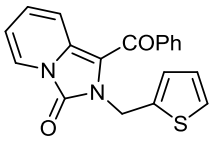

Yellow solid, yield = 78% (52 mg, cHex:AcOEt = 4:1). **M.p.** = 160.5-162.3 °C. **^{1}H NMR** (400 MHz, $CDCl_3$) δ = 7.92 (d, J = 7.1 Hz, 1H), 7.64 (d, J = 6.9 Hz, 2H), 7.58 (s, 1H), 7.48 (t, J = 7.5 Hz, 2H), 7.24 – 7.19 (m, 2H), 6.92 (dd, J = 5.1, 3.5 Hz, 1H), 6.76 (ddd, J = 9.5, 6.5, 0.9 Hz, 1H), 6.46 (dd, J = 10.0, 3.6 Hz, 1H), 6.35 (d, J = 9.5 Hz, 1H), 5.84 (s, 2H). **^{13}C NMR** (100 MHz, $CDCl_3$) δ =183.12, 147.61, 140.45, 138.99, 131.77, 131.61, 128.97, 128.76 (2C), 128.29 (2C), 127.79, 126.65, 125.91, 124.06, 117.84, 111.80, 109.85, 40.81. **LC-MS** (m/z): $[M+H]^+$ = 335.0, $[M+Na]^+$ = 357.0, $[2M+Na]^+$ = 691.2. **Anal. Calc**. for ($C_{19}H_{14}N_2O_2S$: 334.08): C, 68.25; H, 4.22; found: C, 68.01, H, 4.05.

1-Benzoyl-2-pentylimidazo[1,5-a]pyridin-3(2H)-one (**77ha**)

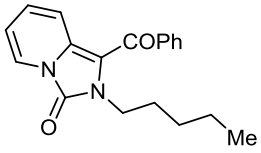

Brown oil, yield = 66% (41 mg, cHex:AcOEt = 5:1). **^{1}H NMR** (400 MHz, $CDCl_3$) δ = 7.94 (d, J = 7.1 Hz, 1H), 7.66 (dd, J = 8.2, 1.4 Hz, 2H), 7.62 – 7.55 (m, 1H), 7.49 (t, J = 7.4 Hz, 2H), 6.77 (ddd, J = 9.5, 6.5, 1.1 Hz, 1H), 6.51 – 6.45 (m, 1H), 6.38 (d, J = 9.5 Hz, 1H), 4.42 – 4.34 (m, 2H), 1.84 – 1.75 (m, 2H), 1.37 (td, J = 7.2, 3.6 Hz, 4H), 0.93 – 0.87 (m, 3H). **^{13}C NMR** (100 MHz, $CDCl_3$) δ = 183.09, 147.97, 140.81, 131.78, 131.61, 128.95 (2C), 128.67, 128.53 (2C), 124.17, 118.06, 111.83, 110.80, 53.56, 43.67, 29.67, 29.07, 22.51. **LC-MS** (m/z): $[M+H]^+$ = 309.0, $[M+Na]^+$ = 331.0. **Anal. Calc**. for ($C_{19}H_{20}N_2O_2$: 308.38): C, 74.00; H, 6.54; found: C, 73.88, H, 6.31.

1-Benzoyl-2-(pentan-3-yl)imidazo[1,5-a]pyridin-3(2H)-one (**77ia**)

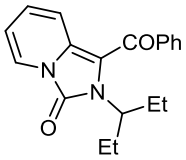

Brown oil, yield = 75% (46 mg, cHex:AcOEt = 5:1). **^{1}H NMR** (400 MHz, $CDCl_3$) δ = 7.89 (d, J = 7.1 Hz, 1H), 7.66 (d, J = 7.9 Hz, 2H), 7.57 (t, J = 7.4 Hz, 1H), 7.47 (t, J = 7.6 Hz, 2H), 6.72 (dd, J = 9.4, 6.5 Hz, 1H), 6.45 (t, J = 6.8 Hz, 1H), 6.25 (d, J = 9.5 Hz, 1H), 4.98 – 4.83 (m, 1H), 2.38 – 2.25 (m, 2H), 1.89 (dd, J = 13.7, 6.6 Hz, 2H), 0.91 (t, J = 7.4 Hz, 6H). **^{13}C NMR** (100 MHz, $CDCl_3$) δ =182.99, 147.31, 140.95, 131.72, 131.34, 128.79 (2C), 128.54 (2C), 128.20, 123.61, 117.90, 112.41, 111.46, 60.00, 25.29 (2C), 11.24 (2C).. **LC-MS** (m/z): $[M+H]^+$ = 309.0, $[M+Na]^+$ = 331.2, $[2M+Na]^+$ = 639.2. **Anal. Calc.** for ($C_{19}H_{20}N_2O_2$: 308.38): C, 74.00; H, 6.54; found: C, 73.83, H, 6.31.

1-Benzoyl-2-(prop-2-yn-1-yl)imidazo[1,5-a]pyridin-3(2H)-one (**77ja**)

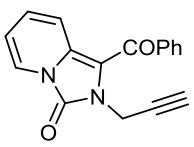

Yellow solid, yield = 88% (49 mg, cHex:AcOEt = 5:1). **M.p.** = 174.9-176.1

°C. **^{1}H NMR** (400 MHz, $CDCl_3$) δ = 7.91 (d, J = 7.1 Hz, 1H), 7.71 (d, J = 7.0 Hz, 2H), 7.59 (t, J = 7.4 Hz, 1H), 7.49 (t, J = 7.5 Hz, 2H), 6.79 (ddd, J = 9.4, 6.5, 0.9 Hz, 1H), 6.46 (m, 2H), 5.22 (d, J = 2.4 Hz, 2H), 2.24 (t, J = 2.4 Hz, 1H). **^{13}C NMR** (100 MHz, $CDCl_3$) δ = 182.83, 147.50, 140.01, 131.84, 131.47, 129.09, 128.74 (2C), 128.49 (2C), 124.01, 117.76, 111.80, 109.87, 78.36, 72.00, 32.95. **LC-MS** (m/z): $[M+H]^+$ = 277.0, $[M+Na]^+$ = 299.0, $[2M+Na]^+$ = 575.2. **Anal. Calc**. for ($C_{17}H_{12}N_2O_2$: 276.30): C, 73.90; H, 4.38; found: C, 73.65, H, 4.21.

2-Allyl-1-benzoylimidazo[1,5-a]pyridin-3(2H)-one (**77ka**)

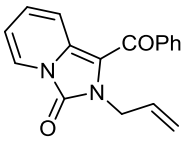

Yellow solid, yield =72% (40 mg, cHex:AcOEt = 5:1). **M.p.** = 119.4-120.7 °C. **^{1}H NMR** (400 MHz, $CDCl_3$) δ = 7.94 (d, J = 7.1 Hz, 1H), 7.68 – 7.65 (m, 2H), 7.58 (t, J = 7.4 Hz, 1H), 7.48 (t, J = 7.5 Hz, 2H), 6.81 – 6.73 (m, 1H), 6.48 (t, J = 6.8 Hz, 1H), 6.40 (d, J = 9.5 Hz, 1H), 6.03 (ddd, J = 15.9, 10.8, 5.7 Hz, 1H), 5.21 (dd, J = 17.3, 13.7 Hz, 2H), 5.02 (d, J = 5.7 Hz, 2H). **^{13}C NMR** (100 MHz, $CDCl_3$) δ = 182.80, 147.67, 140.35, 132.97, 131.68, 131.36, 128.74 (2C), 128.69, 128.37 (2C), 123.99, 117.81, 117.57, 111.71, 110.39, 45.33. **LC-MS** (m/z): $[M+H]^+$ = 279.0, $[M+Na]^+$ = 300.2, $[2M+Na]^+$ = 577.2. **Anal. Calc.** for ($C_{17}H_{14}N_2O_2$: 278.11): C, 73.37; H, 5.07; found: C, 73.21, H, 4.90.

3-Benzoyl-2-benzylimidazo[1,5-a]quinolin-1(2H)-one (**77ma**)

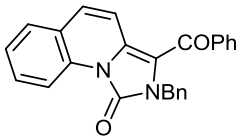

Yellow solid, yield = 35% (27 mg, cHex:AcOEt = 4:1). **M.p.** = 132.5-135.5 °C. **^{1}H NMR** (400 MHz, $CDCl_3$) δ = 9.37 (d, J = 8.5 Hz, 1H), 7.65 – 7.60 (m, 2H), 7.56 (dd, J = 12.2, 4.7 Hz, 2H), 7.49 – 7.42 (m, 3H), 7.39 (d, J = 7.0 Hz, 2H), 7.37 – 7.32 (m, 1H), 7.30 – 7.21 (m, 3H), 6.92 (d, J = 9.7 Hz, 1H), 6.28 (d, J = 9.8 Hz, 1H), 5.57 (s, 2H).**^{13}C NMR** (100 MHz, $CDCl_3$) δ = 184.34, 150.43, 139.98, 137.59, 133.66, 132.24, 130.05, 129.61, 128.77 (2C), 128.73 (2C), 128.50(2C), 128.13 (2C), 127.60, 127.52, 125.41, 123.73, 119.07, 117.43, 115.63, 112.96, 45.75. **LC-MS** (m/z): $[M+H]^+$ = 379.0, $[M+Na]^+$ = 401.2, $[2M+Na]^+$ = 779.2. **Anal. Calc.** for ($C_{25}H_{18}N_2O_2$: 378.43): C, 73.95; H, 4.79; found: C, 73.71, H, 4.61.

1-Benzoyl-2-benzyl-5-bromoimidazo[1,5-a]pyridin-3(2H)-one (**77na**)

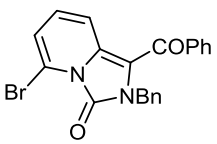

Yellow oil, yield = 54% (44 mg, cHex:AcOEt = 4:1). **^{1}H NMR** (400 MHz, $CDCl_3$) δ= 7.57 (m, 3H), 7.43 (dd, J = 19.2, 7.3 Hz, 4H), 7.26 (dt, J = 11.9, 7.0 Hz, 3H), 6.47 (dd, J = 9.2, 7.1 Hz, 1H), 6.30 (d, J = 6.8 Hz, 1H), 6.25 (d, J = 9.5 Hz, 1H), 5.54 (s, 2H). **^{13}C NMR** (100 MHz, $CDCl_3$) δ = 183.35, 147.96, 140.00,

137.19, 133.40, 132.08, 129.79, 128.83 (2C), 128.50 (2C), 128.46 (2C), 128.42 (2C), 127.66, 127.22, 116.49, 113.20, 110.87, 46.07. **LC-MS** (m/z): $[M+H]^+$ = 407.2, $[M+Na]^+$ = 429.2. **Anal. Calc**. for ($C_{21}H_{15}BrN_2O_2$: 406.03): 61.93; H, 3.71; found: C, 61.71, H, 3.51.

Dimethyl (*R*)-2-(1-benzoyl-3-oxoimidazo[1,5-a]pyridin-2(3H)-yl)succinate (**77oa**)

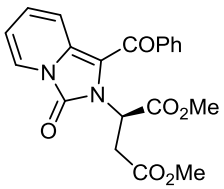

Brown oil, yield = 82% (63 mg, cHex:AcOEt = 2:1). **$[\alpha]_D^{25}$** = -79.7 (c = 0.9, CHCl3). **^{1}H NMR** (400 MHz, $CDCl_3$) δ = 7.95 – 7.91 (m, 1H), 7.65 – 7.62 (m, 2H), 7.60 – 7.54 (m, 1H), 7.48 (t, J = 7.4 Hz, 2H), 6.81 (ddd, J = 9.5, 6.5, 1.1 Hz, 1H), 6.53 – 6.47 (m, 1H), 6.39 (d, J = 9.5 Hz, 1H), 6.17 (dd, J = 8.0, 5.9 Hz, 1H), 3.78 (s, 3H), 3.67 (s, 3H), 3.55 (dd, J = 16.8, 5.7 Hz, 1H), 3.16 (dd, J = 16.8, 8.3 Hz, 1H). **^{13}C NMR** (100 MHz, $CDCl_3$) δ = 182.79, 170.82, 169.01, 147.60, 140.09, 131.86, 131.65, 129.40, 128.76 (2C), 128.27 (2C), 124.13, 117.87, 111.95, 110.14, 52.88 (2C), 51.96, 35.34. **LC-MS** (m/z): $[M+H]^+$ = 383.0, $[M+Na]^+$ = 405.2, $[2M+Na]^+$ = 787.2. **Anal. Calc.** for ($C_{20}H_{18}N_2O_2$: 382.37): C, 62.82; H, 4.75; found: C, 62.59, H, 4.60.

1-Benzoyl-3H-oxazolo[3,4-a]pyridin-3-one (**77pa**)

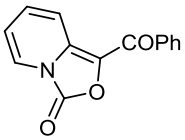

Yellow solid, yield = 65% (31 mg, cHex:AcOEt = 3:1). **M.p.** = 162.7-163.6 °C. **^{1}H NMR** (400 MHz, $CDCl_3$) δ = 8.10 – 8.06 (m, 2H), 7.91 (d, J = 9.4 Hz, 1H), 7.74 (d, J = 7.2 Hz, 1H), 7.59 – 7.53 (m, 1H), 7.52 – 7.47 (m, 3H), 7.18 (dd, J = 9.4, 6.5 Hz, 1H), 6.55 (t, J = 6.8 Hz, 1H). **^{13}C NMR** (100 MHz, $CDCl_3$) δ = 179.17, 148.21, 136.82, 133.60, 133.18, 132.39, 130.12, 129.01 (2C), 128.41 (2C), 123.83, 118.80, 113.32. **LC-MS** (m/z): $[M+H]^+$ = 240.0, $[2M+Na]^+$ = 501.2. **Anal. Calc**. for ($C_{14}H_9NO_3$: 239.23): C, 70.29; H, 3.70; found: C, 70.11, H, 3.51.

1-Benzoyl-5-(thiophen-2-yl)-3H-oxazolo[3,4-a]pyridin-3-one (**77qa**)

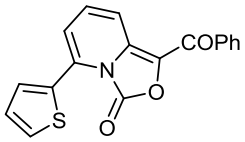

Orange solid, yield = 52% (33 mg, cHex:AcOEt = 3:1). **M.p.** = 124.8-127.7 °C. **^{1}H NMR** (400 MHz, $CDCl_3$) δ = 8.09 (d, J = 7.1 Hz, 2H), 8.00 (d, J = 9.2 Hz, 1H), 7.57 (t, J = 7.3 Hz, 1H), 7.53 – 7.47 (m, 3H), 7.34 (dd, J = 3.7, 1.1 Hz, 1H), 7.16 – 7.09 (m, 2H), 6.53 (d, J = 6.7 Hz, 1H). **^{13}C NMR** (100 MHz, $CDCl_3$) δ = 179.37, 147.28, 136.98, 135.54, 133.29, 132.33, 131.24, 131.01, 129.11 (2C), 129.01 (2C), 128.49, 128.30, 127.47, 127.21, 118.31, 117.24. **LC-MS** = $[M+H]^+$ = 322.0, $[M+Na]^+$ = 344.0, $[2M+Na]^+$ = 665.2. **Anal. Calc.** for ($C_{18}H_{11}NO_3S$: 321.35): C, 67.28; H, 3.45; found: C, 67.01, H, 3.27.

4.5.5. Synthetic Application of Products

1-Benzoyl-2-(pentan-3-yl)-5,6,7,8-tetrahydroimidazo[1,5-a]pyridin-3(2H)-one (**78ia**)

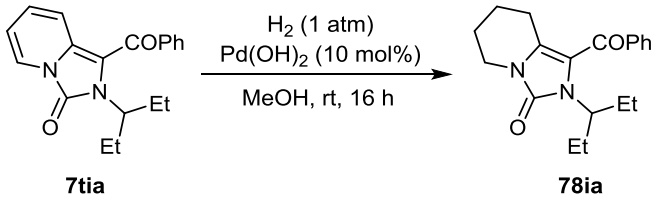

7tia **78ia**

An oven-dried Schlenk tube, filled with nitrogen atmosphere, was charged with MeOH (1.0 mL), dienamide **77ia** (0.1 mmol, 1.0 eq) and $Pd(OH)_2$ (10 mol%, 20 wt% on carbon). Then the nitrogen was evacuated, and the reactor was filled with H_2 (1 atm). This procedure was repeated twice, and then the reaction was left stirring at rt overnight. Finally the solution was directly filtrated over celite, and washed with methanol. The crude product was then purified by flash chromatography (c-Hex:AcOEt = 2:1) to afford pure compound **78ia** as a colorless oil (yield = 88%, 27 mg). **^{1}H NMR** (400 MHz, $CDCl_3$) δ = 7.64 (d, J = 7.0 Hz, 2H), 7.55 (t, J = 7.4 Hz, 1H), 7.45 (t, J = 7.5 Hz, 2H), 4.30 (ddd, J = 15.2, 9.8, 5.6 Hz, 1H), 3.65 (t, J = 6.3 Hz, 2H), 2.26 – 2.06 (m, 4H), 1.89 – 1.70 (m, 4H), 1.56 (dt, J = 12.1, 6.2 Hz, 2H), 0.91 (t, J = 7.4 Hz, 6H). **^{13}C NMR** (100 MHz, $CDCl_3$) δ = 185.47, 152.73, 140.55, 132.18, 132.06, 128.66 (2C), 128.51 (2C), 120.20, 59.12, 40.35, 25.58 (2C), 23.59, 21.83, 19.71, 11.40 (2C). **LC-MS** (m/z): $[M+H]^+$ = 313.2, $[M+Na]^+$ = 335.2, $[2M+Na]^+$ = 647.2. **Anal. Calc.** for ($C_{19}H_{24}N_2O_2$: 312.18): C, 73.05; H, 7.74; found: C, 72.71, H, 7.51.

Methyl 2-benzyl-3-oxo-2,3-dihydroimidazo[1,5-a]pyridine-1-carboxylate (**79aj**)

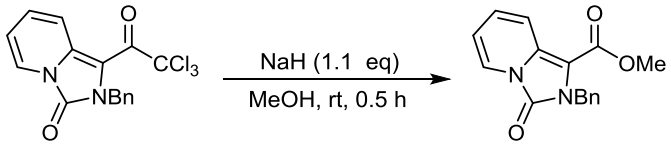

77aj **79aj**

To a solution of **77aj** (0.1 mmol) in MeOH (0.5 mL) at 0 °C, were added NaH (0.11 mmol). Gas evolution was immediately observed. The reaction proceed at rt for 30 minutes, until complete conversion of the starting material (TLC). The reaction was then quenched with water, extracted with EtOAc (2 mL x 3), washed with brine and dried with Na_2SO_4. After removal of the volatiles by means of rotary evaporation, the crude product was purified by flash chromatography (*c*-Hex:AcOEt = 1:1) to afford pure compound **79aj** as a yellow solid (yield = 98%, 28 mg). **M.p.** = 114.8-117.7 °C. **^{1}H NMR** (400 MHz, $CDCl_3$) δ = 7.91 (d, J =

7.1 Hz, 1H), 7.68 (d, J = 9.4 Hz, 1H), 7.40 (d, J = 7.5 Hz, 2H), 7.32 – 7.22 (m, 3H), 6.99 (dd, J = 9.3, 6.6 Hz, 1H), 6.49 (t, J = 6.8 Hz, 1H), 5.51 (s, 2H), 3.86 (s, 3H). **^{13}C NMR** (100 MHz, $CDCl_3$) δ = 160.40, 147.83, 137.45, 129.86, 128.41 (2C), 128.23, 127.97 (2C), 127.48, 123.58, 118.84, 111.29, 100.37, 51.02, 46.21. **LC-MS** = $[M+H]^+$ = 283.0, $[M+Na]^+$ = 305.0, $[2M+Na]^+$ = 587.2. **Anal. Calc.** for ($C_{16}H_{14}N_2O_3$: 282.10): C, 68.08; H, 5.00; found: C, 67.87, H, 4.77.

4.5.6. General procedure for the *trans*-carbonylation between TBD and amine

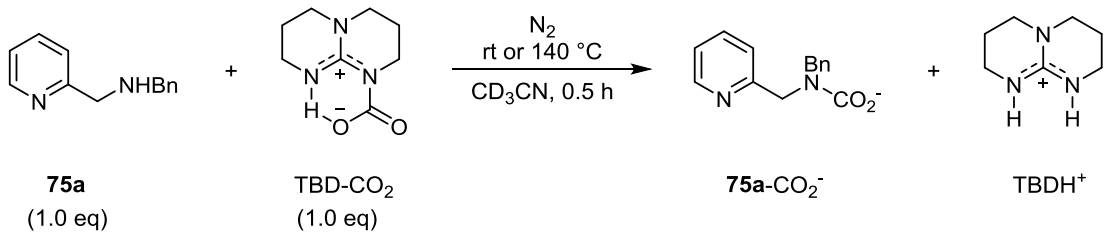

TBD-CO_2 (prepared in accordance to the procedure of Villiers[72]), was dissolved in CD_3CN (0.5 mL), under nitrogen atmosphere. Amine **75a** (0.5 mmol, 1.0 eq) was added and the solution was stirred at the desired temperature. After 30 minutes NMR control proved the formation of the carbamate **75a-CO_2^-** with a ratio with the free amine of 90:10. The solution of **[$TBDH^+$][75a-CO_2^-]** can be directly used for the subsequent carbonylation and acylation at room temperature.

4.5.7. General procedure for the carbonylation/acylation reaction at rt

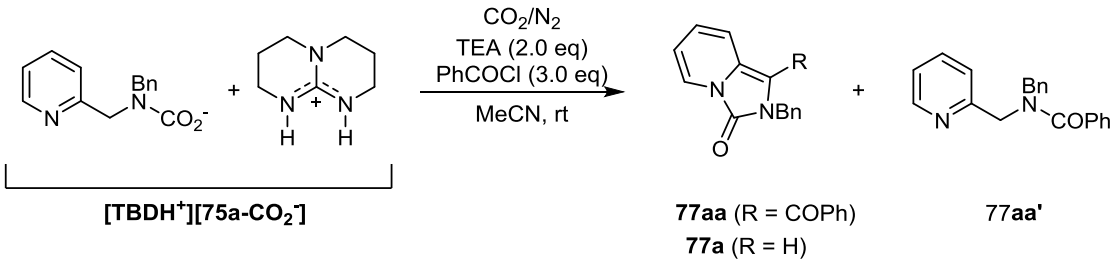

To the pre-formed solution of **[$TBDH^+$][75a-CO_2^-]** (0.2 mmol, 0.2 M), under the desired gas atmosphere, were added TEA (0.4 mmol) and PhCOCl (0.6 mmol). The reaction proceeded stirring for 1 h, then the solution was quenched with NaOH 2M, and extracted three times with AcOEt. The crude mixture of **77aa**, **77a** and **77aa'** has been separated by flash chromatography (*c*Hex:AcOEt 3:1) obtaining **77aa** with a yield of 20% under CO_2 atmosphere, and 54% with nitrogen atmosphere.

[72] C. Villiers, J.-P. Dognon, R. Pollet, P. Thuéry, M. Ephritikhine, *Angew. Chem. Int. Ed.* **2010**, *49*, 3465-3468.

2-Benzylimidazo[1,5-a]pyridin-3(2H)-one (**77a**)

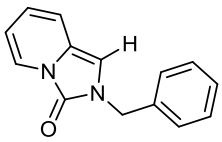

Orange oil. **^{1}H NMR** (400 MHz, $CDCl_3$) δ = 7.55 (d, J = 7.3 Hz, 1H), 7.31 (m, 5H), 6.74 (d, J = 9.3 Hz, 1H), 6.36 (dd, J = 8.8, 6.7 Hz, 1H), 6.26 (s, 1H), 6.05 (t, J = 6.6 Hz, 1H), 5.00 (s, 2H). **^{13}C NMR** (100 MHz, $CDCl_3$) δ = 147.31, 136.48, 128.74 (2C), 127.95 (2C), 127.90, 122.38, 121.63, 120.93, 117.26, 108.66, 98.08, 47.52. **LC-MS** (m/z): $[M+H]^+$ = 225.0; $[2M+Na]^+$ = 471.2. **Anal. Calc.** for ($C_{14}H_{12}N_2O$: 224.09): C, 74.98; H, 5.39; found: C, 74.85, H, 5.21.

N-benzyl-*N*-(pyridin-2-ylmethyl)benzamide (**77aa'**)

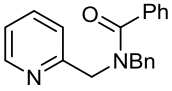

Colorless oil. **^{1}H NMR** (400 MHz, $CDCl_3$) δ = 8.64 (brs, 1H), 7.72 (brs, 1H), 7.60 (d, J = 5.2 Hz, 2H), 7.50 – 7.11 (m, 11H), 4.87 (d, J = 16.9 Hz, 2H), 4.63 (d, J = 42.4 Hz, 2H). **^{13}C NMR** (100 MHz, $CDCl_3$) δ 172.50 – 172.28, 157.14 – 156.66, 149.86 – 149.34, 136.91 (2C), 136.71, 136.19, 129.66, 128.77 – 128.68, 128.46 (2C), 127.56, 127.10, 126.82 (2C), 122.44 – 122.30, 121.36, 104.57, 53.31 – 52.95, 49.59 – 47.94. **LC-MS** (m/z): $[M+H]^+$ = 303.0; $[M+Na]^+$ = 325.2; $[2M+Na]^+$ = 627.2. **Anal. Calc.** for ($C_{20}H_{18}N_2O$: 302.14): C, 79.44; H, 6.00; found: C, 79.29, H, 5.79.

5. Enantioselective CO_2 Fixation Via a Heck-Coupling /Carboxylation Cascade Catalyzed by Nickel

All the procedures and results here described can be found in:

- A. Cerveri, R. Giovanelli, D. Sella, R. Pedrazzani, M. Monari, O. Nieto Faza, C. Silva López, M. Bandini, "Enantioselective CO_2 Fixation Via a Heck-Coupling /Carboxylation Cascade Catalyzed by Nickel" *Chem.Eur.J.* **2021**, *27*, 7657-7662.

ABSTRACT

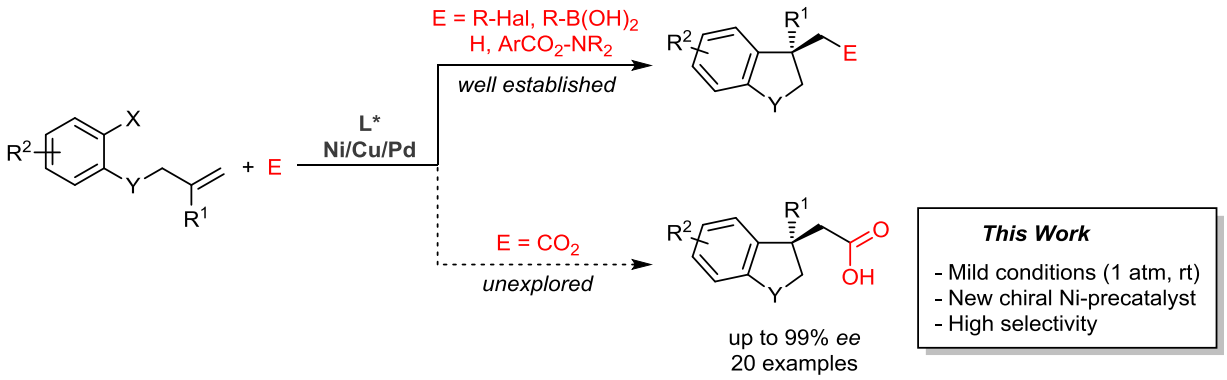

Scheme 40: Proposed Ni-catalyzed enantioselective arylative carboxylation of alkenes.

A novel asymmetric nickel-based carbo-carboxylation procedure has been developed, featuring atmospheric CO_2 as carboxylating reagent. A new rationally designed chiral ligand has been prepared and shown to achieve enantiomeric excesses (up to 99%) and better performances. The overall process efficiently furnishes chiral 2,3-dihydrobenzofuran-3-ylacetic acids, an important class of bioactive products, from readily available starting materials. A combined experimental and computational efforts revealed the key steps of the catalytic cycle and suggested the unexpected participation of Ni(I) species in the stereodetermining cyclization event.

5.1. Background

As exposed in the previous chapter, carbon dioxide has emerged in the past decades as a green and abundant C1-synthon in organic chemistry.[73] Overcoming the challenge of CO_2

[73] a) M. Aresta, Wiley-VCH: Weinheim, **2010**; b) T. Sakakura, J.-C. Choi, Y. Yasuda, *Chem. Rev.* **2007**, *107*, 2365-2387; c) M. Aresta, A. Dibenedetto, A. Angelini, *Chem. Rev.* **2014**, *114*, 1709-1742; d) J. R. Cabrero- Antonino, R. Adam, M. Beller, *Angew. Chem. Int. Ed.* **2019**, *58*, 12820-12838; e) S. Dabral, T. Schaub, *Adv. Synth. Catal.* **2019**, *361*, 223-246.

intrinsic inertness has brough chemists to develop different activation methods, applying it successfully in metal-, light- or base-promoted processes.[74] Particularly, an insightful understanding of the detailed organometallic chemistry of CO_2 is of great importance for the further design of the catalytic processes and the chelating mode between transition metal centres and CO_2 has been investigated intensively via stoichiometric experimental studies (Scheme 41).[75]

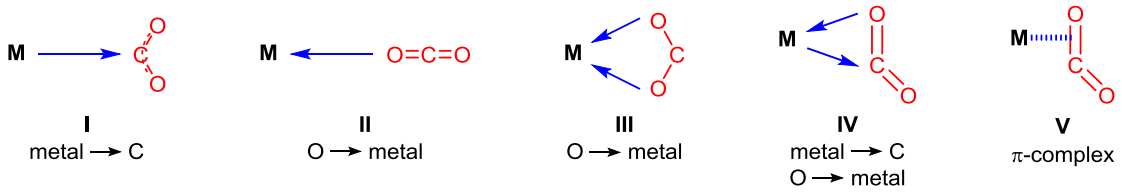

Scheme 41: Activation modes observed between CO_2 and metal centres.

As shown above, CO_2 has multiple reactive sites: the carbon atom is an electrophilic Lewis acid centre and the oxygen atoms act as weak nucleophilic Lewis base. In its ground state, carbon dioxide possesses two equivalent C-O bonds that could coordinate to a transition metal centre. As a result, a series of transition metal CO_2 complexes are known. If a metal centre reacts with one molecule of CO_2, there are five different chelating modes possible. Complex **I** with an M-C bond can be called metallacarboxylate. Electron-rich metal centres are more feasible to form these types of complexes via electron transfer from metal centre to carbon atom. Adduct **II** (end-on type) shows the weak interaction between the lone pair of only one oxygen atom and the metal centre. Compared to it, complex **III** is more stable, since CO_2 acts as a bidentate ligand with two oxygen atoms. In this case, a more electron-deficient metal centre is favoured for the electron transfer from oxygen atom to transition metal. A combination of the above two mentioned electron transfer processed affords the three-membered metallacycle complex **IV**. Moreover, the side-on-bonding p-complex **V** can also be formed in a similar spatial arrangement of atoms through the coordination of the C-O double bond to the central metal. On the basis of these different coordination and activation modes,

[74] a) Q. Liu, L. Wu, R. Jackstell, M. Beller, *Nat. Commun.* **2015**, *6*, 5933; b) Y. Shi, B.-W. Pan, Y. Zhou, J. Zhou, Y.-L. Liu, F. Zhou, *Org. Biomol. Chem.* **2020**, *18*, 8597-8619; c) J. Hou, J.-S. Li, J. Wu, *Asian J. Org. Chem.* **2018**, *7*, 1439-1447; d) J. Song,; Q. Liu, H. Liu, X. Jiang, *Eur. J. Org. Chem.* **2018**, 696-713; e) S. Wang, G. Du, G. Xi, *Org. Biomol. Chem.* **2016**, *14*, 3666-3676; f) C. Maeda, Y. Miyazaki, T. Ema, *Catal. Sci. Technol.* **2014**, *4*, 1482-1497; g) A. Tortajada, F. Julià-Hernàndez, M. Börjesson, T. Morgas, M. Martin, *Angew. Chem. Int. Ed.* **2018**, *57*, 15948-15982; h) Y. Cao, N. Wang, H.-R. Li, L. N. He, *Chin. J. Chem.***2018**, *36*, 644-659.

[75] a) K. Huang, C.-L. Sun, Z.-J. Shi, *Chem. Soc. Rev.* **2011**, *40*, 2435–2452; b) A. Behr, *Angew. Chem.* **1988**, *100*, 681–698.

well-designed transition metal complex catalysts are able to promote the reactivity and also control the selectivity of CO_2 fixation reactions in the organic synthesis.

In his pioneering work, Aresta firstly described a stable Ni-CO_2 complex, characterized by the η^2-coordination between nickel and the C-O bond of carbon dioxide.[76] This complex was based on a nucleophilic phosphine-based Ni(0) species. Successively other complexes have been studied and other coordination modes observed, such as the one reported by Liaw, which achieves a η^1 O → Ni coordination with an anionic Ni(II) complex, or the pincer ligand-based Ni(0) complex shown by Milstein, based on the peculiar η^1 Ni → C coordination mode (Scheme 42).[77]

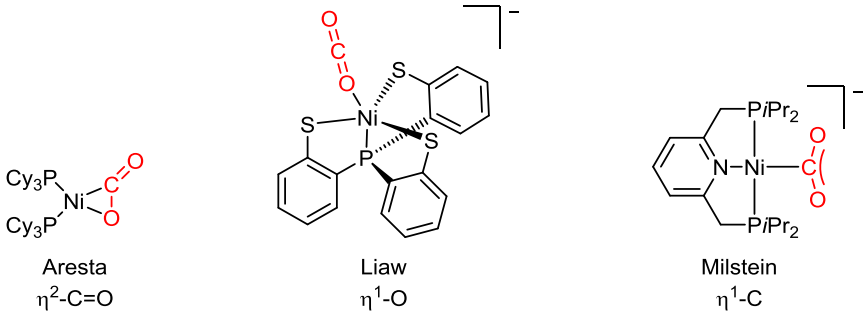

Scheme 42: Examples of coordination modes of CO_2 with nickel complexes.

Direct carboxylation of reactive functional groups, such as aryl/alkyl (pseudo)halides, alcohols, amines and radical precursors, as well as hydro-carboxylation of olefins can rapidly give access to pre-functionalized carboxylate-containing scaffolds of great synthetic interest (Scheme 43a).[78] However, the possibility of enhancing molecular complexity and, at the same time, introducing CO_2 as a carboxylate precursor has recently emerged, giving rise to a number of *tandem functionalization-carboxylation processes*. The advantage of applying this reactive concept is to employ a single activation method (that is a complete set of catalysts, additives, and solvents) to achieve both molecular modification and carboxylation of the same scaffold. The types of functionalizations that have been productively coupled with CO_2-based carboxylation are wide and diversified, ranging from carbo-functionalizations to the introduction of various heteroatoms such as B, F, Si, S, and P. These processes can be divided

[76] M. Aresta, C.F. Nobile, V.G. Albano, E. Forni, M. Manassero, *J. Chem. Soc., Chem. Commun.*, **1975**, 636-637
[77] a) T-W. Chiou, Y-M. Tseng, T-T. Lu, T-C. Weng, D. Sokaras, W-C. Ho, T-S. Kuo, L-Y. Jang, J-F Lee, W-F. Liaw, *Chem. Sci.* **2016**, *7,* 3640-3644; b) D. Sahoo, C. Yoo, Y. *J. Am. Chem. Soc.* **2018**, *140*, 6, 2179–2185.
[78] a) M. Börjesson, T. Morgas, D. Gallego, R. Martin, *ACS Catal.* **2016**, *6*, 6739-6749; b) J. Luo, I. C−H Larrosa, *ChemSusChem* **2017**, *10*, 3317-3332; c) M. Gaydou, T. Morgas, F. Julià-Hernàndez, R. Martin, *J. Am. Chem. Soc.* **2017**, *139*, 12161-12164; d) Y.-G. Chen, X.-T. Xu, K. Zhang, Y.-Q. Li, L.-P. Zhang, P. Fang, T. S. Mei, *Synthesis* **2018**, *50*, 35-48; i) Z. Zhang, J.-H. Ye, T. Ju, L.-L. Liao, H. Huang, Y.-Y. Gui, W.-J. Zhou, D.-G. Yu, *ACS Catal.* **2020**, *10*, 10871–10885.

into three categories, depending on the type of activation employed, namely: light-promoted processes, metal or base-promoted processes and reactions involving nickelalactone intermediates (Scheme 43b).[79]

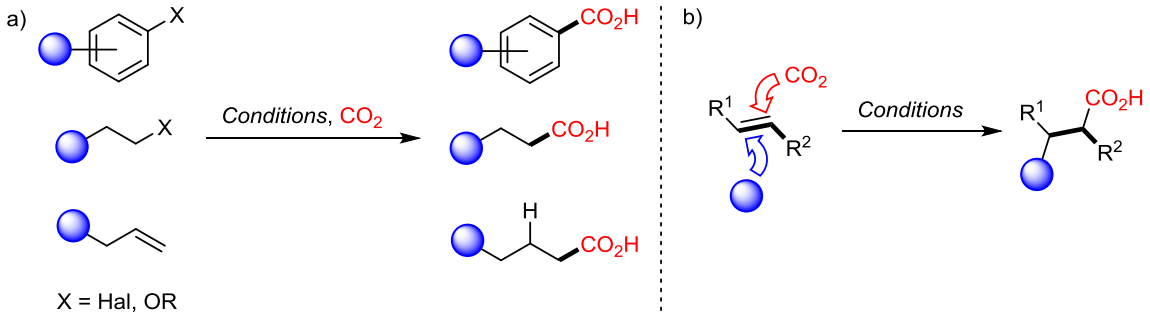

Scheme 43: a) Vastly explored carboxylation of substrates with CO_2; b) Di-functionalization of alkenes in the fixation of carbon dioxide.

In this context, only metal-catalyzed processes will be analyzed, in particular those based on the di-functionalization of π-systems. A number of excellent examples were recently disclosed, highlighting how versatile and productive these tandem reactions can be, as they can be run under a variety of different conditions. Some metal-catalyzed examples of sequential functionalization-carboxylations of olefins[80] have also been reported, however, not being strictly tandem one-pot protocols, these will not be discussed here in detail.

In 2015 Martin, and co-workers developed a substrate-dependent stereodivergent intramolecular cyclization-carboxylation protocol to convert bromides **80** into cyclo-fused acrylic acids **86**.[81] The reaction was promoted by sterically demanding ligand **85** coupled with catalytic nickel, and manganese as stoichiometric reductant. Labeling experiments revealed that the selectivity in the cyclization step, which determines the configuration of the double bond, is closely related to the nature of the substrate. Specifically, the *syn*-addition will be obtained when R^2 = H/D, while the *anti*-product is produced by the steric repulsion with R^2 = alkyl, aryl. The protocol tolerates variously substituted aryl-alkynes **80**, and also aliphatic substrates where successfully subjected to the desired cyclization-carboxylation sequence (Scheme 44). Mechanistically, after the insertion of the Ni(0) to the C-Br bond, a fast *syn*-insertion to the triple bond occurs forming intermediate **82**. Here the nature of the substrate

[79] a) X.-Y. Yu, J.-R. Chen, W.-J. Xiao, *Chem. Rev.* **2021**, *121*, 506-561; b) X.-Q. Hu, Z.-K. Liu, W.-J. Xiao, *Catalysts* **2020**, *19*, 1054; c) G. Li, C. Liu, X. Cui, Y. Yang, F. Shi, *Green Chem.* **2021**, *23*, 689-707; d) S. Ogoshi, Nickel Catalysis in Organic Synthesis (Part IV), Wiley-VCH:Weinheim, **2020**.
[80] a) P. Shao, S. Wang, C. Chen, C. Xi, *Chem. Commun.* **2015**, *51*, 6640-6642; b) W. Hang, S. Zou, C. Xi, *ChemCatChem* **2019**, *11*, 3814-3817.
[81] X. Wang, Y. Liu, R. Martin, *J. Am. Chem. Soc.* **2015**, *137*, 6476-6479.

induces the isomerization of the *in-situ* formed alkene. From previous reports disclosed by the same group, insertion of CO_2 on the Ni-C bond is accessible for the more nucleophilic Ni(I) species, with respect to the Ni(II) complexes. Thus, after the Mn-mediated mono-electronic reduction (intermediates **82'** and **83**), CO_2 is trapped and a second reduction re-generates the Ni(0) active species liberating the product as a Mn-carboxylate.

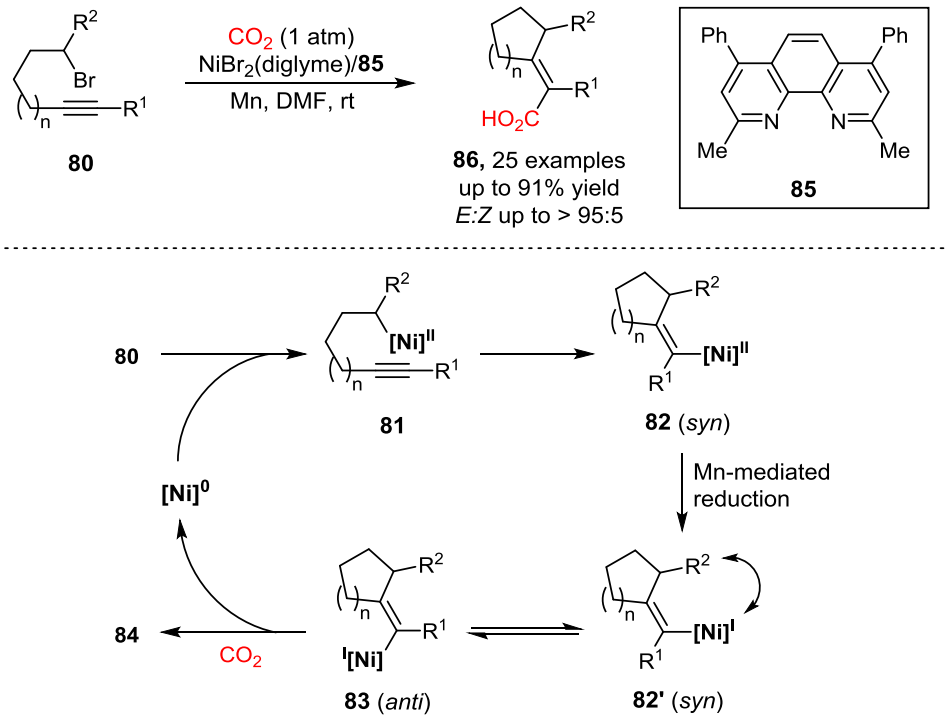

Scheme 44: Ni-catalyzed intramolecular carbo-carboxylation of internal alkynes.

A palladium-catalyzed synthesis of 3-methyleneindoline-2-carboxylates **93** and analogues was disclosed by the group of Sato in 2017 through a Heck-carboxylation sequence on N-allenyl-2-iodoanilines **87** (Scheme 45).[82] The reaction was promoted by the use of slightly electron-poor monodentate phosphine ligands, and Et_2Zn as sacrificial reductant for the turnover of the catalyst. The protocol could accommodate the use of iodoanilines of different electronic nature and 2-iodophenol-tethered allenes. The determining step for the formation of the product is the Et_2Zn mediated activation of the η^3-allylpalladium intermediate **89** generating the less sterically hindered η^1-allylpalladium **90**, which can capture atmospheric carbon dioxide at the γ-position. Finally, the product is obtained as a Zn-carboxylate through Et_2Zn-induced β-hydride elimination of the Pd(II) intermediate **91** and concomitant reduction of the catalyst. This mechanism interestingly forms the non-aromatic product mainly, and the

[82] Y. Higuchi, T. Mita, Y. Sato, *Org. Lett.* **2017**, *19*, 2710-2713.

methylene moiety can be easily functionalized to obtain complex indole-2-carboxylates derivatives through re-aromatization.

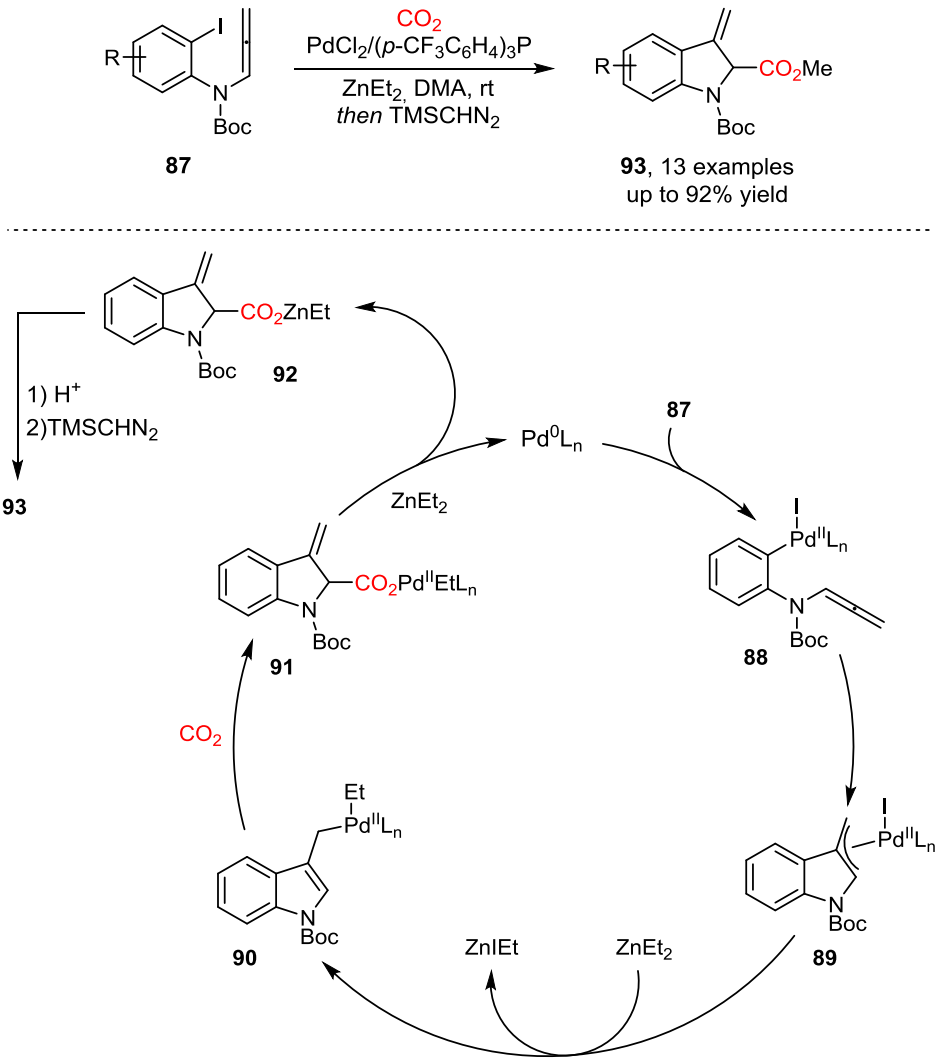

Scheme 45: Pd-catalyzed tandem Heck-carboxylation of allenamides and proposed catalytic cycle.

In 2020, the group of Martin disclosed a novel nickel-catalyzed remote C(sp^2)-H carboxylation of arenes (Scheme 46).[83] Tethered *o*-alkynylaryl bromides **94** underwent cyclization on the triple bond moiety, to generate the alkenyl-nickel complex. Here the carboxylation pathway occurs after a faster 1,4-Ni migration, to give the aryl-nickel intermediate which finally traps the CO_2 to give the final product **96** (Scheme 46a). The protocol could produce a variety of densely functionalized cyclo-fused styrene-2-carboxylates **96**, with a well-defined geometry of the formed alkene, and sterically or electronically demanding substrates are nicely accommodated. Mechanistic insight showed a significant

[83] M. Börjesson, D. Janssen-Müller, B. Sahoo, Y. Duan, X. Wang, M. Martin, *J. Am. Chem. Soc.* **2020**, *142*, 16234-16239.

isotopic effect when the deuterated starting material **97** is engaged in the cascade process, corroborating the [1,4]-Ni migration hypothesis (Scheme 46b). Moreover, differently from the majority of the previous studies, in this case the insertion of CO_2 on the Ni-C bond looks to be accessible from the Ni(II) center. In fact, when the pre-formed Ni(II) complexes **99** and **100** are subjected at the carboxylation protocol, in the absence of the sacrificial reductant, the desired benzoic acid **98** is still obtained. This unusual reactivity could be attributed to particular electronic and steric properties of the substrate, but still represents an important information to add to the Ni-catalyzed reductive coupling portfolio.

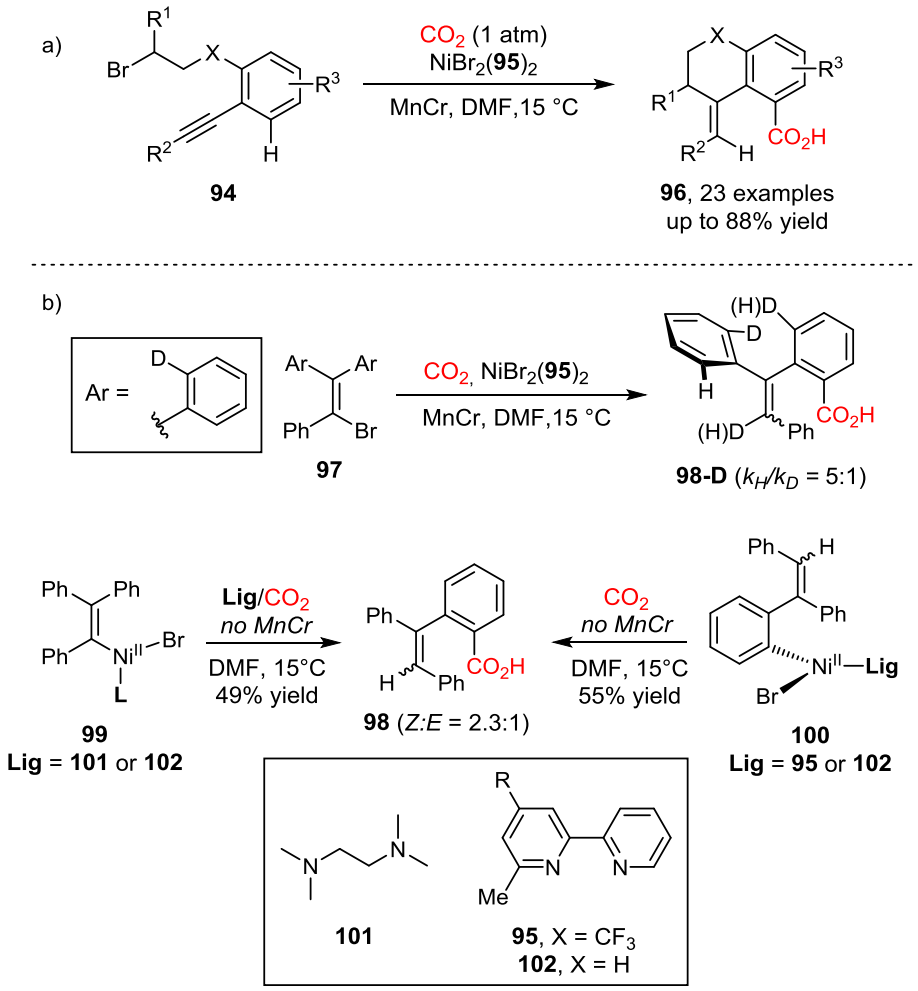

Scheme 46: a) Ni-catalyzed remote C(sp^2)-H carboxylation with CO_2 b) Control experiments with labelled starting materials and preformed Ni(II) complexes.

In 2014 the group of Tsuji developed a copper-catalyzed regiodivergent sila-carboxylation of allenes **103** with $PhMe_2Si$-Bpin and CO_2.[84] In the presence of *rac*-Me-DuPhos ligand (*conditions A*), carboxylated vinyl silanes **104** were obtained as the only regioisomer;

[84] Y. Tani, T. Fujihara, J. Terao, Y. Tsuji, *J. Am. Chem. Soc.* **2014**, *136*, 17706-17709.

however, in the presence of PCy_3 (conditions B) regioisomeric silylated methacrylates **105** were obtained exclusively (Scheme 47). The reversal in regioselectivity might be attributed to the difference in relative steric bulkiness of the CuL (L = Me-DuPhos or PCy_3) and $SiMe_2Ph$ moieties. Indeed, when mono-substituted allenes were employed, the regioselectivity under *conditions B* dropped sensibly, highlighting the steric hinderance at the C-1 position of allenes **103** as a key factor for a high selectivity. The process showed generally high yield, with functional groups such as ketal, alkenyl, bromo and ester being well-tolerated. Products **104** and **105** were also amenable of selective transformations.

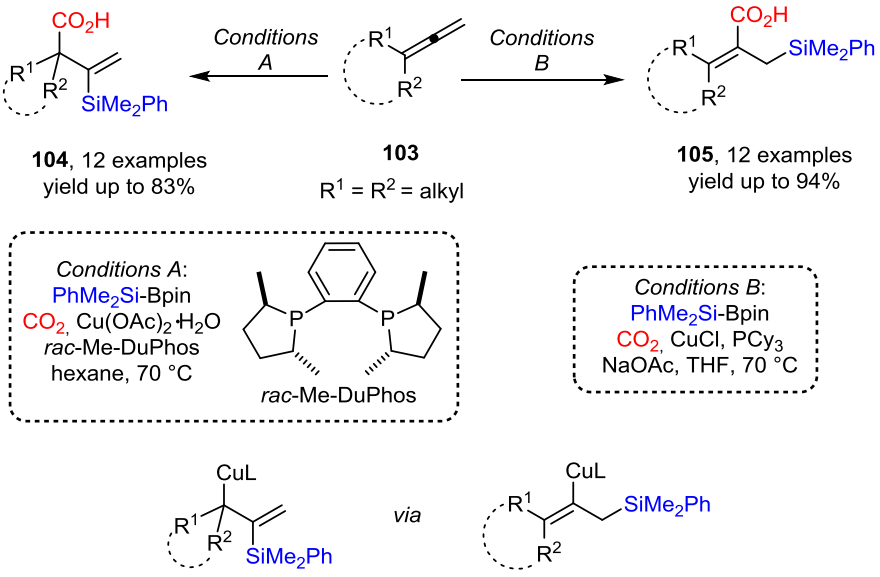

Figura 47: Copper catalyzed regiodivergent sila-carboxylation of allenes.

In 2016, Popp and co-workers disclosed the first hetero-element functionalization-carboxylation of alkenes by developing a redox-neutral copper-catalyzed regioselective bora-carboxylation of styrenes **106**.[85] The process relied on an olefin boryl-cupration by a Cu-B species, followed by CO_2 insertion into the Cu-C bond. The reaction proceeded in the presence of B_2pin_2 as a boron source, catalyst **108** and NaO*t*Bu as a base (conditions *A*, Scheme 48). Under these reaction conditions electron-rich and electron-neutral styrenes could undergo efficiently the desired process for the formation of a variety of α-aryl-β-boryl carboxylic acids **107**. However, electron-poor styrenes failed in delivering any product, suggesting the nucleophilicity of the Cu-alkyl intermediate as a key factor for the carboxylation step. Nevertheless, in 2019, the same group disclosed an improved protocol

[85] T.W. Butcher, E.J. McClain, T.G. Hamilton, T.M. Perrone, K.M. Kroner, G.C. Donohoe, N.G. Akhmedov, J.L. Peterson, B.V. Popp, *Org. Lett.* **2016**, *18*, 6428-6231.

(conditions *B*) relying on the addition of PPh_3 as a co-catalyst. Under these conditions some electron-poor styrenes afforded the desired products **107** in moderate yields.[86]

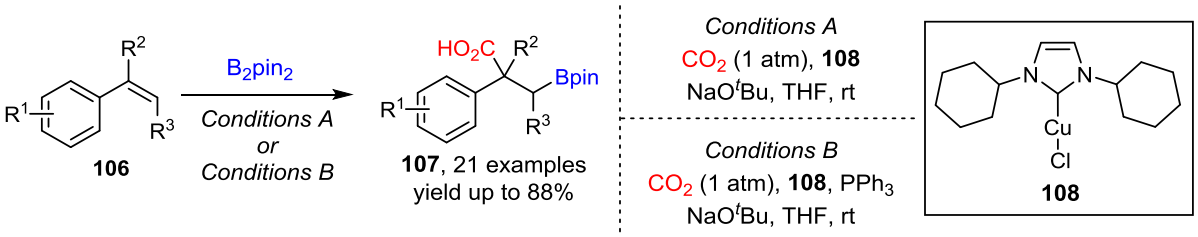

Scheme 48: Redox-neutral Cu-catalyzed bora-carboxylation of styrenes.

In 2020, Li and coworkers disclosed a Rh(I)-catalyzed aryl-carboxylation of acrylamides **109** with arylboronic acids **110** and CO_2.[87] This elegant strategy envisioned the productive merging of 1,4-additions of organometallic reagents to α,β-unsaturated compounds and metal-catalyzed carboxylation reactions, with the aid of a single catalytic species capable of both processes, namely $[Rh(cod)Cl]_2$. Malonate derivatives **111** were thus obtained in high yields when different **109** and substituted **110** were reacted with the abovementioned Rh(I) catalyst. The use of Cs_2CO_3, PMDETA (*N*,*N*,*N*′,*N*″,*N*″-pentamethyldiethylenetriamine) as bases and AgOTf as a co-catalyst completed the reaction conditions (Scheme 49). In particular, the addition of silver salts improved the selectivity of the process greatly, thus increasing the yield in desired products **111** as well. Control experiments pointed to the presence of rhodium-enolates as the nucleophilic species undergoing CO_2 trapping.

[86] T.M. Perrone, A.S. Gregory, S.W. Knowlden, N.R. Ziemer, R.N. Alsulami, J.L. Petersen, B.V. Popp, *ChemCatChem* **2019**, *11*, 5814-5820.
[87] L. Cai, L. Fu, C. Zhou, Y. Gao, S. Li, G. Li, *Green Chem.* **2020**, *22*, 7328-7332.

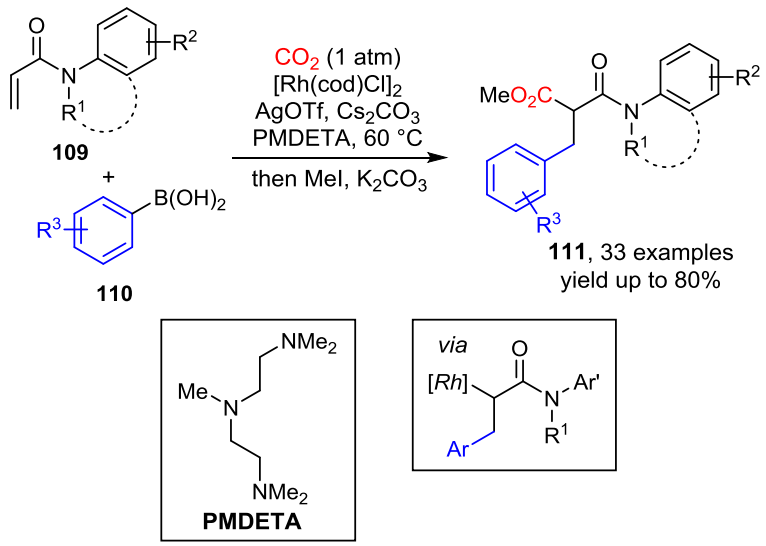

Scheme 49: Rh-catalyzed arylative carboxylation of acrylamides with CO_2 and boronic acids.

In 2020, Zhang, Luo, Hou and co-workers demonstrated that the bora-carboxylation strategy for the tandem functionalization of π-systems is not restricted to C-C double bonds but can be productively achieved on imines **112** as well (Scheme 50).[88] The protocol relies on a copper-catalyzed addition of a B(pin) unit, followed by *N*-carboxylation with atmospheric CO_2 for the preparation of cyclic lithium boracarbamates **114** that can be isolated as such. Alternatively, reaction with Meerwein's salt affords α-amino boronic esters **115** in good to excellent yields.

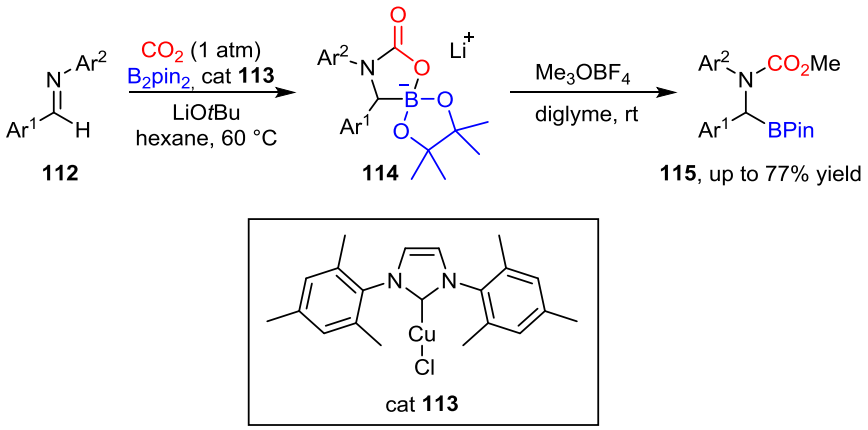

Scheme 50: Cu-catalyzed bora-carboxylation of imines for the synthesis of α-amino acids.

The capability of Ni(0) species to engage oxidative cycloadditions, which yields a nickela-cycle complex with concomitant formation of a C-C bond between two unsaturated partners,[89]

[88] Z. Li, L. Zhang, M. Nishiura, G. Luo, Y. Luo, Z. Hou, *J. Am. Chem. Soc.* **2020**, *142*, 1966-1974.
[89] S. Ogoshi, Nickel Catalysis in Organic Synthesis (Part IV), Wiley-VCH: Weinheim, **2020**.

has been the first exploited strategy for CO_2 fixation. Nickela-lactone complexes are readily obtained via direct oxidative cyclization of CO_2 and monounsaturated systems (alkenes, alkynes, allenes) or via oxidative intramolecular cyclization and subsequent CO_2 insertion with polyunsaturated systems (dienes, diynes). Implementing a reductive transformation of the nickela-lactone complex allows turnover of the nickel catalyst: this approach has prompted the development of catalytic methodologies for the functionalization-carboxylation of unsaturated substrates, either by incorporation of an organic group from an organometallic reductant or by reductive cyclization of the nickela-lactone. On the basis of previously studied co-oligomerization of 1,3-dienes and CO_2 catalyzed by nickel or palladium, in 2002 the group of Mori reported the nickel catalyzed intramolecular ring closing-carboxylation of bis-1,3-dienes **116** (Scheme 51).[90a] The reaction proceeded in the presence of a catalytic amount of $Ni(acac)_2$ and triphenylphosphine, using an excess of a diorganozinc compound as both reductant and transmetalating agent. The selectivity was observed to be absolute: cyclized products **117** or **118** were obtained as single regio- and steroisomers. Shortly after, the same group reported an enantioselective version of the protocol by using (*S*)-MeO-MOP as ligand, with excellent yields and enantioselectivity.[91]

[90] M. Takimoto, M. Mori, *J. Am. Chem. Soc.* **2002**, *124*, 10008-10009.
[91] M. Takimoto, Y. Nakamura, K. Kimura, M. Mori, *J. Am. Chem. Soc.* **2004**, *126*, 5956-5957.

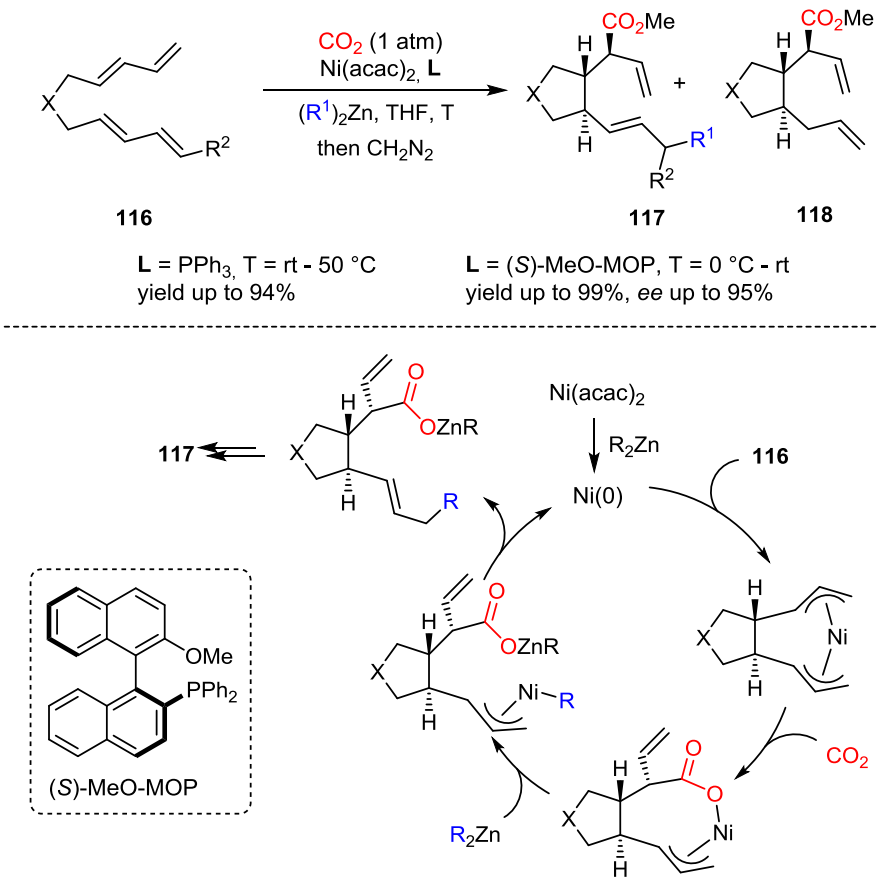

Scheme 51: Enantioselective Ni-catalyzed carboxylation of dienes via nickelalactone.

Various tethering units were found to be competent in the transformation, and unsymmetrical dienes **116**, bearing a terminal methyl group reacted smoothly as well, with carboxylation occurring exclusively at the unsubstituted diene. The proposed mechanism involves oxidative cyclization of the diene to from a bis-η^3-allyl nickel complex, which undergoes CO_2 insertion followed by transmetalation with the organozinc species. Reductive elimination allows the catalyst turnover and furnishes the desired product as methyl ester upon treatment with diazomethane. Particularly worth to mention is that this is one of the very few examples of enantioselective carboxylation with CO_2 nickel-catalyzed.

In the context of nickel-promoted cross-coupling, adopting a stoichiometric reductant makes accessible an interesting catalytic strategy, namely *cross-electrophile coupling*. This expedient has been vastly explored in the last years, becoming a popular tool in the nickel chemistry (Scheme 52a).[92] Exploiting this method on a higher level of complexity brought the

[92] C.E.I. Knappke, S. Grupe, D. Gärtner, M. Corpet, C. Gosmini, A. Jacobi von Wangelin, Chem. Eur. J., **2014**, *20*, 6828-6842.

scientific community to produce different alkene di-functionalization, both in intra- and intermolecular fashions (Scheme 52b).[93]

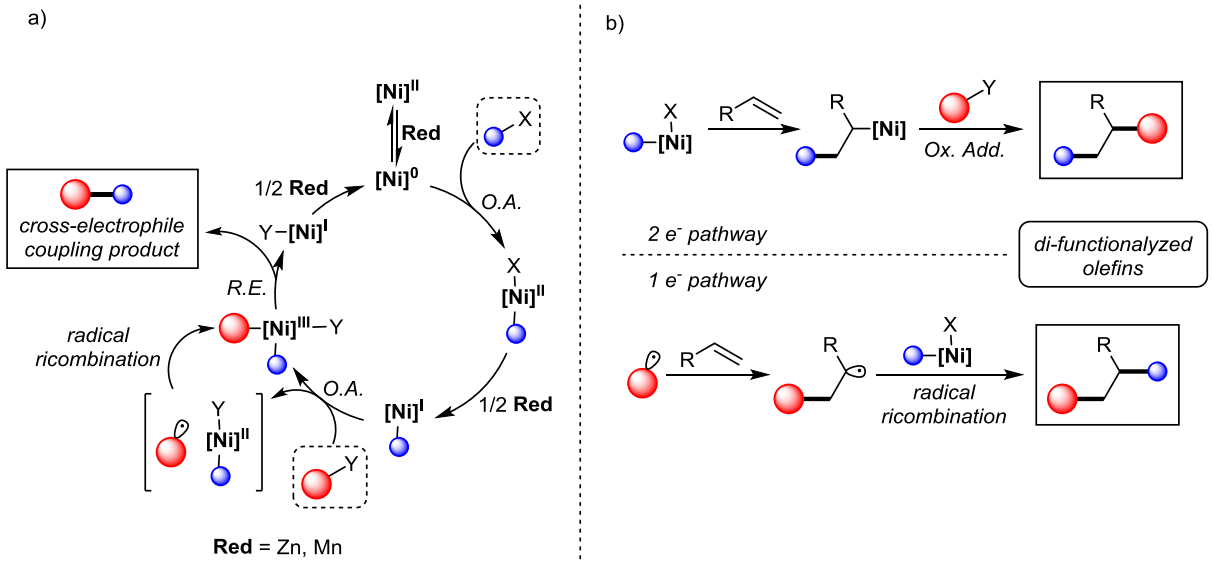

Scheme 52: a) Cross electrophile coupling; b) Reductive alkene di-(carbo)functionalization.

An important field in the nickel catalysis realm is the intramolecular di-functionalization of alkenes, which is being subjected to an exponential growth, particularly in the context of obtaining highly efficient enantioselective processes. This chemistry, which can be traced back to some seminal palladium based examples from the 90s,[94] has been widely explored, but only in the few last years it reached a particularly improved efficiency. Yet only in 2019 three pivotal examples of the synthetic opportunities opened by this strategy were reported independently from three different research groups employing various electrophiles, chiral ligands and conditions (Scheme 53). A range of enantioenriched dihydrobenzofurans, indolines and indanes **122-124** were successfully synthesized from simple 2-iodo-tethered alkenyl arenes **119-121** coupled with alkenyl triflates **126** (Shu)[95], alkyl bromides **128** (Wang)[96] and benzoyloxy amines **130** (Wang and Zhu)[97] with mild conditions and ligands easily obtainable by the *chiral pool* (*i.e.* amino-acids).

[93] Y. Ping, W. Kong, *Synthesis* **2020**, *52*(07), 979-992.
[94] a) R. Grigg, J. V. Sriti, D. Wilson, *Tetrahedron Letters,* **1994,** *35*(25), 4429-4432; b) R. Grigg, V. Sridharan, C. Terrier, *Tetrahedron Letters,* **1996,** *37*(24), 4221-4224; c) R. Grigg, J. M. Sansano, V. Santhakumar, V. Sridharan, *Tetrahedron,* **1997,** *53*(34), 11803-11826; d) M. Yamane, Y. Kubota, K. Narasaka, *Bull. Chem. Soc. Jpn*., **2005,** *78*, 331–340.
[95] Z.-X. Tian, J.-B. Qiao, G.-L. Xu, X. Pang, L. Qi, W.-Y. Ma, Z.-Z. Zhao, J. Duan, Y.-F. Du, P. Su, X.-Y. Liu, X.-Z. Shu, *J. Am. Chem. Soc.* **2019**, *141*, 7637-7643.
[96] Y. Jin, C. Wang, *Angew. Chem. Int. Ed.* **2019**, *58*, 6794-6799.
[97] J. He, Y. Xue, B. Han, C. Zhang, Y. Wang, S. Zhu, *Angew. Chem. Int. Ed.* **2019**, *58*, 1-6.

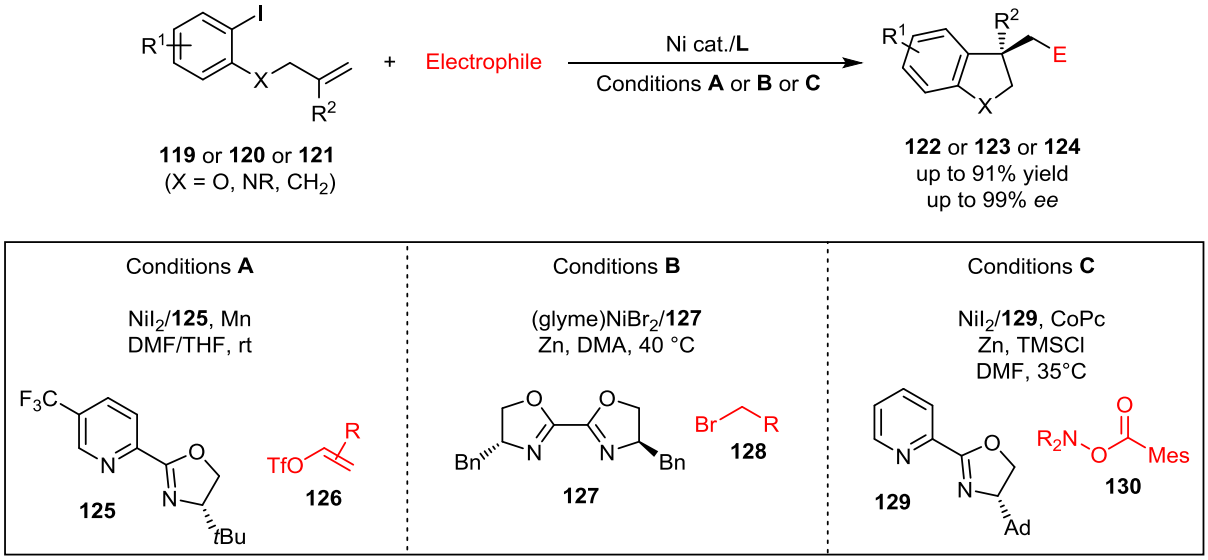

Figura 53: Recent examples of Ni-catalyzed enantioselective di-functionalization of alkenes.

5.2. Aim of the Project

In organic synthesis, catalytic carboxylation[98] and carbonylation[99] protocols, based on a low-pressure CO_2 atmosphere, represent important cornerstones in the creation of chemical complexity/diversity via C1-homologation reactions. However, despite the titanic efforts deployed in this direction by means of metal-based and metal-free catalysis, the realization of added value compounds via enantioselective CO_2-based catalytic carboxylation reactions is still far from being fully developed.[100] In this context, the enantiopure 2,3-dihydrobenzofuran-3-ylacetic acid scaffold **A** (Scheme 54) is of pivotal importance in naturally occurring compounds.[101] However a direct and stereoselective catalytic approach to this motif has not been found yet.[102]

[98] a) D. Yu, S. P. Teong, Y. Zhang, *Coord. Chem. Rev.* **2015**, *293*, 279–291; b) M. Borjesson, T. Moragas, D. Gallego, R. Martin, *ACS Catal.* **2016**, *6*, 6739–6749; c) I. Tommasi, *Catalysts* **2017**, *7*, 380; d) J. Song, Q. Liu, H. Liu, X. Jiang, *Eur. J .Org. Chem.* **2018**, 696–713.

[99] a) L. Wang, W. Sun, C. Liu, *Chin. J. Chem.* **2018**, *38*, 353–362; b) L. Song, Y.-X. Jiang, Z. Zhang, Y.-Y. Gui, X.-Y. Zhou, D.-G. Yu, *Chem. Commun.* **2020**, *56*, 8355–8367.

[100] a) N. Kielland, C. J. Whiteoak, A. W. Kleij, *Adv. Synth. Catal.* **2013**, *355*, 2115–2138; b) X.-B. Lu, Top. *Organomet. Chem.* **2016**, *53*, 171–198; c) J. Vaitla, Y. Guttormsen, J. K. Mannisto, A. Nova, T. Repo, A. Bayer, K. H. Hopmann, *ACS Catal.* **2017**, *7*, 7231–7244.

[101] a) N. Negoro, S. Sasaki, S. Mikami, M. Ito, M. Suzuki, Y. Tsujihata, R. Ito, A. Farada, K. Takeuchi, N. Suzuki, J. Miyazeki, T. Santou, T. Odani, N. Kanzaki, M. Funami, T. Tanaka, A. Kogame, S. Matsunaga, T. Yasuma, Y. Momose, *ACS Med. Chem. Lett.* **2010**, *1*, 290–294; b) M. B. Vekariya, H. S. Joshi, N. C. Desai, K. A. Jadeja, *ChemistrySelect* **2019**, *4*, 10381–10384.

[102] a) S. Olivero, E. Dunach, *Eur. J. Org. Chem.* **1999**, 1885–1891; b) H. Senboku, J. Michinishi, S. Hara, *Synlett* **2011**, *11*, 1567–1572.

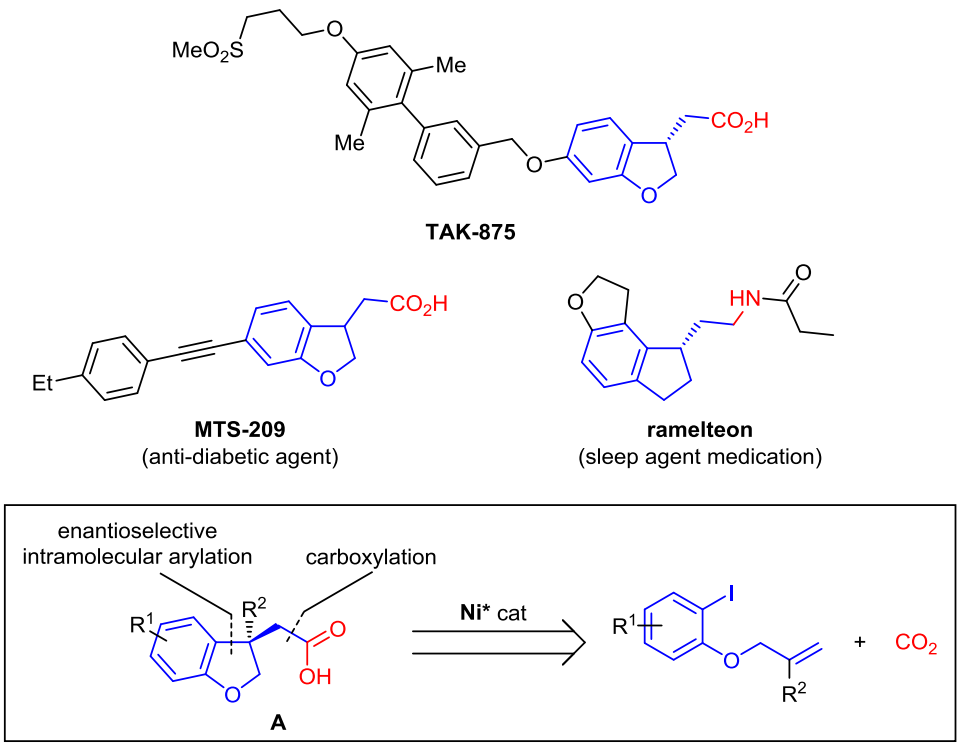

Scheme 54: Working project for the enantioselective aryl-carboxylation of alkenes with CO_2.

Given these assumptions was envisioned the possibility to apply metal catalyzed CO_2 fixation reactions to the direct synthesis of motif **A**, and an unprecedented Ni-catalyzed intramolecular reductive Heck-coupling[103] followed by CO_2-based carboxylation was mustered to this end. It is worth mentioning that, although a number of enantioselective metal-catalyzed truncated Heck-couplings have been reported,[104] the use of CO_2 as the final "electrophilic" trapping agent of the *in situ* generated organometallic intermediate has never been associated so far to this methodology.

5.3. Discussion and Results

At the outset of the investigation, was envisioned that iodoarylether **119a** could act as a suitable model acyclic precursor to yield the desired dihydrobenzofuran-3-ylacetic acid scaffold under reductive cross-coupling/carboxylative conditions. Targeting abundant and low toxic 3d-TMs as catalysts, nickel complexes were assessed along with a survey of reaction parameters. The use of the *in situ* formed **L3**/NiI_2 (20/10 mol%) precatalyst, Zn (3 eq) as

[103] a) S. Bhakta, T. Ghosh, *Adv. Synth. Catal.* **2020**, *362*, 5257–5274; b) F. A. Siqueira, J. C. Taylor, C. R. D. Correia, *Tetrahedron Lett.* **2010**, *51*, 2101–2102; c) H. Senboku, J. Michinishi, S. Hara, *Synlett*, **2011**, 1567–1572.
[104] a) W. You, M. K. Brown, *J. Am. Chem. Soc*. **2015**, *137*, 14578–14581; b) K. Wang, Z. Ding, Z. Zhou, W. Kong, *J. Am. Chem. Soc.* **2018**, *140*, 12364–12368; c) B. Ju, S. Chen, W. Kong, *Chem. Commun.* **2019**, *55*, 14311–14314; d) Z.-M. Zhang, B. Xu, L. Wu, Y. Wu, Y. Qian, L. Zhou, Y. Liu, J. Zhang, *Angew. Chem. Int. Ed.* **2019**, *58*, 14653–14659; e) F. Yang, Y. Jin, C. Wang, *Org. Lett.* **2019**, *21*, 6989–6994; f) Y. Jin, H. Yang, C. Wang, *Org. Lett*. **2020**, *22*, 2724–2729; g) J. He, Y. Xue, B. Han, C. Zhang, Y. Wang, S. Zhu, *Angew. Chem. Int. Ed*. **2020**, *59*, 2328–2332.

reducing agent, TMSCl (3 eq) and TBAI (20 mol%) as additives, released the desired benzofused acetic acid (*R*)-**122** in 52% yield and 93% *ee* via exposure to an atmosphere of CO_2 in DMF (0.07 mM, rt, 16 h, Table 3 entry 3). The main by-products **i-iv** (Scheme of Table 3) were identified in variable amounts in the Ni-catalysis and accounts for the moderate yield.

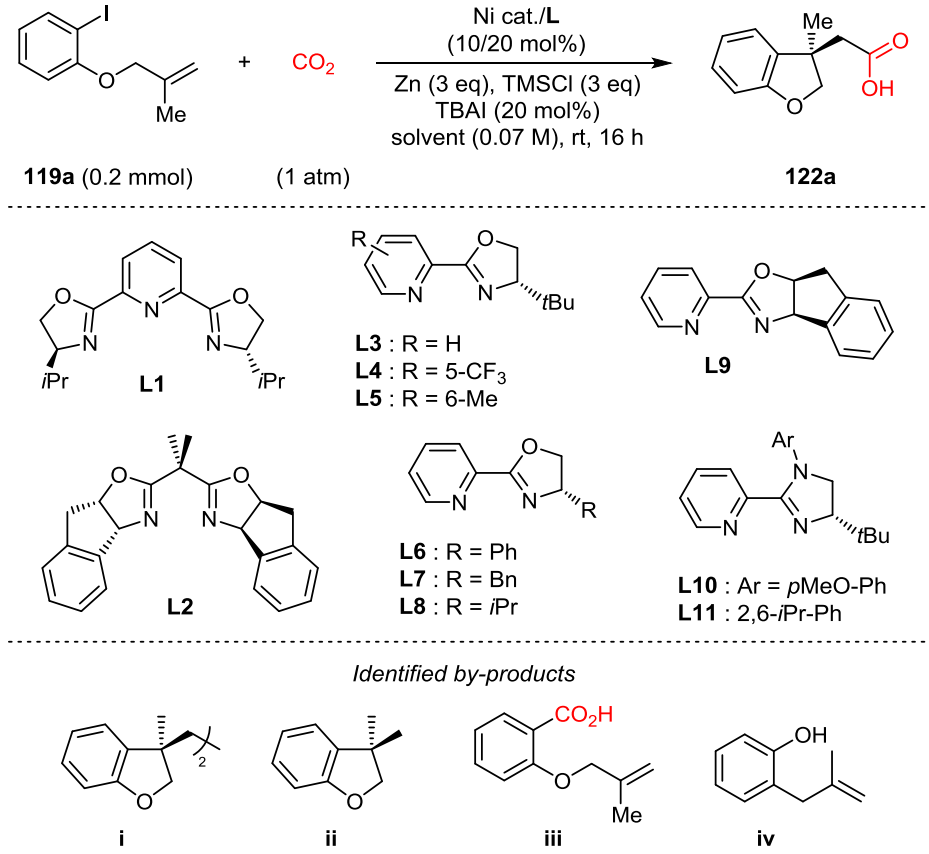

Entry	Conditions	Yield **122a** (%)[b]	*Ee* **122a** (%)[c]
1	**L1**	traces	ND
2	**L2**	13	-21[d]
3	**L3**	52	93
4	**L4**	traces	ND[e]
5	**L5**	8	-7
6	**L6**	18	41
7	**L7**	traces	ND
8	**L8**	30	71
9	**L9**	11	-72[d]
10	**L10**	36	90

11	**L11**	58	96
12	**L11**/$NiBr_2$(glyme)	66	96
13	**L11**/$NiCl_2$(glyme)	60	93
14	No TMSCl, **L11**	NR	-
15	No CO_2, **L11**	NR	-
16	No TBAI, **L11**	47	96
17[f]	0 °C, **L11**	31	98
18[g]	60 °C, **L11**	14	95
19	Mn instead of Zn, **L11**	traces	ND
20	THF, MeCN, dioxane instead of DMF, **L11**	NR	ND
21	Br-**119** was used, **L11**	43	97

Table 3: [a] Reaction conditions: **119a** (0.07 M). Under anhydrous conditions. [b] Determined after flash chromatography. [c] Determined via chiral HPLC. The absolute configuration of **122a** was determined via X-Ray analysis. [d] Inverted stereoinduction was observed. NR: no reaction. ND: not determined. [e] By-products derived from dehalogenation, rearrangement and dimerization of de-iodinated **119a** were isolated as major outcomes. [f] By-product **III** was isolated in 56% yield. [g] Substantial decomposition of the starting material was recorded.

From the screening of reaction conditions, the use of C2-symmetric chiral PyBox **L1** and Box **L2** ligands did not yield synthetically useful results (entries 1,2). The introduction of an electron-withdrawing unit into the C1-symmetric PyOx (*i.e.* CF_3, **L4**) at the C5-position of the pyridyl ring resulted in a marked degrading of chemical outcomes (entry 4). The presence of a mild donor with reduced steric volume (*i.e.* Me, **L5**) in proximity to the coordinating pyridyl nitrogen atom proved not only highly detrimental for the turnover of the process but also led to an inversion of the stereochemical induction. Modifying the *t*Bu steric probe on the oxazoline framework also produced undesired effects (**L6**-**L9**). In order to test if more profound changes to the electronic structure of the ligand would improve the output of this process, was tested some imidazoline variants (**L10**-**L11**). Gladly, the replacement of PyOx **L3** with pyridyl imidazoline ligand **L11** (DIPP: 2,6-*i*Pr-phenyl)[105] resulted in substantial improvements in both reproducibility and chemical outcomes (yield = 66%, *ee* = 96%) in the presence of (glyme)$NiBr_2$ (entry 12). Focusing on the role of additives, the use of catalytic amounts (20 mol%) of TBAI (tetrabutylammonium iodide) improved the turnover of the process (yield = 47%, *ee* = 96%, entry 16) likely facilitating the release of the metal from the

[105] a) C. Karmel, C. Z. Rubel, E.V. Kharitonova, J. F. Hartwig, *Angew. Chem. Int. Ed.* **2020**, *59*, 6074-6081; Y. He, C. Liu, L. Yu, S. Zhu, *Angew. Chem. Int. Ed.* **2020**, *59*, 21530-21534.

final carboxylates. Even more pronounced was found to be the impact of TMSCl on the mechanism (entry 14): its omission caused complete inhibition of the process. This can be attributed to multiple actions such as: 1) activation of the metal powder reductant; 2) co-activation of the CO_2 and 3) metal scavenging of the final carboxylates. Room temperature led to optimal results with respect to 0 °C or 60 °C (entries 17,18) and Zn as a stoichiometric sacrificial metal reductant proved superior to Mn (entry 19). Interestingly only DMF among the common polar aprotic solvents promoted the reactivity, while others failed even in giving any chemical output (entry 20). Finally, the bromo derivative Br-**119a** could also be employed as a model substrate, although at the expense of a light decrease in the chemical yield (yield = 43%, *ee* = 97%, entry 21).

In an attempt to simplify the protocol and in order to get further insight into the real nature of the catalytically active chiral Ni complex, was envisioned the possibility of using a pre-formed Ni-adduct in the carboxylation event. Here, the synthesis of **L11**-$NiCl_2$ was attempted by refluxing in THF a 2:1 mixture of **L11** and dried $NiCl_2$. Interestingly, a single-crystal X-ray study (in collaboration with Prof. Magda Monari, University of Bologna) carried out on one crystal grown from the resulting pale-green solid revealed the formation of the cationic aquo complex $[(\mathbf{L11})_2Ni(H_2O)Cl]^+(Cl^-$ as counterion). The Ni(II) center exhibits a distorted octahedral geometry (Scheme 55a) being coordinated by one chloride, one H_2O molecule and two pairs of N atoms of the bidentate **L11** ligand. The Cl^- and H_2O ligands are in mutual *cis* position whereas in the bidentate N ^ N ligands (**L11)** the pyridyl N atoms adopt a *trans* arrangement and the imidazolyl N atoms have a *cis* disposition.

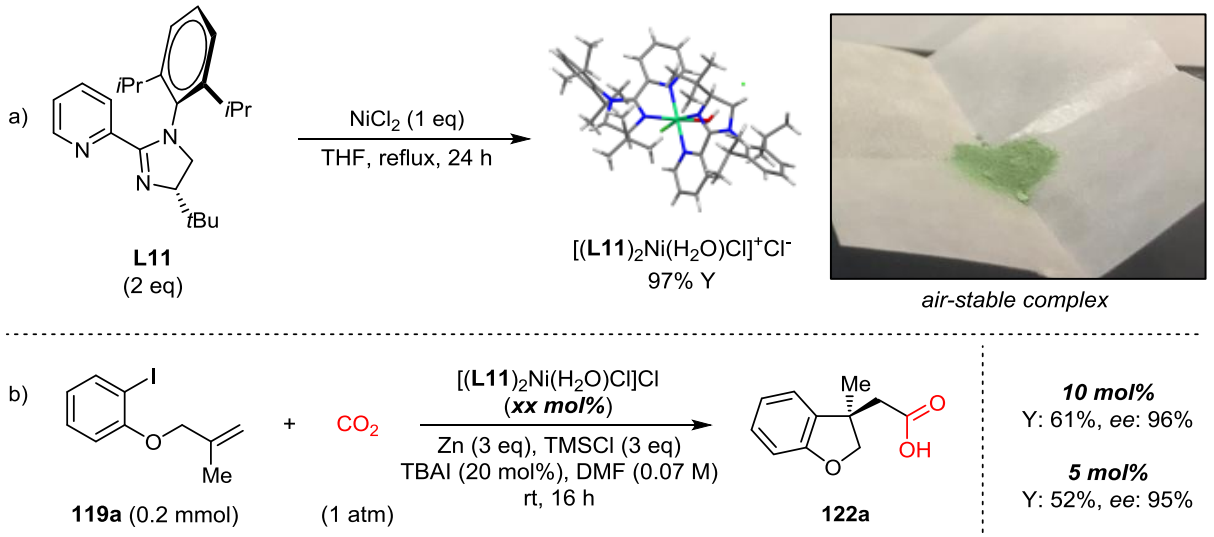

Scheme 55: a) Synthesis of the chiral nickel complex; b) Catalytic performances of the pre-formed catalyst.

The Ni-Npy distances [2.073 and 2.084(3) Å] are similar and shorter than the Ni-Nim ones [2.092 and 2.122(3) Å] being the latter N atom positioned *trans* to the chloride ligand. The Ni-O and Ni-Cl distances [2.126 and 2.141(3) Å] fall in the range typical for Ni complexes. The Npy-Ni-Nim bite angles in the two five-membered metallacycles are almost identical [78.4(2) and 77.8(1)°, respectively]. The pyridyl and imidazoline rings in each **L11** ligand are not coplanar but have dihedral angles of 18.2 and 17.7(2)°, respectively, due to steric congestion generated by the bulky substituents. Interestingly, this cationic aquo complex [**(L11**)$_2$Ni(H_2O)Cl]Cl (5-10 mol%) proved high competence in promoting the carboxylative truncated Heck-coupling of **119a** delivering the dihydrobenzofuran **122a** in similar extent to the *in situ* approach (Scheme 55b *vs* entry 13, Table 1). Having established the optimal reaction conditions, the generality of the enantioselective carboxylative Heck cross-coupling was assessed by subjecting a range of diversely functionalized *ortho*-aryliodines (**119b-o**) to the cascade protocol in the presence of [(**L11**)$_2$Ni(H_2O)Cl]Cl (10 mol%). The chemical outcomes of these essays have been collected in Scheme 56 and from the results some preliminary conclusions can be drawn.

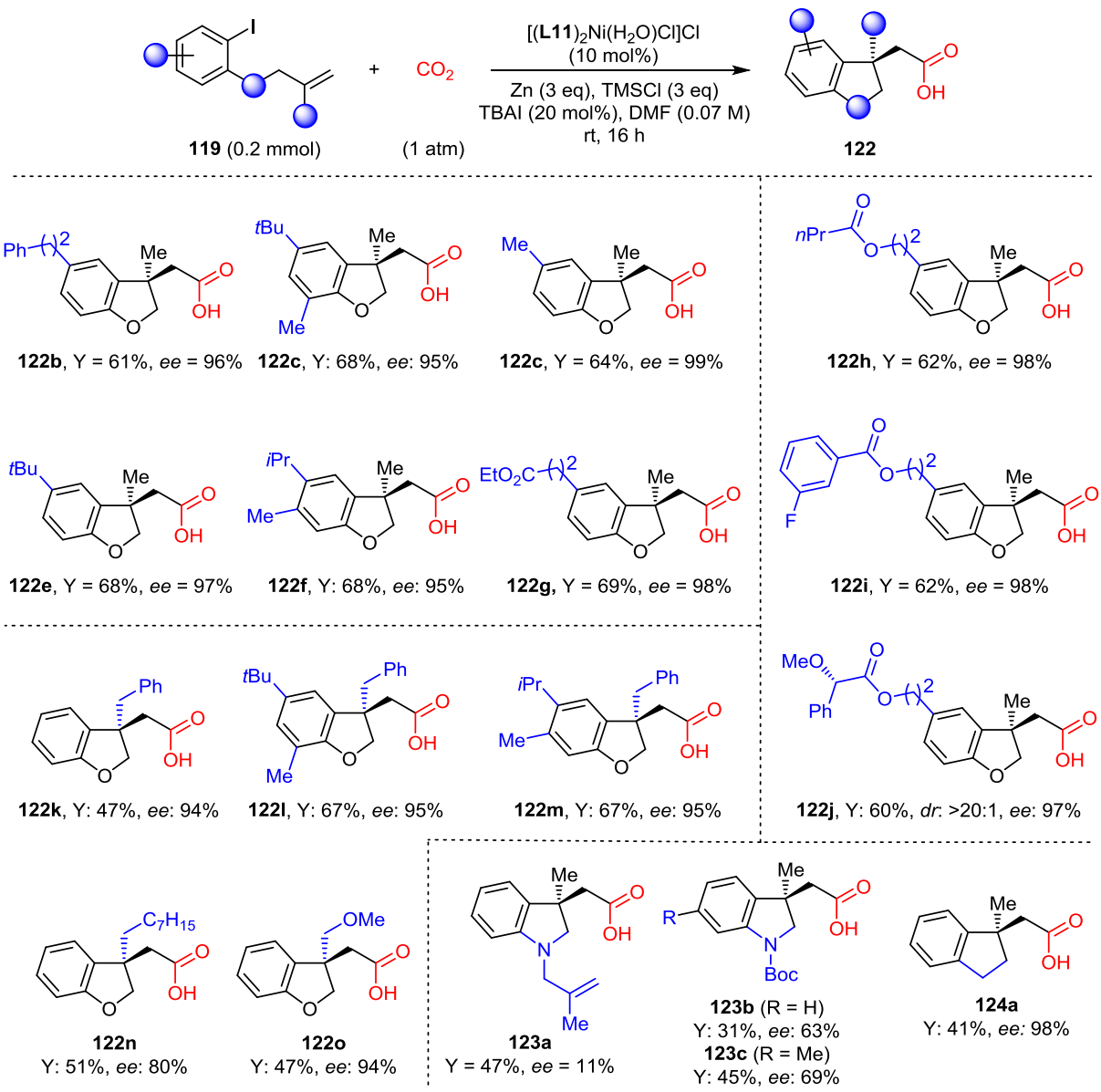

Scheme 56: Scope for the enantioselective tandem Heck/carboxylation.

Tolerance towards decoration of the phenolic ring with electron-donating substituents (Me, *i*Pr, *t*Bu) was recorded through substrates **119b-j**. In particular, the corresponding 2,3-dihydrobenzofuran-3-ylacetic acids **122b-j** were isolated in synthetically useful yields (61-69%) and enantiomeric excesses systematically higher than 90% were obtained (Scheme 56). On the contrary, limitations of the method emerged from the accommodation of EWGs at the aromatic ring (*i.e.* 4-Cl, 4-CF_3) that prevalently led to the direct carboxylation of the benzene ring, prevalently.[106] The possibility to decorate the newly formed all carbon quaternary

[106] a) T. Fujihara, K. Nogi, T. Xu, J. Terao, Y. Tsuji, *J. Am. Chem. Soc*. **2012**, *134*, 9106-9109; b) F. Rebih, M. Adreini, A. Moncomble, A. Harrison-Marchand, J. Maddaluno, M. Durandetti, *Chem.-Eur. J.* **2016**, *22*, 3758-3760; c) A. Correa, T. Leon, R. Martin, *J. Am. Chem. Soc.* **2014**, *136*, 1062-1069; c) C. Ma, C.-Q. Zhao, X.-T. Xu, Z.

stereogenic centers with different substituents was then considered. In particular, aliphatic, aromatic and OMe groups were successfully installed at different distances from the stereogenic center (**122k-o**) resulting in similar and remarkable chemical and optical outcomes (*ee* up to 98%). Finally, the role of the tethering unit was investigated by replacing the oxygen atom with *C*- as well as *N*-based connectors. Here, although *N*-allyl- and *N*-Boc-indoline scaffolds **123a-c** were isolated in moderate extents (*ee*: 11-69%), the enantio-enriched dihydroindene acetic acid **124a** was obtained in excellent stereochemical yield (*ee* = 98%). Then, the absolute configuration of compound **122a** was unambiguously determined to be *R* via single crystal X-ray analysis of the corresponding bromo-amide **131a** (Scheme 57a). Additionally, the pivotal role of CO_2 in generating the carboxylic unit of targeted compounds **122** was determined via a labelled ^{13}C-experiment. As a matter of fact, a full incorporation of ^{13}C-carbon dioxide (99.8% labelling) was obtained in the final compound **122a** when $^{13}CO_2$ was employed under optimal reaction conditions (^{13}C-**122a**, yield = 65%, *ee* = 98%, Scheme 57b).

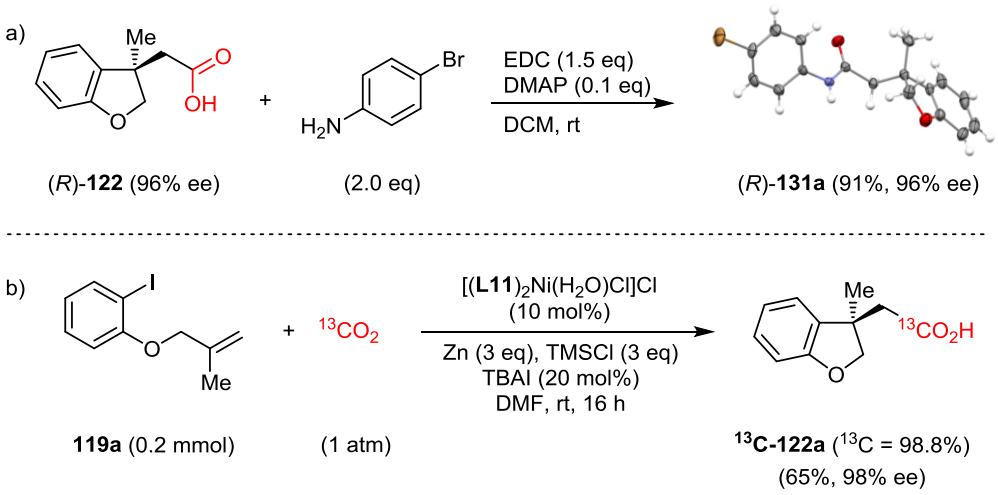

Scheme 57: a) Synthesis of the *p*-bromoamide **131a** to establish the absolute configuration; b) Isotopic labelling of the model substrate.

In order to gain further insight into this reaction, a mechanistic exploration was carried out in parallel by DFT simulations. Crucial questions that are key to the understanding of this reactivity are, at least: 1) what is the structural model of enantiodiscrimination, 2) which is the active catalyst. Initially was assumed that the [(**L**)$_2$Ni(H$_2$O)Cl]Cl complex, with a 2:1 **L**:Ni ratio, would dissociate delivering the **L**Ni species **I** as the active catalyst (*see* the NLE

M. Li, X.-Y. Wang, K. Zhang, T.S. Mei, *Org. Lett.* **2019**, *21*, 2464-2467; d) T. Yanagi, R. J. Somerville, K. Nogi, R. Martin, H. Yorimutsu, *ACS Catal.* **2020**, *10*, 2117-2123.

Scheme 59). Was also assumed that [Ni(0)] would be the oxidation state of the catalyst, after reduction with the excess of zinc.[107] Catalytic cycles were simulated via DFT calculations (In collaboration with Prof. Carlos Silva Lopez, University of Vigo) for the PyOx (**L3**) and its imidazoline variant **L11**. Both ligands yielded similar reaction profiles. First was explored a [Ni(0)]/[Ni(II)] catalytic cycle in which Zn would only participate at the end, to restore the active [Ni(0)] catalyst **I** (**path A** - Scheme 58). From this, a facile oxidative addition of **119a** occurs to form intermediate **II**. Then, the stereodiscriminating addition of the Ni-C bond to the alkene must occur. The barriers associated to the formation of the two diastereomers favor (by 2.5 kcal/mol) the formation of intermediate **III**. Attempts to describe this step also on the neutral complex **II** were unsuccessful, while was possible find only the associated transition state assuming prior loss of iodine. This is explained through the need to open a coordinating vacant site such that the double bond can be pre-activated for the addition step. However, the insertion of CO_2 onto intermediates **III** and **III-diast**, to yield the final carboxylates **IV** and **IV-diast**, featured high activation energies (26.3 and 36.7 kcal/mol, respectively) rendering these paths unlikely. Was therefore considered whether a zinc-mediated [Ni(II)]/[Ni(I)] reduction step along the reaction pathway could facilitate the carboxylation event,[108] and indeed, the reaction proceeds much more favorably if Ni is reduced right before CO_2 insertion (**path C** - Scheme 58). This reduction step could also be occurring earlier in the mechanism, right after the oxidative addition (**path B** - Scheme 58). Interestingly the latter alternative, which involves a rare Heck step occurring at a Ni(I) species, also produces very competitive barriers for the subsequent steps. Analyzing the experimental chemical output of the reaction, even in different conditions from optimal (*see* Table 3, entry 17), stands up one very common side product of this protocol, which is the benzoic acid derivative (**SP**) deriving by a direct carboxylation of the aryl-Ni intermediates. Was computed the transition state for this carboxylation both at the [Ni(II)] and [Ni(I)] complexes. Was found that this step is very costly for the [Ni(II)] complex (a computed barrier of about 30 kcal/mol) and that it is feasible when acting on the [Ni(I)] species. These results therefore not only help explain the formation of this byproduct but also strongly candidate the **path B** (Scheme 58) as the mechanism at work, involving an unusual Heck step on a [Ni(I)] complex.[109]

[107] J. B. Diccianni, T. Diao, *Trends in Chem.* **2019**, *1*, 830-844.
[108] a) R. J. Somerville, R. Martin, *in* Nickel catalysis in organic synthesis: methods and reactions, chap. 12, pp. 285-330, Wiley-VCH, **2019**; b) F. B. Sayyed, Y. Tsuji, S. Sakaki, *Chem. Commun.* **2013**, *49*, 10715-10717.
[109] M. Borjesson, T. Moragas, D. Gallego, R. Martin, *ACS Catal.* **2016**, *6*, 6739-6749.

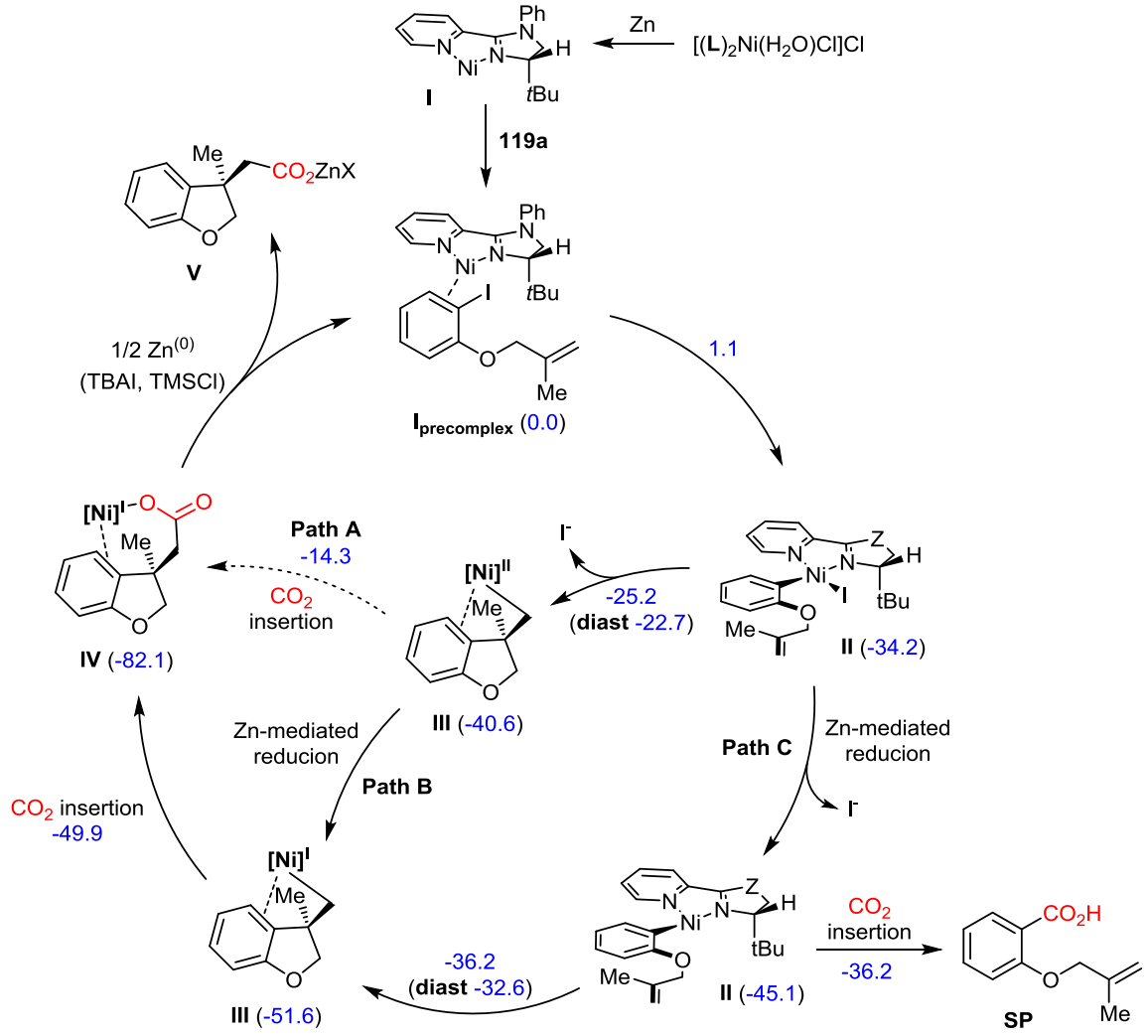

Scheme 58: Proposed mechanism for the aryl-carboxylation of alkenes.

In an attempt to unequivocally determine the nature of the active catalyst, was performed a non-linear effect study[110] on the model transformation **119a** → **122a**, by varying the enantiopurity of the chiral ligand **L3**. Interestingly, a perfect linear correlation between *ee*(**L3**) and *ee*(**122a**) was observed (Scheme 59). This finding led to the conclusion that indeed the isolated [(**L11**)$_2$Ni(H$_2$O)Cl]Cl species should be considered a pre-catalytic unit, capable of delivering the active 1:1 active organometallic species through an *in situ* ligand dissociation event.

[110] a) C. Girard, H. B. Kagan, *Angew. Chem., Int. Ed.* **1998**, *37*, 4000-4037; b) H.B. Kagan, *Adv. Synth. Catal.* **2001**, *343*, 227-233.

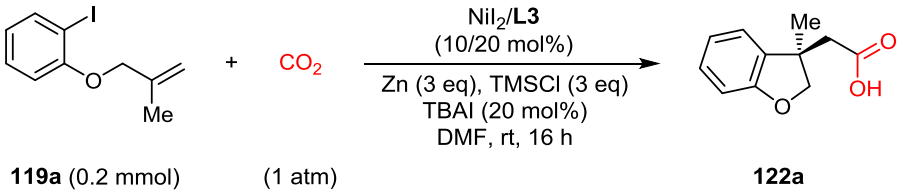

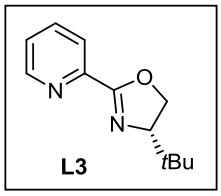

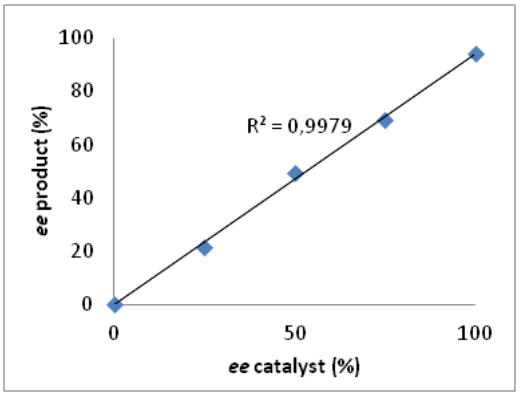

Scheme 59: Non-linear experiments with ligand **L3**.

Non-covalent interactions (NCI) analysis performed onto transition states $\mathbf{TS_{II\text{-}III}}$ and $\mathbf{TS_{II\text{-}IIIdiast}}$ provides an interesting picture of the stereodiscriminating mechanism where the *t*Bu group location is pivotal to differentiate between the two available trajectories for the cyclization (Scheme 60).

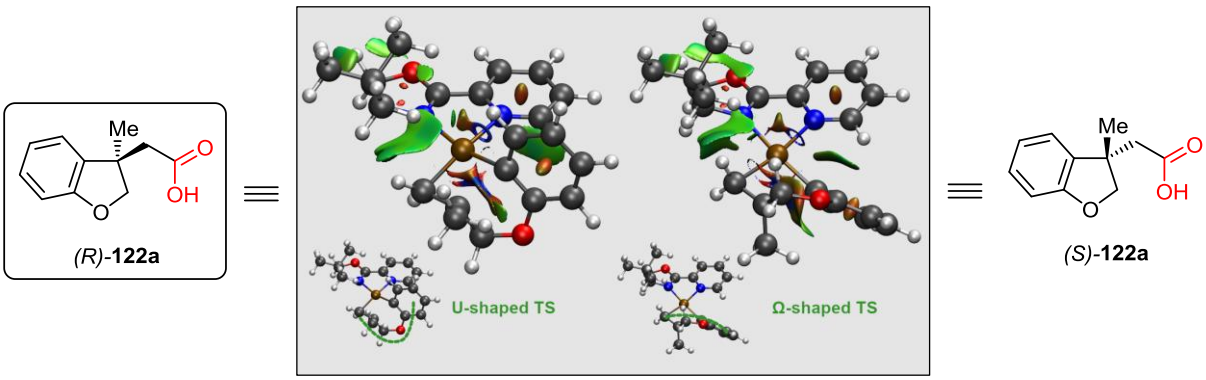

Figura 60: Non-covalent interactions analysis of the stereodiscriminating transition state.

In both cases there is steric contact with this group, however, it is considerably stronger in the Ω trajectory than in the U alternative. In the former the *t*Bu group is pushed back by the incoming alkene which also translates into stronger steric contacts with the heterocyclic fragment of the chiral ligand in the back (Scheme 60).

5.4. Conclusion

In conclusion, an asymmetric nickel catalyzed tandem Heck-coupling/CO_2-carboxylation reaction is documented and its scope was evaluated to be wide enough to provide an unprecedented and versatile protocol for the synthesis of stereodefined hetero-benzofused acetic acids. A range of valuable enantioenriched hetero-cyclic scaffolds were produced, and the possibility to synthesize fully labeled carboxylic acids in mild conditions is particularly attractive in the bio-medicinal field. A fully elucidated mechanistic profile, comprising an unusual Ni(I)-mediated Heck-type elementary step, was also proposed based on a combined experimental/computational analysis.

5.5. General Procedures and Product Characterization

5.5.1. Materials and Methods

^{1}H-NMR spectra were recorded on Varian 400 (400 MHz) spectrometers. Chemical shifts are reported in ppm from TMS with the solvent resonance as the internal standard (deuterochloroform: 7.24 ppm). Data are reported as follows: chemical shift, multiplicity (s = singlet, d = doublet, dd= doublet doublet, t = triplet, td = triple doublet, dt = double triplet, q = quartet, sext = sextet, sept = septet, p = pseudo, b = broad, m = multiplet), coupling constants (Hz). ^{13}C-NMR spectra were recorded on a Varian 400 (100 MHz) spectrometers with complete proton decoupling. Chemical shifts are reported in ppm from TMS with the solvent as the internal standard (deuterochloroform: 77.0 ppm). GC-MS spectra were taken by EI ionization at 70 eV on a Hewlett-Packard 5971 with GC injection. They are reported as: *m/z* (rel. intense). LC-electrospray ionization mass spectra were obtained with Agilent Technologies MSD1100 single-quadrupole mass spectrometer. HRMS-ESI were obtained with column Luna Omega 3um Polar C18 (size 100*3 mm) and Xevo G2-XS QTof. The enantiomeric excess (*ee*) were determined by chiral HPLC, on an Agilent Technologies Series 1200 instrument using chiral columns. The enantiomeric compositions were checked against the corresponding racemic products. Chromatographic purification was done with 240-400 mesh silica gel. Other anhydrous solvents were supplied by Sigma Aldrich in Sureseal® bottles and used without any further purification. Commercially available chemicals were purchased from Sigma Aldrich, Fluorochem, Alfa Aeser and TCI and used without any further purification. Melting points were determined with Bibby Stuart Scientific Melting Point Apparatus SMP 3 and are not corrected. Agilent Technologies LC/MSD Trap 1100 series (nebulizer: 15.0 PSI, dry Gas: 5.0 L/min, dry temperature: 325 °C, capillary voltage positive scan: 4000 mA, capillary voltage negative scan: 3500 mA). The X-ray intensity data for [(**L11**)$_2$Ni(H$_2$O)Cl]Cl and (*R*)-**122a** were measured on a Bruker Apex III CCD diffractometer. Cell dimensions and the orientation matrix were initially determined from a least-squares refinement on reflections measured in four sets of 20 exposures, collected in three different ω regions, and eventually refined against all data. A full sphere of reciprocal space was scanned by 0.5° ω steps. The software SMART[3] was used for collecting frames of data, indexing reflections and determination of lattice parameters. The collected frames were then processed for integration by the SAINT program,[111] and an empirical absorption

[111] *SMART & SAINT Software Reference Manuals*, version 5.051 (Windows NT Version), Bruker Analytical X-ray Instruments Inc.: Madison, Wi, **1998.**

correction was applied using SADABS.[112] The structures were solved by direct methods (SIR 2014)[113] and subsequent Fourier syntheses and refined by full-matrix least-squares on F^2 (SHELXTL)[114] using anisotropic thermal parameters for all non-hydrogen atoms. The aromatic, methyl, methylenic and methine hydrogen atoms were placed in calculated positions, refined with isotropic thermal parameters *U(H)* = 1.2 *Ueq*(C) and allowed to ride on their carrier carbons. Known compounds were prepared following the known procedures: **119a, 119d, 119e, 119f, 119k** (ref. 5)[115], Br-**119a** (ref. 6)[116], **121a** (ref. 7)[117], **119o** (ref. 8)[118], **120b** (ref. 9)[119], **119n, 120c** (ref. 10)[120], **120a** (ref. 11)[121].

[112] G. M. Sheldrick, *SADABS-2008/1 - Bruker AXS Area Detector Scaling and Absorption Correction*, Bruker AXS: Madison, Wisconsin, USA, **2008**.
[113] M.C. Burla, R. Caliandro, B. Carrozzini, G.L. Cascarano, C. Cuocci, C. Giacovazzo, M. Mallamo, A. Mazzone, G. Polidori, *J. Appl. Cryst.* **2015**, *48*, 306-309.
[114] G. M. Sheldrick, *Acta Cryst C71***, 2015**, 3-8.
[115] G. Yang, X. Wenfang, C. Huoji, W. Wanqing, P. Jianwen, G. Yinglan, J. Huanfeng, *J. Org. Chem.* **2015,** *80*, 7456-7467.
[116] W. Wang, R. Zhou, Z.-J. Jiang, X. Wang, H.-Y. Fu, X.-L. Zheng, H. Chen, R.-X. Li, *Eur. J. Org. Chem.* **2015**, 2579-2584.
[117] D. G. W. Iain, R. Stefanie,; F. T. Dean, *J.Am.Chem.Soc.* **2009**, *131*, 2056-2057.
[118] A. G. Samantha, V-C. Suhelen, A. S. Ryan, *J. Am. Chem. Soc.* **2018**, *140*, 11317-11324
[119] S. Daniel, M. Francesco, F. Israel, A. S. Miguel, *J. Org.Chem.* **2012**, *77*, 10272-10284.
[120] T. Zhi-Xiong, Q. Jin-Bao, X. Guang-Li, P. Xiaobo, Q. Liangliang, M. Wei-Yuan, Z. Zhen-Zhen, D. Jicheng, D. Yun-Fei, S. Peifeng, L. Xue-Yuan. S. Xing-Zhong, *J. Am. Chem. Soc.* **2019,** *141*, 7637-7643.
[121] K. Ramesh, S. Basuli, G. Satyanarayana, *Eur.J.Org.Chem.* **2018**, 2171-2177.

5.5.2. General Procedure A for the synthesis of acyclic precursor by S_N2 reaction[122]

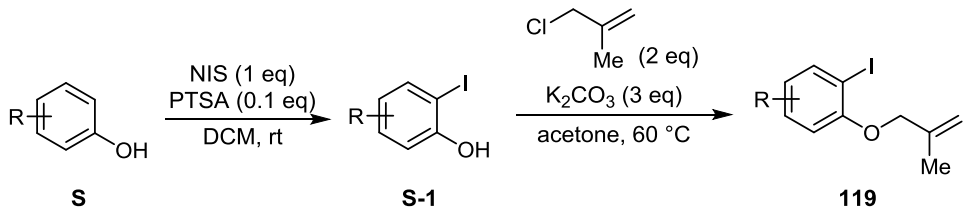

A solution of phenol **S** (5.0 mmol) in DCM (15 mL) was treated with *N*-iodosuccinimide (1.12 g, 5.0 mmol) and *p*-toluenesulfonic acid monohydrate (95.1 mg, 10 mol%) at room temperature for 6 h. The reaction was quenched with water (15 mL), extracted with DCM (3 x 15 mL), and the reunited organic phases were washed with $Na_2S_2O_3$ (10 mL), dried over anhydrous Na_2SO_4, and concentrated under reduced pressure, to obtain the *o*-iodophenol **S-1** quantitatively. The iodinated phenol was then dissolved in acetone (30 mL), and K_2CO_3 (2.07 g, 15.0 mmol) was added. After 10 min methallyl chloride (0.97 mL, 10 mmol) was added, and the solution was stirred at reflux for 5 h. At complete consumption of the starting material (TLC) the solvent was removed, and the crude was dissolved in ethyl acetate (20 mL) and extracted with water (20 mL), washed with brine (15 mL), dryed over anhydrous Na_2SO_4, and concentrated under reduced pressure. The residue was purified by flash chromatography on silica gel to give the desired product **119**.

2-Iodo-1-((2-methylallyl)oxy)-4-phenethylbenzene (**119b**)

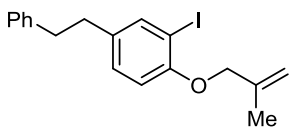

Colorless oil, yield = 95% (1.79 g, *n*-Hex). **^{1}H NMR** (400 MHz, $CDCl_3$) δ = 7.64 (t, *J* = 2.3 Hz, 1H), 7.30 (ddd, *J* = 8.1, 6.6, 2.1 Hz, 2H), 7.26 – 7.14 (m, 3H), 7.06 (dt, *J* = 8.4, 2.1 Hz, 1H), 6.71 (dd, *J* = 8.3, 1.7 Hz, 1H), 5.22 (s, 1H), 5.04 (s, 1H), 4.47 (s, 2H), 2.92 – 2.86 (m, 2H), 2.84 (m, 2H), 1.89 (s, 3H). **^{13}C NMR** (100 MHz, $CDCl_3$) δ = 155.48, 141.43, 140.37, 139.28, 136.12, 129.30, 128.49 (2C), 128.40 (2C), 126.03, 112.86, 112.10, 86.51, 72.64, 38.00, 36.56, 19.55. **GC-MS** (m/z): 287 (100), 378 (27). **Anal. Calc.** for ($C_{18}H_{19}IO$: 378.05): C, 57.16; H, 5.06; found: C, 57.00, H, 4.96.

5-(*tert*-Butyl)-1-iodo-3-methyl-2-((2-methylallyl)oxy)benzene (**119c**)

[122] M. Pierre-Yves, F. B. Marcus, C. Jyun-Hung, A. G. Timothy, S. K. Donald, D. L. Mark, L. Sha, A. M. Dale, M. M. Christopher, R-M. Anne, M. O. Katheen, R. Deepa, W. T. Anthony, S. T. John, Y. Nathan, J. A. Robert, *Bioorg. & Med. Chem. Lett.* **2003**, *13*, 4071-4075.

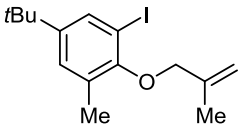

Colorless oil, yield = 91% (1.56 g, *n*-Hex). **^{1}H NMR** (400 MHz, $CDCl_3$) δ = 7.58 (s, 1H), 7.13 (s, 1H), 5.19 (s, 1H), 5.00 (s, 1H), 4.24 (s, 2H), 2.31 (t, *J* = 2.3 Hz, 3H), 1.92 (s, 3H), 1.27 (t, *J* = 2.4 Hz, 9H). **^{13}C NMR** (100 MHz, $CDCl_3$) δ = 153.77, 148.16, 140.50, 133.36, 130.72, 127.99, 112.20, 91.30, 75.22, 33.41, 30.62 (3C), 19.17, 16.65. **GC-MS** (m/z): 162 (100), 334 (16), 329 (14). **Anal. Calc.** for ($C_{15}H_{21}IO$: 344.06): C, 52.34; H, 6.15; found: C, 52.21, H, 6.01.

Ethyl 3-(3-iodo-4-((2-methylallyl)oxy)phenyl)propanoate (**119g**)

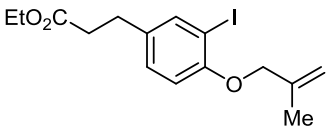

Colorless oil, yield = 93% (1.74 g, *n*-Hex). **^{1}H NMR** (400 MHz, $CDCl_3$) δ = 7.60 (d, *J* = 2.2 Hz, 1H), 7.11 – 7.04 (m, 1H), 6.68 (d, *J* = 8.4 Hz, 1H), 5.15 (s, 1H), 4.98 (s, 1H), 4.42 (s, 2H), 4.10 (qd, *J* = 7.1, 0.9 Hz, 2H), 2.82 (t, *J* = 7.7 Hz, 2H), 2.54 (dd, *J* = 8.2, 7.2 Hz, 2H), 1.83 (s, 3H), 1.21 (t, *J* = 7.1 Hz, 3H). **^{13}C NMR** (100 MHz, $CDCl_3$) δ = 172.61, 155.67, 140.25, 139.14, 134.85, 129.18, 112.83, 112.13, 86.49, 72.58, 60.43, 35.96, 29.55, 19.45, 14.22. **GC-MS** (m/z): 159 (100), 374 (65), 287 (61). **Anal. Calc.** for ($C_{15}H_{19}IO_3$: 374.04): C, 48.14; H, 5.12; found: C, 48.00, H, 5.11.

5.5.3. General Procedure B for the synthesis of acyclic precursor by Mitsunobu reaction[123]

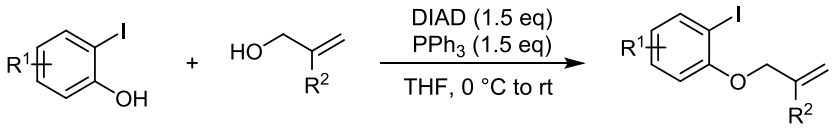

S-1 (1.0 eq) **119**

To a solution of allylic alcohol (5.0 mmol) and phenol **S-1** (5.0 mmol) in THF (15 mL), under nitrogen atmosphere, was added PPh_3 (1.96 g, 7.5 mmol) at 0 °C, followed after 20 min by slow addition of DIAD (1.51 g, 7.5 mmol). The reaction mixture was allowed to warm to room temperature, and stirred for 12 h. The reaction was quenched with water (20 mL) and extracted with AcOEt (3 x 15 mL), and the organic layers were washed with brine, dried over anhydrous Na_2SO_4, and concentrated under reduced pressure. The residue was purified by flash chromatography on silica gel to give the desired product **119**.

[123] H. Zheng, Y. Zhu, Y. Shi, *Angew. Chem. Int. Ed.* **2014**, 53: 11280-11284.

2-((2-Benzylallyl)oxy)-5-(*tert*-butyl)-1-iodo-3-methylbenzene (**119l**)

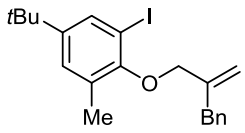

Colorless oil, yield = 74%, (1.55 g, *n*-Hex). **^{1}H NMR** (400 MHz, $CDCl_3$) δ = 7.56 (d, *J* = 2.4 Hz, 1H), 7.33 – 7.22 (m, 4H), 7.24 – 7.16 (m, 1H), 7.10 (dd, *J* = 2.4, 0.8 Hz, 1H), 5.38 (s, 1H), 5.02 (s, 1H), 4.23 (s, 2H), 3.58 (s, 2H), 2.23 (s, 3H), 1.25 (s, 9H). **^{13}C NMR** (100 MHz, $CDCl_3$) δ = 154.48, 148.90, 144.34, 138.93, 134.04, 131.42, 129.10 (2C), 128.69, 128.35 (2C), 126.24, 114.21, 92.02, 74.29, 40.18, 34.12, 31.31 (3C), 17.34. **GC-MS** (m/z): 275 (100), 420 (11). **Anal. Calc.** for ($C_{21}H_{25}IO_3$: 420.10): C, 60.01; H, 6.00; found: C, 59.75, H, 5.88.

1-((2-Benzylallyl)oxy)-2-iodo-4-isopropyl-5-methylbenzene (**119m**)

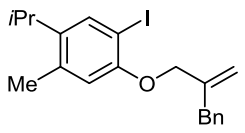

Colorless oil, yield = 79% (1.60 g, *n*-Hex). **^{1}H NMR** (400 MHz, $CDCl_3$) δ = 7.55 (s, 1H), 7.31 – 7.22 (m, 4H), 7.23 – 7.18 (m, 1H), 6.44 (s, 1H), 5.29 (dd, *J* = 1.5, 0.7 Hz, 1H), 5.05 (d, *J* = 1.3 Hz, 1H), 4.39 (s, 2H), 3.53 (s, 2H), 2.98 (sept, *J* = 6.9 Hz, 1H), 2.21 (s, 3H), 1.17 (dd, *J* = 6.9, 0.6 Hz, 6H). **^{13}C NMR** (100 MHz, $CDCl_3$) δ = 154.67, 143.75, 141.45, 138.79, 136.41, 135.66, 129.05 (2C), 128.41 (2C), 126.30, 114.27, 114.03, 83.25, 70.75, 39.95, 28.61, 23.26 (2C), 19.38. **GC-MS** (m/z): 315 (100), 406 (38). **Anal. Calc.** for ($C_{20}H_{23}IO_3$: 406.08): C, 59.12; H, 5.71; found: C, 58.95, H, 5.55.

5.5.4. General Procedure C for the synthesis of acyclic precursor by Mitsunobu reaction[124]

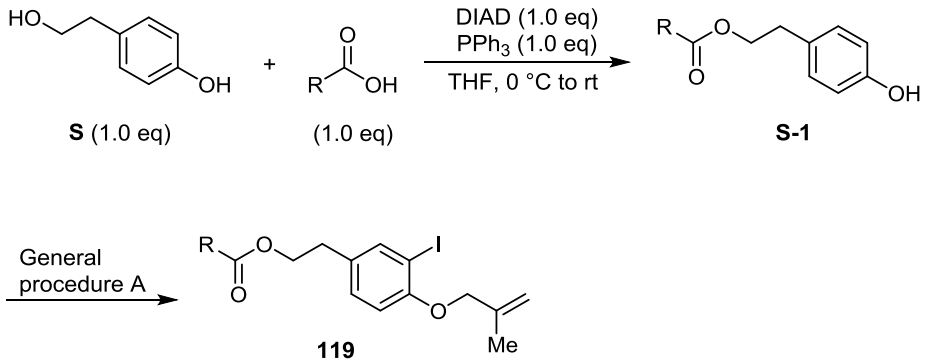

To a solution of tyrosol **S** (0.69 g, 5.0 mmol) and the desired carboxylic acid (5.0 mmol) in THF (12 mL) at 0°C were added PPh_3 (1.31 g, 5.0 mmol) and diisopropyl azodicarboxylate (1.01 g, 5.0 mmol). The reaction mixture was allowed to rise at room temperature, and stirred for 24 h. At complete consumption of the starting material (TLC) the solvent was remooved

[124] A.B. Belnaser, I.F. Ahmed, M. Tina, A.E. Khalid, *Bioorg. & Med. Chem.* **2013**, *21*, 2117-2127.

under reduced pressure, and the residue was dissolved in ethyl acetate (30 mL) and washed with saturated acqueous solution of $NaHCO_3$ (3 x 30 mL) and brine (3 x 30 mL). The organic layer was then dried over Na_2SO_4 and concentrated under reduced pressure. The crude so obtained was directly engaged in the General procedure A, giving the desired compound **119**.

3-Iodo-4-((2-methylallyl)oxy)phenethyl butyrate (**119h**)

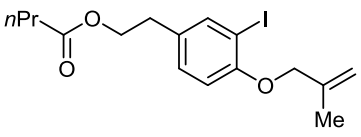

Colorless oil, yield = 76% (1.47 g, *n*-Hex). **^{1}H NMR** (400 MHz, $CDCl_3$) δ = 7.61 (d, *J* = 2.1 Hz, 1H), 7.08 (dd, *J* = 8.3, 2.1 Hz, 1H), 6.69 (d, *J* = 8.4 Hz, 1H), 5.15 (s, 1H), 4.97 (s, 1H), 4.41 (s, 2H), 4.20 (t, *J* = 6.9 Hz, 2H), 2.80 (t, *J* = 6.9 Hz, 2H), 2.24 (t, *J* = 7.4 Hz, 2H), 1.83 (s, 3H), 1.60 (sext, *J* = 7.4 Hz, 2H), 0.89 (t, *J* = 7.4 Hz, 3H). **^{13}C NMR** (100 MHz, $CDCl_3$) δ = 173.43, 155.90, 140.19, 139.74, 132.16, 129.69, 112.86, 112.12, 86.47, 72.56, 64.49, 36.15, 33.73, 19.46, 18.41, 13.66. **GC-MS** (m/z): 300 (100), 245 (43). **Anal. Calc.** for ($C_{16}H_{21}IO_3$: 388.05): C, 49.50; H, 5.45; found: C, 49.21, H, 5.21.

3-Iodo-4-((2-methylallyl)oxy)phenethyl 3-fluorobenzoate (**119i**)

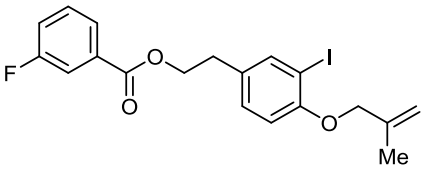

Colorless oil, yield = 71%, (1.56 g, *n*-Hex). **^{1}H NMR** (400 MHz, $CDCl_3$) δ = 7.77 (d, *J* = 7.8 Hz, 1H), 7.69 (d, *J* = 2.2 Hz, 1H), 7.66 (ddd, *J* = 9.3, 2.7, 1.6 Hz, 1H), 7.38 (td, *J* = 8.0, 5.5 Hz, 1H), 7.22 (td, *J* = 8.4, 2.8 Hz, 1H), 7.15 (dd, *J* = 8.4, 2.2 Hz, 1H), 6.71 (d, *J* = 8.4 Hz, 1H), 5.16 (s, 1H), 4.98 (s, 1H), 4.49 – 4.40 (m, 4H), 2.94 (t, *J* = 6.9 Hz, 2H), 1.83 (s, 3H). **^{13}C NMR** (100 MHz, $CDCl_3$) δ = 165.20 (d, *J*C-F = 3.0 Hz), 162.49 (d, *J*C-F = 247.2 Hz), 156.02, 140.17, 139.85, 132.33 (d, *J*C-F = 7.3 Hz), 131.93, 130.05 (d, *J*C-F = 7.8 Hz), 129.75, 125.29 (d, *J*C-F = 3.1 Hz), 120.01 (d, *J*C-F = 21.3 Hz), 116.41 (d, *J*C-F = 23.2 Hz), 112.89, 112.19, 86.57, 72.56, 65.62, 33.75, 19.46. **^{19}F NMR** (376 MHz, $CDCl_3$) δ = -112.14 (td, *J* = 8.8, 5.5 Hz). **GC-MS** (m/z): 300 (100), 123 (43), 158 (36). **Anal. Calc.** for $C_{19}H_{18}FIO_3$: 440.03; C, 51.84; H, 4.12; found: C, 51.65, H, 4.01.

3-Iodo-4-((2-methylallyl)oxy)phenethyl (*R*)-2-methoxy-2-phenylacetate (**119j**)

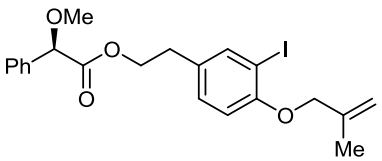

Colorless oil ,yield = 68% (1.58 g, *n*-Hex). **$[\alpha]_D^{20}$** = -10.5 (*c* = 1.0, $CHCl_3$). **^{1}H NMR** (400 MHz, $CDCl_3$) δ = 7.54 (d, *J* = 2.1 Hz, 1H), 7.40 – 7.29 (m, 5H), 6.92 (dd, *J* = 8.4, 2.2 Hz, 1H), 6.61 (d, *J* = 8.4 Hz, 1H), 5.17 (s, 1H), 5.00 (s, 1H), 4.71 (s, 1H), 4.42 (s, 2H), 4.26 (td, *J* = 6.8, 1.1 Hz, 2H), 3.36 (s, 3H), 2.75 (td, *J* = 6.8, 3.1 Hz, 2H), 1.85 (s, 3H). **^{13}C NMR** (100 MHz,

$CDCl_3$) δ = 170.54, 155.90, 140.21, 139.68, 136.12, 131.73, 129.67, 128.69, 128.64 (2C), 127.15 (2C), 112.90, 112.09, 86.45, 82.52, 72.57, 65.35, 57.36, 33.50, 19.47. **GC-MS** (m/z): 300 (100), 466 (14). **Anal. Calc.** for ($C_{21}H_{23}IO_3$: 466.06): C, 54.09; H, 4.97; found: C, 53.85, H, 4.68.

5.5.5. General procedure for the synthesis of 2-pyridyl imidazoline ligands[125]

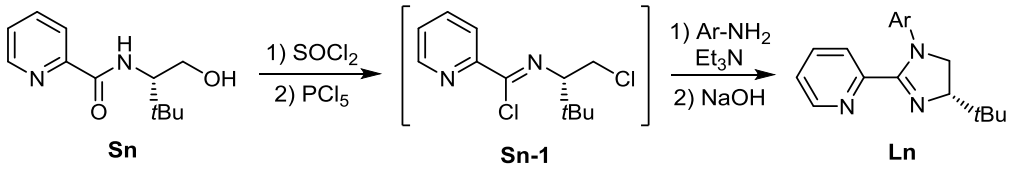

To a solution of *N*-(pyridinoyl)-amino alcohol **Sn** (1.11 g, 5.0 mmol) in chloroform (1.0 M solution), thionyl chloride (0.4 mL, 5.5 mmol) was added dropwise at room temperature, and the resulting mixture was stirred at reflux for 2 h. After completion of the reaction (TLC), phosphorus pentachloride (1.14 mg, 5.5 mmol) was added at room temperature, and the resulting suspension was refluxed until the reaction completion, determined by ^{1}H-NMR spectroscopy. The solvent was evaporated, and the $POCl_3$ was removed under high vacuum. The resulting residue was re-dissolved in chloroform (1.0 M) and the solution cooled at 0 °C when a solution of the desired aniline (6.0 mmol) and triethylamine (15 mmol) in chloroform was added dropwise. The mixture was stirred at 0 °C for 30 min and then refluxed for 12 h. After removal of the volatiles, aqueous NaOH (20% w/v, 10 mL) was added to the residue. The mixture was extracted with dichloromethane, and the combined organic layers were washed with brine, dried over Na_2SO_4, filtered and concentrated. The residue was purified by column chromatography on silica gel.

(*S*)-2-(4-(tert-butyl)-1-(4-methoxyphenyl)-4,5-dihydro-1H-imidazol-2-yl)pyridine (**L10**)

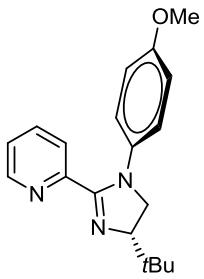

Sticky Yellow oil, yield = 27% (417.4 mg, *n*-Hex:AcOEt = 2:1). **[α]$_D^{20}$** = +11.4 (*c* = 1.0, $CHCl_3$). **^{1}H NMR** (400 MHz, $CDCl_3$) δ = 8.46 (d, *J* = 2.6 Hz, 1H), 7.72 – 7.59 (m, 2H), 7.20 (dd, *J* = 4.8, 2.4 Hz, 1H), 6.75 – 6.62 (m, 4H), 4.02 (q, *J* = 11.4, 9.0 Hz, 2H), 3.69 (s, 3H), 3.66 – 3.60 (m, 1H), 0.98 (s, 9H). **^{13}C NMR** (100 MHz, $CDCl_3$) δ = 159.48, 154.31, 149.13, 147.56, 135.05, 134.71, 122.56, 122.54 (2C), 122.44, 112.32 (2C), 72.73, 54.13, 53.70, 32.54, 24.35 (3C). **LC-MS** (m/z): $[M+H]^+$ = 310.2, $[M+Na]^+$ = 332.2, $[2M+H]^+$ = 619.4. **Anal. Calc.** for ($C_{19}H_{23}N_3O$: 309.18): C, 73.76; H, 7.49; found: C, 73.51, H, 7.21.

[125] T. L. Bo Su, F. H. John, *J. Am. Chem. Soc.* **2018**, *140*, 18032-18038.

(*S*)-2-(4-(tert-butyl)-1-(2,6-diisopropylphenyl)-4,5-dihydro-1H-imidazol-2-yl)pyridine (**L11**)

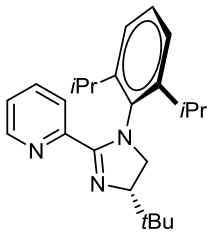

Sticky Yellow oil, yield = 33%, (599.4 mg, *n*-Hex : AcOEt = 2 : 1). $[\alpha]_D^{20}$ = -65.8 (c = 1.0, $CHCl_3$). **^{1}H NMR** (400 MHz, $CDCl_3$) δ = 8.26 (d, *J* = 4.8 Hz, 1H), 7.66 (d, *J* = 7.8 Hz, 1H), 7.50 (td, *J* = 7.7, 1.6 Hz, 1H), 7.18 (t, *J* = 7.7 Hz, 1H), 7.09 – 7.02 (m, 2H), 7.00 (d, *J* = 7.6 Hz, 1H), 4.13 (t, *J* = 11.1 Hz, 1H), 3.73 – 3.64 (m, 1H), 3.55 (t, *J* = 10.2 Hz, 1H), 3.33 (sept, *J* = 6.5 Hz, 1H), 3.11 (sept, *J* = 6.7 Hz, 1H), 1.20 (dd, *J* = 13.2, 6.9 Hz, 6H), 1.04 (s, 9H), 0.96 (d, *J* = 6.8 Hz, 3H), 0.78 (d, *J* = 6.8 Hz, 3H). **^{13}C NMR** (100 MHz, $CDCl_3$) δ = 162.58, 149.86, 148.50, 147.59, 146.90, 136.88, 135.58, 127.62, 123.80 (2C), 123.75, 123.72, 74.51, 56.34, 34.21, 28.06, 27.94, 26.29 (3C), 25.37, 24.99, 23.61, 23.24. **LC-MS** (m/z): $[M+H]^+$ = 364.2, $[M+Na]^+$ = 386.4, $[2M+H]^+$ = 749.4. **Anal. Calc.** for ($C_{24}H_{33}N_3$: 363.27): C, 79.29; H, 9.15; found: C, 79.15, H, 9.00.

5.5.6. General procedure for the synthesis of the nickel complex $[(L11)_2Ni(H_2O)Cl]Cl$

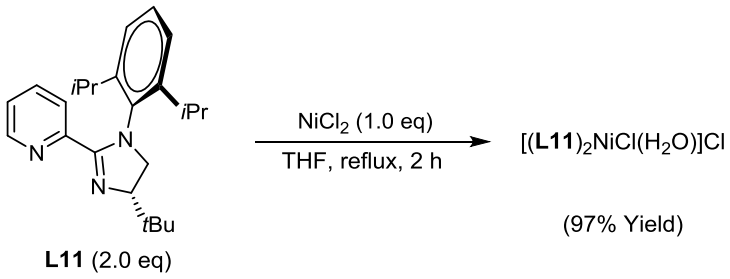

A solution of flame and dried $NiCl_2$ (129.6 mg, 1.0 mmol), ligand **L11** (727.1 mg, 2.0 mmol) in anhydrous THF (1.5 mL) was refluxed for 2 h (complete consumption of the ligand, monitored by TLC). Then the mixture was slowly cooled, and the solvent was cannulated out. The pale-green solid was washed three times with Et_2O, and dried under vacuum, yielding the desired nickel complex as a fine light-green powder air-stable (yield = 97%, 848.5 mg). **NMR (*d*^{6}-DMSO)** spectra appeared extremely broad. **Melting point** = 190-193 °C. **HRMS-ESI:** $[M+H^+]$ calcd for $C_{46}H_{63}Cl_2N_6Ni^+$ 829.46692, found 829.46702.

5.5.7. General procedure for the enantioselective Heck-carboxylation reaction

a) *In-situ* formation of the nickel complex (the case for compound **119a** is presented).

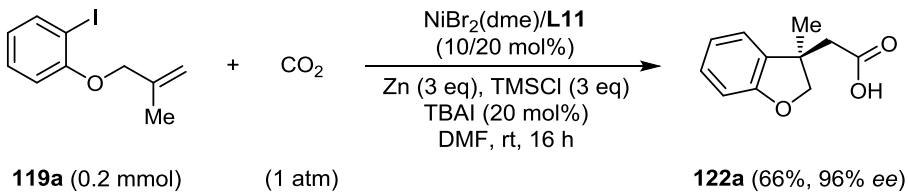

A flame-dried, nitrogen filled Schlenk tube equipped with a stirring bar was charged with Nickel catalyst (10 mol%, 6.2 mg), zinc (0.6 mmol, 39.2 mg) and TBAI (20 mol%, 14.8 mg). The nitrogen atmosphere was evacuated, and the tube was backfilled with CO_2 (1 bar). This operation was repeated three times. Then DMF (3 mL, 0.07 M) and ligand **L11** (20 mol %, 14.5 mg) were added under flow of CO_2, and the reaction mixture was stirred for 15 min. Under flow of CO_2, substrate **119a** (0.2 mmol) was added, and CO_2 was bubbled in the solution. Then TMSCl (0.6 mmol, 76 μL) was added by syringe, and the reaction mixture was stirred (1000 rpm) for 16 h at rt. The reaction was quenched with HCl (10 mL, 1.0 M), and extracted with ethyl acetate (3 x 10 mL). The combined organic layers were washed with HCl twice (2 mL, 1.0 M), dried over anhydrous Na_2SO_4, and concentrated under reduced pressure. The residue was purified by flash chromatography on silica gel (*n*-Hex:AcOEt = 7:3) to afford the desired product **122a** (yield = 66%, 25.3 mg). A small amount of the product (ca. 1 mg) was then dissolved in MeOH and $TMSCHN_2$ (25 μL) was added. The solvent was removed, and the so obtained methyl ester was injected in chiral HPLC (*ee* = 96%).

a) Use of preformed complex.

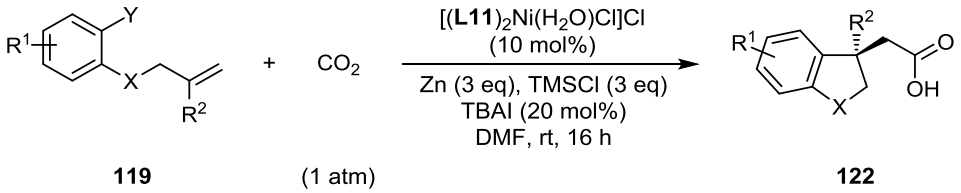

119 (1 atm) **122**

A flame dried, nitrogen filled Schlenk tube equipped with a stirring bar was charged with Nickel catalyst (10 mol%, 17.5 mg), zinc (0.6 mmol, 39.2 mg) and TBAI (20 mol%, 14.8 mg). The nitrogen atmosphere was evacuated, and the tube was backfilled with CO_2 (1 bar). This operation was repeated three times. Then DMF (3 mL, 0.07 M) was added under flow of CO_2, and the reaction mixture was stirred for 15 min. Under flow of CO_2, substrate **119** (0.2 mmol) was added, and CO_2 was bubbled in the solution. Then, TMSCl (0.6 mmol, 76 μL) was added by syringe, and the reaction mixture was stirred (1000 rpm) for 16 h at rt. The reaction was quenched with HCl (10 mL, 1.0 M), and extracted with ethyl acetate (3 x 10 mL). The combined organic layers were washed with HCl twice (2 mL, 1.0 M), dried over anhydrous Na_2SO_4, and concentrated under reduced pressure. The residue was purified by flash chromatography on silica gel to afford the desired product **122**. A small amount of the product (ca 1 mg) was then dissolved in MeOH and $TMSCHN_2$ (25 μL) was added. The solvent was removed, and the so obtained methyl ester was injected in chiral HPLC.

(*R*)-2-(3-methyl-2,3-dihydrobenzofuran-3-yl)acetic acid (**122a**)

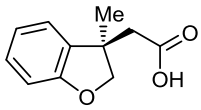

White solid, yield = 61%, *ee* = 96% (23.4 mg, *n*-Hex:AcOEt = 7:3). **M.p.** = 88-90 °C. **[α]$_D^{20}$** = +46.2° (*c* = 0.5, $CHCl_3$). **^{1}H NMR** (400 MHz, $CDCl_3$) δ = 7.19 – 7.06 (m, 2H), 6.88 (td, *J* = 7.4, 1.0 Hz, 1H), 6.80 (d, *J* = 8.0 Hz, 1H), 4.61 (dd, *J* = 9.2, 1.3 Hz, 1H), 4.31 (dd, *J* = 9.2, 1.3 Hz, 1H), 2.80 – 2.65 (m, 2H), 1.45 (s, 3H). **^{13}C NMR** (100 MHz, $CDCl_3$) δ = 177.18, 159.25, 134.22, 128.93, 122.90, 120.97, 110.21, 82.43, 44.24, 43.85, 25.22. **GC-MS** (m/z): calcd for $C_{20}H_{22}O_3$ 206.09 (M-OMe) 133 (100), 206 (36). **Anal. Calc.** for ($C_{11}H_{12}O_3$: 192.04): C, 68.74, H, 6.29; found: C, 68.65, H, 6.21.

(*R*)-2-(3-methyl-5-phenethyl-2,3-dihydrobenzofuran-3-yl)acetic acid (**122b**)

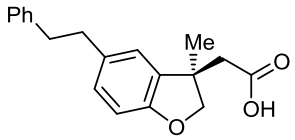

White solid, yield = 61%, *ee* = 96% (36.1 mg, *n*-Hex:AcOEt = 7:3). **M.p.** = 87-89 °C. **[α]$_D^{20}$** = +24.2° (*c* = 1.0, $CHCl_3$). **^{1}H NMR** (400 MHz, $CDCl_3$) δ = 7.26 (t, *J* = 7.9 Hz, 2H), 7.16 (m, 3H), 6.96 (dd, *J* = 8.1, 1.8 Hz, 1H), 6.82 (d, *J* = 1.9 Hz, 1H), 6.72 (d, *J* = 8.1 Hz, 1H), 4.60 (d, *J* = 9.2 Hz, 1H), 4.30 (d, *J* = 9.2 Hz, 1H), 2.86 (s, 4H), 2.68 (s, 2H), 1.42 (s, 3H). **^{13}C NMR** (100 MHz, $CDCl_3$) δ = 177.07, 157.27, 141.70, 134.18, 133.95, 128.63, 128.53 (2C), 128.27 (2C), 125.86, 122.72, 109.58, 82.33, 43.95, 43.63, 38.44, 37.50, 24.86. **GC-MS** (m/z): calcd for $C_{20}H_{22}O_3$ 310.16 (M-OMe) 219 (100), 310 (9). **Anal. Calc.** for ($C_{19}H_{20}O_3$: 296.14): C, 77.00, H, 6.80; found: C, 76.90, H, 6.61.

(*R*)-2-(5-(tert-butyl)-3,7-dimethyl-2,3-dihydrobenzofuran-3-yl)acetic acid (**122c**)

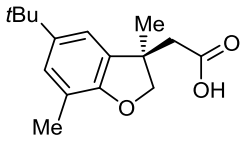

Colorless oil, yield = 68%, *ee* = 95% (35.6 mg, *n*-Hex:AcOEt = 8:2). **[α]$_D^{20}$** = +24.7° (*c* = 1.0, $CHCl_3$). **^{1}H NMR** (400 MHz, $CDCl_3$) δ = 7.00 (s, 1H), 6.95 (s, 1H), 4.59 (d, *J* = 9.1 Hz, 1H), 4.30 (d, *J* = 9.1 Hz, 1H), 2.80 – 2.63 (m, 2H), 2.21 (s, 3H), 1.45 (s, 3H), 1.28 (s, 9H). **^{13}C NMR** (100 MHz, $CDCl_3$) δ = 177.30, 155.11, 143.85, 132.89, 126.93, 119.06, 116.72, 82.26, 44.13, 44.07, 34.31, 31.73 (3C), 24.62, 15.31. **GC-MS** (m/z): calcd for $C_{17}H_{24}O_3$ 276.17 (M-OMe) 261 (100), 276 (18). **Anal. Calc.** for ($C_{16}H_{22}O_3$: 262.16): C, 73.25, H, 8.45; found: C, 73.15, H, 8.33.

(*R*)-2-(3,5-dimethyl-2,3-dihydrobenzofuran-3-yl)acetic acid (**122d**)

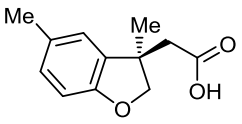

White solid, yield = 64%, *ee* = 99% (26.4 mg, *n*-Hex:AcOEt = 7:3). **M.p.** = 98-100 °C. $[\alpha]_D^{20}$ = +33.4° (*c* = 1.0, $CHCl_3$). **^{1}H NMR** (400 MHz, $CDCl_3$) δ = 7.01 – 6.84 (m, 2H), 6.68 (d, *J* = 8.1 Hz, 1H), 4.58 (d, *J* = 9.2 Hz, 1H), 4.29 (d, *J* = 9.2 Hz, 1H), 2.80 – 2.61 (m, 2H), 2.27 (s, 3H), 1.43 (s, 3H). **^{13}C NMR** (100 MHz, $CDCl_3$) δ = 176.45, 157.14, 134.27, 130.28, 129.30, 123.40, 109.74, 82.52, 44.08, 43.90, 25.12, 21.08. **GC-MS** (m/z): calcd for $C_{13}H_{16}O_3$ 220.11 (M-OMe) 147 (100), 119 (41), 220 (20). **Anal. Calc.** for ($C_{12}H_{14}O_3$: 206.09): C, 69.89, H, 6.84; found: C, 69.75, H, 6.61.

(*R*)-2-(5-(tert-butyl)-3-methyl-2,3-dihydrobenzofuran-3-yl)acetic acid (**122e**)

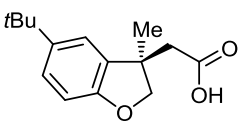

White solid, yield = 68%, *ee* = 97% (33.7 mg, *n*-Hex:AcOEt = 7:3). **M.p.** = 99-101 °C. $[\alpha]_D^{20}$ = +34.6° (*c* = 1.0, $CHCl_3$). **^{1}H NMR** (400 MHz, $CDCl_3$) δ = 7.19 (dd, *J* = 8.4, 2.1 Hz, 1H), 7.16 – 7.10 (m, 1H), 6.74 (dd, *J* = 8.4, 0.5 Hz, 1H), 4.61 (d, *J* = 9.2 Hz, 1H), 4.32 (d, *J* = 9.2 Hz, 1H), 2.84 – 2.61 (m, 2H), 1.48 (s, 3H), 1.30 (s, 9H). **^{13}C NMR** (100 MHz, $CDCl_3$) δ = 177.15, 156.75, 143.86, 133.54, 125.51, 119.43, 109.11, 82.48, 44.05, 43.79, 34.40, 31.69, 24.68. **GC-MS** (m/z): calcd for $C_{16}H_{22}O_3$ 262.16 (M-OMe) 247 (100), 262 (41). **Anal. Calc.** for ($C_{15}H_{20}O_3$: 248.14): C, 72.55, H, 8.12; found: C, 72.34, H, 8.01.

(*R*)-2-(5-isopropyl-3,6-dimethyl-2,3-dihydrobenzofuran-3-yl)acetic acid (**122f**)

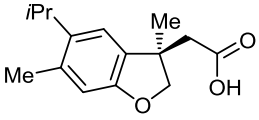

Colorless oil, yield = 63%, *ee* = 95% (31.3 mg, *n*-Hex:AcOEt = 7:3). $[\alpha]_D^{20}$ = +23.4° (*c* = 1.0, $CHCl_3$). **^{1}H NMR** (400 MHz, $CDCl_3$) δ = 6.96 (s, 1H), 6.59 (s, 1H), 4.56 (d, *J* = 9.1 Hz, 1H), 4.27 (d, *J* = 9.1 Hz, 1H), 3.06 (sept, *J* = 6.8 Hz, 1H), 2.78 – 2.62 (m, 2H), 2.27 (s, 3H), 1.44 (s, 3H), 1.18 (dd, *J* = 6.9, 3.4 Hz, 6H). **^{13}C NMR** (100 MHz, $CDCl_3$) δ = 176.39, 156.76, 139.34, 135.64, 131.66, 118.67, 111.32, 82.43, 44.00, 43.73, 28.88, 24.74, 23.50 (2C), 19.63. **GC-MS** (m/z): calcd for $C_{16}H_{22}O_3$ 262.16 (M-OMe) 189 (100), 147 (92), 262 (86). **Anal. Calc.** for ($C_{15}H_{20}O_3$: 248.14): C, 72.55, H, 8.12; found: C, 72.41, H, 8.05.

(*R*)-2-(5-(3-ethoxy-3-oxopropyl)-3-methyl-2,3-dihydrobenzofuran-3-yl)acetic acid (**122g**)

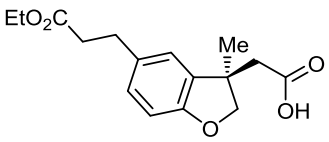

Colorless oil, yield = 69%, *ee* = 98% (40.3 mg, *n*-Hex:AcOEt = 2:1). $[\alpha]_D^{20}$ = +21.7° (*c* = 1.0, $CHCl_3$). **^{1}H NMR** (400 MHz, $CDCl_3$) δ = 6.96 (dd, *J* = 8.1, 1.9 Hz, 1H), 6.93 (d, *J* = 1.8 Hz,

1H), 6.70 (d, *J* = 8.1 Hz, 1H), 4.58 (d, *J* = 9.2 Hz, 1H), 4.29 (d, *J* = 9.2 Hz, 1H), 4.10 (q, *J* = 7.1 Hz, 2H), 2.87 (t, *J* = 7.8 Hz, 2H), 2.76 – 2.63 (m, 2H), 2.56 (t, *J* = 7.8 Hz, 2H), 1.43 (s, 3H), 1.21 (td, *J* = 7.1, 0.8 Hz, 3H). **^{13}C NMR** (100 MHz, $CDCl_3$) δ = 176.67, 173.27, 157.78, 134.47, 133.24, 128.77, 122.78, 109.96, 82.63, 60.65, 44.11, 43.88, 36.68, 30.77, 25.10, 14.44. **GC-MS** (m/z): calcd for $C_{17}H_{22}O_5$ 306.15 (M-OMe) 145 (100), 233 (51), 306 (30). **Anal. Calc.** for ($C_{16}H_{20}O_5$: 292.13): C, 65.74, H, 6.90; found: C, 65.58, H, 6.74.

(*R*)-2-(5-(2-(butyryloxy)ethyl)-3-methyl-2,3-dihydrobenzofuran-3-yl)acetic acid (**122h**)

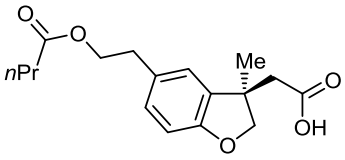

Colorless oil, yield = 57%, *ee* = 98% (34.9 mg, *n*-Hex:AcOEt = 2:1). **$[\alpha]_D^{20}$** = +16.6° (*c* = 1.0, $CHCl_3$). **^{1}H NMR** (400 MHz, $CDCl_3$) δ = 7.01 – 6.92 (m, 2H), 6.72 (d, *J* = 8.1 Hz, 1H), 4.60 (d, *J* = 9.2 Hz, 1H), 4.30 (d, *J* = 9.2 Hz, 1H), 4.22 (t, *J* = 7.1 Hz, 2H), 2.86 (t, *J* = 7.1 Hz, 2H), 2.76 – 2.62 (m, 2H), 2.25 (t, *J* = 7.4 Hz, 2H), 1.61 (sext, *J* = 7.4 Hz, 2H), 1.44 (s, 3H), 0.91 (t, *J* = 7.4 Hz, 3H). **^{13}C NMR** (100 MHz, $CDCl_3$) δ = 176.56, 173.72, 157.80, 134.30, 130.15, 129.18, 123.12, 109.76, 82.40, 65.03, 43.90, 43.63, 36.21, 34.64, 24.89, 18.40, 13.62. **LC-MS** (m/z): $[M-H]^-$ = 305.0. **Anal. Calc.** for ($C_{17}H_{22}O_5$: 306.15): C, 66.65, H, 7.24; found: C, 65.50, H, 7.10.

(*R*)-2-(5-(2-((3-fluorobenzoyl)oxy)ethyl)-3-methyl-2,3-dihydrobenzofuran-3-yl)acetic acid (**122i**)

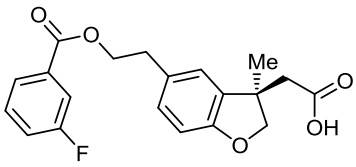

Colorless oil, yield = 62%, *ee* = 98% (44.4 mg, *n*-Hex:AcOEt = 2:1). **$[\alpha]_D^{20}$** = +14.2° (*c* = 1.0, $CHCl_3$). **^{1}H NMR** (400 MHz, $CDCl_3$) δ = 7.79 (dt, *J* = 7.7, 1.2 Hz, 1H), 7.67 (ddd, *J* = 9.3, 2.7, 1.5 Hz, 1H), 7.39 (td, *J* = 8.0, 5.5 Hz, 1H), 7.28 – 7.19 (m, 1H), 7.07 – 6.97 (m, 2H), 6.74 (d, *J* = 8.1 Hz, 1H), 4.60 (d, *J* = 9.2 Hz, 1H), 4.47 (t, *J* = 7.0 Hz, 2H), 4.31 (d, *J* = 9.2 Hz, 1H), 2.99 (t, *J* = 7.0 Hz, 2H), 2.76 – 2.62 (m, 2H), 1.43 (s, 3H). **^{13}C NMR** (100 MHz, $CDCl_3$) δ = 176.17, 165.33 (d, *J*C-F = 3.0 Hz), 162.51 (d, *J*C-F = 247.1 Hz), 157.92, 134.43, 132.43 (d, *J*C-F = 7.5 Hz), 130.02, 129.98 (d, *J*C-F = 7.8 Hz), 129.18, 125.25 (d, *J*C-F = 3.1 Hz), 123.30, 120.01 (d, *J*C-F = 21.3 Hz), 116.42 (d, *J*C-F = 22.9 Hz), 109.89, 82.43, 66.10, 43.84, 43.63, 34.69, 24.89. **^{19}F NMR** (376 MHz, $CDCl_3$) δ = -112.37 (td, *J* = 8.8, 5.5 Hz). **LC-MS** (m/z): $[M-H]^-$ = 357.2. **Anal. Calc.** for ($C_{20}H_{19}FO_5$: 358.12): C, 67.03; H, 5.34; F, 5.30; found: C, 66.81, H, 5.21.

2-((*R*)-5-(2-((*R*)-2-methoxy-2-phenylacetoxy)ethyl)-3-methyl-2,3-dihydrobenzofuran-3-yl)acetic acid (**122j**)

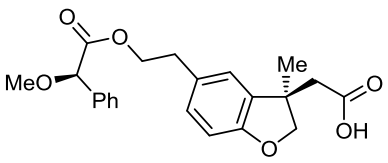

Colorless oil, yield = 60%, dr = 25:1, *ee* = 97% (43.7 mg, *n*-Hex:AcOEt = 2:1). $[\alpha]_D^{20}$ = +5.4° (*c* = 1.0, $CHCl_3$). **^{1}H NMR** (400 MHz, $CDCl_3$) δ = 7.41 – 7.29 (m, 5H), 6.87 (d, *J* = 1.9 Hz, 1H), 6.82 (dd, *J* = 8.2, 1.9 Hz, 1H), 6.64 (d, *J* = 8.1 Hz, 1H), 4.73 (d, *J* = 2.5 Hz, 1H), 4.58 (d, *J* = 9.2 Hz, 1H), 4.32 – 4.24 (m, 3H), 3.36 (d, *J* = 1.0 Hz, 3H), 2.80 (t, *J* = 7.2 Hz, 2H), 2.72 – 2.59 (m, 2H), 1.40 (s, 3H). **^{13}C NMR** (100 MHz, $CDCl_3$) δ = 175.91, 170.61, 157.83, 136.10, 134.38, 129.72, 129.17, 128.72, 128.62 (2C), 127.21 (2C), 123.02, 109.71, 82.57, 82.48, 65.89, 57.26, 43.90, 43.62, 34.44, 24.86. **LC-MS** (m/z): $[M-H]^-$ = 383.2. **Anal. Calc.** for ($C_{22}H_{24}O_6$: 384.16): C, 68.74; H, 6.29; found: C, 68.55, H, 6.15.

(*R*)-2-(3-benzyl-2,3-dihydrobenzofuran-3-yl)acetic acid (**122k**)

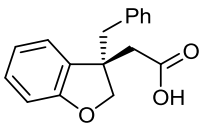

White solid, yield = 49%, *ee* = 98% (26.3 mg, *n*-Hex:AcOEt = 7:3). **M.p.** = 137-139 °C. $[\alpha]_D^{20}$ = +44.3° (*c* = 1.0, $CHCl_3$). **^{1}H NMR** (400 MHz, $CDCl_3$) δ = 7.24 – 7.18 (m, 3H), 7.14 (td, *J* = 7.7, 1.4 Hz, 1H), 6.92 – 6.86 (m, 2H), 6.81 (td, *J* = 7.4, 1.0 Hz, 1H), 6.79 – 6.71 (m, 2H), 4.66 (d, *J* = 9.4 Hz, 1H), 4.46 (d, *J* = 9.3 Hz, 1H), 3.13 – 3.01 (m, 2H), 2.93 (d, *J* = 16.4 Hz, 1H), 2.71 (d, *J* = 16.4 Hz, 1H). **^{13}C NMR** (100 MHz, $CDCl_3$) δ = 176.90, 159.50, 136.41, 131.40, 130.54 (2C), 128.92, 127.97 (2C), 126.74, 124.26, 120.11, 109.88, 81.01, 47.94, 43.67, 41.11. **GC-MS** (m/z): calcd for $C_{18}H_{18}O_3$ 282.13 (M-OMe) 131 (100), 191 (41), 282 (7). **Anal. Calc.** for ($C_{17}H_{16}O_3$: 268.11): C, 76.10; H, 6.01; found: C, 75.95, H, 5.80.

(*R*)-2-(3-benzyl-5-(tert-butyl)-7-methyl-2,3-dihydrobenzofuran-3-yl)acetic acid (**122l**)

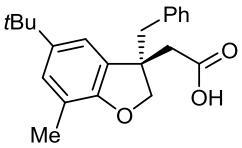

Colorless oil, yield = 67%, *ee* = 95% (45.3 mg, *n*-Hex:AcOEt = 7:3). $[\alpha]_D^{20}$ = +26.1° (*c* = 1.0, $CHCl_3$). **^{1}H NMR** (400 MHz, $CDCl_3$) δ = 7.21 (dd, *J* = 4.9, 1.8 Hz, 3H), 7.01 – 6.96 (m, 1H), 6.92 – 6.85 (m, 2H), 6.39 (d, *J* = 2.1 Hz, 1H), 4.66 (d, *J* = 9.3 Hz, 1H), 4.45 (d, *J* = 9.3 Hz, 1H), 3.14 (d, *J* = 13.3 Hz, 1H), 3.01 (d, *J* = 13.2 Hz, 1H), 2.92 (d, *J* = 16.5 Hz, 1H), 2.66 (d, *J* = 16.4 Hz, 1H), 2.20 (s, 3H), 1.19 (s, 9H). **^{13}C NMR** (100 MHz, $CDCl_3$) δ = 177.24, 155.43, 142.81, 136.67, 130.77 (2C), 130.16, 127.87 (2C), 126.96, 126.58, 119.03, 118.84, 81.87, 48.30, 43.15, 40.44, 34.16, 31.59 (3C), 15.33. **GC-MS** (m/z): calcd for $C_{23}H_{28}O_3$ 352.20 (M-

OMe) 205 (100), 261 (21), 352 (10). **Anal. Calc.** for ($C_{22}H_{26}O_3$: 338.19): C, 78.07; H, 7.74, found: C, 77.91, H, 7.59.

(*R*)-2-(3-benzyl-5-isopropyl-6-methyl-2,3-dihydrobenzofuran-3-yl)acetic acid (**122m**)

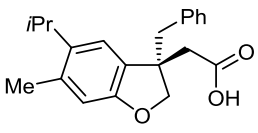

White solid, yield = 56%, *ee* = 98% (36.3 mg, *n*-Hex:AcOEt = 7:3). **M.p.** = 111-113 °C. **$[\alpha]_D^{20}$** = +20.7° (*c* = 1.0, $CHCl_3$). **^{1}H NMR** (400 MHz, $CDCl_3$) δ = 7.25 – 7.19 (m, 3H), 6.90 (dd, *J* = 6.5, 2.9 Hz, 2H), 6.58 (s, 1H), 6.43 (s, 1H), 4.64 (d, *J* = 9.3 Hz, 1H), 4.44 (d, *J* = 9.3 Hz, 1H), 3.14 (d, *J* = 13.3 Hz, 1H), 3.07 – 2.96 (m, 2H), 2.93 (d, *J* = 16.5 Hz, 1H), 2.66 (d, *J* = 16.5 Hz, 1H), 2.28 (s, 3H), 1.08 (dd, *J* = 10.3, 6.8 Hz, 6H). **^{13}C NMR** (100 MHz, $CDCl_3$) δ = 177.47, 157.07, 138.46, 136.67, 135.74, 130.74 (2C), 128.88, 127.94 (2C), 126.60, 120.84, 111.20, 81.95, 47.99, 43.24, 40.65, 28.69, 23.40, 23.38, 19.68. **GC-MS** (m/z): calcd for $C_{22}H_{26}O_3$ 338.19 (M-OMe) 189 (100), 338 (12). **Anal. Calc.** for ($C_{21}H_{24}O_3$: 324.17): C, 77.75; H, 7.46; found: C, 77.60; H, 7.31.

(*R*)-2-(3-octyl-2,3-dihydrobenzofuran-3-yl)acetic acid (**122n**)

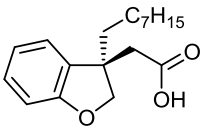

Colorless oil, yield = 51%, *ee* = 80% (29.6 mg, *n*-Hex:AcOEt = 7:3). **$[\alpha]_D^{20}$** = +68.4° (*c* = 1.0, $CHCl_3$). **^{1}H NMR** (400 MHz, $CDCl_3$) δ = 7.13 (ddd, *J* = 8.0, 7.4, 1.4 Hz, 1H), 7.07 (dd, *J* = 7.4, 1.4 Hz, 1H), 6.86 (td, *J* = 7.4, 1.0 Hz, 1H), 6.78 (d, *J* = 8.0 Hz, 1H), 4.53 (d, *J* = 9.4 Hz, 1H), 4.46 (d, *J* = 9.4 Hz, 1H), 2.83 (d, *J* = 15.7 Hz, 1H), 2.71 (d, *J* = 15.6 Hz, 1H), 1.80 (td, *J* = 12.9, 4.3 Hz, 1H), 1.65 (td, *J* = 13.2, 12.5, 4.3 Hz, 1H), 1.29 (m, 1H), 1.25 – 1.17 (m, 10H), 1.03 (m, 1H), 0.84 (t, *J* = 6.9 Hz, 3H). **^{13}C NMR** (100 MHz, $CDCl_3$) δ = 175.48, 159.62, 132.05, 128.65, 123.28, 120.42, 109.75, 80.75, 47.16, 42.66, 38.30, 31.77, 29.91, 29.34, 29.18, 24.12, 22.58, 14.05. **GC-MS** (m/z): calcd for $C_{19}H_{28}O_3$ 304.20 (M-OMe) 131 (100), 191 (36), 231 (17), 304 (7). **Anal. Calc.** for ($C_{18}H_{26}O_3$: 290.19): C, 74.45; H, 9.02; found: C, 74.35, H, 8.85.

(*R*)-2-(3-(methoxymethyl)-2,3-dihydrobenzofuran-3-yl)acetic acid (**122o**)

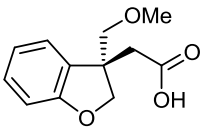

Colorless oil, yield = 47%, *ee* = 94% (20.9 mg, *n*-Hex:AcOEt = 7:3). **$[\alpha]_D^{20}$** = +21.4° (*c* = 1.0, $CHCl_3$). **^{1}H NMR** (400 MHz, $CDCl_3$) δ = 7.22 – 7.11 (m, 2H), 6.85 (td, *J* = 7.5, 1.0 Hz, 1H), 6.79 (dt, *J* = 8.0, 0.7 Hz, 1H), 4.53 (d, *J* = 9.6 Hz, 1H), 4.47 (d, *J* = 9.6 Hz, 1H), 3.55 (m, 2H), 3.32 (s, 3H), 2.96 (d, *J* = 15.9 Hz, 1H), 2.74 (d, *J* = 15.8 Hz, 1H). **^{13}C NMR** (100 MHz, $CDCl_3$) δ = 176.77, 159.65, 130.28, 129.17, 124.14, 120.54, 109.89, 78.69, 76.80, 59.32, 48.19, 39.55. **GC-MS** (m/z): calcd for $C_{13}H_{16}O_4$

236.10 (M-OMe) 131 (100), 191 (31), 236 (10). **Anal. Calc.** for ($C_{12}H_{14}O_4$: 222.09): C, 64.85; H, 6.35; found: C, 64.75, H, 6.22.

(*R*)-2-(3-methyl-1-(2-methylallyl)indolin-3-yl)acetic acid (**123a**)

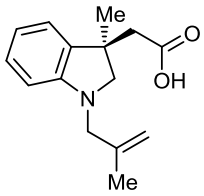

Orange oil, yield = 47%, *ee* = 11% (23.1 mg, *n*-Hex:AcOEt = 2:1). **$[\alpha]_D^{20}$** = +8.4° (*c* = 1.0, $CHCl_3$). **^{1}H NMR** (400 MHz, $CDCl_3$) δ = 7.07 (td, *J* = 7.6, 1.3 Hz, 1H), 7.01 (dd, *J* = 7.3, 1.3 Hz, 1H), 6.67 (td, *J* = 7.4, 1.0 Hz, 1H), 6.48 (d, *J* = 7.9 Hz, 1H), 4.95 (s, 1H), 4.88 (s, 1H), 3.65 – 3.50 (m, 2H), 3.46 (d, *J* = 9.3 Hz, 1H), 3.13 (d, *J* = 9.3 Hz, 1H), 2.66 (s, 2H), 1.76 (s, 3H), 1.42 (s, 3H). **^{13}C NMR** (100 MHz, $CDCl_3$) δ = 177.29, 151.07, 141.99, 136.17, 128.10, 122.13, 117.53, 112.18, 107.06, 65.23, 55.14, 43.85, 41.99, 24.62, 20.30. **GC-MS** (m/z): calcd for $C_{15}H_{19}NO_2$ 259.16 (M-OMe) 186 (100), 130 (59), 144 (56), 259 (44). **Anal. Calc.** for ($C_{15}H_{19}NO_2$: 245.14): C, 66.65, H, 7.24; found: C, 66.25, H, 7.04.

(*R*)-2-(1-(tert-butoxycarbonyl)-3-methylindolin-3-yl)acetic acid (**123b**)

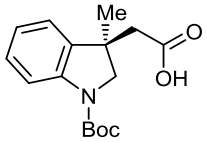

Orange oil, yield = 31%, *ee* = 63% (18.0 mg, *n*-Hex:AcOEt = 2:1, as a 83:17 inseparable mixture with the benzoic acid by-product). **$[\alpha]_D^{20}$** = +5.0° (*c* = 1.0, $CHCl_3$). **^{1}H NMR** (400 MHz, $CDCl_3$) δ = [7.83 (m), 7.55 – 7.42 (m), 1H], 7.18 (t, *J* = 7.7 Hz, 1H), 7.10 (dd, *J* = 7.6, 1.3 Hz, 1H), 6.95 (td, *J* = 7.5, 1.1 Hz, 1H), 4.11 (d, *J* = 11.7 Hz, 1H), 3.82 – 3.73 (m, 1H), 2.74 – 2.60 (m, 2H), 1.56 (s, 9H), 1.43 (s, 3H). **^{13}C NMR** (100 MHz, $CDCl_3$) δ = 175.36, 152.54, 141.55, 135.42, 128.24, 122.42, 114.86, 110.95, 77.18, 59.88, 44.40, 28.44 (3C), 26.34, 20.29. **GC-MS** (m/z): calcd for $C_{17}H_{23}NO_4$ 305.16 (M-OMe) 290 (100), 190 (41), 305 (6). **Anal. Calc.** for ($C_{16}H_{21}NO_4$: 291.15): C, 65.96; H, 7.27; found: C, 65.80, H, 7.12.

(*R*)-2-(1-(tert-butoxycarbonyl)-3,6-dimethylindolin-3-yl)acetic acid (**123c**)

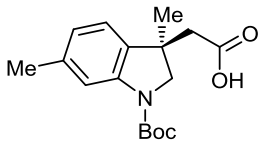

Orange oil, yield = 45%, *ee* = 69% (27.5 mg, *n*-Hex:AcOEt = 2:1, as a 76:24 inseparable mixture with the benzoic acid by-product). **$[\alpha]_D^{20}$** = +11.3° (*c* = 1.0, $CHCl_3$). **^{1}H NMR** (400 MHz, $CDCl_3$) δ = 7.69 (m), 7.28 (m), 1H], 6.97 (d, *J* = 7.6 Hz, 1H), 6.76 (d, *J* = 7.6 Hz, 1H), 4.09 (d, *J* = 11.6 Hz, 1H), 3.75 (d, *J* = 11.2 Hz, 1H), 2.70 – 2.56 (m, 2H), 2.31 (s, 3H), 1.55 (s, 9H), 1.40 (s, 3H). **^{13}C NMR** (100 MHz, $CDCl_3$) δ = 176.15, 152.59, 141.93, 131.71, 129.32, 127.48, 123.13, 112.02, 80.53, 60.22, 44.72, 28.42 (3C), 28.10, 26.39, 20.39. **GC-MS** (m/z): calcd for

$C_{18}H_{25}NO_4$ 319.18 (M-OMe) 304 (100), 319 (20). **Anal. Calc.** for ($C_{17}H_{23}NO_4$: 305.16): C, 66.86; H, 7.59; found: C, 66.75, H, 7.44.

(*R*)-2-(1-methyl-2,3-dihydro-1H-inden-1-yl)acetic acid (**124a**)

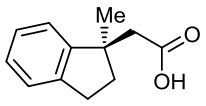

Colorless oil, yield = 41%, *ee* = 98% (15.6 mg, *n*-Hex:AcOEt = 8:2). **$[\alpha]_D^{20}$** = +20.9° (*c* = 1.0, $CHCl_3$). **^{1}H NMR** (400 MHz, $CDCl_3$) δ = 7.23 – 7.11 (m, 4H), 2.92 (t, *J* = 7.2 Hz, 2H), 2.64 (d, *J* = 14.2 Hz, 1H), 2.54 (d, *J* = 14.2 Hz, 1H), 2.36 – 2.25 (m, 1H), 1.98 (dt, *J* = 12.8, 7.4 Hz, 1H), 1.39 (s, 3H). **^{13}C NMR** (100 MHz, $CDCl_3$) δ = 177.67, 149.95, 142.72, 126.88, 126.45, 124.70, 122.36, 46.02, 44.86, 38.68, 29.97, 26.17. **GC-MS** (m/z): calcd for $C_{13}H_{16}O_2$ 204.12 (M-OMe) 131 (100), 115 (43), 204 (8). **Anal. Calc.** for ($C_{12}H_{14}O_2$: 190.10): C, 75.76; H, 7.42; found: C, 75.66, H, 7.31.

5.5.8. General procedure for the synthesis of the amide derivative

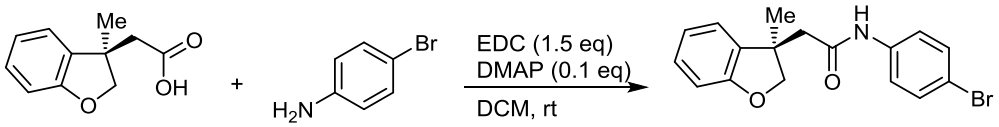

(*R*)-**122a** (96% *ee*) (2.0 eq) (*R*)-**131a** (91%, 96% *ee*)

To a solution of acid (*R*)-**122a** (96.1 mg, 0.5 mmol, *ee* = 96%), 4-bromoaniline (172.0 mg, 1.0 mmol) and DMAP (6.0 mg, 10 mol%) in CH_2Cl_2 (2.5 mL) was added EDC (148.2 mg, 1.5 mmol) and the reaction mixture was stirred at room temperature for 6 h. Then CH_2Cl_2 (2.5 mL) was added, and the solution was washed with 1 M HCl (3 x 3 mL), water (3 x 3 mL) and brine (3 mL) and dried with Na_2SO_4 and concentrated. The residue was purified by flash chromatography on silica gel (*n*-Hex:AcOEt = 8:2), to obtain the amide (*R*)-**131a** as a pale yellow solid (yield = 91%, *ee* = 96%, 157.5 mg). **M.p.** = 127-129 °C. **$[\alpha]_D^{20}$** = -10.4° (*c* = 1.0, $CHCl_3$). **^{1}H NMR** (400 MHz, $CDCl_3$) δ = 7.35 (d, *J* = 8.7 Hz, 2H), 7.24 – 7.01 (m, 5H), 6.90 (t, *J* = 7.4 Hz, 1H), 6.80 (d, *J* = 8.0 Hz, 1H), 4.65 (d, *J* = 9.1 Hz, 1H), 4.30 (d, *J* = 9.1 Hz, 1H), 2.70 – 2.56 (m, 2H), 1.49 (s, 3H). **^{13}C NMR** (100 MHz, $CDCl_3$) δ = 168.67, 159.37, 136.45, 133.83, 131.88 (2C), 128.95, 122.61, 121.60 (2C), 120.80, 117.09, 110.28, 82.24, 47.93, 44.48, 25.11. **LC-MS** (m/z): $[M+H]^+$ = 346.2, $[2M+Na]^+$ = 713.2. **Anal. Calc.** for ($C_{17}H_{16}BrNO_2$: 345.04): C, 58.98; H, 4.66; found: C, 58.74, H, 4.41.

5.5.9. General procedure for labeling experiment with marked carbon dioxide

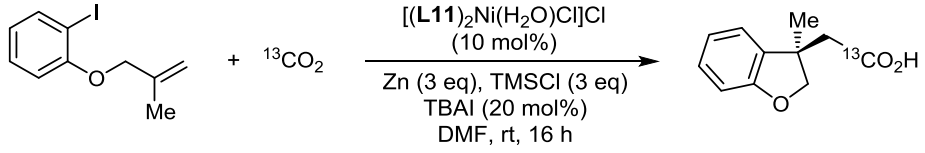

119a (0.2 mmol) (1 atm) **^{13}C-122a** (^{13}C = 98.8%) (65%, 98% *ee*)

A flame dried, nitrogen filled Schlenk tube equipped with a stirring bar was charged with Nickel catalyst (17.5 mol%, 9.8 mg), Zn (0.6 mmol, 39.2 mg) and TBAI (20 mol%, 14.8 mg). The nitrogen atmosphere was evacuated, and the tube was backfilled with CO_2 (1 bar). This operation was repeated three times. Then DMF (3 mL, 0.07 M) was added under flow of CO_2, and the reaction mixture was stirred for 15 min. Under flow of CO_2, substrate **119a** (54.8 mg, 0.2 mmol) was added, and CO_2 was bubbled in the solution. Then, TMSCl (0.6 mmol, 76 µL) was added by syringe, and the reaction mixture was stirred (1000 rpm) for 16 h at rt. The reaction was quenched with HCl (10 mL, 1.0 M), and extracted with ethyl acetate (3 x 10 mL). The combined organic layers were washed with HCl twice (2 mL, 1.0 M), dried over anhydrous Na_2SO_4, and concentrated under reduced pressure. The residue was purified by flash chromatography on silica gel (*n*-Hex:AcOEt = 7:3) to afford the desired product **122a-*^{13}C*** as a white solid (yield = 65%, *ee* = 98%, ^{13}C = 98.8%, 25.0 mg). **^{1}H NMR** (400 MHz, $CDCl_3$) δ = 7.18 – 7.08 (m, 2H), 6.88 (t, *J* = 7.4 Hz, 1H), 6.80 (d, *J* = 8.0 Hz, 1H), 4.61 (d, *J* = 9.2 Hz, 1H), 4.31 (d, *J* = 9.2 Hz, 1H), 2.73 (t, *J* = 6.3 Hz, 2H), 1.45 (s, 3H). **^{13}C NMR** (100 MHz, $CDCl_3$) δ = 176.54, 159.02, 133.98 (d, *J* = 4.2 Hz), 128.68, 122.66, 120.72, 109.97, 82.20, 43.98 (d, *J* = 57.3 Hz), 43.63, 24.98. **HRMS-ESI:** $[M-H]^-$ calcd for $C_{10}{}^{13}CH_{11}O_3^-$ 192.07429, found 192.07433.

6. CO_2 Fixation Through Ni-Catalyzed Reductive C-C Bond Activation/Carboxylation Sequence

- G. Bertuzzi, L. Lombardi, A. Cerveri, L. Ceccon, R. Pedrazzani, M. Monari, M. Bandini, " CO_2 Fixation Through Ni-Catalyzed Reductive C-C Bond Activation/Carboxylation Sequence " *Manuscript in preparation.*

ABSTRACT

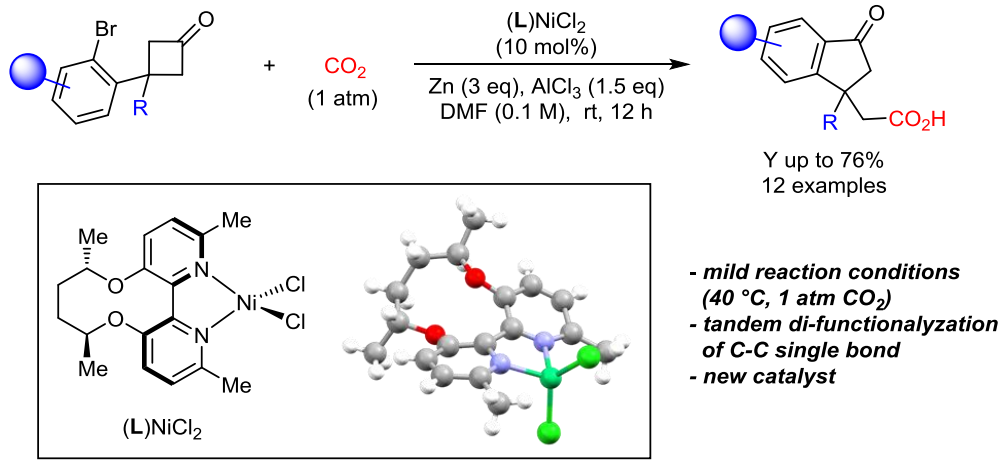

The nickel catalyzed cascade C-C bond activation/carboxylation of cyclobutanones derivatives is described. Through mild conditions and the use of carbon dioxide as environmentally benign carboxylating agent, a range of dihydroindanones bearing a quaternary carbon centre and a carboxylic moiety were synthesized (12 examples) in moderate to good yields (up to 76% yield). A new tetrahedral sterically demanding nickel complex has been prepared for this transformation and has been characterized by means of X-ray spectroscopy. Moreover, based on previous reports and experimental observation a rationally designed mechanism is proposed.

6.1. Background

Given the ubiquity of carbon-carbon (C-C) and carbon-hydrogen (C-H) bonds, the ability to disconnect and/or functionalize either selectively would provide synthetic chemists an atom-economic[126] and straightforward method to construct biologically interesting or complex molecules.[127] In contrast to the area of C-H functionalization,[128] C-C

[126] B.M. Trost, *Science* **1991**, *254*, 1471–1477

[127] a) EJ. Corey, X-M. Cheng, The logic of chemical synthesis. **2009**, Wiley-VCH, Weinheim; b) KC, Nicolaou, EJ. Sorensen, Classics in total synthesis: targets, strategies, methods. **1996**, Wiley-VCH, Weinheim; c) KC, Nicolaou,

activation/functionalization is still underdeveloped in the synthetic community.[129] In general, there are two primary modes of C-C single bond cleavage: direct oxidative addition (Scheme 61a), and β-carbon elimination (Scheme 61b).

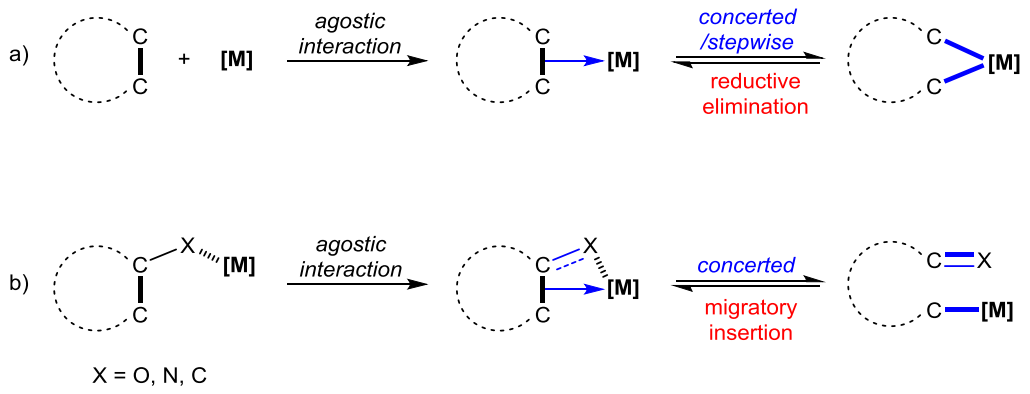

Scheme 61: Diverse modes of insertion of a metal in to a C-C bond.

The challenges associated with oxidative addition of a C-C bond onto a transition metal are twofold. First, the reductive elimination is usually an exo-ergonic reaction and thus thermodynamically favored, which makes the oxidative addition of C-C bonds disfavored. Usually, oxidative additions take place at high temperature or need other driving forces such as strain release, forming aromatic compounds, and/or chelation-derived assistance.[130] Second, C-C bonds typically have neighboring C-H bonds that are more "exposed" which causes kinetic competition to C-C bond activation,[131] causing that during interaction with a transition metal, C-H activation is often more likely due to the statistical abundance and favorable orbital trajectory of C-H bonds. Regarding the second mode of C-C activation, β-carbon elimination poses similar challenges, though as a primarily intramolecular process it does not involve the same kinetic barriers with a transition metal. Furthermore, when acyclic substrates are employed, a byproduct is generated alongside the β-C elimination reaction. In this case, the β-C elimination process generates an entropy increase, lowering the activation barrier. However, generally, transition metal-mediated β-C elimination reactions are still

---

SA. Snyder, Classics in total synthesis II: more targets, strategies, methods. **2003**, Wiley-VCH, Weinheim; d) KC. Nicolaou, J. Chen, Classics in total synthesis III. **2011**, Wiley-VCH, Weinheim.

[128] J-Q. Yu, Z-J. Shi, C–H activation. *Springer*, **2010**, Berlin, Heidelberg

[129] a) C. Winter, N. Krause, *Angew Chem Int Ed* **2009**, *48*, 2460–2462; b) C. Najera, JM. Snasano, *Angew Chem Int Ed* **2009,** *48*, 2452–2456; c) T. Seiser, N. Cramer *Org Biomol Chem* **2009,** *7*, 2835–2840.

[130] a) B. Rybichinski, D. Milstein, *Angew Chem Int Ed* **1999** *38*, 870–883; b) C-H. Jun, *Chem Soc Rev* **2004**, *33*, 610–618.

[131] a) M. Murakami, Y. Ito Top *Organomet Chem* **1999**, *3*, 97–129; b) C. Perthuisot, BJ. Edelbach, DL. Zubirs, H. Simhai, CN. Iverson, C. Muller, T. Satoh, WD. Jones, *J Mol Catal A* **2002**, *189*:157–168; c) K. Ruhland, *Eur J Org Chem* **2012**, *14*, 2683–2706.

thermodynamically challenging due to formation of weak metal-carbon bonds, and often less competitive compared to the more common β-H elimination. Due to the above-mentioned thermodynamic and kinetic challenges to cleave C-C σ bonds, strain-release provided by small-sized rings serves as one of the most important driving forces for C-C activation. A large number of novel and synthetically useful transformations based on this mode of reactivity have been realized, particularly during the past two decades. For example, reactions with cyclopropanes are of high synthetic value, and have been extensively developed.[132] However, activation of the related four-membered ring compounds has received much less attention.[133] In particular, the four-membered ring compounds containing a ketone moiety (namely cyclobutanones) are unique substrates, because the carbonyl can serve as a reacting group or a convenient handle to control site-selectivity. On the other hand, given the possibility for decarbonylation, these compounds can behave as either a four-carbon or a three-carbon synthon, leading to distinct transformations.

In 1994, Murakami and co-workers pioneered the field[134] founding that when cyclobutanone **132** was treated with an equimolar amount of $(PPh_3)_3RhCl$ in refluxing toluene, decarbonylation took place to produce cyclopropane **135** in quantitative yield along with the unreactive complex trans-$[Rh(CO)Cl(PPh_3)_2]$ (Scheme 62).

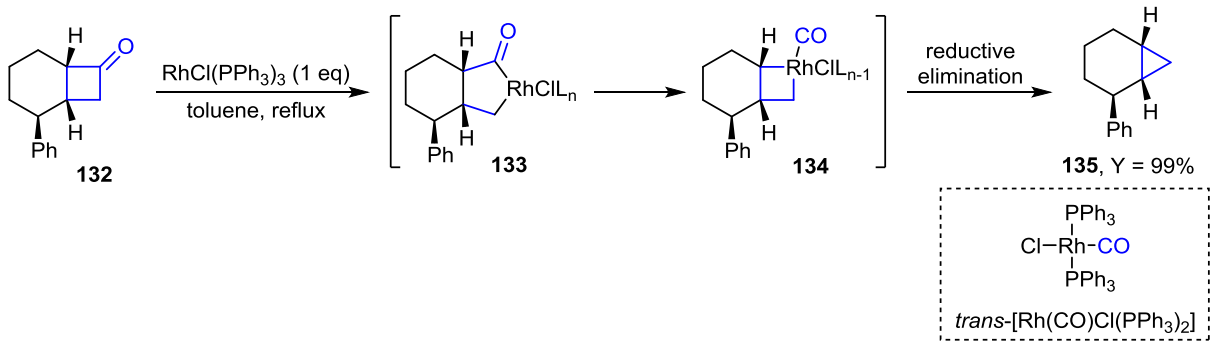

Scheme 62: Rhodium catalyzed cyclobutanone C-C activation.

This decarbonylation reaction was initially believed to proceed through direct oxidative addition of Rh onto the less hindered C-C bond adjacent to the carbonyl group to give five-membered rhodacycle **133**, followed by carbon monoxide extrusion to yield the four-membered rhodacycle **134**, which then undergoes reductive elimination to furnish the observed product **135**. These results are in firm agreement with a stoichiometric

[132] M. Ruben, M. Rubina, V. Gevorgyan, *Chem Rev* **2007**, *107*,3117–3179.
[133] T. Seiser, T. Saget, DN. Tran, N. Cramer, *Angew Chem Int Ed* **2011**, *50*, 7740–7752
[134] M. Murakami, H. Amii, Y. Ito, *Nature* **1994**, *370*, 540–541

decarbonylation reaction previously reported by Rusina.[135] Formation of the thermodynamically stable but catalytically inert trans-[$Rh(CO)Cl(PPh_3)_2$] and release of the ring strain are two major driving forces for this reaction.

A sequential C-C bond activation/C-O bond cleavage reaction was subsequently reported by the same group in 1998.[136] It was discovered that alternative reaction pathways are possible with different bidentate ligands (Scheme 63a). While two possible C-C bonds in cyclobutanone **136** can be activated, Murakami and co-workers suggested bond "a" would preferably undergo C-C bond activation resulting from the directing ability of the benzylic ether. Alternatively, cleavage of bond "b" followed by decarbonylation and CO reinsertion can give the same intermediate **141** (Scheme 63b). The ether (-OPh) directing effects apparently do not govern the reaction, as cyclopentanone **138** was the predominant product (condition B in Scheme 63a). Cleavage of bond "a" can be induced by addition of diphenylacetylene **140** in the reaction media to produce ester **137** (condition A in Scheme 63a). Presumably coordination of the diphenylacetylene **140** competes with the olefin in intermediate **142** to prevent OPh reinsertion, thus favoring reductive elimination to produce **137**. Also, the decarbonylation product cyclopropane **139** could be achieved if a ligand with a large bite angle, such as dppb, was employed (condition C in Scheme 63a).

[135] A. Rusina, A. Vlcek, *Nature* **1965**, *206*, 295–296.
[136] M. Murakami, T. Takahashi, H. Amii, Y. Ito, *J Am Chem Soc* **1998**, *120*, 9949–9950.

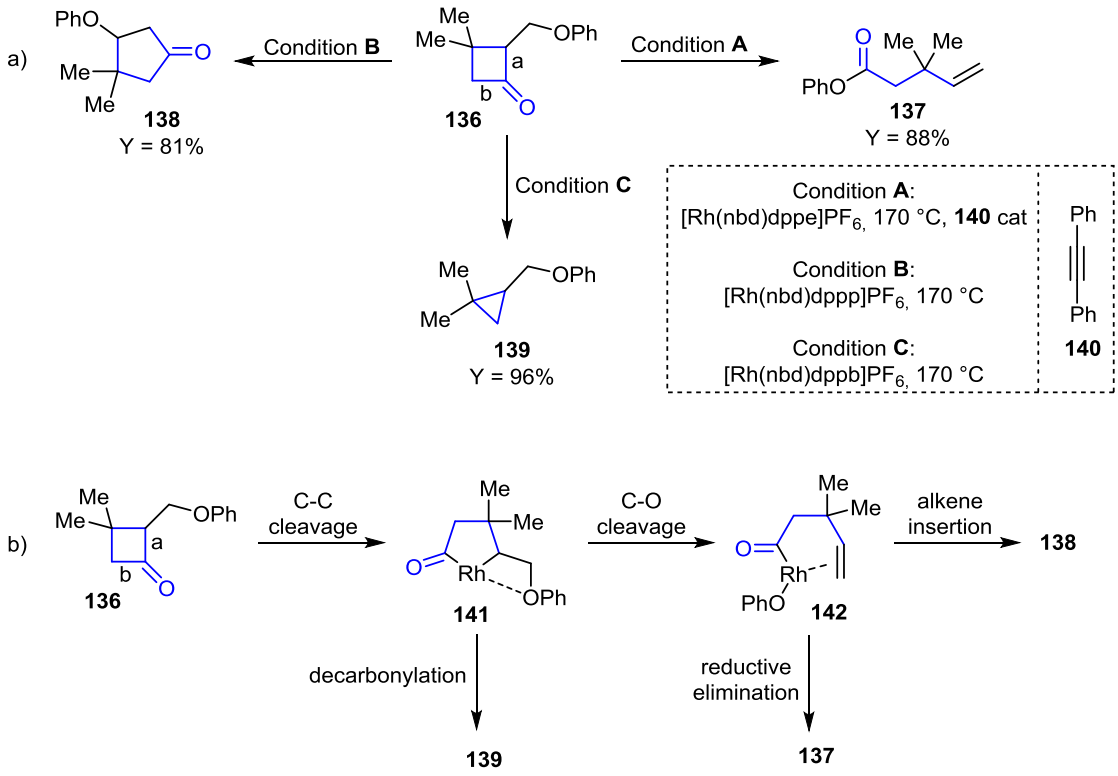

Scheme 63: Ligand-dependant divergent C-C activation of cyclobutanones bearing a coordinating group.

In the area of C-C bond activation via β-C elimination, Ni shows complementary reactivity to Rh and in fact has unique characteristics: 1) as a first row transition metal, Ni is usually more reactive than its second and/or third row counterparts when cyclometalation[137] is involved; 2) Ni(0)-catalyzed aldehyde and alkyne/alkene coupling reactions have been largely developed.[138] In 2005 Murakami and co-workers showed how using a Ni(0) catalyst, an intermolecular [4+2] cycloaddition reaction with cyclobutanone **143** and 4-octyne **144** produced cyclohexenone **145** in 95% yield (Scheme 64).[139] Presumably the reaction of **143** and **144** with Ni(0) would proceed through oxidative cyclization to give oxanickelacyclopentene **146**. β-C elimination cleaves the cyclobutane ring to generate **147** and leads to formation of product **145** after reductive elimination. Overall, a formal [4+2] cycloaddition was accomplished with Ni(0) via β-C elimination. In contrast, Rh was not an effective catalyst for this transformation.

[137] J. Montgomery, Organonickel chemistry. In: Organometallics in synthesis: fourth manual. Wiley, Hoboken, **2013,** pp 319–428.
[138] E. Oblinger, J. Montgomery, *J Am Chem Soc* **1997**, *119*, 9065–9066.
[139] M. Murakami, S. Ashida, T. Matsuda, *J Am Chem Soc* **2005**, *127*, 6932–6933

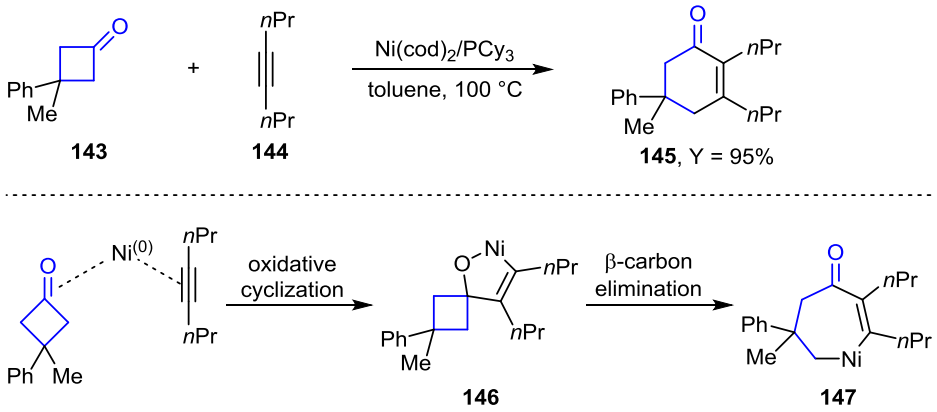

Scheme 64: Ni-catalyzed formal [4+2] cycloaddition with symmetrical alkynes.

Successively, both the Louie and Aissa groups reported similar transformations by activation of Boc-protected azetidinone and/or 3-oxetane as the coupling partner.[140] A [4+2] coupling between protected azetidinones and internal alkynes was independently reported by the Louie[141] and Murakami groups in 2012.[142] As shown in Scheme 65, protected azetidinone **148** and internal alkynes **149** can undergo oxidative metallocyclization to afford the sterically more favored intermediate **151b**, which will afford the piperidone **152** after β-C elimination and reductive elimination.

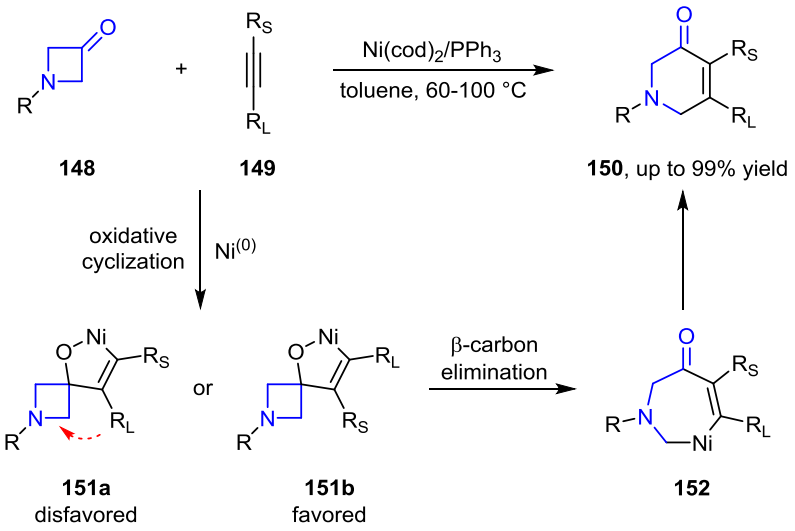

Scheme 65: Regioselective Ni-catalyzed [4+2] cycloaddition between azetidinones and unsymmetrical alkynes.

[140] a) P. Kumar, K. Zhang, J. Louie, *Angew Chem Int Ed* **2021**, *51*, 8602–8606; b) KYT. Ho, C. Aissa, *Chem Eur J* **2012**, *18*, 3486–3489.
[141] P. Kumar, J. Louie, *Org Lett* ***2012***, *14*; 2026–2029.
[142] N. Ishida, T. Yuhki, M. Murakami, *Org Lett* **2012**, *14*, 3898–3901

Besides coupling with alkynes, in 2006 Murakami and co-workers reported a Ni-catalyzed intramolecular coupling of cyclobutanones with alkenes.[143] An asymmetric version of this reaction was reported by the same group in 2012,[144] where the phosphoramidite chiral ligand **154** was employed (Scheme 66). A similar mechanism was proposed and benzobicyclo[2,2,2]octenone **155** was isolated in high yield (up to 97%) and *ee* (up to 92%). Thus far, this is a rare example of an intramolecular carboacylation of alkenes via C-C bond activation.

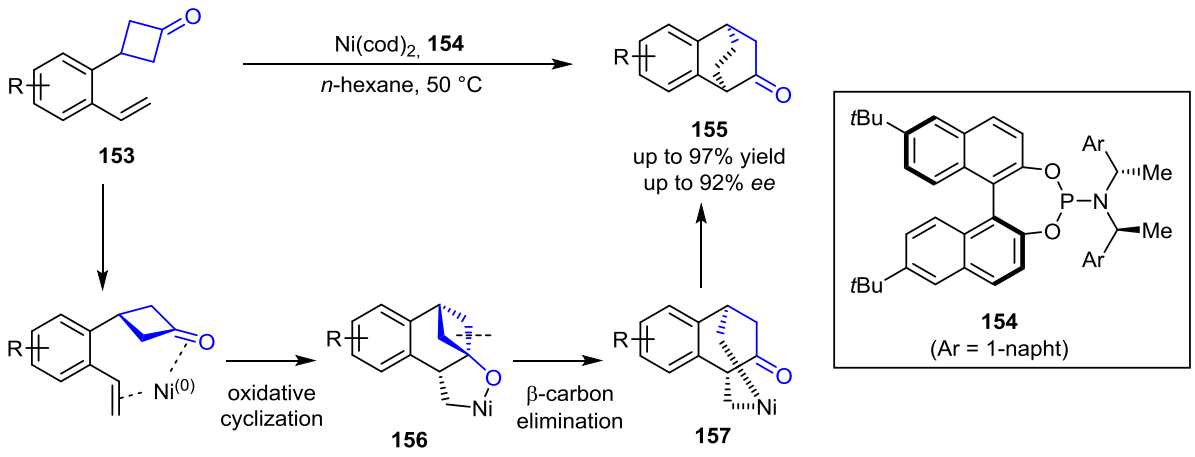

Scheme 66: Intramolecular asymmetric cascade olefin insertion/C-C activation.

In 2020 Wang and co-workers developed a reductive strategy for ring opening of prochiral cyclobutanones via sequential C-C bond cleavage and electrophilic trapping.[145] Under the catalysis of a chiral Ni-complex in assistance of Mn as reducing agent, various cyclobutanones tethering an aryl iodide **158** were reacted with both primary and secondary alkyl bromides **159**, furnishing a variety of chiral indanones **161** containing a quaternary stereogenic center in good to high enantioselectivities (Scheme 67). Various stoichiometric and catalytic control experiments showed that only a Ni(I) intermediate, afterward to oxidative addition to the carbon-iodine bond, can actually catalyze the ring opening step. Moreover, evidences of the presence of radical species (Scheme 67b) and the inertness of the aryl-Ni intermediate through tethered ketone moiety (Scheme 67c), convincingly point to the C-C oxidative addition (mechanism **A**) as most likely. Interestingly this stands in contraposition to the majority of the reactivity observed in other reaction conditions (*see* the examples above), which are based on the β-carbon elimination (mechanism **B**, Scheme 67a).

[143] M. Murakami, S. Ashida, *Chem Commun* **2006**, 4599–4601.
[144] L. Liu, N. Ishida, M. Murakami, *Angew Chem Int Ed* **2012**, *51*, 2485–2488.
[145] D. Ding, H. Dong, C. Wang, *iScience* **2020**, *23*, 101017.

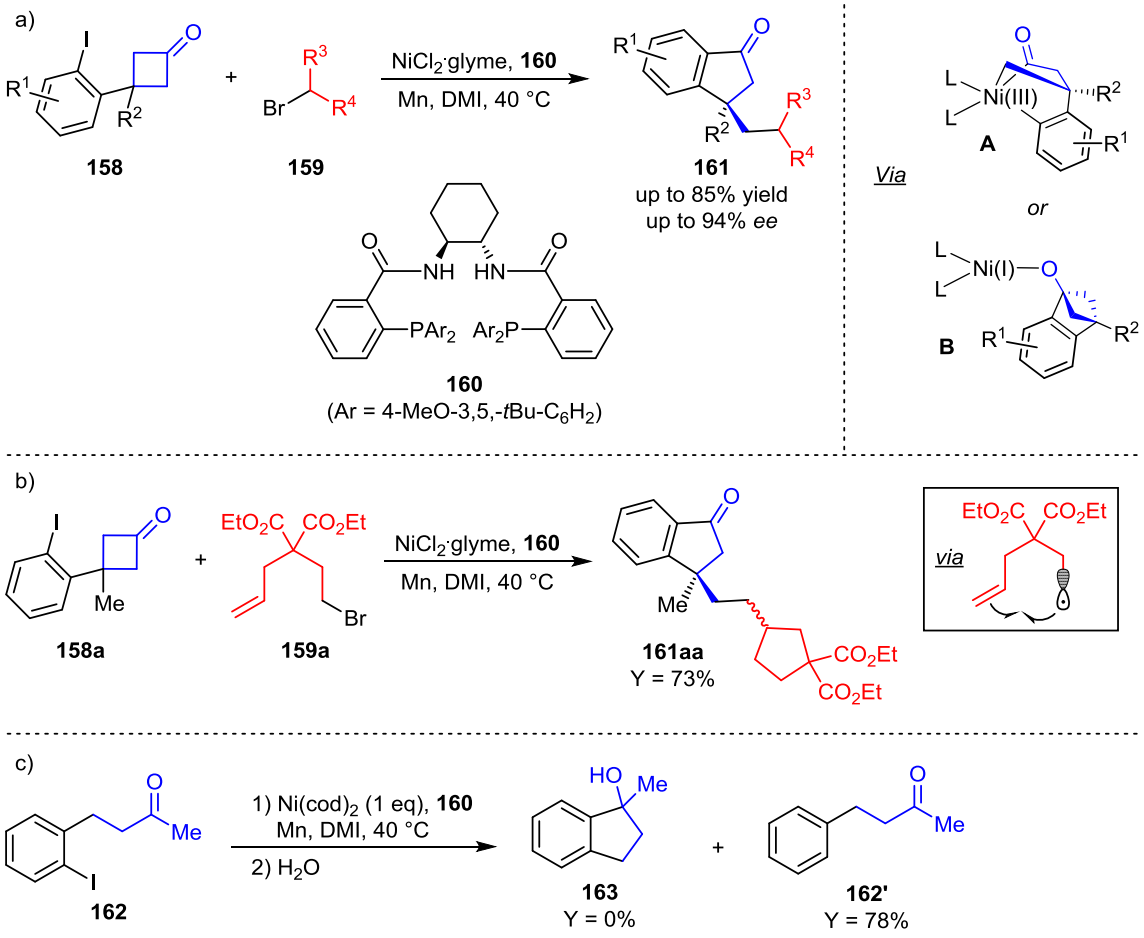

Scheme 67: Enantioselective Ni-catalyzed ring opening of cyclobutanones and control experiments on the reaction mechanism.

Carbonylation reactions have often been coupled with cross-coupling reaction to obtain efficient tandem processes, given the interest in catalytic processes for the generation of high chemical complexity.[146] Although palladium based carbonylation reactions based on the use of carbon monoxide are so far efficient and well understood,[147] many efforts are continuously undertaken to replace this hazardous gas with more benign entities.[148] With this purpose, in 2021 Xu and co-workers investigated a new tandem C-C bond activation/carbonylation sequence, employing aryl formates derivatives as CO surrogate.[149] Particularly under palladium catalysis the C-C bond activation/cyclization of **158** can be coupled with a substituted aryl formate **164** to directly install the carboxylic moiety and obtain the indanone

[146] a) L. Kollar, in *Modern Carbonylation Methods*, Wiley-VCH, **2008**; b) M. Beller, X.-F. Wu, Transition Metal Catalyzed Carbonylation Reactions Carbonylative Activation of C-X Bonds, Springer, **2013**; c) S. Zhao, N.P. Mankad, *Catal. Sci. Technol.* **2019**, *9*, 3603-3613.
[147] A. Brennführer, H. Neumann, M. Beller, *ChemCatChem*, **2009,** 1, 28-41.
[148] a) D. Yu, S. P. Teong, Y. Zhang, *Coord. Chem. Rev.* **2015**, *293-294*, 279-291; b) J. Klankermayer; S. Wesselbaum, K. Beydoun, W. Leitner, *Angew. Chem. Int. Ed.* **2016**, *55*, 7296-7343.
[149] K.L. Song, B. Wu, W-E. Gan, W-C. Yang, X-B. Cheng, J. Cao, L-W. Xu, *Org. Chem. Front*., **2021**, *8*, 3398-3403.

165. Interestingly using the highly reactive aryl formate **TFBen** is possible to *in situ* form the desired ester derivative **165** in a three-component fashion (Scheme 68).

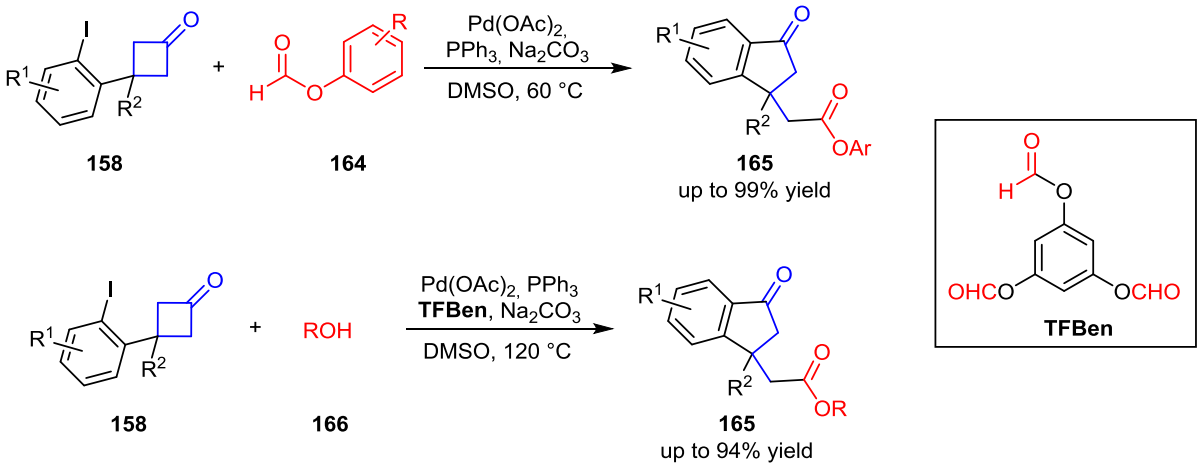

Scheme 68: Pd-catalyzed cascade C-C activation/carbonylation via C-H activation of formates.

6.2. Aim of the Project

Single carbon-carbon bond activation is a powerful tool for the skeletal editing of easily accessible substrates into more complex and useful scaffolds.[150] Although this strategy has been discovered and developed since the dawn of synthetic organic chemistry,[151] in the last decades this intriguing research field has been deeply investigated to obtain more general and reliable catalytic and not methodologies.[152] The need of precious transition metals (*i.e.* Rh, Pd) and drastic conditions such as high temperatures for overcoming the high energy barriers of those processes are main drawbacks of this chemical scenario, and titanic efforts are directed in the development of protocols based on milder reaction conditions and more accessible metal catalysts.[153] Given these assumptions, a Ni-catalyzed cascade C-C bond activation/carboxylation sequence was proposed for the formal ring-expansion of cyclobutanones into dihydroindenes, characterized by a highly congested quaternary carbon centre and a carboxylic functionality (Scheme 69).

[150] S.H. Kennedy, B.D. Dherange, K.J. Berger, *et al. Nature* **2021**, *593*, 223–227.
[151] J. R. Donald, W. P. Unsworth, *Chem. Eur. J.* **2017**, *23*, 8780.
[152] C.H. Jun, *Chem Soc Rev.* **2004**, 33(9), 610-8.
[153] F. Song, T. Gou, B-Q. Wang, Z-J. Shi, *Chem. Soc. Rev.*, **2018**, *47*, 7078-7115.

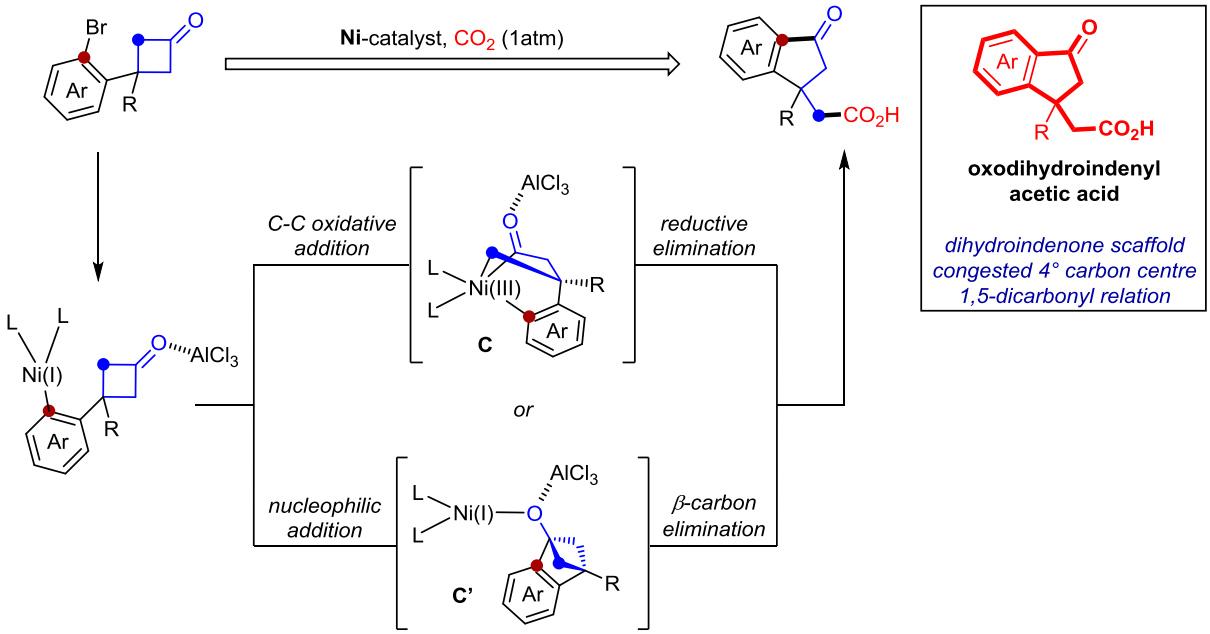

Figura 69: Reaction design for the tandem C-C activation/carboxylation with CO_2.

Depending on the working mechanism, a skeletal editing of the four-membered cyclic ketone should be obtained by β-carbon elimination or direct oxidative insertion of the nickel catalyst into the C-C(O) bond, furnishing a straightforward method for the synthesis of added value cyclo-fused products. The installation of the carboxylic moiety was entrusted to the low toxic feedstock CO_2, with the purpose of developing a mild and sustainable process.

6.3. Discussion and Results

At the outset of the investigation, the conditions from the previous tandem Heck/carboxylation protocol were translated to this parallel system. Interestingly, by employing the pyridine-oxazoline ligand **L1** in the presence of TMSCl as an additive under nickel catalyzed reductive conditions, no conversion of the bromo arene derivative **XX** into the corresponding dihydroindenone was observed. A survey of Lewis acids were tested as additives, and was found the best promoter of the process in the oxophilic $AlCl_3$ used in stoichiometric amount, which delivered the carboxylate product in 43% yield (Table 4, entry 4). Surprisingly the analogue $Al(OTf)_3$ was completely unable to deliver the desired product, while the less acidic $MgCl_2$ gave an intermediate result (Table 4, entry 5 and 2). Similarly to the majority of the Ni-catalyzed reductive cross-coupling protocols, only the highly polar aprotic amide solvents are able to properly promote the process, and DMF resulted the only effectively working reaction media. Once confirmed the reaction conditions, a range of different class of ligands were subjected to the tandem process (**L2-L13**).

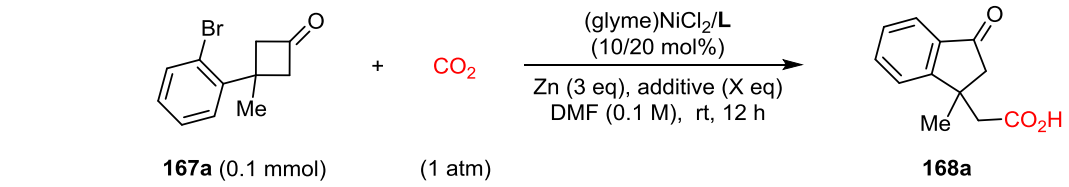

167a (0.1 mmol) (1 atm) **168a**

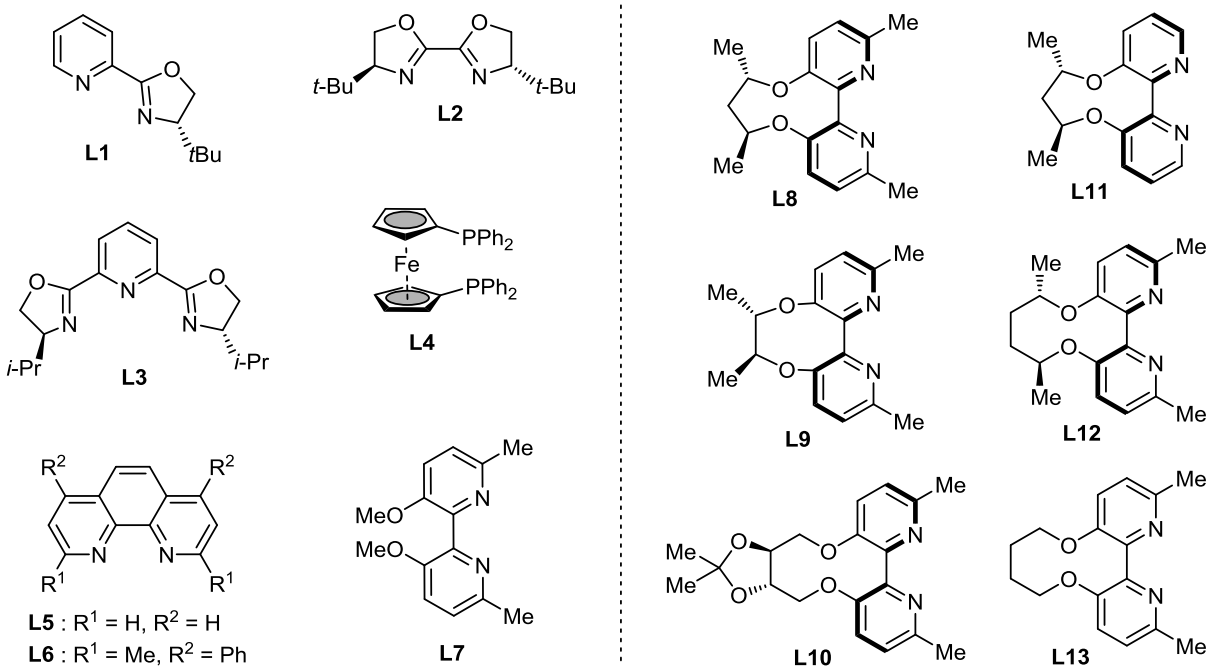

Entry[a]	Ligand	Conditions	Yield **168a** (%)[b]
1	**L1**	TMSCl (1.5 eq)	NR[c]
2	**L1**	$MgCl_2$ (1.5 eq)	22
3	**L1**	LiCl (1.5 eq)	NR
4	**L1**	$AlCl_3$ (1.5 eq)	43
5	**L1**	$Al(OTf)_3$ (1.5 eq)	NR[c]
6	**L2**	$AlCl_3$ (1.5 eq)	NR
7	**L3**	$AlCl_3$ (1.5 eq)	NR
8	**L4**	$AlCl_3$ (1.5 eq)	NR
9	**L5**	$AlCl_3$ (1.5 eq)	NR
10	**L6**	$AlCl_3$ (1.5 eq)	22

11	**L7**	$AlCl_3$ (1.5 eq)	43
12	**L8**	$AlCl_3$ (1.5 eq)	59
13	**L9**	$AlCl_3$ (1.5 eq)	Traces
14	**L10**	$AlCl_3$ (1.5 eq)	23
15	**L11**	$AlCl_3$ (1.5 eq)	18
16	**L8**	$AlCl_3$ (1.5 eq), 40 °C	64
17	**L12**	$AlCl_3$ (1.5 eq), 40 °C	70
18	**L13**	$AlCl_3$ (1.5 eq), 40 °C	12
19	**L12**	$AlCl_3$ (1.5 eq), 60 °C	38
20	**L12**	No CO_2 or Zn or Ni catalyst	NR

Table 4: [a] Reaction conditions: **167a** (0.1 mmol) under anhydrous conditions. [b] Determined after flash chromatography. [c] By-product from de-halogenation of **167a** was isolated as major outcome.

Initially was observed the inertness toward the process using C2-symmetric Bi-Ox **L2** and PyBOx **L3** (Table 4, entry 6 and 7), and similar output was registered by changing class of ligand and employing phosphine based bi-dentate **L4** (Table 4, entry 8). Particularly relevant is the contraposition between entry 9 and entry 10; while phenantroline results un-effective in the target transformation, the simple installation of two methyl groups in the *ortho* positions respect to the nitrogen atoms make **L6** capable of producing the cyclic ketone **168a** in 22% yield (Table 4, entry 9 and 10). This evidence strongly suggest that the steric hinderance caused on the nickel complex is beneficial for the process. As a support of this hypothesis, the bi-pyridine ligand **L7** worked smoothly in the process giving an improved 43% yield (Table 4, entry 11), hinting that another important characteristic needed by the ligand for an efficient activation of the substrate is the presence of electron-rich groups and the twisted conformation of the associated nickel complex. Accordingly, various bpy-based ligands exhibiting those key features were synthesized and tested in the model reaction (**L8-L13**) and after setting the optimal reaction temperature at 40 °C (Table 4, entry 16) the ideal ligand was found in **L12** bearer of the larger back-bone ring, able to deliver the target compound in 70% yield at 40 °C (Table 4, entry 17). Unfortunately every search of enantioselectivity resulted

futile, and no appreciable enantiomeric excess were recorded (with **L12** was obtained 18% *ee* of the product).

To further enhance the performances of the catalytic system in terms of reproducibility and reliability a 1:1 Ni/**L12** complex was prepared by simply mixing the ligand and a nickel salt in DMF (Scheme 70). The nickel complex (**L12**)$NiCl_2$ is obtained in a quantitative yield, and it is characterized by a peculiar tetrahedral geometry, as clearly evidenced by the single-crystal X-ray analysis (in collaboration with Prof. Magda Monari, University of Bologna), and exhibits perfectly comparable catalytic activity to the *in situ* approach.

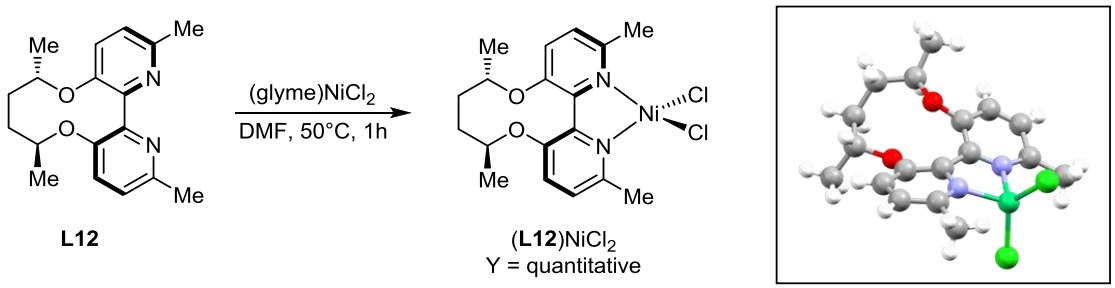

Scheme 70: Synthesis of the tetrahedral Ni complex and X-ray characterization.

With these optimal conditions was then tested the generality of the tandem C-C bond activation/carboxylation by subjecting to catalysis various *o*-bromoaryl cyclobutanone derivatives **167b-l** decorated with a range of functionalities (Scheme 71). Slight modifications of the arene scaffold (5- and 6-Me) brought to no significant changes in the chemical output (**168b-c**, 64-76% yield), in contraposition with a drop in performances when a naphthyl derivative is employed in the process (**168d**, 43% yield). The cascade protocol showed an appreciable tolerance toward electronic perturbation and steric hindrance of the model substrates, and various functionalities were successfully tolerated by the catalytic system (**168e-k**). In particular oxygenated (OMe, OBn) *o*-bromoarenes reacted smoothly forming the carboxylated cycloadduct in satisfying yields (50-73%) in comparison with the model substrate. Similarly electron-poor substitutions (F, CF_3) were installed in different positions on the aromatic moiety, and the corresponding dihydroindanones were isolated in moderate yields (**168i-k**, 35-52% yield). It's worth to notice the particular robustness of this methodology to sterically hindered substrates at the arene portion, both at the *ortho* position in respect to the cyclobutanone (**168f**, 73% yield) and to the bromo (**168i**, 45% yield) suggesting a low dependence on this parameter for the cascade process to happen. Finally the possibility to increase the complexity of the cyclo-fused scaffold at the level of the generated

quaternary carbon centre was investigated subjecting a *n*-butyl substituted cyclobutanone. Interestingly the desired product can be isolated even in a higher yield to the respect of its methyl-substituted counterpart (**168l**, 76% yield).

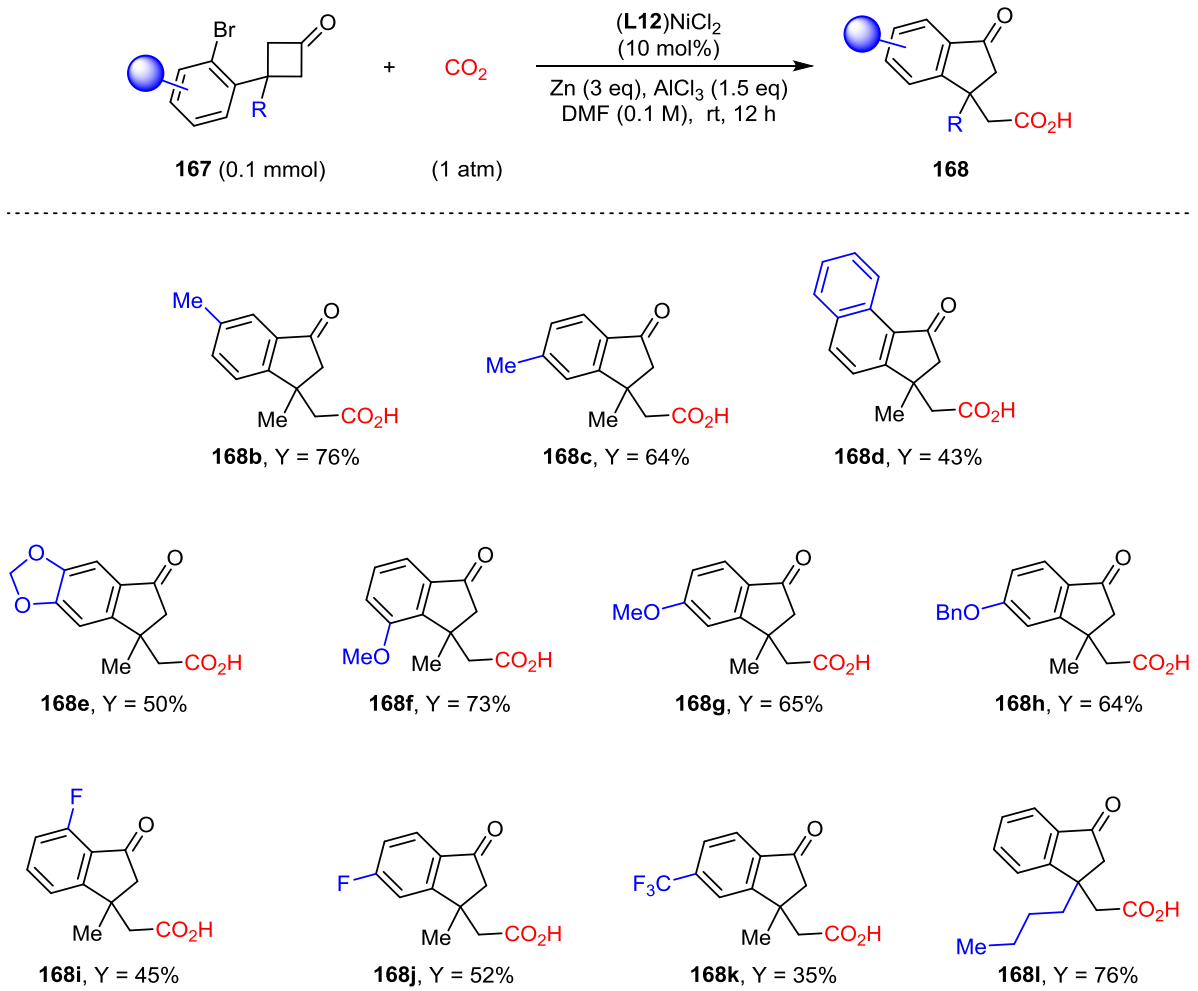

Scheme 71: Reaction scope for the Ni-catalyzed cascade C-C activation/carboxylation.

Finally a mechanistic hypothesis has been evaluated for the present catalytic process, based on previously reported insights of this chemical scenario and experimental evidences. As for the intramolecular arylative carboxylation of alkenes (*see* chapter 5) was assumed the participation of a single 1:1 nickel-ligand complex in the productive pathway for the formation of the carboxylic acid derivative. Similarly the reductive conditions employed (stoichiometric Zn as a reductant) probably implies the formation of a Ni(0)**L** as active catalyst, which initiates the catalytic cycle by oxidatively insert on the C-Br bond, to form the aryl-Ni(II) intermediate **I** (Scheme 72).

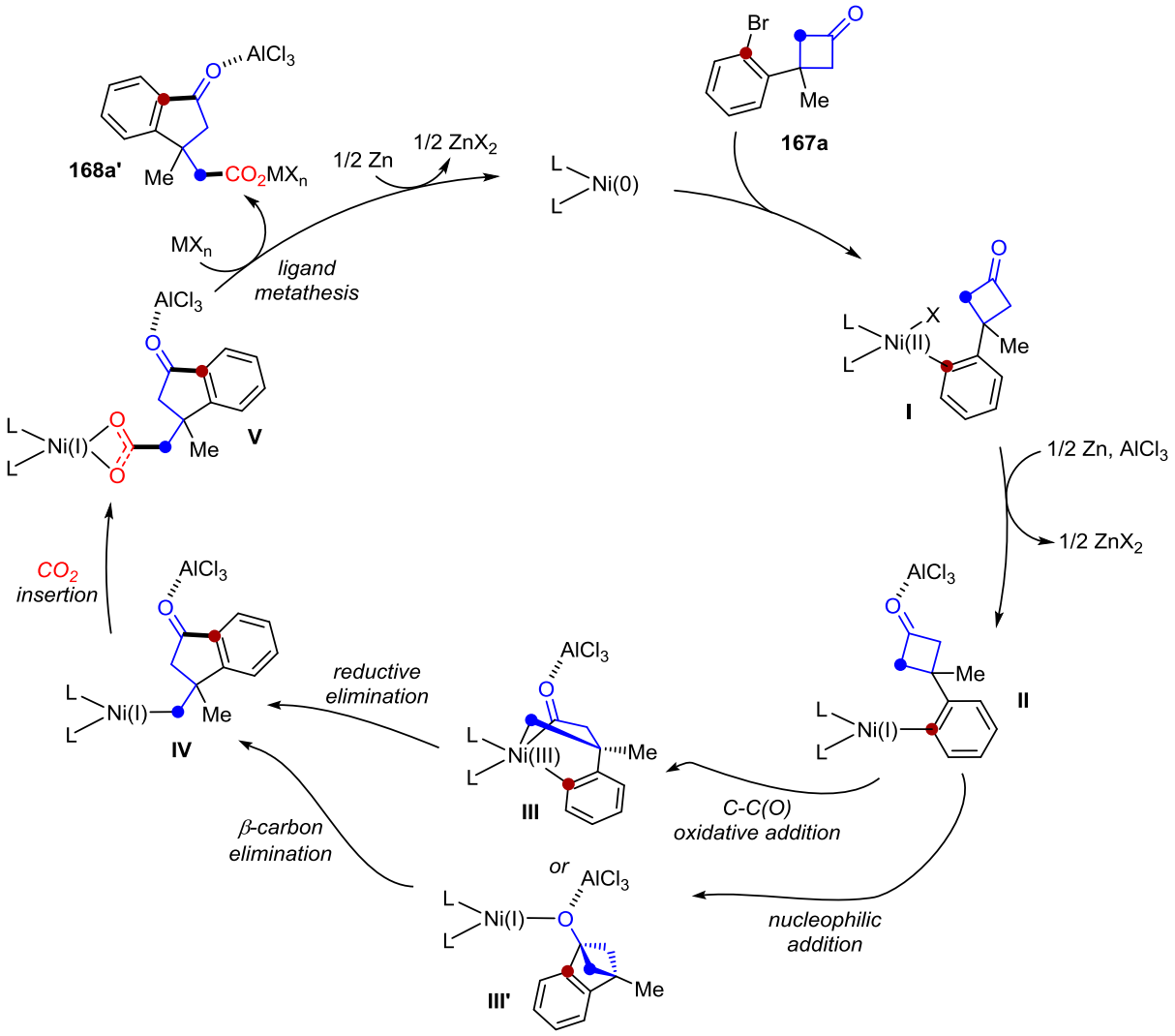

Scheme 72: Proposed mechanism.

A single electron reduction operated by zinc is then responsible for the formation of the aryl-Ni(I) species **II**, and a fast coordination of the carbonyl moiety to the aluminium centre weakens the cyclobutanone skeleton in respect to nucleophilic attack from the tethered organometallic portion, which can take place at the C=O bond, keeping unvaried the oxidation state of nickel (intermediate **III'**), or at the level of the C-C(O) bond by oxidative addition and concomitantly formation of the bridged nickelacycle **III**. Depending on the reaction path undertaken, a β-carbon elimination or a reductive elimination have to happen to release the strain, forming the five-membered intermediate **IV** which can finally be trapped by carbon dioxide by insertion of the alkyl-Ni(I) to the C-O bond. The Ni-carboxylate **V** can then engage coordinatively a different metal from the reaction media (Zn, Al other Ni source) to free the Ni(I) salt that can be further reduced from zinc to generate back the active catalyst.

6.4. Conclusion

A novel cascade procedure for the sequential C-C bond activation/carboxylation of four-membered ketones has been developed. The protocol employs mild reaction conditions and atmospheric pressure of carbon dioxide as C(1)-synthon for the synthesis of densely functionalized dihydroindenone scaffolds by means of a newly defined nickel catalyst. The scope has been evaluated, and the results obtained suggest a good generality and a potential applicability of the methodology. A rational catalytic cycle has been proposed on the basis of previous acquaintances and attempts to further develop the present methodology are underway.

6.5. General Procedures and Product Characterization

6.5.1. Materials and Methods

^{1}H-NMR spectra were recorded on Varian 400 (400 MHz) spectrometers. Chemical shifts are reported in ppm from TMS with the solvent resonance as the internal standard (deuterochloroform: 7.24 ppm). Data are reported as follows: chemical shift, multiplicity (s = singlet, d = doublet, dd= doublet doublet, t = triplet, td = triple doublet, dt = double triplet, q = quartet, sext = sextet, sept = septet, p = pseudo, b = broad, m = multiplet), coupling constants (Hz). ^{13}C-NMR spectra were recorded on a Varian 400 (100 MHz) spectrometers with complete proton decoupling. Chemical shifts are reported in ppm from TMS with the solvent as the internal standard (deuterochloroform: 77.0 ppm). GC-MS spectra were taken by EI ionization at 70 eV on a Hewlett-Packard 5971 with GC injection. They are reported as: *m/z* (rel. intense). LC-electrospray ionization mass spectra were obtained with Agilent Technologies MSD1100 single-quadrupole mass spectrometer. HRMS-ESI were obtained with column Luna Omega 3um Polar C18 (size 100*3 mm) and Xevo G2-XS QTof. The enantiomeric excess (*ee*) were determined by chiral HPLC, on an Agilent Technologies Series 1200 instrument using chiral columns. The enantiomeric compositions were checked against the corresponding racemic products. Chromatographic purification was done with 240-400 mesh silica gel. Other anhydrous solvents were supplied by Sigma Aldrich in Sureseal® bottles and used without any further purification. Commercially available chemicals were purchased from Sigma Aldrich, Fluorochem, Alfa Aeser and TCI and used without any further purification. Melting points were determined with Bibby Stuart Scientific Melting Point Apparatus SMP 3 and are not corrected. Agilent Technologies LC/MSD Trap 1100 series (nebulizer: 15.0 PSI, dry Gas: 5.0 L/min, dry temperature: 325 °C, capillary voltage

positive scan: 4000 mA, capillary voltage negative scan: 3500 mA). The X-ray intensity data for [(**L12**)$NiCl_2$] were measured on a Bruker Apex III CCD diffractometer.

6.5.2. General Procedure for the synthesis of tethered 2-bromoaryl cyclobutanones

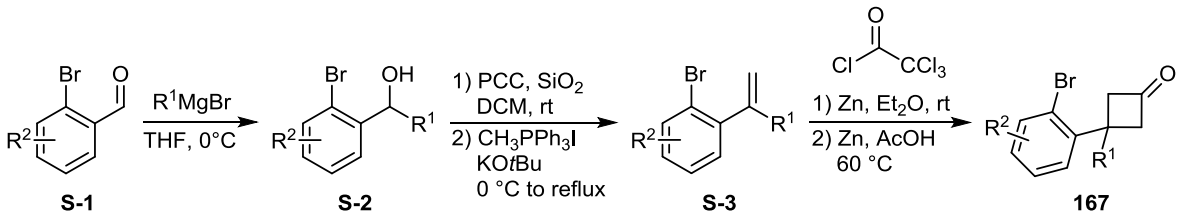

A 50 mL two necked flask under nitrogen atmosphere at 0 °C was charged with a solution of *o*-bromoaryl aldehyde **S-1** (10.8 mmol, 1 eq) in THF (12 mL). Then a solution of MeMgBr (1.2 eq, 3 M) was added dropwise, and the mixture was stirred at 0 °C for 1 h. Then a saturated solution of NH_4Cl was added (15 mL), and the aqueous phase was extracted with AcOEt (3 x 10 mL). The combined organic phases were washed with water (3 x 10 mL), dried over anhydrous Na_2SO_4, and concentrated under reduced pressure, to obtain the benzyl alcohol **S-2** quantitatively, and was used directly in the following step.

A one necked flask was charged with **S-2** (10.8 mmol, 1 eq), silica gel (4.6 g), PCC (21.6 mmol, 2 eq) and DCM (90 mL) at room temperature, and the solution was stirred for 12 h. The solution was concentrated under reduced pressure, and the crude was purifier by flash chromatography (100% AcOEt) to obtain the aromatic ketone, that was involved in the next step. A solution of KO*t*Bu (24.3 mmol, 2.5 eq) and $MePPh_3I$ (19.4 mmol, 2 eq) in THF (40 mL) was stirred at room temperature for 1 h. Then the solution was cooled at 0 °C and a solution of 2-bromoacetophenone (9.7 mmol, 1 eq) in THF (5 mL) was added dropwise. The mixture was slowly warmed at reflux and stirred for 12 h. The reaction was quenched with water (50 mL), extracted with AcOEt (3 x 30 mL), and the reunited organic phases were washed with water (3 x 30 mL), dried over anhydrous Na_2SO_4, and concentrated under reduced pressure, to obtain the *o*-bromo styrene **S-3** quantitatively, that was used directly in the following step.

To a suspension of styrene **S-3** (8.7 mmol, 1 eq) and Zn (35 mmol, 4 eq) in Et_2O (70 mL) at 0 °C was added dropwise trichloroacetyl chloride (26.2 mmol, 3 eq), and the resulting mixture was stirred at room temperature for 12 h. The solution was filtered on a celite pad, and the crude was purified by flash chromatography giving the dichloro cyclobutanone, which was directly involved in the following step. A suspension of dichloro cyclobutanone (7 mmol, 1 eq) and Zn (14 mmol, 2 eq) in AcOH (30 mL) was stirred at 60 °C for 12 h. The solvent was removed under reduced pressure, suspended in AcOEt and filtered on a celite pad. The crude was purified by flash chromatography to obtain the *o*-bromoaryl cyclobutanone **167**.

3-(2-bromophenyl)-3-methylcyclobutan-1-one (**167a**)

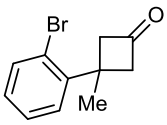

Pale yellow oil. **^{1}H NMR** (400 MHz, $CDCl_3$) δ = 7.61 (dt, *J* = 7.6, 3.1 Hz, 1H), 7.38 – 7.30 (m, 2H), 7.14 (ddt, *J* = 11.3, 8.2, 4.0 Hz, 1H), 3.60 – 3.52 (m, 2H), 3.27 – 3.20 (m, 2H), 1.65 (s, 3H). **^{13}C NMR** (100 MHz, $CDCl_3$) δ = 206.5, 145.9, 134.3, 128.3, 128.2, 127.6, 122.2, 59.2 (2C), 36.2, 27.7. **GC-MS** (m/z): 239 (9), 197 (100).

3-(2-bromo-4-methylphenyl)-3-methylcyclobutan-1-one (**167b**)

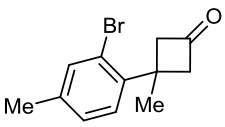

Pale yellow oil. **^{1}H NMR** (400 MHz, $CDCl_3$) δ = 7.41 – 7.39 (m, 1H), 7.16 (d, *J* = 7.9 Hz, 1H), 7.10 (ddd, *J* = 7.9, 1.7, 0.7 Hz, 1H), 3.53 – 3.45 (m, 2H), 3.23 – 3.13 (m, 2H), 2.31 (s, 3H), 1.59 (s, 3H). **^{13}C NMR** (100 MHz, $CDCl_3$) δ = 206.8, 142.8, 138.4, 134.7, 128.3, 127.8, 121.9, 59.2 (2C), 35.8, 27.8, 20.4. **GC-MS** (m/z): 253 (8), 211 (100).

3-(2-bromo-5-methylphenyl)-3-methylcyclobutan-1-one (**167c**)

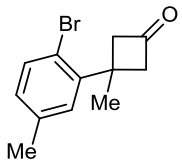

Pale yellow oil. **^{1}H NMR** (400 MHz, $CDCl_3$) δ = 7.43 (d, *J* = 8.1 Hz, 1H), 7.08 (d, *J* = 1.9 Hz, 1H), 6.94 – 6.90 (m, 1H), 3.56 – 3.47 (m, 2H), 3.22 – 3.13 (m, 2H), 2.31 (s, 3H), 1.60 (s, 3H). **^{13}C NMR** (100 MHz, $CDCl_3$) δ = 207.0, 145.5, 137.5, 134.0, 129.1, 128.9, 118.8, 59.1 (2C), 36.1, 27.8, 21.0. **GC-MS** (m/z): 253 (5), 211 (100).

3-(1-bromonaphthalen-2-yl)-3-methylcyclobutan-1-one (**167d**)

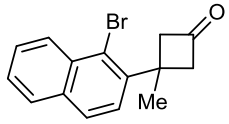

White solid. **^{1}H NMR** (400 MHz, $CDCl_3$) δ = 8.38 (d, *J* = 8.6 Hz, 1H), 7.81 (*pseudo*d, *J* = 8.4 Hz, 2H), 7.60 (t, *J* = 7.7 Hz, 1H), 7.51 (t, *J* = 7.5 Hz, 1H), 7.40 (d, *J* = 8.6 Hz, 1H), 3.71 – 3.61 (m, 2H), 3.36 – 3.26 (m, 2H), 1.70 (s, 3H). **^{13}C NMR** (100 MHz, $CDCl_3$) δ = 206.6, 143.7, 133.2, 132.8, 128.1, 128.0, 127.8, 127.1, 126.5, 125.5, 122.2, 59.6 (2C), 37.3, 27.5. **GC-MS** (m/z): 289 (10), 247 (100).

3-(6-bromobenzo[d][1,3]dioxol-5-yl)-3-methylcyclobutan-1-one (**167e**)

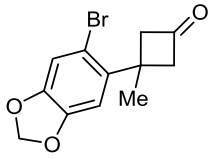

White solid. **^{1}H NMR** (400 MHz, $CDCl_3$) δ = 7.00 (s, 1H), 6.76 (s, 1H), 5.96 (s, 2H), 3.49 – 3.39 (m, 2H), 3.20 – 3.11 (m, 2H), 1.56 (s, 3H). **^{13}C NMR** (100 MHz, $CDCl_3$) δ = 206.4, 147.5, 147.1, 139.2, 113.9, 112.4,

108.0, 101.9, 59.3 (2C), 36.2, 27.7. **GC-MS** (m/z): 283 (10), 241 (100).

3-(2-bromo-6-methoxyphenyl)-3-methylcyclobutan-1-one (**167f**)

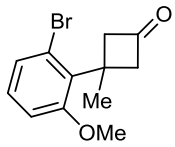

Pale yellow oil. **^{1}H NMR** (400 MHz, $CDCl_3$) δ = 7.18 (dd, *J* = 8.0, 1.2 Hz, 1H), 7.05 (t, *J* = 8.1 Hz, 1H), 6.84 (dd, *J* = 8.2, 1.0 Hz, 1H), 3.80 (s, 3H), 3.56 – 3.47 (m, 2H), 3.24 – 3.14 (m, 2H), 1.53 (s, 3H). **^{13}C NMR** (100 MHz, $CDCl_3$) δ = 210.1, 158.7, 134.1, 128.3, 126.5, 123.1, 110.3, 60.5 (2C), 55.6, 34.6, 25.6. **GC-MS** (m/z): 269 (7), 227 (100).

3-(2-bromo-5-methoxyphenyl)-3-methylcyclobutan-1-one (**167g**)

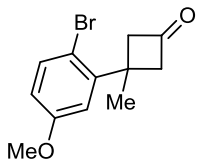

Pale yellow oil. **^{1}H NMR** (400 MHz, $CDCl_3$) δ = 7.46 (d, *J* = 8.7 Hz, 1H), 6.83 (d, *J* = 3.0 Hz, 1H), 6.67 (dd, *J* = 8.7, 3.0 Hz, 1H), 3.80 (s, 3H), 3.57 – 3.47 (m, 2H), 3.24 – 3.10 (m, 2H), 1.61 (s, 3H). **^{13}C NMR** (100 MHz, $CDCl_3$) δ = 201.7, 154.2, 142.2, 130.2, 110.1, 108.2, 107.8, 54.3 (2C), 50.7, 31.5, 22.9. **GC-MS** (m/z): 269 (8), 227 (100).

3-(5-(benzyloxy)-2-bromophenyl)-3-methylcyclobutan-1-one (**167h**)

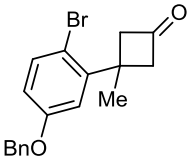

Yellow oil. **^{1}H NMR** (400 MHz, $CDCl_3$) δ = 7.45 (d, *J* = 8.7 Hz, 1H), 7.42 – 7.30 (m, 5H), 6.90 (d, *J* = 3.0 Hz, 1H), 6.73 (dd, *J* = 8.7, 3.0 Hz, 1H), 5.03 (s, 2H), 3.52 – 3.43 (m, 2H), 3.21 – 3.12 (m, 2H), 1.59 (s, 3H). **^{13}C NMR** (100 MHz, $CDCl_3$) δ = 206.4, 158.1, 147.0, 136.3, 134.9, 128.7 (2C), 128.2 (2C), 127.5, 115.8, 113.9, 112.8, 70.3, 59.1 (2C), 36.2, 27.6. **GC-MS** (m/z): 345 (8), 303 (31), 91 (100).

3-(2-bromo-3-fluorophenyl)-3-methylcyclobutan-1-one (**167i**)

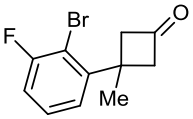

Yellow oil. **^{1}H NMR** (400 MHz, $CDCl_3$) δ = 7.28 (td, *J* = 8.0, 5.6 Hz, 1H), 7.08 (dt, *J* = 7.9, 1.3 Hz, 1H), 7.03 (td, *J* = 8.2, 1.5 Hz, 1H), 3.59 – 3.49 (m, 2H), 3.30 – 3.17 (m, 2H), 1.65 – 1.61 (m, 3H). **^{13}C NMR** (100 MHz, $CDCl_3$) δ = 205.9, 159.6 (d, *J* = 246.5 Hz), 148.4, 128.6 (d, *J* = 8.4 Hz), 123.3 (d, *J* = 3.2 Hz), 114.6 (d, *J* = 23.5 Hz), 109.6 (d, *J* = 21.0 Hz), 59.3 (2C), 36.4 (d, *J* = 2.1 Hz), 27.6 (2C). **^{19}F NMR** (376 MHz, $CDCl_3$) δ = -103.46 (dd, *J* = 8.1, 5.5 Hz, 1F). **GC-MS** (m/z): 257 (5), 215 (100).

3-(2-bromo-5-fluorophenyl)-3-methylcyclobutan-1-one (**167j**)

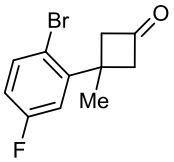

Pale yellow oil. **^{1}H NMR** (400 MHz, $CDCl_3$) δ = 7.52 (dd, *J* = 8.7, 5.4 Hz, 1H), 7.01 (dd, *J* = 9.7, 3.0 Hz, 1H), 6.91 – 6.80 (m, 1H), 3.54 – 3.45 (m, 2H), 3.25 – 3.16 (m, 2H), 1.61 (s, 3H). **^{13}C NMR** (100 MHz, $CDCl_3$) δ = 205.6, 162.0 (d, *J* = 247.6 Hz), 148.1 (d, *J* = 6.6 Hz), 135.6 (d, *J* = 8.0 Hz), 116.2 (d, *J* = 3.0 Hz), 115.6 (d, *J* = 2.4 Hz), 115.3 (d, *J* = 3.4 Hz), 59.0 (2C), 36.3 (d, *J* = 1.4 Hz), 27.5; **^{19}F NMR** (376 MHz, $CDCl_3$) δ = -114.21 – -114.32 (m, 1F). **GC-MS** (m/z): 257 (8), 215 (100).

3-(2-bromo-5-(trifluoromethyl)phenyl)-3-methylcyclobutan-1-one (**167k**)

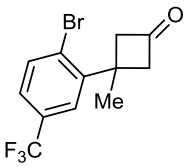

Colorless oil. **^{1}H NMR** (400 MHz, $CDCl_3$) δ = 7.71 (d, *J* = 8.2 Hz, 1H), 7.51 (d, *J* = 2.2 Hz, 1H), 7.37 (dd, *J* = 8.3, 2.2 Hz, 1H), 3.59 – 3.48 (m, 2H), 3.31 – 3.20 (m, 2H), 1.64 (s, 3H). **^{13}C NMR** (100 MHz, $CDCl_3$) δ = 205.1, 147.0, 135.0, 130.2 (q, *J* = 33.1 Hz), 126.1 (q, *J* = 1.6 Hz), 125.1 (q, *J* = 3.6 Hz), 124.9 (q, *J* = 3.6 Hz), 123.6 (q, *J* = 259.4 Hz) 59.1 (2C), 36.4, 27.5. **^{19}F NMR** (376 MHz, $CDCl_3$) δ = --62.66 (s, 3F). **GC-MS** (m/z): 307 (11), 265 (100).

3-(2-bromophenyl)-3-butylcyclobutan-1-one (**167l**)

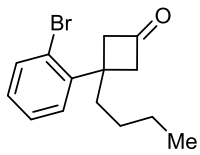

Yellow oil. **^{1}H NMR** (400 MHz, $CDCl_3$) δ = 7.57 (dd, *J* = 7.9, 1.3 Hz, 1H), 7.28 (td, *J* = 7.6, 1.3 Hz, 1H), 7.19 (dd, *J* = 7.8, 1.7 Hz, 1H), 7.10 (td, *J* = 7.6, 1.3 Hz, 1H), 3.50 – 3.40 (m, 2H), 3.28 – 3.17 (m, 2H), 1.94 (bs, 2H), 1.26 – 1.16 (m, 2H), 1.06 - 0.95 (m, 2H), 0.80 (t, *J* = 7.3 Hz, 3H). **^{13}C NMR** (100 MHz, $CDCl_3$) δ = 209.5, 143.8, 134.3, 129.8, 128.3, 127.0, 122.3, 57.8 (b, 2C), 39.8, 38.4, 27.7, 22.7, 13.8. **GC-MS** (m/z): 281 (8), 239 (100).

6.5.3. General Procedure for the synthesis of the tetrahedral Ni-complex

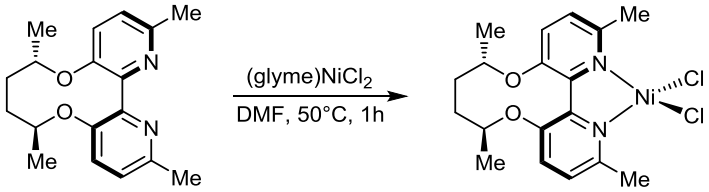

L12 (**L12**)$NiCl_2$

To a solution, under nitrogen atmosphere, of (glyme)$NiCl_2$ (65.9 mg, 0.3 mmol, 1 eq) in DMF (1 mL) was added **L12** (89.4 mg, 0.3 mmol, 1 eq), and the system was heated at 50 °C for 1 h. Then the nickel complex was precipitated by adding Et_2O (10 mL) and filtered to obtain (**L12**)$NiCl_2$ quantitatively as a brown powder.

6.5.4. General Procedure for the tandem C-C bond activation/carboxylation protocol

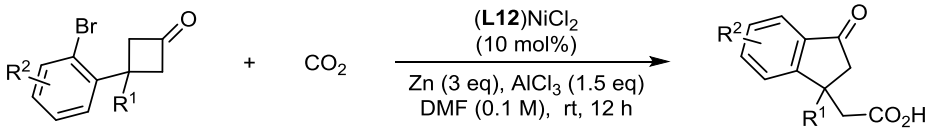

167 (0.1 mmol) (1 atm) **168**

A flame dried, nitrogen filled Schlenk tube equipped with a stirring bar was charged with Nickel catalyst (10 mol%, 4.3 mg), zinc (0.3 mmol, 19.8 mg) and $AlCl_3$ (0.15 mmol, 20 mg). The nitrogen atmosphere was evacuated, and the tube was backfilled with CO_2 (1 bar). This operation was repeated three times. Then DMF (1 mL) was added under flow of CO_2, and the reaction mixture was stirred for 15 min. Under flow of CO_2, substrate **167** (0.1 mmol) was added, and CO_2 was bubbled in the solution. Then the reaction mixture was stirred (1000 rpm) at 40 °C for 12 h. The reaction was quenched with HCl (5 mL, 1.0 M), and extracted with ethyl acetate (3 x 5 mL). The combined organic layers were washed with HCl twice (2 mL, 1.0 M), dried over anhydrous Na_2SO_4, and concentrated under reduced pressure. The residue was purified by flash chromatography on silica gel to afford the desired product **168**.

2-(1-methyl-3-oxo-2,3-dihydro-1H-inden-1-yl)acetic acid (**168a**)

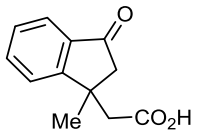

Colorless oil, yield = 70% (14.3 mg, *n*-Hex:AcOEt = 7:2 + 1% HCO_2H). **^{1}H NMR** (400 MHz, $CDCl_3$) δ = 7.70 (d, *J* = 7.6 Hz, 1H), 7.61 (t, *J* = 7.5 Hz, 1H), 7.47 (d, *J* = 7.8 Hz, 1H), 7.38 (t, *J* = 7.4 Hz, 1H), 3.02 (d, *J* = 19.0 Hz, 1H), 2.80 (d, *J* = 15.4 Hz, 1H), 2.66 (d, *J* = 15.3 Hz, 1H), 2.56 (d, *J* = 19.0 Hz, 1H), 1.47 (s, 3H). **^{13}C NMR** (100 MHz, $CDCl_3$) δ = 200.0, 170.7, 155.6, 130.5, 129.9, 122.8, 118.4, 118.4, 45.0, 40.0, 34.9, 23.4. **LC-MS** (m/z): $[M-H]^-$ = 203.2.

2-(1,5-dimethyl-3-oxo-2,3-dihydro-1H-inden-1-yl)acetic acid (**168b**)

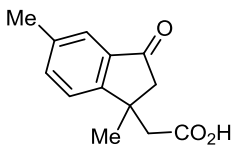

Colorless oil, yield = 76% (16.6 mg, *n*-Hex:AcOEt = 7:2 + 1% HCO_2H). **^{1}H NMR** (400 MHz, $CDCl_3$) δ = ^{1}H NMR (401 MHz, cdcl$_3$) δ 7.49 (s, 1H), 7.43 (d, *J* = 7.9 Hz, 1H), 7.35 (d, *J* = 7.9 Hz, 1H), 3.02 (d, *J* = 19.0 Hz, 1H), 2.78 (d, *J* = 15.3 Hz, 1H), 2.64 (d, *J* = 15.3 Hz, 1H), 2.55 (d, *J* = 19.0 Hz, 1H), 2.38 (s, 3H), 1.45 (s, 3H). **^{13}C NMR** (100 MHz, $CDCl_3$) δ = 205.2, 176.0, 158.2, 138.1, 136.3, 135.9, 123.5, 123.3, 50.5, 45.2, 39.8, 28.6, 21.0. **LC-MS** (m/z): $[M-H]^-$ = 217.2.

2-(1,6-dimethyl-3-oxo-2,3-dihydro-1H-inden-1-yl)acetic acid (**168c**)

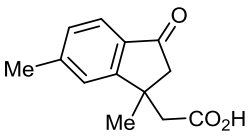

Colorless oil, yield = 64% (13.9 mg, *n*-Hex:AcOEt = 7:2 + 1% HCO_2H). **^{1}H NMR** (400 MHz, $CDCl_3$) δ = 7.59 (d, *J* = 7.8 Hz, 1H), 7.26 (s, 1H), 7.18 (d, *J* = 7.8 Hz, 1H), 6.26 (bs, 1H), 3.01 (d, *J* = 19.0 Hz, 1H), 2.79 (d, *J* = 15.4 Hz, 1H), 2.64 (d, *J* = 15.4 Hz, 1H), 2.54 (d, *J* = 19.0 Hz, 1H), 2.43 (s, 3H), 1.46 (s, 3H). **^{13}C NMR** (100 MHz, $CDCl_3$) δ = 204.8, 175.9, 161.3, 146.3, 133.4, 129.3, 123.9, 123.4, 50.4, 45.1, 39.9, 28.5, 22.2. **LC-MS** (m/z): $[M-H]^-$ = 217.0.

2-(3-methyl-1-oxo-2,3-dihydro-1H-cyclopenta[a]naphthalen-3-yl)acetic acid (**168d**)

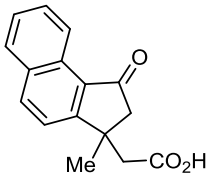

White solid, yield = 43% (10.9 mg, *n*-Hex:AcOEt = 7:2 + 1% HCO_2H). **^{1}H NMR** (400 MHz, $CDCl_3$) δ = 9.13 (d, *J* = 8.3 Hz, 1H), 8.07 (d, *J* = 8.5 Hz, 1H), 7.87 (d, *J* = 8.1 Hz, 1H), 7.66 (ddd, *J* = 8.3, 7.0, 1.1 Hz, 1H), 7.55 (ddd, *J* = 6.9, 6.2, 1.6 Hz, 1H), 7.52 (d, *J* = 8.5 Hz, 1H), 3.14 (d, *J* = 18.8 Hz, 1H), 2.86 (d, *J* = 15.2 Hz, 1H), 2.71 (s, *J* = 15.2 Hz, 1H), 2.67 (d, *J* = 18.8 Hz, 1H), 1.52 (s, 3H). **^{13}C NMR** (100 MHz, $CDCl_3$) δ = 205.5, 175.7, 163.2, 136.3, 132.7, 129.5, 129.2, 129.0, 128.1, 126.9, 124.4, 120.5, 50.7, 44.8, 39.8, 28.2. **LC-MS** (m/z): $[M-H]^-$ = 253.2.

2-(5-methyl-7-oxo-6,7-dihydro-5H-indeno[5,6-d][1,3]dioxol-5-yl)acetic acid (**168e**)

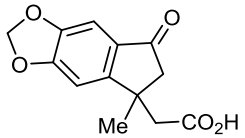

White solid, yield = 50% (12.4 mg, *n*-Hex:AcOEt = 7:2 + 1% HCO_2H). **^{1}H NMR** (400 MHz, acetone-d_6) δ = 7.25 (s, 1H), 7.02 (s, 1H), 6.24 (s, 2H), 3.09 (d, *J* = 18.6 Hz, 1H), 2.91 (d, *J* = 15.5 Hz, 1H), 2.81 (d, *J* = 15.5 Hz, 1H), 2.55 (d, *J* = 18.6 Hz, 1H). **^{13}C NMR** (100 MHz, acetone-d_6) δ = 204.2, 174.5, 161.4, 156.8, 151.2, 133.3, 106.2, 105.3, 103.6, 52.9, 46.9, 42.4, 30.8. **LC-MS** (m/z): $[M-H]^-$ = 247.2.

2-(7-methoxy-1-methyl-3-oxo-2,3-dihydro-1H-inden-1-yl)acetic acid (**168f**)

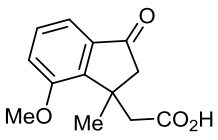

Colorless oil, yield = 73% (17.1 mg, *n*-Hex:AcOEt = 7:2 + 1% HCO_2H). **^{1}H NMR** (400 MHz, $CDCl_3$) δ = 7.34 (t, *J* = 7.6 Hz, 1H), 7.29 (d, *J* = 6.9 Hz, 1H), 7.04 (d, *J* = 7.3 Hz, 1H), 3.87 (s, 3H), 3.03 (d, *J* = 6.6 Hz, 1H), 2.98 (d, *J* = 10.3 Hz, 1H), 2.90 (d, *J* = 15.6 Hz, 1H), 2.53 (d, *J* = 19.2 Hz, 1H), 1.52 (s, 3H). **^{13}C NMR** (100 MHz, $CDCl_3$) δ = 205.5, 176.8, 157.1, 147.4, 138.0, 130.0, 116.3, 115.3, 55.4, 50.8, 42.4, 40.3, 26.3. **LC-MS** (m/z): $[M-H]^-$ = 233.2.

2-(6-methoxy-1-methyl-3-oxo-2,3-dihydro-1H-inden-1-yl)acetic acid (**168g**)

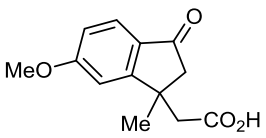

Colorless oil, yield = 65% (15.2 mg, *n*-Hex:AcOEt = 7:2 + 1% HCO_2H). **^{1}H NMR** (400 MHz, $CDCl_3$) δ = 7.64 (d, *J* = 8.5 Hz, 1H), 6.90 (dd, *J* = 8.5, 2.1 Hz, 1H), 6.87 (d, *J* = 2.0 Hz, 1H), 3.87 (s, 3H), 3.01 (d, *J* = 18.9 Hz, 1H), 2.78 (d, *J* = 15.3 Hz, 1H), 2.65 (d, *J* = 15.3 Hz, 1H), 2.55 (d, *J* = 18.9 Hz, 1H), 1.46 (s, 3H). **^{13}C NMR** (100 MHz, $CDCl_3$) δ = 200.9, 173.2, 163.0, 161.2, 126.4, 122.9, 112.8, 104.8, 53.1, 47.9, 42.5, 37.4, 25.9. **LC-MS** (m/z): $[M-H]^-$ = 233.2.

2-(6-(benzyloxy)-1-methyl-3-oxo-2,3-dihydro-1H-inden-1-yl)acetic acid (**168h**)

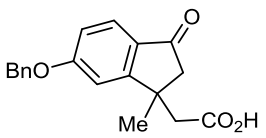

Colorless oil, yield = 64% (19.8 mg, *n*-Hex:AcOEt = 7:2 + 1% HCO_2H). **^{1}H NMR** (400 MHz, $CDCl_3$) δ = 7.64 (d, *J* = 8.7 Hz, 1H), 7.45 – 7.31 (m, 5H), 7.00 – 6.94 (m, 2H), 5.12 (s, 2H), 3.01 (d, *J* = 18.9 Hz, 1H), 2.75 (d, *J* = 15.3 Hz, 1H), 2.63 (d, *J* = 15.3 Hz, 1H), 2.54 (d, *J* = 18.9 Hz, 1H), 1.45 (s, 3H). **^{13}C NMR** (100 MHz, $CDCl_3$) δ = 203.5, 175.3, 164.7, 163.8, 135.8, 129.2, 128.7 (2C), 128.3, 127.6 (2C), 125.5, 115.9, 108.5, 70.4, 50.5, 45.1, 40.0, 28.4. **LC-MS** (m/z): $[M-H]^-$ = 309.2.

2-(4-fluoro-1-methyl-3-oxo-2,3-dihydro-1H-inden-1-yl)acetic acid (**168i**)

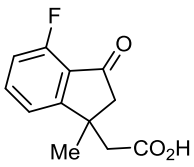

Colorless oil, yield = 45% (10.0 mg, *n*-Hex:AcOEt = 7:2 + 1% HCO_2H). **^{1}H NMR** (400 MHz, $CDCl_3$) δ = 7.61 (tt, *J* = 12.6, 6.3 Hz, 1H), 7.27 (d, *J* = 7.5 Hz, 1H, sovrapposto con il picco di $CHCl_3$), 7.03 (t, *J* = 8.6 Hz, 1H), 3.07 (d, *J* = 18.9 Hz, 1H), 2.84 (d, *J* = 15.6 Hz, 1H), 2.74 (d, *J* = 15.6 Hz, 1H), 2.61 (d, *J* = 18.9 Hz, 1H), 1.51 (s, 3H). **LC-MS** (m/z): $[M-H]^-$ = 221.0.

2-(6-fluoro-1-methyl-3-oxo-2,3-dihydro-1H-inden-1-yl)acetic acid (**168j**)

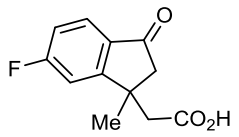

Colorless oil, yield = 52% (11.5 mg, *n*-Hex:AcOEt = 7:2 + 1% HCO_2H). **^{1}H NMR** (400 MHz, $CDCl_3$) δ = 7.71 (dd, *J* = 8.4, 5.3 Hz, 1H), 7.14 – 7.04 (m, 2H), 3.02 (d, *J* = 19.0 Hz, 1H), 2.79 (d, *J* = 15.6 Hz, 1H), 2.68 (d, *J* = 15.6 Hz, 1H), 2.58 (d, *J* = 19.0 Hz, 1H), 1.47 (s, 3H). **^{13}C NMR** (100 MHz, $CDCl_3$) δ = 203.0, 167.3 (d, *J* = 256.9 Hz), 175.3, 163.6 (d, *J* = 8.9 Hz), 132.2 (d, *J* = 1.9 Hz), 126.1 (d, *J* = 10.4 Hz), 116.3 (d, *J* = 23.8 Hz), 110.5 (d, *J* = 22.5 Hz), 50.4, 44.7, 40.0 (d, *J* = 2.0 Hz), 28.6; **^{19}F NMR** (376 MHz, $CDCl_3$) δ = -101.49 - -101.59 (m, 1F). **LC-MS** (m/z): $[M-H]^-$ = 221.2.

2-(1-methyl-3-oxo-6-(trifluoromethyl)-2,3-dihydro-1H-inden-1-yl)acetic acid (**168k**)

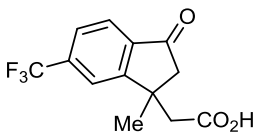

Colorless oil, yield = 35% (9.5 mg, *n*-Hex:AcOEt = 7:2 + 1% HCO_2H). **^{1}H NMR** (400 MHz, $CDCl_3$) δ = 7.84 (d, *J* = 7.9 Hz, 1H), 7.76 (s, 1H), 7.68 (d, *J* = 7.9 Hz, 1H), 3.10 (d, *J* = 19.2 Hz, 1H), 2.88 (d, *J* = 15.8 Hz, 1H), 2.77 (d, *J* = 15.8 Hz, 1H), 2.66 (d, *J* = 19.1 Hz, 1H), 1.55 (s, 3H). **LC-MS** (m/z): $[M-H]^-$ = 271.2.

2-(1-butyl-3-oxo-2,3-dihydro-1H-inden-1-yl)acetic acid (**168l**)

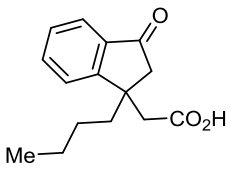

Colorless oil, yield = 76% (18.7 mg, *n*-Hex:AcOEt = 7:2 + 1% HCO_2H). **^{1}H NMR** (400 MHz, $CDCl_3$) δ = 7.69 (d, *J* = 7.6 Hz, 1H), 7.63 – 7.57 (m, 1H), 7.42 (d, *J* = 7.8 Hz, 1H), 7.38 (t, *J* = 7.4 Hz, 1H), 2.92 (d, *J* = 19.1 Hz, 1H), 2.83 (d, *J* = 15.3 Hz, 1H), 2.70 (d, *J* = 15.3 Hz, 1H), 2.63 (d, *J* = 19.1 Hz, 1H), 1.88 – 1.78 (m, 1H), 1.74 – 1.63 (m, 1H), 1.30 – 1.04 (m, 4H), 0.78 (t, *J* = 7.2 Hz, 3H). **^{13}C NMR** (100 MHz, $CDCl_3$) δ = 205.2, 175.7, 159.1, 136.7, 134.9, 128.0, 123.8, 123.5, 47.6, 44.0, 43.6, 40.6, 26.5, 22.9, 13.8. **LC-MS** (m/z): $[M-H]^-$ = 245.2.